The Chlorination of Pharmaceuticals and Other Phenolic Compounds in the Presence of Iodide

Edward Matthew Fiss

Dissertation submitted to the faculty of the Virginia Polytechnic Institute and State University in partial fulfillment of the requirements for the degree of

Doctor of Philosophy

In

Civil and Environmental Engineering

Peter J. Vikesland
Andrea M. Dietrich
Marc A. Edwards
John C. Little
James M. Tanko

April 1, 2009
Blacksburg, Virginia

Keywords: halogenation, free chlorine, iodide, PPCPs, drinking water

The Chlorination of Pharmaceuticals and Other Phenolic Compounds
in the Presence of Iodide

Edward Matthew Fiss

ABSTRACT

Pharmaceuticals and personal care products (PPCPs) include a wide range of chemicals such as prescription and over-the-counter drugs, fragrances, diagnostic agents, and a litany of other compounds commonly added to household products such as sunscreens, soaps, toothpastes, and deodorants. If present in natural waters, PPCPs can come into contact with disinfectants during drinking water treatment processes. PPCPs are already known to form a variety of disinfection byproducts (DBPs) when oxidized by free chlorine, including trihalomethanes (THMs) and haloacetic acids (HAAs), many of which are known carcinogens.

Salts, such as iodide, are also often present in natural water systems. Iodide is known to form a much more reactive oxidant, free iodine, when it reacts with free chlorine. Free iodine can react with organic compounds in waters to form iodinated byproducts, many of which have been shown to form in higher yields and to be more toxic than their chlorinated analogues. For this reason, it is necessary to more fully understand the fate of PPCPs during drinking water processes. The overall goals of this study are to 1) elucidate reaction mechanisms and product formation potentials for PPCP oxidation by free chlorine in the presence of iodide and 2) develop a computer model that can act as a predictive tool to aid in the assessment of potential risks resulting from PPCPs in source waters.

Through the course of this research, a model was developed that could fit reaction rate parameters and accurately predict solution reactivity for a range of substituted phenols as well as PPCPs including bisphenol-A and triclosan. Past studies utilizing pseudo-first-order rate constants to determine a reaction rate over-simplified the analysis of halogen substitution reactions. Free chlorine reaction rate constant values were updated from the literature since the mechanism for electrophilic substitution was found to be different than stated in currently published literature. The involvement of H_2OCl^+ was found to be negligible. The mechanism for the electrophilic substitution of phenolic compounds by free iodide was also different from current literature findings. We found that I_2, rather than H_2OI^+, was an extremely important species for free iodine reactions and must be considered when analyzing the reaction kinetics. Finally, we found that small amounts of iodide can significantly affect product formation pathways thereby causing preferential formation of iodinated products and a potential increase in the total product formation.

In general, the reaction kinetics were highly dependent upon the pH, iodide to free chlorine ratio, and the reactivity of the phenolic compound, and our model was able to successfully address changes in each of these variables. An LFER was developed that showed a linear relationship between reaction rates and the pK_a of a phenolic compound. It is believed that the model developed can be used as a predictive tool to estimate reactivity of natural waters for a range of phenolic PPCPs simply by using the compounds pK_a.

Acknowledgements

I thank the National Science Foundation for providing funding for this research.

I especially would like to thank Peter Vikesland for his support throughout my time here at Virginia Tech. Without his guidance, I would never have been able to find my way through my research projects (all 8 of them) and make sense of my time here. Our conversations always helped me figure out my problems, no matter what they were, while also calming me when my stress level was on the rise (whether it be from a looming deadline or a dysfunctional computer). Working with him has taught me more about chemistry than I ever thought possible and has prepared me for success no matter where I end up.

Thanks also to my committee members (Marc Edwards, Andrea Dietrich, John Little, and James Tanko) who have all taught me tremendous amounts.

A heartfelt thanks goes to Jody Smiley for her never-ending help in the instrumentation lab. I also could not have finished without the help of Krista Rule and Rob Rebodos, who have been here with me since the beginning and never refused to lend a hand.

I also must thank my father, without whom I would have never hung in this long. I look forward to working alongside you and learning from you for years to come.

And last but far from least, I must thank my wife Lauren. She moved from everything she knew to give us a chance, replacing the city she was used to with a new view of farmland. I look forward to our new home and our lives after school. Without her love and support, I would never have completed this work.

Table of Contents

List of Figures

List of Tables

Chapter 1: Introduction

Continual expansion of the world's human population has resulted in the increased consumption of potable water while also creating inflated waste production. Pollution and overuse increase the environmental stresses on the natural environment by diminishing the usefulness of an already limited supply of fresh water. The surge in demand for consumer goods, such as pharmaceuticals and personal care products, naturally leads to their eventual release to the environment and their detection in aquatic systems. Through exposure pathways such as consumption, inhalation, and dermal sorption, people are continuously exposed to many of these compounds in their everyday lives. Continual advances in science and technology have made it possible to identify and detect these compounds in the environment at levels previously unattainable and it has subsequently become apparent that a number of these substances can cause negative health effects. With these discoveries comes the inherent need to understand the fate of such compounds in the natural environment to enable proper risk assessments to be performed.

Pharmaceuticals and personal care products (PPCPs) include a wide range of chemicals such as prescription and over-the-counter drugs, fragrances, diagnostic agents, and a litany of other compounds commonly added to household products such as sunscreens, soaps, toothpastes, and deodorants. By both excretion and simply by washing products down the drain, PPCPs and their degradation products are constantly introduced into wastewater treatment utilities. As a result of incomplete removal, sludge disposal processes, and PPCP persistence in natural systems, these chemicals can be found in nearly every aquatic environment (1-4). Recent

studies have detected PPCP contamination of both raw and treated drinking waters at the ng/L to μg/L level. Two of the most commonly measured are bisphenol-A and triclosan (3, 5-10). Prior studies have shown that the reactive phenolic rings found in these PPCPs readily react with free chlorine and the mechanisms by which these reactions occur have been established. These reactions result in the formation of a variety of disinfection byproducts (DBPs) including chlorinated phenoxy-phenols, chlorophenols, benzonquinones, trihalomethanes (THMs) and haloacetic acids (HAAs) (11-26). The initial reactions that occur are electrophilic substitution reactions by free chlorine as described by reactions 1.1-1.3 (19, 27).

Cl_2 + phenol → products (1.1)

HOCl + phenol → products (1.2)

HOCl + phenolate → products (1.3)

An issue that has been overlooked in the majority of the PPCP-disinfectant studies to date is the potential complicating effect of the presence of salts such as bromide and iodide. Most natural waters contain bromide and iodide at concentrations ranging from 0.01-3.0 mg/L (10) and from 0.5-212 μg/L (8), respectively. Both species react with free chlorine to produce reactive intermediates (28) that in turn can react with organic matter and PPCPs to form iodinated and brominated DBPs (25, 29-31). This study focused on the interactions and effects of iodide. Iodide quickly reacts with free chlorine to form hypoiodous acid, which is believed to then react with phenols via electrophilic substitution as described by reactions 1.4-1.7 (31).

I_2 + phenol → products (1.4)

HOI + phenol → products (1.5)

HOI + phenolate → products (1.6)

OI^- + phenol → products (1.7)

The potential formation of iodinated products is especially troublesome since some have been shown to be significantly more toxic than their chlorinated analogues (32), although the toxicities of individual species are largely unknown.

The overall goal of this study was to increase our understanding of how the presence of iodide affects the kinetics of PPCP/disinfectant interactions under conditions simulating drinking water treatment. Specifically, the reactivity of phenolic compounds with free chlorine in the presence and absence of iodide was assessed. Three different types of phenolic compounds were used: substituted phenols, triclosan, and bisphenol-A. The studies with the substituted phenols discussed in **Chapter 3** were conducted to facilitate the development of a comprehensive kinetic model that simultaneously accounts for the speciation of free chlorine and free iodine as well as the electrophilic substitution reactions that each species can undergo with a given phenol. Our use of a series of substituted phenols facilitated the parameterization of this model. **Chapter 4** describes experimental results obtained with triclosan and discusses the steps taken to model the kinetics of triclosan/disinfectant interactions. Similarly, **Chapter 5** describes experimental results obtained with bisphenol-A and discusses the steps taken to model the kinetics of bisphenol-A/disinfectant interactions. **Chapter 6** summarizes the collected results and quantitatively compares the rate constants obtained with each phenolic compound. **Chapter 2** provides a brief review of the literature to illustrate the current state of knowledge in the field of iodine/free chlorine interactions and their potential implications to PPCP reactivity.

1.2: References

1. Vieno, N. M.; Harkki, H.; Tuhkanen, T.; Kronberg, L., Occurrence of pharmaceuticals in river water and their elimination a pilot-scale drinking water treatment plant. *Environ. Sci. Technol.* **2007,** *41*, (14), 5077-5084.

2. Stackelberg, P. E.; Gibs, J.; Furlong, E. T.; Meyer, M. T.; Zaugg, S. D.; Lippincott, R. L., Efficiency of conventional drinking-water-treatment processes in removal of pharmaceuticals and other organic compounds. *Science of the Total Environment* **2007,** *377*, (2-3), 255-272.

3. Boyd, G. R.; Palmeri, J. M.; Zhang, S. Y.; Grimm, D. A., Pharmaceuticals and personal care products (ppcps) and endocrine disrupting chemicals (edcs) in stormwater canals and bayou st. John in new orleans, louisiana, USA. *Science of the Total Environment* **2004,** *333*, (1-3), 137-148.

4. Snyder, S. A.; Westerhoff, P.; Yoon, Y.; Sedlak, D. L., Pharmaceuticals, personal care products, and endocrine disruptors in water: Implications for the water industry. *Environmental Engineering Science* **2003,** *20*, (5), 449-469.

5. Boyd, G. R.; Reemtsma, H.; Grimm, D. A.; Mitra, S., Pharmaceuticals and personal care products (ppcps) in surface and treated waters of louisiana, USA and ontario, canada. *Science of the Total Environment* **2003,** *311*, (1-3), 135-149.

6. Kolpin, D. W.; Furlong, E. T.; Meyer, M. T.; Thurman, E. M.; Zaugg, S. D.; Barber, L. B.; Buxton, H. T., Pharmaceuticals, hormones, and other organic wastewater contaminants in u.S. Streams, 1999-2000: A national reconnaissance. *Environ. Sci. Technol.* **2002,** *36*, 1202-1211.

7. Halling-Sorensen, B.; Nielsen, S. N.; Lanzky, P. F.; Ingerslev, F.; Lutzhoft, H. C. H.; Jorgensen, S. E., Occurrence, fate and effects of pharmaceutical substances in the environment - a review. *Chemosphere* **1998,** *36*, (2), 357-394.

8. Moran, J. E.; Oktay, S. D.; Santschi, P. H., Sources of iodine and iodine 129 in rivers. *Water Resources Research* **2002,** *38*, (8).

9. Amy, G.; M., S.; Zhai, W.; DeBroux, J.; Odem, W., *Survey of bromide in drinking water and impacts on dbp formation*. AWWARF: Denver, CO, 1994.

10. Westerhoff, P.; Siddiqui, M.; Debroux, J.; Zhai, W.; Ozekin, K.; Amy, G. In *Nation-wide bromide occurrence and bromate formation potential in drinking water supplies*, National Conference on Environmental Engineering, Boulder, CO, 1994; Edwards, J. N. R. a. M., Ed. ASCE: Boulder, CO, 1994; pp 670-677.

11. Pinkston, K. E.; Sedlak, D. L., Transformation of aromatic ether-and amine-containing pharmaceuticals during chlorine disinfection. *Environ. Sci. Technol.* **2004,** *38*, (14), 4019-4025.

12. Onodera, S.; Nishikawa, T.; Suzuki, S., Chemical-changes of organic-compounds in chlorinated water .14. Characterization and determination of halogenated organics formed during chlorination of water from the tama river. *J. Chromatogr.* **1987,** *409*, 259-270.

13. Kanetoshi, A.; Ogawa, H.; Katsura, E.; Kaneshima, H., Chlorination of irgasan dp300 and formation of dioxins from its chlorinated derivatives. *J. Chromatogr.* **1987,** *389*, 139-153.

14. Canosa, P.; Morales, S.; Rodriguez, I.; Rubi, E.; Cela, R.; Gomez, M., Aquatic degradation of triclosan and formation of toxic chlorophenols in presence of low concentration of free chlorine. *Anal. Bioanal. Chem.* **2005,** *383*, (7-8), 1119-1126.

15. Rule, K. L.; Ebbett, V. R.; Vikesland, P. J., Formation of chloroform and chlorinated organics by free-chlorine-mediated oxidation of triclosan. *Environmental Science and Technology* **2005,** *39*, 3176-3185.

16. Lee, G. F.; Morris, J. C., Kinetics of chlorination of phenol-chlorophenolic tastes and odors. *Int. J. Air Water Pollut.* **1962,** *6*, 419-431.

17. Soper, F. G.; Smith, G. F., The halogenation of phenols. *J. Am. Chem. Soc.* **1926,** *6*, 1582-1591.

18. Gallard, H.; von Gunten, U., Chlorination of natural organic matter: Kinetics of chlorination and of thm formation *Water Res.* **2002,** *36*, (1), 65-74.

19. Gallard, H.; Von Gunten, U., Chlorination of phenols: Kinetics and formation of chloroform. *Environ. Sci. Technol.* **2002,** *36*, (5), 884-890.

20. Onodera, S.; Iino, N.; Matsuda, M.; Ishikura, S., Chemical-changes of organic-compounds in chlorinated water .6. Gas-chromatographic and mass-spectrometric studies of the reactions of phenylphenols with hypochlorite in dilute aqueous-solution. *J. Chromatogr.* **1983,** *265*, (2), 201-213.

21. Onodera, S.; Yamada, K.; Yamaji, Y.; Ishikura, S.; Suzuki, S., Chemical-changes of organic-compounds in chlorinated water .10. Formation of polychlorinated methylphenoxymethylphenols (predioxins) during chlorination of methylphenols in dilute aqueous-solution. *J. Chromatogr.* **1986,** *354*, 293-303.

22. Bedner, M.; Maccrehan, W. A., Transformation of acetaminophen by chlorination produces the toxicants 1,4-benzoquinone and n-acetyl-p-benzoquinone imine. *Environ. Sci. Technol.* **2006,** *40*, (2), 516-522.

23. Fiss, E. M.; Rule, K. L.; Vikesland, P. J., Formation of chloroform and other chlorinated byproducts by chlorination of triclosan-containing antibacterial products. *Environ. Sci. Technol.* **2007,** *41*, (7), 2387-2394.

24. Greyshock, A. E.; Vikesland, P. J., Triclosan reactivity in chloraminated waters. *Environmental Science and Technology* **2006,** *40*, 2615-2622.

25. Vikesland, P. J.; Rule, K. L.; Greyshock, A. E.; Ebbett, V. R.; Fiss, E. M., *Triclosan reactivity in chlorinated and monochloraminated waters*. AWWA Research Foundation: Denver, 2006.

26. Trussell, R. R.; Umphres, M. D., Formation of trihalomethanes. *Journal American Water Works Association* **1978,** *70*, (11), 604-612.

27. Cherney, D. P.; Duirk, S. E.; Tarr, J. C.; Collette, T. W., Monitoring the speciation of aqueous free chlorine from ph 1 to 12 with raman spectroscopy to determine the identity of the potent low-ph oxidant. *Applied Spectroscopy* **2006,** *60*, (7), 764-772.

28. Bichsel, Y.; von Gunten, U., Oxidation of iodide and hypoiodous acid in the disinfection of natural waters. *Environ. Sci. Technol.* **1999,** *33*, (22), 4040-4045.

29. Rook, J. J., Formation of haloforms during chlorination of natural waters. *Water Treatment and Examination* **1974,** *23*, 234-243.

30. Symons, J. M.; Krasner, S. W.; Simms, L. A.; Sclimenti, M., Measurement of thm and precursor concentrations revisited - the effect of bromide ion. *Journal American Water Works Association* **1993,** *85*, (1), 51-62.

31. Bichsel, Y.; von Gunten, U., Formation of iodo-trihalomethanes during disinfection and oxidation of iodide containing waters. *Environ. Sci. Technol.* **2000,** *34*, (13), 2784-2791.

32. Plewa, M. J.; Wagner, E. D.; Richardson, S. D.; Thruston, A. D.; Woo, Y. T.; McKague, A. B., Chemical and biological characterization of newly discovered lodoacid drinking water disinfection byproducts. *Environ. Sci. Technol.* **2004,** *38*, (18), 4713-4722.

Chapter 2: Literature Review

2.1: Drinking Water Disinfection

Access to safe drinking water is an essential part of the maintenance of good health in humans. Free chlorine has been used for drinking water disinfection in the U.S. since 1908 and is amongst the biggest breakthroughs in public health protection to date. Since that time, research performed around the world has led to more complex disinfection practices using additional disinfectants such as ozone and chloramines, and the addition of filtration and membrane technologies to further ensure consumer safety. Free chlorine disinfection is a relatively inexpensive and highly reliable treatment practice and thus over 70% of drinking water utilities in the U.S. continue to use free chlorine for water disinfection today (1). In the developed world, drinking water today is safer and healthier for the consumer than it has ever been in history.

The benefits of disinfectants are undeniable as a matter of public health protection, but there are also many drawbacks to drinking water disinfection including the formation of potentially harmful disinfection byproducts. The effectiveness of drinking water treatment practices have increased through the expansion of knowledge and technology and simultaneously our ability to detect and study the effects of other contaminants in drinking water has also been greatly improved. Though effective for disinfection, it has been found that the use of free chlorine in drinking water treatment can lead to the formation of a range of potentially harmful byproducts. Repeatedly, trihalomethanes (THMs), such as chloroform, have been shown to form from the chlorination of organic compounds such as fulvic and humic substances during

drinking water treatment. These aromatic precursors are converted into several trichloromethyl-substituted intermediates that subsequently decompose to chloroform through a series of hydrolysis and decarboxylation steps (2, 3). It was found that the phenolic moieties present within humic substances react with chlorine, and that the reaction rates were proportional to free chlorine concentration, TOC concentration, temperature, and pH (4), with the optimal reaction pH ranging from 8 to 10 (2). The reaction between humic or fulvic acids and low chlorine concentrations yields substantial amounts of polyhalogenated intermediates, while reactions performed at high chlorine levels do not (2). Other studies have shown that resorcinol-type structures (i.e., aromatic, phenolic structures including *m*-dihydroxybenzene, β-diketone, and β-ketoacid structures) in NOM are responsible for the fast reacting THM precursors ($k>100\ M^{-1}s^{-1}$, pH=8.0), while more slowly reacting precursors consist of phenolic moieties ($k=0.026\ M^{-1}s^{-1}$, pH=8.0) (5, 6). Other compounds, including additional THMs, haloacetic acids (HAAs), and chlorinated phenols, have also been shown to form from these reactions.

The EPA has set a maximum contaminant level of 80 μg/L for total trihalomethanes since these volatile byproducts have been established as potentially carcinogenic compounds (7). The MCL was set by extrapolating a dose-response curve created by testing acute high-level exposure effects on animals to the estimated human effects from chronic, low-level exposure. Although the risk assessment method likely results in high levels of error, the evaluation is necessary since only 20 chemicals have adequate epidemiological exposure data to prove human carcinogenicity. Both 2,4-dichlorophenol and 2,4,6-trichlorophenol have been placed on the EPA Drinking Water Contaminant Candidate List (CCL) since they are suspected

carcinogens and are thus suspected to increase an individual's risk of cancer by their presence in drinking water; however, at this time these compounds are not regulated due to an insufficient amount of data. The EPA is currently researching all 51 contaminants on the candidate list to determine if they need to be regulated (8). In addition to potential health effects, many aromatic disinfection by-products also are a concern because they can cause problems with respect to the taste and odor of treated water.

2.2: The Effects of Iodide.

An issue that has largely been overlooked in drinking water disinfection is the potential complicating effect caused by the presence of common salts, such as iodide (I^-) , on these reactions. The predominant reservoir of iodine, which is a minor element in the environment and a vital nutrient for human health, is the ocean. Within the ocean, iodine is largely present in the thermodynamically stable form, iodate (IO_3^-), although it can be reduced to I^- by biological processes or phytoplankton (9-11). Marine algae can release iodoorganic compounds including iodoform (CHI_3) and other iodine-containing trihalomethanes, methyl iodide, and ethyl iodide, among others, into seawater (12, 13). Many of these iodoalkanes are volatile and are subject to evaporation thus transferring iodine into the atmosphere (14). Atmospheric iodine can then enter clouds and rainwater where concentrations have been found as high as 20 μg/L (14, 15). Iodine is also found in rocks at concentrations ranging from 0.08 to 0.50 mg/kg and in soils at concentrations between 0.5 to 20 mg/kg (16). By precipitation and weathering of rocks and sediments, iodine is then introduced into fresh waters where it is typically found at concentrations ranging from 0.5 to 212 μg/L (17). As opposed to oceanic

iodine, which is primarily in the form of IO_3^-, fresh water iodine is almost completely in the iodide (I^-) form (18).

During drinking water treatment processes, naturally present iodide can come into contact with disinfectants such as free chlorine. If this occurs, any available iodide is oxidized by HOCl to form hypoiodous acid (HOI) by a complex series of reactions involving the intermediates $HOClI^-$ and ICl (19-22). The resulting product is the highly reactive species hypoiodous acid (19, 21, 23-26). Studies have shown that $HOClI^-$ and ICl are present at trace levels and react instantaneously to form HOI, so their presence can be considered negligible (21). As such, the overall, irreversible reaction between HOCl and iodide can therefore be described by a single overall equation (equation 2.1):

$$HOCl + I^- \xrightarrow{k_{3.8}} HOI + Cl^- \qquad k_{2.1} = 4.3 \times 10^8\ M^{-1}s^{-1} \qquad (2.1)$$

An HOI-species equilibrium is then quickly established as illustrated by equations 2.2-2.6 to form I_2, OI^-, I_3^-, H_2OI^-, and HOI_2^- (27-30), any of which is potentially reactive.

$$I_2 + H_2O \longleftrightarrow HOI + I^- + H^+ \qquad K_{2.2} = 5.44\times10^{-13}\ M^2 \qquad (2.2)$$

$$HOI \longleftrightarrow OI^- + H^+ \qquad K_{2..3} = 2.3\times10^{-11}\ M \qquad (2.3)$$

$$I_2 + I^- \longleftrightarrow I_3^- \qquad K_{2.4} = 715\ M^{-1} \qquad (2.4)$$

$$H_2OI^- \longleftrightarrow HOI + H^+ \qquad K_{2.5} = 2\ M \qquad (2.5)$$

$$HOI_2^- \longleftrightarrow HOI + I^- \qquad K_{2.6} = 3.1\times10^{-3}\ M \qquad (2.6)$$

A plot illustrating the speciation of iodide as a function of pH is shown in Figure 2.1.

At alkaline pH, iodide is predominantly in the I_2 form while HOI dominates in neutral to basic solutions. The OI^- form only accounts for greater than 10% of total iodine above a pH of 9.5. All other reactive iodine species make up less than 0.7% of total species combined. HOI can

subsequently form iodate (IO_3^-) as a result of disproportionation reactions (Reactions 2.7-2.9) or through further oxidation of HOI by excess HOCl (Reaction 2.10).

$$HOI + HOI \longrightarrow IO_2^- + 2H^+ + I^- \quad (2.7)$$

$$HOI + OI^- \longrightarrow IO_2^- + H^+ + I^- \quad (2.8)$$

$$IO_2^- + HOI \xrightarrow{\text{fast}} IO_3^- + H^+ + I^- \quad (2.9)$$

$$HOI + HOCl + HOCl \longrightarrow IO_3^- + 3H^+ + 2Cl^- \quad (2.10)$$

Iodate is stable and non-reactive, making it a desirable sink for iodide during treatment processes because iodinated DBP formation potentials are reduced (31). However, for HOCl and I^- concentrations typical of drinking water treatment processes, the half-life of I^- is on the order of milliseconds (23), so under conditions where free chlorine is in excess, iodide is immediately and completely converted to HOI. The half-life of the HOI disproportionation reaction is on the order of ≈4 days (23), while the half-life due to oxidation by HOCl is on the order of hours (31). This means that disproportionation and HOCl-mediated oxidation reactions are of little importance relative to HOI reactivity with phenols since HOI-phenol reactions have a half-life on the order of seconds.

Similar to free chlorine, reactive iodinated species can readily react with organic matter. In fact, HOI has been shown to react with natural organic matter 15 times faster than HOCl (24) resulting in the formation of iodinated THMs and HAAs (26, 32-34). These iodinated byproducts have been estimated to be 50-500× more toxic than their chlorinated analogues (25) and in addition have much lower odor threshold concentrations (35). Because these reactive iodine-containing species cannot be differentiated from HOCl by common oxidant measurements (e.g., DPD based methods), the presence of these species during water disinfection has been

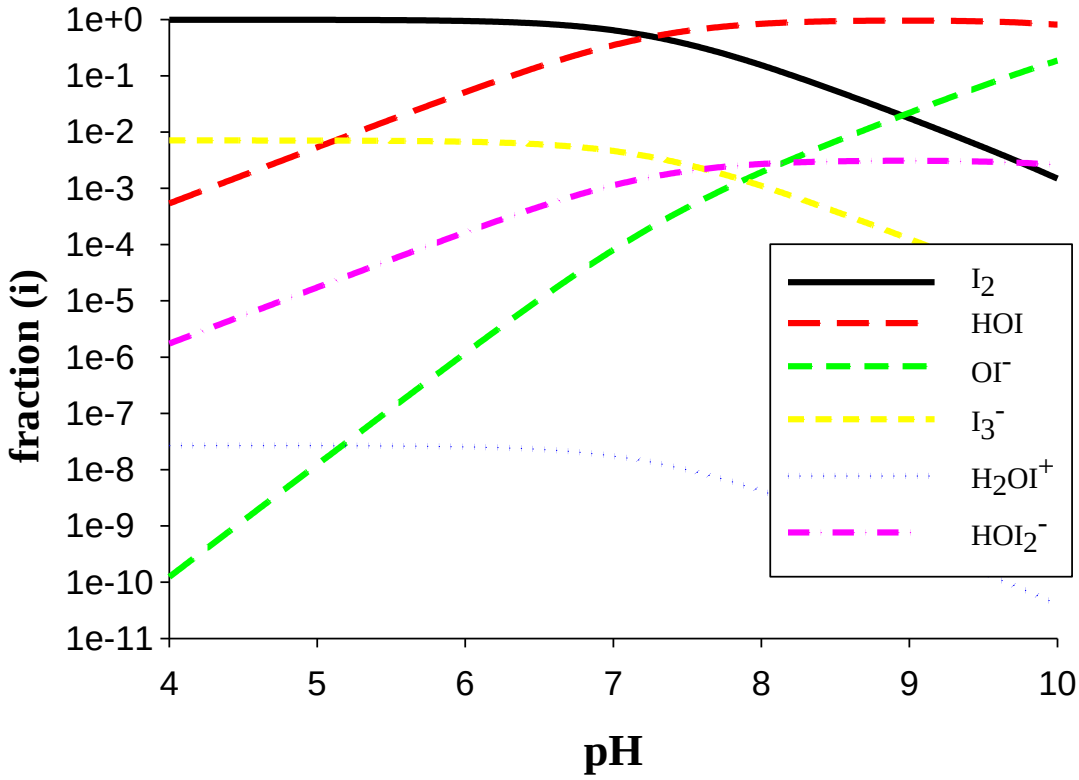

Figure 2.1: Speciation of iodide versus pH for a solution containing 10 μM total iodide.

underappreciated in the past. Based upon the observations of increased reactivity and product toxicity, the effects from the presence of iodide in natural systems needs to be further studied.

2.3: Pharmaceutical and personal care products.

Pharmaceuticals and personal care products (PPCPs) include a wide range of chemicals such as prescription and over-the-counter drugs, fragrances, diagnostic agents, and a litany of other compounds commonly added to household items such as sunscreens, soaps, toothpastes, and deodorants. By both excretion and simply by washing products down the drain, PPCPs and their degradation products are constantly introduced into wastewater treatment plant influents. As a result of incomplete removal and sludge disposal processes and their persistence in natural systems, PPCPs can be detected in nearly every aquatic environment (36-39). Numerous studies have shown PPCP contamination of both raw and treated drinking waters at the ng/L to μg/L level (17, 38, 40-44). Because of increased public concern about microbial pathogens, as well as the ever increasing human populations, the amounts and types of PPCPs being introduced into the environment continue to increase. For instance, currently over 75% of liquid soaps and 30% of bar soaps on the market contain an antibacterial chemical such as triclosan or triclocarban (45). It should therefore not be a surprise that triclosan was detected in 57.6% of waters during a recent survey of 139 U.S. streams (41). These facts suggest that PPCPs are continually input into the environment and thus are ubiquitous, which reinforces the need to understand the ultimate fate of these compounds in natural waters.

Many PPCPs are continuously released into the environment and as such, are commonly found in source waters used for drinking water supply. These source waters are then pumped to utilities so that these potentially reactive compounds can be present during drinking water

disinfection. Studies have shown that PPCPs and chlorinated disinfectants react to form a variety of disinfection byproducts (DBPs) including chlorinated phenoxy-phenols, chlorophenols, benzonquinones, trihalomethanes (THMs) and haloacetic acids (HAAs). The formation rates for these products are normally fastest near circumneutral pH (5, 6, 46-59). Since ≈90% of utilities maintain a pH between 7 and 9.5 (1), the presence of PPCPs in source waters may be cause for concern. In addition, a number of PPCPs are designed for use during common household activities, such as showering and washing dishes, and can be in contact with a consumer's skin for extended periods of time at elevated water temperatures (60, 61). During these activities, conditions are optimized for free chlorine reactions and elevated temperatures may further enhance product formation rates. The potential presence of iodide in these systems and its acknowledged reactivity requires an in-depth understanding of how its presence affects PPCP stability and reactivity.

Substituted phenols. In this study, the reactivity of a range of differentially substituted phenols was studied to determine the effects of iodide on reaction kinetics and product formation during drinking water disinfection. Differentially substituted phenols were used because they have historically been used as model compounds for similar but more complex or more highly toxic materials, such as natural organic matter and organic micro-pollutants such as PPCPs. Phenols are useful model compounds because they exhibit chemical behaviors similar to other phenolic compounds, but are more readily available for purchase, are easier to quantify, and are generally safer to handle (5, 62). The pH-dependant relationships describing the reactivity of differentially substituted phenolic compounds and free chlorine have historically been described by reactions 2.11-2.16 (6, 63-65).

$$Cl_2 + H_2O \longleftrightarrow HOCl + Cl^- + H^+ \qquad K_{2.11} = 5.1\times10^{-4}\ M^2 \qquad (2.11)$$

$$HOCl \longleftrightarrow OCl^- + H^+ \qquad K_{2.12} = 2.9\times10^{-8}\ M \qquad (2.12)$$

$$\text{phenol} \longleftrightarrow \text{phenolate} + H^+ \qquad K_{2.13} \qquad (2.13)$$

$$Cl_2 + \text{phenol} \longrightarrow \text{products} \qquad k_{2.14} \qquad (2.14)$$

$$HOCl + \text{phenol} \longrightarrow \text{products} \qquad k_{2.15} \qquad (2.15)$$

$$HOCl + \text{phenolate} \longrightarrow \text{products} \qquad k_{2.16} \qquad (2.16)$$

Reaction 2.14 has long been believed to be the reaction between H_2OCl^+ and phenol, although a recent study suggests that Cl_2 is the active electrophile at low pH (65). The dominant mechanism at circumneutral pH is the reaction between HOCl and the phenolate form of phenol with second-order rate constants ranging from 12.8 to 2.71×10^4 $M^{-1}s^{-1}$ for 2,4,6-trichlorophenol and unsubstituted phenol, respectively (6). Similar reactions between substituted phenols and HOI have been described by reactions 4.1-4.3 (24).

$$H_2OI^+ + \text{phenol} \longrightarrow \text{products} \qquad k_{2.17} \qquad (2.17)$$

$$HOI + \text{phenol} \longrightarrow \text{products} \qquad k_{2.18} \qquad (2.18)$$

$$HOI + \text{phenolate} \longrightarrow \text{products} \qquad k_{2.19} \qquad (2.19)$$

As with HOCl, it is possible that the H_2OI^+ species in reaction 4.1 should be replaced with I_2 (66), although such a conclusion requires additional studies. And again as has been observed for HOCl, the dominant pathway at circumneutral pH is thought to be between HOI and the phenolate form of phenol with a second-order rate constant of 2×10^6 $M^{-1}s^{-1}$ published for unsubstituted phenol (24). Formation of chlorinated trihalomethanes such as chloroform results from HOCl oxidation of phenols (6), while iodinated trihalomethanes such as iodoform were observed when HOI was the oxidant (24).

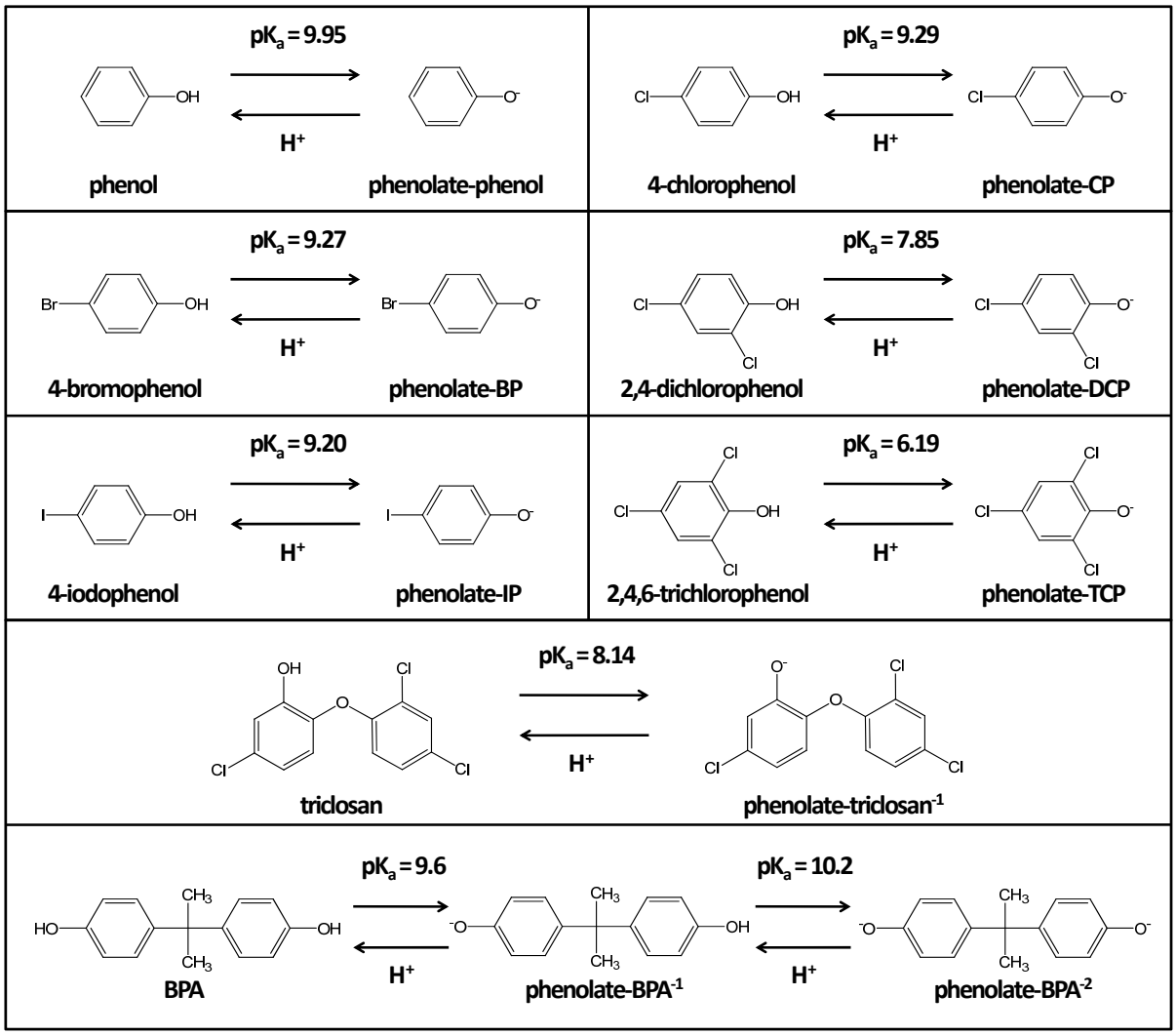

Figure 2-2: Structures of all experimental species.

Triclosan. Triclosan (5-chloro-2-(2,4- dichlorophenoxy)phenol) is an antimicrobial agent found in many common household hygienic products to prevent bacterial infections and for oral applications (67). Triclosan is a synthetic, broad spectrum antimicrobial agent that takes the form of an off-white, odorless, tasteless, crystalline powder (67). It is virtually insoluble in water and has a molecular weight of 289.5 g/mole (67). Although triclosan was introduced for use in health care settings over 30 years ago, its use dramatically expanded over the last fifteen years as a result of increased concern about microbial pathogens. Many companies currently add triclosan to products such as hand soaps, surgical scrubs, deodorants, dish soaps, body washes, and toothpastes at concentrations of up to 0.3%. Although its actual effectiveness is a topic of some debate, triclosan has been added to many personal care products because it exhibits antibacterial as well as some antifungal and antiviral properties (68).

Phenoxy-phenols such as triclosan are a class of compounds that exhibit a broad spectrum of antimicrobial activity. The two most widely used members of this group are triclosan and hexachlorophene, although use of the latter in consumer products has been limited due to toxicity concerns (69). Historically, it was thought that triclosan worked as a non-specific biocide that disturbs membrane functionality in bacteria by preventing RNA and protein synthesis (70, 71) Proponents of triclosan have also suggested that high triclosan concentrations, such as those observed with normal antibacterial product use, cause a multitude of different effects on numerous targets resulting in cell lysis (72). During the last decade, however, it was found that triclosan works as a site-specific biocide that inhibits a defined target in the bacterial fatty acid biosynthetic pathway. Studies have shown that triclosan can prevent fatty acid synthesis by inhibition of the NADH-dependent enoyl acyl

carrier protein reductase enzyme (FabI) in *E. coli* (73), *P. aeruginosa* (74), *S. aureus* (75) or its homolog InhA in *M. smegmatis* (76) and *M. tuberculosis* (77).

In the US, over 75% of liquid soaps and nearly 30% of bar soaps currently on the market contain some type of antibacterial product (45). An estimated 700 antibacterial products, the vast majority of which contain triclosan as the active ingredient, entered the consumer market between 1992 and 1999 (69). On average, a typical American uses approximately 5 mg of triclosan each day, resulting in a total nationwide usage of almost 1500 kg/day (78). When coupled with its relative chemical stability, the wide-spread use of triclosan has led to its presence in nearly every aquatic environment. Triclosan is washed down consumer's drains during product use and is present in wastewater treatment plant (WWTP) influents. Triclosan is common in WWTP biosolids (79), and due to incomplete removal by biological treatment processes, it is also detected in treatment plant effluents (80, 81). Incomplete removal by treatment plants and land-application of triclosan containing biosolids result in its continued release into lake and river waters (79, 82). A comprehensive study by the U.S. Geological Survey detected triclosan in 57.6% of 139 highly susceptible streams (41). Triclosan has also regularly been detected in drinking water source waters (83).

Many European countries, such as Denmark and Germany, have limited the use of triclosan-containing products because of increasing fears about the acute toxicity of the compound, its potential to lead to bacterial resistance, and other long-term ill effects (84). Several recent studies have shown that some bacteria, such as *escherichia coli* and *mycobacterium smegmatis*, can readily build resistance to triclosan (76, 85). *Pseudomonas putida* and *alcaligenes*

xylosoxidans bacteria that have been exposed to triclosan for a long period of time will even adopt triclosan as their sole carbon source (86).

In a household environment, it is not clear that the use of triclosan containing products provides enhanced antibacterial protection relative to triclosan-free products (84). The minimum inhibitory concentration of triclosan varies from 0.01 to over 1000 mg/L depending on the organism in question (87). The wide range in effective concentrations, when combined with the large variability of tolerance within an individual species, has resulted in weak statistical findings in studies analyzing triclosan's effectiveness. Because of this, no study to date has been able to definitively show that antibacterial products work any better than regular soap and water. In fact, several studies have claimed that triclosan-containing soap use does not provide any prolonged antibacterial effect when compared to non-medicated soap, although it did cause skin irritation in several cases (88, 89). Larson et al. showed that there was no statistically significant advantage to washing hands with triclosan-containing soap over triclosan-free soap, and that there was no reduction of an individual's risk of acquiring an infectious household disease. After performing a risk analysis, Larson argues in favor of the use of plain soap and water (90, 91).

Studies have shown that triclosan and free chlorine readily react to form several different byproducts including chlorinated phenoxy-phenols, chlorinated phenols, and trihalomethanes with an optimal pH ranging from 7 to 9 (48-50, 92). It has also been shown that these and other phenols can act as trihalomethane precursors when they come in contact with free-chlorine (5, 6, 51-54, 93). In a past study by Rule et al. (50), a reaction scheme was proposed that illustrates the products that form during the free chlorine-triclosan reactions. From this study, and

subsequent work by Canosa et al. (49), it is apparent that when triclosan reacts in the presence of free chlorine, a number of simultaneous reaction pathways result in production of several byproducts. Chlorine substitution into triclosan can result in formation of 5,6-dichloro-2-(2,4-dichlorophenoxy)phenol, 4,5-dichloro-2-(2,4-dichlorophenoxy)phenol, and 4,5,6-trichloro-2-(2,4-dichlorophenoxy)phenol intermediates. Any of these products, or triclosan itself, reacts to produce 2,4-dichlorophenol and then 2,4,6-trichlorophenol after an ether cleavage reaction. Additionally, triclosan and all byproducts mentioned above can form chloroform directly by ring cleavage and chlorination. The effects of iodide on triclosan oxidation have not been studied to date.

Bisphenol-A. Bisphenol-A (BPA, 2,2-bis(4-hydroxyphenyl)propane) is a widely produced chemical used in the manufacture of a range of consumer products. It is used as a monomer in the synthesis of polycarbonates, a type of polymer utilized in the manufacture of plastic food containers, as well as a polymerization inhibitor in PVC pipes (94). BPA is an organic compound that exists as a white to light brown powder with an aqueous solubility of 300 mg/L at 25 ^{o}C (95). The estimated U.S. production in 2004 of BPA was ≈2.3 billion pounds, 75% of which was used to manufacture polycarbonate resins for various consumer products (95). Such resins are commonly used in the production of food containers because they are highly transparent, low weight, highly heat resistant, and virtually indestructible (95).

BPA has well documented estrogenic and other endocrine disrupting capabilities that can have harmful effects on human health (96) including effects on the reproductive system as well as increasing neurobehavioral problems like ADHD and autism (97). BPA exposure is mostly due to the leaching of BPA from containers into food and other consumer products that are

then ingested. For example, one study detected BPA in over 50% of samples taken from canned tomatoes (98). Much evidence suggests that BPA exposures typical of an average human living in a developed county are well within the range to cause adverse health effects (97).

Bisphenol-A is regularly introduced into the environment by sewage treatment plant effluents, landfill leachates, and natural degradation of plastics leading to their detection in natural waters at concentrations up to 700 ng/L (99). During water treatment and due to the common use of PVC pipes in distribution systems, BPA regularly comes in contact with free chlorine. In addition, BPA migration from plastics into water used for cooking and storing water and food products can result in substantial contact periods. Several recent studies have shown that free chlorine can oxidize BPA to form a range of products including chlorinated BPA congeners, polychlorinated phenoxyphenols, and differentially substituted chlorophenols (100-102). The predominant reactions responsible for these reactions at circumneutral pH are believed to be between HOCl and $PhOH^-$ and PhO^{2-}, respectively (102). In addition, the binding affinity of chlorinated BPAs towards estrogen receptors are 24× greater than before chlorination, meaning that a chlorinated BPA is better able to mimic the effects of estrogen hormones than un-chlorinated BPA and can bind to receptors in the body more easily. The chlorination of BPA increases the estrogenic activity of the compound and is more apt to alter endocrine systems and disrupt growth in humans (100). To date, no studies have been performed to assess the effects of iodine in this system.

2.4: References

1. Drinking water utility database. In *AWWA*, American Water Works Association Water Quality Section: 1997.

2. Boyce, S. D.; Hornig, J. F., Reaction pathways of trihalomethane formation from the halogenation of dihydroxyaromatic model compounds for humic acid. *Environ. Sci. Technol.* **1983,** *17*, 202-211.

3. Rook, J. J., Chlorination reactions of fulvic acids in natural waters. *Environ. Sci. Technol.* **1977,** *11*, 478-482.

4. Urano, K.; Wada, H.; Takemasa, T., Empirical rate equation for trihalomethane formation with chlorination of humic substances in water. *Water Res.* **1983,** *17*, 1797-1802.

5. Gallard, H.; von Gunten, U., Chlorination of natural organic matter: Kinetics of chlorination and of thm formation *Water Res.* **2002,** *36*, (1), 65-74.

6. Gallard, H.; Von Gunten, U., Chlorination of phenols: Kinetics and formation of chloroform. *Environ. Sci. Technol.* **2002,** *36*, (5), 884-890.

7. EPA, Stage 1 disinfectants and disinfection byproducts rule. In US Environmental Protection Agency: 1998; Vol. EPA 815-F-98-010.

8. EPA *Drinking water contaminant candidate list 2*; U.S. Environmental Protection Agency: 2005.

9. Councell, T. B.; Landa, E. R.; Lovley, D. R., Microbial reduction of iodate. *Water, Air, and Soil Pollution* **1997,** *100*, (1-2), 99-106.

10. Luther III, G. W.; Wu, J.; Cullen, J. B., Redox chemistry of iodine in seawater- frontier molecular orbital theory considerations. In *Advances in Chemistry*, C.P. Huang, C. R. O. M., and J.J. Morgan, Ed. American Chemical Society: Washington DC, 1995; Vol. 244.

11. Moisan, T. A.; Dunstan, W. M.; Udomkit, A.; Wong, G. T. F., The uptake of iodate by marine phytoplankton. *Journal of Phycology* **1994,** *30*, (4), 580-587.

12. Moore, R. E., Volatile compounds from marine algae. *Accounts of Chemical Research* **1977,** *10*, 40-47.

13. Gschwend, P. M.; MacFarlane, J. K.; Newman, K. A., Volatile halogenated organice compounds released to seawater from temperate marine macroalgae. *Science* **1985,** *227*, 1033-1035.

14. Fuge, R., Iodine in the environment: Its distribution and relationship to human health. *Trace Substances in Environmental Health* **1987,** *21*, 74-87.

15. Duce, R. A.; Wasson, J. T.; Winchester, J. W.; Burns, F., Atmospheric iodine, bromine, and chlorine. *Journal of Geophysical Research* **1963,** *68*, (13), 3943-3947.

16. Whitehead, D. C., The distribution and transformations of iodine in the environment. *Environment International* **1984,** *10*, (4), 321-339.

17. Moran, J. E.; Oktay, S. D.; Santschi, P. H., Sources of iodine and iodine 129 in rivers. *Water Resources Research* **2002,** *38*, (8).

18. Bichsel, Y. Behavior of iodine species in oxidative processes during drinking water treatment. Swiss Federal Institute of Technology Zurich, Zurich, 2000.

19. Nagy, J. C.; Kumar, K.; Margerum, D. W., Non-metal redox kinetics - oxidation of iodide by hypochlorous acid and by nitrogen trichloride measured by the pulsed-accelerated-flow method. *Inorganic Chemistry* **1988,** *27*, (16), 2773-2780.

20. Nagy, K.; Kortvelyesi, T.; Nagypal, I., Iodine hydrolysis equilibrium. *Journal of Solution Chemistry* **2003,** *32*, (5), 385-393.

21. Lengyel, I.; Li, J.; Kustin, K.; Epstein, I. R., Rate constants for reactions between iodine- and chlorine-containing species: A detailed mechanism of the chlorine dioxide/chlorite-iodide reaction. *J. Am. Chem. Soc.* **1996,** *118*, (15), 3708-3719.

22. Kazantseva, N. N.; Ernepesova, A.; Khodjamamedov, A.; Geldyev, O. A.; Krumgalz, B. S., Spectrophotometric analysis of iodide oxidation by chlorine in highly mineralized solutions. *Analytica Chimica Acta* **2002,** *456*, (1), 105-119.

23. Bichsel, Y.; von Gunten, U., Oxidation of iodide and hypoiodous acid in the disinfection of natural waters. *Environ. Sci. Technol.* **1999,** *33*, (22), 4040-4045.

24. Bichsel, Y.; von Gunten, U., Formation of iodo-trihalomethanes during disinfection and oxidation of iodide containing waters. *Environ. Sci. Technol.* **2000,** *34*, (13), 2784-2791.

25. Plewa, M. J.; Wagner, E. D.; Richardson, S. D.; Thruston, A. D.; Woo, Y. T.; McKague, A. B., Chemical and biological characterization of newly discovered lodoacid drinking water disinfection byproducts. *Environmental Science & Technology* **2004,** *38*, (18), 4713-4722.

26. Hua, G. H.; Reckhow, D. A.; Kim, J., Effect of bromide and iodide ions on the formation and speciation of disinfection byproducts during chlorination. *Environmental Science & Technology* **2006,** *40*, (9), 3050-3056.

27. Gottardi, W., Iodine and disinfection: Theoretical study on mode of action, efficiency, stability, and analytical aspects in the aqueous system. *Archiv Der Pharmazie* **1999,** *332*, (5), 151-157.

28. Gottardi, W.; Arnitz, R.; Nagl, M., N-chlorotaurine and ammonium chloride: An antiseptic preparation with strong bactericidal activity. *International Journal of Pharmaceutics* **2007,** *335*, (1-2), 32-40.

29. Schmitz, G., Inorganic reactions of iodine(+1) in acidic solutions. *International Journal of Chemical Kinetics* **2004,** *36*, (9), 480-493.

30. Lengyel, I.; Epstein, I. R.; Kustin, K., Kinetics of iodine hydrolysis. *Inorganic Chemistry* **1993,** *32*, (25), 5880-5882.

31. Bichsel, Y.; von Gunten, U., Hypoiodous acid: Kinetics of the buffer-catalyzed disproportionation. *Water Res.* **2000,** *34*, (12), 3197-3203.

32. Hua, G. H.; Reckhow, D. A., Comparison of disinfection byproduct formation from chlorine and alternative disinfectants. *Water Res.* **2007,** *41*, (8), 1667-1678.

33. Cancho, B.; Ventura, F.; Galceran, M.; Diaz, A.; Ricart, S., Determination, synthesis and survey of iodinated trihalomethanes in water treatment processes. *Water Res.* **2000,** *34*, (13), 3380-3390.

34. Krasner, S. W.; Weinberg, H. S.; Richardson, S. D.; Pastor, S. J.; Chinn, R.; Sclimenti, M. J.; Onstad, G. D.; Thruston, A. D., Occurrence of a new generation of disinfection byproducts. *Environ. Sci. Technol.* **2006,** *40*, (23), 7175-7185.

35. Dietrich, A. M.; Mirlohi, S.; DaCosta, W. F.; Dodd, J. P.; Sauer, R.; Homan, M.; Schultz, J., Flavor profile analysis and gc/ms detection of phenolic iodinated disinfection byproducts in drinking water for the USA space program. *Water Science and Technology* **1999,** *40*, (6), 45-51.

36. Vieno, N. M.; Harkki, H.; Tuhkanen, T.; Kronberg, L., Occurrence of pharmaceuticals in river water and their elimination a pilot-scale drinking water treatment plant. *Environ. Sci. Technol.* **2007,** *41*, (14), 5077-5084.

37. Stackelberg, P. E.; Gibs, J.; Furlong, E. T.; Meyer, M. T.; Zaugg, S. D.; Lippincott, R. L., Efficiency of conventional drinking-water-treatment processes in removal of

pharmaceuticals and other organic compounds. *Science of the Total Environment* **2007,** *377*, (2-3), 255-272.

38. Boyd, G. R.; Palmeri, J. M.; Zhang, S. Y.; Grimm, D. A., Pharmaceuticals and personal care products (ppcps) and endocrine disrupting chemicals (edcs) in stormwater canals and bayou st. John in new orleans, louisiana, USA. *Science of the Total Environment* **2004,** *333*, (1-3), 137-148.

39. Snyder, S. A.; Westerhoff, P.; Yoon, Y.; Sedlak, D. L., Pharmaceuticals, personal care products, and endocrine disruptors in water: Implications for the water industry. *Environmental Engineering Science* **2003,** *20*, (5), 449-469.

40. Boyd, G. R.; Reemtsma, H.; Grimm, D. A.; Mitra, S., Pharmaceuticals and personal care products (ppcps) in surface and treated waters of louisiana, USA and ontario, canada. *Science of the Total Environment* **2003,** *311*, (1-3), 135-149.

41. Kolpin, D. W.; Furlong, E. T.; Meyer, M. T.; Thurman, E. M.; Zaugg, S. D.; Barber, L. B.; Buxton, H. T., Pharmaceuticals, hormones, and other organic wastewater contaminants in u.S. Streams, 1999-2000: A national reconnaissance. *Environ. Sci. Technol.* **2002,** *36*, 1202-1211.

42. Halling-Sorensen, B.; Nielsen, S. N.; Lanzky, P. F.; Ingerslev, F.; Lutzhoft, H. C. H.; Jorgensen, S. E., Occurrence, fate and effects of pharmaceutical substances in the environment - a review. *Chemosphere* **1998,** *36*, (2), 357-394.

43. Amy, G.; M., S.; Zhai, W.; DeBroux, J.; Odem, W., *Survey of bromide in drinking water and impacts on dbp formation*. AWWARF: Denver, CO, 1994.

44. Westerhoff, P.; Siddiqui, M.; Debroux, J.; Zhai, W.; Ozekin, K.; Amy, G. In *Nation-wide bromide occurrence and bromate formation potential in drinking water supplies*, National Conference on Environmental Engineering, Boulder, CO, 1994; Edwards, J. N. R. a. M., Ed. ASCE: Boulder, CO, 1994; pp 670-677.

45. Perencevich, E. N.; Wong, M. T.; Harris, A. D., National and regional assessment of the antibacterial soap market: A step toward determining the impact of prevalent antibacterial soaps. *Am. J.Infect. Control* **2001,** *29*, 281-283.

46. Pinkston, K. E.; Sedlak, D. L., Transformation of aromatic ether-and amine-containing pharmaceuticals during chlorine disinfection. *Environ. Sci. Technol.* **2004,** *38*, (14), 4019-4025.

47. Onodera, S.; Nishikawa, T.; Suzuki, S., Chemical-changes of organic-compounds in chlorinated water .14. Characterization and determination of halogenated organics formed during chlorination of water from the tama river. *J. Chromatogr.* **1987,** *409*, 259-270.

48. Kanetoshi, A.; Ogawa, H.; Katsura, E.; Kaneshima, H., Chlorination of irgasan dp300 and formation of dioxins from its chlorinated derivatives. *J. Chromatogr.* **1987,** *389*, 139-153.

49. Canosa, P.; Morales, S.; Rodriguez, I.; Rubi, E.; Cela, R.; Gomez, M., Aquatic degradation of triclosan and formation of toxic chlorophenols in presence of low concentration of free chlorine. *Anal. Bioanal. Chem.* **2005,** *383*, (7-8), 1119-1126.

50. Rule, K. L.; Ebbett, V. R.; Vikesland, P. J., Formation of chloroform and chlorinated organics by free-chlorine-mediated oxidation of triclosan. *Environmental Science and Technology* **2005,** *39*, 3176-3185.

51. Lee, G. F.; Morris, J. C., Kinetics of chlorination of phenol-chlorophenolic tastes and odors. *Int. J. Air Water Pollut.* **1962,** *6*, 419-431.

52. Soper, F. G.; Smith, G. F., The halogenation of phenols. *J. Am. Chem. Soc.* **1926,** *6*, 1582-1591.

53. Onodera, S.; Iino, N.; Matsuda, M.; Ishikura, S., Chemical-changes of organic-compounds in chlorinated water .6. Gas-chromatographic and mass-spectrometric studies of the reactions of phenylphenols with hypochlorite in dilute aqueous-solution. *J. Chromatogr.* **1983,** *265*, (2), 201-213.

54. Onodera, S.; Yamada, K.; Yamaji, Y.; Ishikura, S.; Suzuki, S., Chemical-changes of organic-compounds in chlorinated water .10. Formation of polychlorinated methylphenoxymethylphenols (predioxins) during chlorination of methylphenols in dilute aqueous-solution. *J. Chromatogr.* **1986,** *354*, 293-303.

55. Bedner, M.; Maccrehan, W. A., Transformation of acetaminophen by chlorination produces the toxicants 1,4-benzoquinone and n-acetyl-p-benzoquinone imine. *Environ. Sci. Technol.* **2006,** *40*, (2), 516-522.

56. Fiss, E. M.; Rule, K. L.; Vikesland, P. J., Formation of chloroform and other chlorinated byproducts by chlorination of triclosan-containing antibacterial products. *Environ. Sci. Technol.* **2007,** *41*, (7), 2387-2394.

57. Greyshock, A. E.; Vikesland, P. J., Triclosan reactivity in chloraminated waters. *Environmental Science and Technology* **2006,** *40*, 2615-2622.

58. Vikesland, P. J.; Rule, K. L.; Greyshock, A. E.; Ebbett, V. R.; Fiss, E. M., *Triclosan reactivity in chlorinated and monochloraminated waters*. AWWA Research Foundation: Denver, 2006.

59. Trussell, R. R.; Umphres, M. D., Formation of trihalomethanes. *Journal American Water Works Association* **1978,** *70*, (11), 604-612.

60. Tancrede, M.; Yanagisawa, Y.; Wilson, R., Volatilization of volatile organic-compounds from showers .1. Analytical method and quantitative assessment. *Atmos. Environ. A-Gen.* **1992,** *26*, (6), 1103-1111.

61. Howard, C.; Corsi, R. L., Volatilization of chemicals from drinking water to indoor air: The role of residential washing machines. *J. Air Waste. Manage.* **1998,** *48*, (10), 907-914.

62. Ge, F.; Zhu, L. Z.; Wang, J., Distribution of chlorination products of phenols under various phs in water disinfection. *Desalination* **2008,** *225*, (1-3), 156-166.

63. Wang, T. X.; Margerum, D. W., Kinetics of reversible chlorine hydrolysis - temperature-dependence and general acid base-assisted mechanisms. *Inorganic Chemistry* **1994,** *33*, (6), 1050-1055.

64. Morris, J. C., The acid ionization constant of hocl from 5 to 35^{o}. *Journal of Physical Chemistry* **1966,** *70*, (12), 3798-3805.

65. Cherney, D. P.; Duirk, S. E.; Tarr, J. C.; Collette, T. W., Monitoring the speciation of aqueous free chlorine from ph 1 to 12 with raman spectroscopy to determine the identity of the potent low-ph oxidant. *Applied Spectroscopy* **2006,** *60*, (7), 764-772.

66. Warner, J. A.; Casey, W. H.; Dahlgren, R. A., Interaction kinetics of i-2(aq) with substituted phenols and humic substances. *Environ. Sci. Technol.* **2000,** *34*, (15), 3180-3185.

67. Bhargava, H. N.; Leonard, P. A., Triclosan: Applications and safety. *Am. J.Infect. Control* **1996,** *24*, 157-222.

68. Jones, R. D.; Jampani, H. B.; Newman, J. L.; Lee, A. S., Triclosan: A review of effectiveness and safety in health care settings. *Am. J.Infect. Control* **2000,** *28*, 184-196.

69. Schweizer, H. P., Triclosan: A widely used biocide and its link to antibiotics. *FEMS Microbiol. Lett.* **2001,** *202*, (1), 1-7.

70. Regos, J.; Hitz, H. R., Investigations on the mode of action of triclosan, a broad spectrum sntimicrobial agent. *Zbl. Bakt. Mik. Hyg. A* **1974,** *226*, 390-401.

71. Meincke, B. E.; Kranz, R. G.; Lynch, D. L., Effect of irgasan on bacterial growth and its adsorption into the cell wall. *Microbios* **1980,** *1980*, 133-147.

72. McDonnell, G.; Russell, A. D., Antiseptics and disinfectants: Activity, action, and resistance. *Clin. Microbiol. Rev.* **1999,** *12*, (1), 147-179.

73. McMurry, L. M.; Oethinger, M.; Levy, S. B., Triclosan targets lipid synthesis. *Nature* **1998,** *394*, (6693), 531-532.

74. Hoang, T. T.; Schweizer, H. P., Characterization of *pseudomonas aeruginosa* enoyl-acyl carrier protein reductase (fabi): A target for the antimicrobial triclosan and its role in acylated homoserine lactone synthesis. *Journal of Bacteriology* **1999,** *181*, 5489-5497.

75. Heath, R. J.; Li, S.; Roland, G. E.; Rock, C. O., Inhibition of the *staphylococcus aureus* nadph-dependent enoyl-acyl carrier protein reductase by triclosan and hexachlorophene. *Journal of Biological Chemistry* **1999,** *7*, 4654-4659.

76. McMurry, L. M.; McDermott, P. F.; Levy, S. B., Genetic evidence that inha of mycobacterium smegmatis is a target for triclosan. *Antimicrob. Agents Chemother.* **1999,** *43*, (3), 711-713.

77. Slayden, R. A.; Lee, R. E.; Barry, C. E., Isoniazid affects multiple components of the type ii fatty acid synthase system of *mycobacterium tuberculosis*. *Mol. Microbiol* **2000,** *38*, (3), 514-525.

78. McAvoy, D. C.; Schatowitz, B.; Jacob, M.; Hauk, A.; Eckhoff, W. S., Measurement of triclosan in wastewater treatment systems. *Environmental Toxicology and Chemistry* **2002,** *21*, 1323-1329.

79. Singer, H.; Muller, S.; Tixier, C.; Pillonel, L., Triclosan: Occurence and fate of a widely used biocide in the aquatic environment: Field measurements in wastewater treatment plants, surface waters, and lake sediments. *Environ. Sci. Technol.* **2002,** *36*, 4998-5004.

80. Kanda, R.; Griffin, P.; James, H. A.; Fothergill, J., Pharmaceutical and personal care products in sewage treatment works. *Journal of Environmental Monitoring* **2003,** *5*, 823-830.

81. Federle, T. W.; Kaiser, S. K.; Nuck, B. A., Fate and effects of triclosan in activated sludge. *Environmental Toxicology and Chemistry* **2001,** *21*, 1330-1337.

82. Lindstrom, A.; Buerge, I. J.; Poiger, T.; Bergqvist, P.-A.; Muller, M. D.; Buser, H.-R., Occurrence and environmental behavior of the bactericide triclosan and its methyl

derivative in surface waters and in wastewater. *Environ. Sci. Technol.* **2002,** *36*, 2322-2329.

83. Boyd, G. R.; Reemtsma, H.; Grimm, D. A.; Mitra, S., Pharmaceuticals and personal care products (ppcps) in surface and treated waters of louisiana, USA and ontario, canada. *the Science of the Total Environment* **2003,** *311*, 135-149.

84. Glaser, A., The ubiquitous triclosan: A common antibacterial agent exposed. *Pesticides and You- Beyond Pesticides/ National Coalition Against the Misuse of Pesticides* 2004, pp 12-17.

85. McMurry, L. M.; Oethinger, M.; Levy, S. B., Overexpression of mara, soxs, or acrab produces resistance to triclosan in laboratory and clinical strains of escherichia coli. *FEMS Microbiol. Lett.* **1998,** *166*, (2), 305-309.

86. Meade, M. J.; Waddell, R. L.; Callahan, T. M., Soil bacteria pseudomonas putida and alcaligenes xylosoxidans subsp denitrificans inactivate triclosan in liquid and solid substrates. *FEMS Microbiol. Lett.* **2001,** *204*, (1), 45-48.

87. Vischer, W. A.; Regos, J., Antimicrobial spectrum of triclosan: A broad spectrum antimicrobial agent. *Zbl. Bakt. Mik. Hyg. A* **1974,** *226*, 376-389.

88. Bendig, J. W. A., Surgical hand disinfection - comparison of 4-percent chlorhexidine detergent solution and 2-percent triclosan detergent solution. *J. Hosp. Infect.* **1990,** *15*, (2), 143-148.

89. Kampf, G.; Kramer, A., Epidemiologic background of hand hygiene and evaluation of the most important agents for scrubs and rubs. *Clin. Microbiol. Rev.* **2004,** *17*, (4), 863-+.

90. Larson, E.; Aiello, A.; Lee, L. V.; Della-Latta, P.; Gomez-Duarte, C.; Lin, S., Short- and long-term effects of handwashing with antimicrobial or plain soap in the community. *J. Commun. Health* **2003,** *28*, (2), 139-150.

91. Larson, E. L.; Lin, S. X.; Gomez-Pichardo, C.; Della-Latta, P., Effect of antibacterial home cleaning and handwashing products on infectious disease symptoms. *Ann. Intern. Med.* **2004,** *140*, (5), 321-329.

92. Onodera, S.; Ogawa, M.; Suzuki, S., Chemical-changes of organic-compounds in chlorinated water .13. Gas-chromatographic mass-spectrometric studies of the reactions of irgasan dp-300 [5-chloro-2-(2,4-dichlorophenoxy)phenol]with chlorine in dilute aqueous-solution. *J. Chromatogr.* **1987,** *392*, 267-275.

93. Burttschell, R. H.; Rosen, A. A.; Middleton, F. M.; Ettinger, M. B., Chlorine derivatives of phenol causing taste and odor. *J. Am. Water Works Assoc.* **1959,** *51*, 205-214.

94. Ash, M.; Ash, I., *Handbook of plastic and rubber additives*. Gower, Hampshire, UK, 1995.

95. *Ntp-cerhr expert panel report on the reproductive and developmental toxicity of bishpehnol a*; Center for the Evaluation of Risks to Human Reproduction: 2007.

96. Wetherill, Y. B.; Akingbemi, B. T.; Kanno, J.; McLachlan, J. A.; Nadal, A.; Sonnenscheing, C.; Watson, C. S.; Zoeller, R. T.; Belcher, S. M., In vitro molecular mechanisms of bisphenol a action. *Reproductive Toxicology* **2007,** *24*, (2), 178-198.

97. vom Saal, F. S.; Akingbemi, B. T.; Belcher, S. M.; Birnbaum, L. S.; Crain, D. A.; Eriksen, M.; Farabollini, F.; Guillette, L. J.; Hauser, R.; Heindel, J. J.; Ho, S. M.; Hunt, P. A.; Iguchi, T.; Jobling, S.; Kanno, J.; Keri, R. A.; Knudsen, K. E.; Laufer, H.; LeBlanc, G. A.; Marcus, M.; McLachlan, J. A.; Myers, J. P.; Nadal, A.; Newbold, R. R.; Olea, N.; Prins, G. S.; Richter, C. A.; Rubin, B. S.; Sonnenschein, C.; Soto, A. M.; Talsness, C. E.; Vandenbergh, J. G.; Vandenberg, L. N.; Walser-Kuntz, D. R.; Watson, C. S.; Welshons, W. V.; Wetherill, Y.; Zoeller, R. T., Chapel hill bisphenol a expert panel consensus statement: Integration of mechanisms, effects in animals and potential to impact human health at current levels of exposure. *Reproductive Toxicology* **2007,** *24*, (2), 131-138.

98. Grumetto, L.; Montesano, D.; Seccia, S.; Albrizio, S.; Barbato, F., Determination of bisphenol a and bisphenol b residues in canned peeled tomatoes by reversed-phase liquid chromatography. *Journal of Agricultural and Food Chemistry* **2008,** *56*, (22), 10633-10637.

99. Crain, D. A.; Eriksen, M.; Iguchi, T.; Jobling, S.; Laufer, H.; LeBlanc, G. A.; Guillette, L. J., An ecological assessment of bisphenol-a: Evidence from comparative biology. *Reproductive Toxicology* **2007,** *24*, (2), 225-239.

100. Hu, J. Y.; Aizawa, T.; Ookubo, S., Products of aqueous chlorination of bisphenol a and their estrogenic activity. *Environ. Sci. Technol.* **2002,** *36*, (9), 1980-1987.

101. Yamamoto, T.; Yasuhara, A., Chlorination of bisphenol a in aqueous media: Formation of chlorinated bisphenol a congeners and degradation to chlorinated phenolic compounds. *Chemosphere* **2002,** *46*, (8), 1215-1223.

102. Gallard, H.; Leclercq, A.; Croue, J. P., Chlorination of bisphenol a: Kinetics and by-products formation. *Chemosphere* **2004,** *56*, (5), 465-473.

Chapter 3: Halogenation of Phenolic Compounds in Chlorinated Waters Containing Iodide

3.1: Introduction

Pharmaceuticals and personal care products (PPCPs) include chemicals such as prescription and over-the-counter drugs, fragrances, diagnostic agents, and a litany of other compounds commonly added to household products. PPCPs are constantly washed down the drain and, as a result, are present in wastewater treatment plant influents. Incomplete removal of PPCPs during wastewater treatment and disposal of PPCP laden sludge, as well as the persistence of many PPCPs in natural systems has led to detection of these compounds in aquatic environments at the ng/L to μg/L level (3-9). Multiple studies have shown that the phenolic substituents present in many PPCPs (e.g., triclosan, acetaminophen, and bisphenol-A) can readily react with free chlorine to form a variety of byproducts (10-16). The initial reaction between free chlorine and a phenolic compound typically involves the electrophilic substitution of chlorine to the phenol ring (1, 2, 17, 18). Electrophilic substitution is most commonly the rate controlling reaction dictating parent phenol loss with subsequent reactions resulting in cleavage of the phenol ring (1, 2, 16). Phenol ring cleavage ultimately leads to the formation of a variety of disinfection byproducts (DBPs), including trihalomethanes (THMs) and haloacetic acids (HAAs), as well as a variety of chlorinated phenols. Because the electrophilic substitution reaction determines phenol reactivity it is important to quantify the kinetics of these reactions. At moderate pH values reactions between hypochlorous acid (HOCl) and the phenolate-form

(PhO^-) of a phenol (Figure 2.2) generally dictate the kinetics of electrophilic substitution (1, 12-16, 18-28). Although they are several orders of magnitude smaller than those measured for PhO^-, rate constants for the substitution of neutral phenol (PhOH) have also been determined for many phenolic compounds (1). Under acidic conditions, the substitution reaction has historically been believed to involve H_2OCl^+ as the electrophile; however, a recent Raman spectroscopy study has shown that Cl_2 is the low pH electrophile (29).

An issue that has been overlooked in the majority of PPCP-free chlorine and phenol-free chlorine studies to date is the potential complicating effect caused by the presence of common salts, such as iodide, on these reactions. In natural waters, iodide is typically found at concentrations ranging from 0.5-200 μg/L (0.004 to 2 μM) with a mean concentration of 20 μg/L (0.2 μM; ref. 30). During drinking water disinfection, I^- is oxidized by free chlorine to produce highly reactive hypoiodous acid (HOI; refs. 2, 31-35) by a complex series of reactions involving the intermediates $HOClI^-$ and ICl (34-37). Studies have shown that these intermediates are present at trace levels and react instantaneously to form HOI, so their possible interactions with other species, such as phenols, are generally neglected in comparison to reactions with HOI (35). The overall irreversible reaction for I^- oxidation can be described by equation 3.8:

$$HOCl + I^- \xrightarrow{k_{3.8}} HOI + Cl^- \qquad k_{3.8} = 4.3 \times 10^8\ M^{-1}s^{-1} \qquad (3.8)$$

Once formed, HOI rapidly equilibrates to form I_2, OI^-, I_3^-, H_2OI^+, and HOI_2^- as described by equations 3.3-3.7 (Table 3.1; refs. 38-41). Potentially any of these free iodine species can react with organic compounds such as PPCPs. Unfortunately, reactive iodine-containing species cannot be differentiated from free chlorine by DPD based measurement methods (Figure 3.1) and thus the presence of these species during water disinfection is often underappreciated. In

Table 3.1: Reactions and equilibrium rate constants for HOCl and HOI in solution.

	Reaction	Equilibrium Constant	Ref
3.1	$Cl_2 + H_2O \longleftrightarrow HOCl + Cl^- + H^+$	$K_{3.1} = 5.1\times10^{-4}\ M^2$	(42)
3.2	$HOCl \longleftrightarrow OCl^- + H^+$	$K_{3.2} = 2.9\times10^{-8}\ M$	(43)
3.3	$I_2 + H_2O \longleftrightarrow HOI + I^- + H^+$	$K_{3.3} = 5.44\times10^{-13}\ M^2$	(38)
3.4	$HOI \longleftrightarrow OI^- + H^+$	$K_{3.4} = 2.3\times10^{-11}\ M$	(41)
3.5	$I_2 + I^- \longleftrightarrow I_3^-$	$K_{3.5} = 715\ M^{-1}$	(40)
3.6	$H_2OI^- \longleftrightarrow HOI + H^+$	$K_{3.6} = 2\ M$	(40)
3.7	$HOI_2^- \longleftrightarrow HOI + I^-$	$K_{3.7} = 3.1\times10^{-3}\ M$	(40)

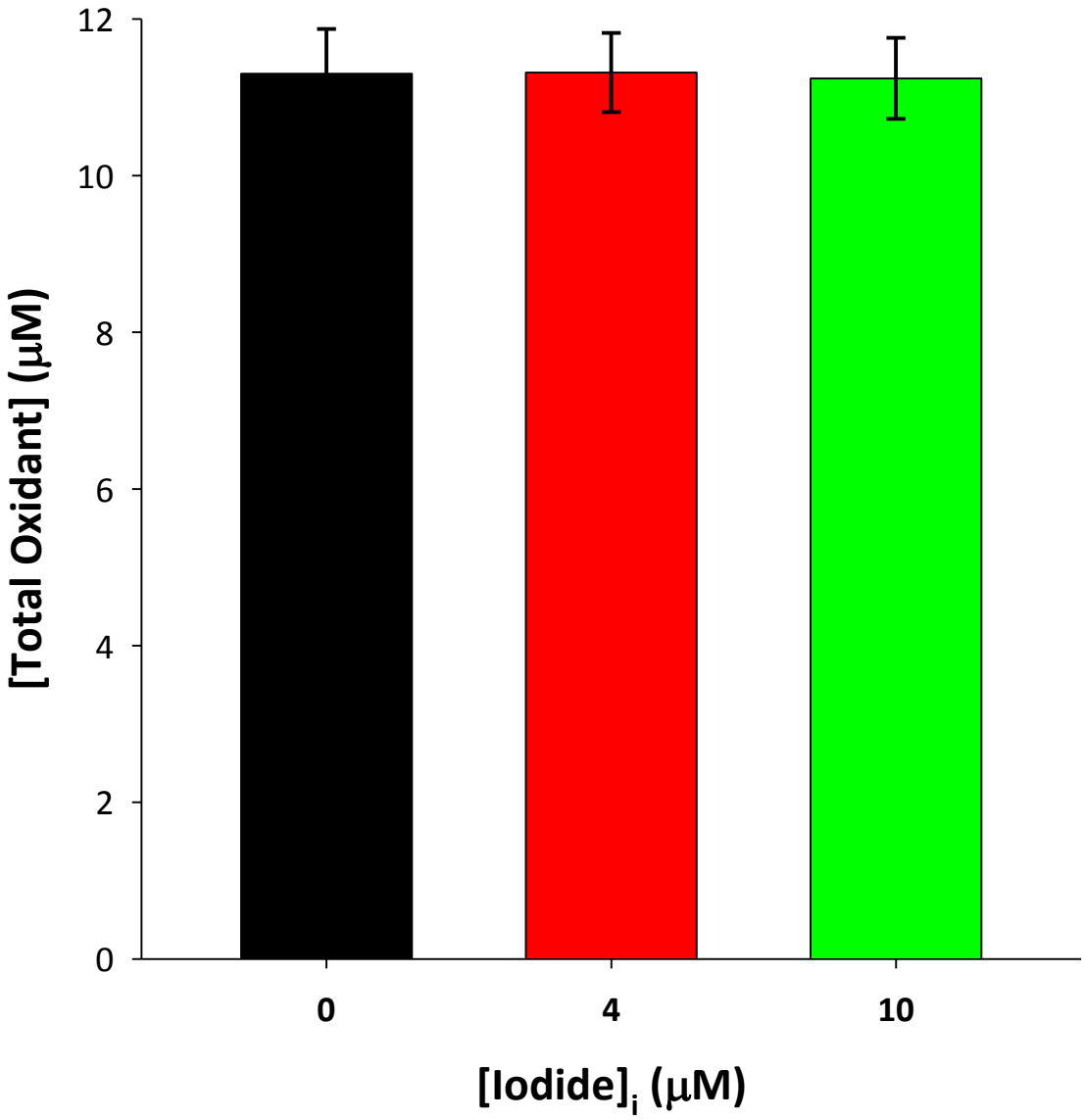

Figure 3.1: Comparison of average total oxidant concentration measured using DPD colorimetric method for solutions containing 10 μM HOCl and iodide concentrations of 0, 4, and 10 μM initially. As shown, DPD-based methods cannot differentiate between chlorinated and iodinated oxidants.

general, relatively little is known about the implications of PPCP iodination in natural waters. HOI has been shown to react with natural organic matter nearly 15 times faster than HOCl (2). Iodination of phenolic compounds is of concern because some iodinated DBPs have been shown to be 50-500× more toxic than their chlorinated analogues (32), and the presence of iodide during organic matter oxidation has been shown to produce iodinated THMs (2) and HAAs (33). Accelerated reactions and increased product formation necessitate the need to better understand iodide-free chlorine interactions so that a true assessment of public health risk is possible.

Substituted phenols have historically been used as model compounds for similar but more complex or more highly toxic materials, such as natural organic matter and organic micro-pollutants such as PPCPs. Phenols are useful model compounds because they exhibit chemical behaviors similar to other phenolic compounds, but are more readily available for purchase, are easier to quantify, and are generally safer to handle (23, 44). This study utilized a range of substituted phenols as PPCP mimics to analyze the effect of changes in the iodide to free chlorine ratio on electrophilic substitution.

Free chlorine reacts with phenols by stepwise electrophilic substitution of the *ortho* (2 and 6) positions and *para* (4) position (1, 17, 18, 45, 46). Initial halogenation occurs at either the *ortho* or *para* position, though the activating effect of the charged hydroxyl group tends to preferentially result in *ortho* substitution (17). The electron withdrawing effects of chlorine, due to the higher electronegativity of chlorine over that of hydrogen, causes the chlorine to preferentially attack the *ortho* position where the negative charge of the phenol is centralized. This is especially the case for a negatively charged (phenolate) phenol (47). The primary

reaction pathway for the iodination of phenols is also known to occur by electrophilic substitution, preferentially in the *ortho* position (45, 48, 49). In general, the kinetics of HOI mediated reactions with phenolic compounds are significantly faster than the corresponding reactions with HOCl, with rate constants typically 2 orders of magnitude larger for iodination reactions than for chlorination reactions (1, 2). The increased rates for iodination are due to the decreased electrophilicity of iodine as compared to chlorine. Because chlorine is more electronegative than iodine, Cl^+ pulls harder on the oxygen in the hydroxyl group in an HOCl molecule than I^+ would in a HOI molecule. Chlorine is a stronger electron acceptor, so it pulls more of the negative charge from the oxygen towards itself, meaning that H^+ can dissociate from the hydroxyl group with less difficulty. This makes HOCl a stronger acid and more stable in its deprotonated form than HOI. Because the iodine-oxygen bond is weaker than the chlorine-oxygen bond, the negative charge of the oxygen retains a stronger bond with the H^+, so the hydrogen is more difficult to remove. Since the H^+ remains bound to the HOI molecule, the molecule retains a stronger polarity, thus making it more reactive towards a negatively charged phenolic compound. Additionally, the lower bond strength of the oxygen- iodine bond means that it requires less energy to be broken, thereby increasing the chance for substitution reactions to occur.

Prior studies have examined the effects of iodide on electrophilic substitution in the presence of free chlorine; however, these studies concentrated on product distributions (33, 50-52) rather than on the determination of reaction rates since data for extremely short reaction periods are difficult to accurately obtain. Published kinetic studies with iodide and free chlorine have focused on the disproportionation of HOI to produce iodate rather than reactions with

organic matter or phenols (31, 36, 53-56). The few kinetic studies that looked at the kinetics of electrophilic substitution by free iodine have either utilized conditions that call the applicability of the results to drinking water into question (57), or used too simplistic of a reaction model (2) to capture the complexity of this system. The objectives of the present study were two-fold: 1) to perform a comprehensive analysis of the effects of iodide on the kinetics of the halogen substitution reactions that occur during drinking water chlorination, and 2) to develop a comprehensive model to calculate reaction rate constants and predict the overall behavior for each reactive oxidant and phenol.

3.2 Materials and Methods

Reagent grade water was purified by deionization and distillation. Glassware was cleaned by sequentially soaking it in a 10% nitric acid bath and then in a concentrated chlorine bath. Phenol, 4-chlorophenol, 4-bromophenol, 4-iodophenol, 2,4-dichlorophenol, and 2,4,6-trichlorophenol were purchased from Alfa Aesar. Stocks of free chlorine were prepared using a commercial solution of sodium hypochlorite (purified grade 4-6% NaOCl; Fisher Scientific). pH measurements were obtained with a Fisher Scientific model 60 pH meter coupled with a Thermo-Orion Ross PerpHect Combination Electrode.

Preparation of Experimental Solutions. Experimental solutions were prepared using reagent grade water containing 2 mM sodium bicarbonate buffer adjusted to the desired pH. Aliquots of stock solution were spiked into experimental solutions to obtain a desired concentration. After allowing 5 minutes for the solutions to equilibrate, the pH of each was adjusted to the desired pH. Solution pH was modified using sodium hydroxide and sulfuric acid. Sulfuric acid was used to minimize chloride addition since chloride ions shift the solution equilibrium from

HOCl towards Cl_2/H_2OCl^+ at low pH values thereby causing enhanced reaction rates (16). All experiments were performed at 25 ^oC.

Total oxidant consumption. Oxidant consumption experiments were performed using a quench flow system (QFS) similar to a design by Buffle et al. (Appendix A, Discussion A.1 and Figure A.1; ref. 58). By keeping the flow-rate of the QFS constant, we achieved highly accurate, short reaction times (ranging from 0.25-10 seconds) by simply changing the volume of each flow loop. Total oxidant concentrations (defined as the sum of the Cl_2, H_2OCl^+, HOCl, OCl^-, I_2, H_2OI^+, HOI, and OI^- concentrations) were determined using a modified DPD colorimetric method with photometric detection at 515 nm developed for use with the QFS (59). To promote pseudo-first order conditions, oxidant demand experiments were performed with phenol concentrations in 10× excess relative to the oxidant concentration. Following the reaction period, the final solution was mixed with DPD reagent and phosphate buffer to quench the reaction. The quenched solution then flowed through an additional flow loop to allow one minute for color development – at which time the solution was analyzed using a Cary5000 (Varian Inc.) UV-Vis-NIR spectrophotometer (λ = 515 nm) with a 1 cm pathlength flowcell. The absorbance of each solution was measured for each reaction time until the absorbance signal stabilized for a minimum of 30 seconds (Appendix A, Figure A.2). Total oxidant concentration was then determined using the average absorbance over the 30-second collection period in conjunction with a total oxidant calibration curve. All experiments were performed in at least duplicate to ensure the precision of the data. Results obtained with these replicate experiments show <1% deviation from one another (Appendix A, Figure A.3).

PPCP and Byproduct Analysis. Byproduct experiments were performed with a 10× excess of oxidant using both the QFS system and batch reactors (14). Following an allotted reaction period, the experimental solutions were mixed with a slight excess of sodium sulfite to quench the reaction. Sodium sulfite was chosen as the quenching agent because it is generally unreactive towards PPCPs and their daughter products (16). QFS solutions were collected in 40 mL amber vials. Products were extracted from solution and analyzed using GC-MS for phenolic byproducts and using GC-ECD for THMs. Detailed experimental methods are described elsewhere (14, 16). Compounds and byproducts were identified by m/z ratios of fragment ions from their GC chromatograms. Calibration curves were produced for phenol, 4-chlorophenol, 2,4-dichlorophenol, 2,4,6-trichlorophenol, 2,4,5,6-tetrachlorophenol, 4-iodophenol, 2,4,6-triiodophenol, 4-chloro-3-iodophenol, 4-bromophenol to assess product concentrations. However, standards for the remaining byproducts, including diiodophenol and phenols with multiple chlorine and iodide substitutions, were not available for purchase. As such, relative abundance (defined as the ratio of analyte peak area to that of the 1,3,5-tribromobenzene internal standard) of these compounds were determined.

Model Development. A computer model was developed using the chemical kinetics program MicroMath Scientist (Salt Lake City, UT) that can predict oxidant reactivity towards substituted phenols (Appendix B). Variables such as species concentration, pH, and temperature are assigned unique names. Differential equations and mass balances were developed that describe the chemical reactions for each reactant. The program utilizes differential equations that describe the dependence of reaction rates on temperature to calculate the specific rate constants for a given system. Using a sequential fitting approach, unknown rate parameters

were systematically determined. These equations were then used to write a computer program where each equation is solved for a given set of variables over a number of iterations. The model initially sets each variable to the value that is input by the user. Scientist then inputs the assigned values to an EPISODE numerical integration package to solve the set of simultaneous differential equations for the variables of interest. As the equations are solved, the input values are updated by the software following each iteration. By setting the model to perform a large number of iterations, it is able to make highly accurate predictions for complex chemical relationships over time (15, 60).

3.3: Results and Discussion

Oxidant consumption kinetics. For all tested phenolic compounds the kinetics of total oxidant loss were significantly enhanced in the presence of iodide. Figure 3.2 illustrates this behavior for 2,4-dichlorophenol. Similar results were obtained with other substituted phenols. Our initial discussion focuses exclusively on 2,4-dichlorophenol because it was studied the most extensively. The behavior of other substituted phenols will be discussed in a later section.

The electrophilic substitution of phenolic compounds commonly is described by second order kinetics; first-order in phenol and first-order in oxidant (1). The kinetic analysis can further be simplified by using a technique called flooding, in which the one reactant concentration is set to at least 10-fold that of the second reactant. This practice forces the concentration of the excess reactant to remain relatively constant so that the consumption of the limiting reactant over time is linear (i.e., first-order). The reaction rate constant can then be determined from the pseudo-first-order data. Studies have shown that both iodide and chlorine substitution reactions with phenols can be described as second order (1, 2). As such, initial experiments

were performed containing excess 2,4-dichlorophenol and a pseudo-first-order approximation was utilized to describe the reaction kinetics:

$$-\frac{d[\text{Total Oxidant}]}{dt} = k_{obs}[\text{Total Oxidant}] \quad (3.9)$$

where [Total Oxidant] reflects the combined concentrations of free chlorine (= [HOCl] + [OCl^-] + [H_2OCl^+] + [Cl_2]) and free iodine (= [HOI] + [I_2] + [OI^-] + [I_3^-] + [H_2OI^-] + [HOI_2^-]) measured using the DPD-FAS colorimetric method, and k_{obs} is the product of the reaction rate and the initial 2,4-dichlorophenol concentration. In addition to simplifying the reaction analysis, the utilization of excess phenol ensures that the measured rates only reflect a single halogenation event (49).

To facilitate comparisons between our results and observed rate constants from the literature (1, 2, 18, 61), apparent second-order rate constants ($k_{app} = k_{obs}/[\text{Total Phenol}]_i$, $M^{-1}s^{-1}$) were calculated. The use of k_{app} normalizes experimentally determined k_{obs} values by dividing each observed rate constant by the initial phenol concentration. This normalization enables direct comparisons between rates obtained under different experimental conditions. Our k_{app} values for 2,4-dichlorophenol are plotted versus solution pH as shown in Figure 3.3. Experiments show that both free chlorine and free iodine readily react with 2,4-dichlorophenol and that the kinetics are a function of the solution pH as well as the iodide to free chlorine ratio. Based upon comparison of the relative k_{app} values, the free iodine mediated reactions are generally 10× faster than reactions with free chlorine at circumneutral pH and the observed rates with iodine are more than twice those for free chlorine at the pH extremes. Control experiments were run to eliminate the possibility that other reactions could result in these observations. The oxidants were stable when 2,4-DCP was not present (Figure 3.2) and 2,4-DCP was stable

when free chlorine was absent (results not shown), thus indicating that the behavior was not the result of an oxidant demand exerted by the QFS tubing.

Previous studies examining *p*-methoxyphenol, *p*-cresol, phenol, *p*-chlorophenol, *p*-iodophenol, and *p*-cyanophenol reactivity in free iodine solutions suggest that the kinetic behavior as a function of pH can be explained by three reactions (28):

$$H_2OI^+ + PhOH \xrightarrow{k_{3.10}} \text{products} \quad (3.10)$$

$$HOI + PhOH \xrightarrow{k_{3.11}} \text{products} \quad (3.11)$$

$$HOI + PhO^- \xrightarrow{k_{3.12}} \text{products} \quad (3.12)$$

where PhOH and PhO^- reflect the neutral and negatively charged forms of a given phenolic compound, respectively. Rate constants reported in the literature for the electrophilic substitution of substituted phenols suggest that $k_{3.12}$ is generally four orders of magnitude larger than that for reaction 3.11 and two orders of magnitude larger than that for reaction 3.10. Althhough 2,4-dichlorophenol was not included in the study mentioned above values of $k_{3.12}$ are reported at magnitudes ranging from 10^5-10^8 for substituted phenols (2). These trends reflect that HOI is a weaker oxidant than H_2OI^+ and that PhO^- is considerably more reactive than PhOH. The decreased reactivity of HOI relative to H_2OI^+ is expected due to its lower electrophilic character and the increased reactivity of PhO^- is the result of a stronger electron donating effect for the phenolate form of phenols because of their negative charge. At face value, our 2,4-dichlorophenol results seem to be consistent with this model since our reaction rates increase as the concentration of the phenolate form of 2,4-DCP increases. The experimentally determined apparent reaction rates increase as solution pH is raised from 5 to 7.5, as would be expected if reaction 3.12 dominates the overall kinetics. However, upon close

inspection a major discrepancy is evident. If reaction 3.12 was indeed controlling the observed kinetics, the maximum apparent reaction rate would occur around a pH of 9.24 because it coincides with the highest simultaneous concentrations of HOI and PhO^-. However, our experimental results exhibit the greatest observed reactivity at a pH of 7.5. The discrepancy results from the fact that prior studies did not address the potential for I_2 mediated reactions to occur. Historically, thermodynamic analyses led to the belief that H_2OI^+ was the rate controlling reactive iodinated electrophile at low pH (61, 62). Recent studies have shown, however, that I_2 is actually the active agent under acidic conditions and must be included in any analysis of iodine-species reactivity (38, 55), while H_2OI^+ is "without any relevance under the conditions occurring in practice" (38). The study suggesting the reaction mechanism summarized by equations 3.10-3.12 analyzed six different phenolic compounds, only one of which had a pK_a less than 9, and their experimental pH range never exceeded 8.6 (2). By performing a simple evaluation on the speciation of free iodide, several conclusions can be drawn. The pK_a of the H_2OI^+-HOI equilibrium, as reported by Bichsel and von Gunten, is 1.4 and the pK_a of the $HOI\text{-}OI^-$ equilibrium is 10.4 (2). If the rate controlling reaction at circumneutral pH is between HOI and PhO^- for phenolic compounds, then the maximum observed reaction rate should occur at a pH half way between the pK_a of the phenolic compound and the pK_a of the $HOI\text{-}OI^-$ equilibrium. Since the reaction is "first-order in phenol and first-order in HOI (2)", the maximum reaction rate should occur at the pH where the concentrations of both species are simultaneously maximized (i.e., half-way between the respective pK_a values). Because the experiments were not conducted at pH values exceeding the pK_a value of any compound, there was no way to tell if the maximum reaction rate did occur at the suspected pH. For our experiments, the

maximum reaction rate of 2,4-dichlorophenol and HOI should have occurred at a pH of 9.1 if this were in fact the rate controlling reaction, but the maximum rate occurred at a pH of 7.5 suggesting that this conclusion was incorrect. Instead, if I_2 was the active species at low pH instead of H_2OI^+, the maximum apparent reaction rate should occur half way between pH 7.2 (below which I_2 is the prevailing iodinated oxidant) and pH 7.85 (above which PhO^- dominates in the case of 2,4-dichlorophenol) since the simultaneous concentrations of both would be maximized. The resulting maximum reaction rate would theoretically occur around a pH of 7.5, which closely matches the maximum pH observed in our experiments.

Iodide hydrolysis. An in-depth analysis of iodine speciation was deemed necessary to fully understand free iodine/free chlorine reactivity towards 2,4-dichlorophenol. The speciation of free chlorine and its reaction with I^- are described by equations 3.1-3.2 (Table 3.1) and equation 3.8, respectively. The behavior of iodine-containing species is described by equations 3.3-3.7 (Table 3.1). The speciation of free iodine (i.e., total reactive iodine) as HOI, H_2OI^+, I^-, I_2, I_3^-, OI^-, and HOI_2^- is pH dependant. A speciation model was developed (Figure 3.4) similar to ones described in the literature (35, 38, 40, 41) that predicts the pH-dependant distribution of chlorinated and iodinated species at any given time using equations 3.1-3.8. Because the rate of I^- oxidation by free chlorine is extremely fast, the solution reaches steady state within seconds. I_2 is the most prevalent iodinated species below pH 7.25, while HOI predominates at higher pH values. OI^- makes up less than 10% of the total iodinated oxidant until the pH exceeds 9.75. From pH 0 to 14, all other species combined account for less than 1% of total reactive iodine. In the case of H_2OI^+, the maximum concentration obtained was on the order of 10^{-7} μM. To compete with reactions involving I_2 or HOI, which have concentrations as high as 5-

10 μM, rate constants for H_2OI^+ would need to be at least 7 orders of magnitude larger than the rate constant for the most abundant species if H_2OI^+ is to affect the overall reactivity at a given pH. If two compounds react immediately when they come into contact, the observed reaction kinetics are limited by the diffusion controlled rate constant, which describes reaction rates limited only by the maximum speed they can move through solution and interact. In water, that rate is 7.4×10^9 $M^{-1}s^{-1}$ (63). If H_2OI^+ reaction rates must automatically be 10^7 larger than the reactivity of the predominant species in acidic conditions, which the speciation model concludes will be I_2, then the reaction rate constant of I_2 with a phenolic compound would have to be below a value of 10^2 $M^{-1}s^{-1}$ in order for the H_2OI^+ reaction to be seven orders of magnitude larger than the I_2 rate without exceeding the diffusion controlled rate limit. Since I_2 is known to be a relatively reactive species, it follows that there is very little chance that H_2OI^+ reactions will be important to the overall reactivity.

In addition to reactions with phenolic compounds, it was also considered that the pH dependant behavior of total oxidant loss could be the result of other interactions. One potential loss pathway would be the result of oxidant demand reactions exerted by the QFS system. However, as noted previously, negligible oxidant demand was detected in the absence of reactive phenol. Another explanation for total oxidant loss is that it is a result of the disproportionation of HOI (reactions 3.13-3.15) or the oxidation of HOI by excess HOCl (reaction 3.16), both of which form iodate (IO_3^-) as an end product (53).

$$HOI + HOI \xrightarrow{k_{3.13}} IO_2^- + 2H^+ + I^- \qquad k_{3.13} = 0.3\ M^{-1}s^{-1} \qquad (3.13)$$

$$HOI + OI^- \xrightarrow{k_{3.14}} IO_2^- + H^+ + I^- \qquad k_{3.14} = 15\ M^{-1}s^{-1} \qquad (3.14)$$

$$IO_2^- + HOI \xrightarrow{\text{fast}} IO_3^- + H^+ + I^- \qquad (3.15)$$

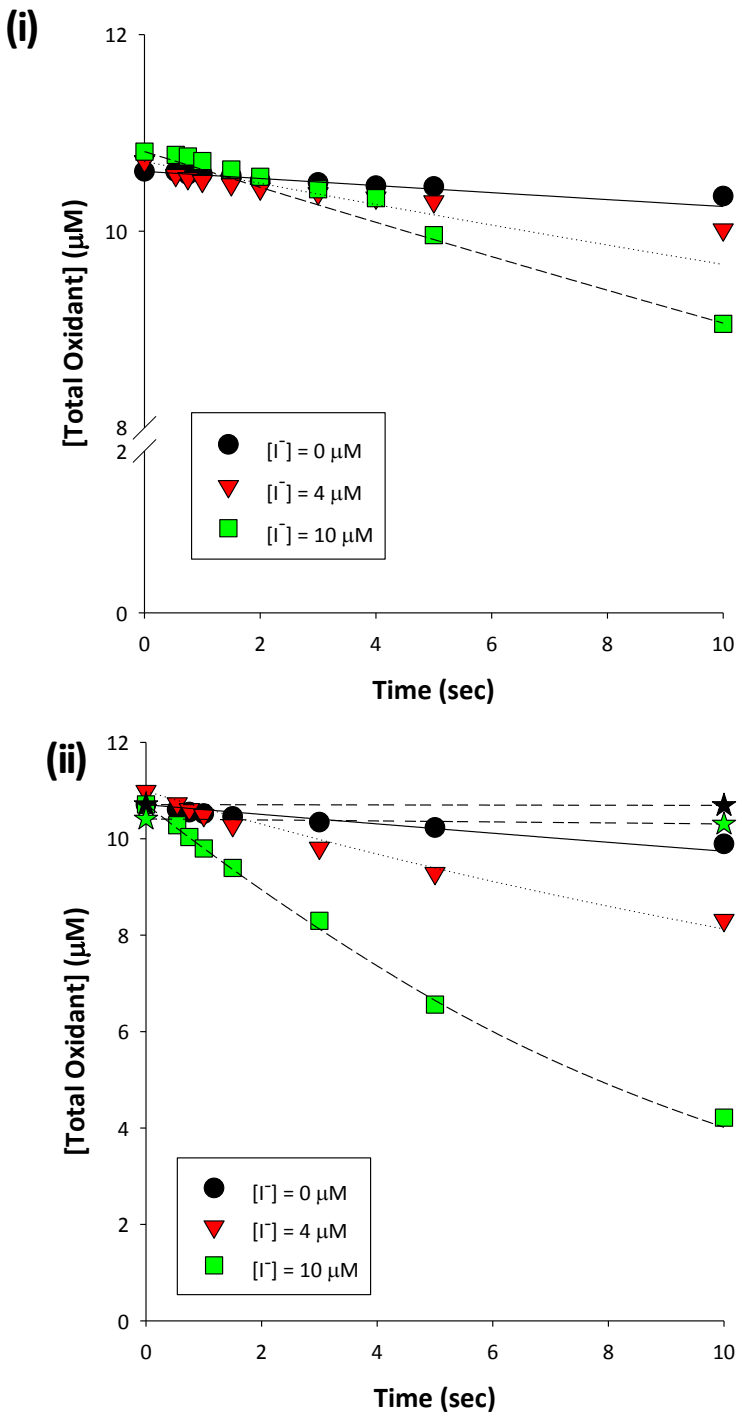

Figure 3.2: Total oxidant loss resulting from reactions with 2,4-dichlorophenol in the presence of iodide. Curves are model predictions. Star symbols represent controls with no 2,4-DCP present. Standard errors for individual points are <0.1%. Conditions: [Total oxidant]$_i$ = 10.6-10.9 μM, [2,4-DCP]$_i$ = 100 μM, [$NaHCO_3$] = 2 mM, pH = 6.0 (i) and 8.0 (ii).

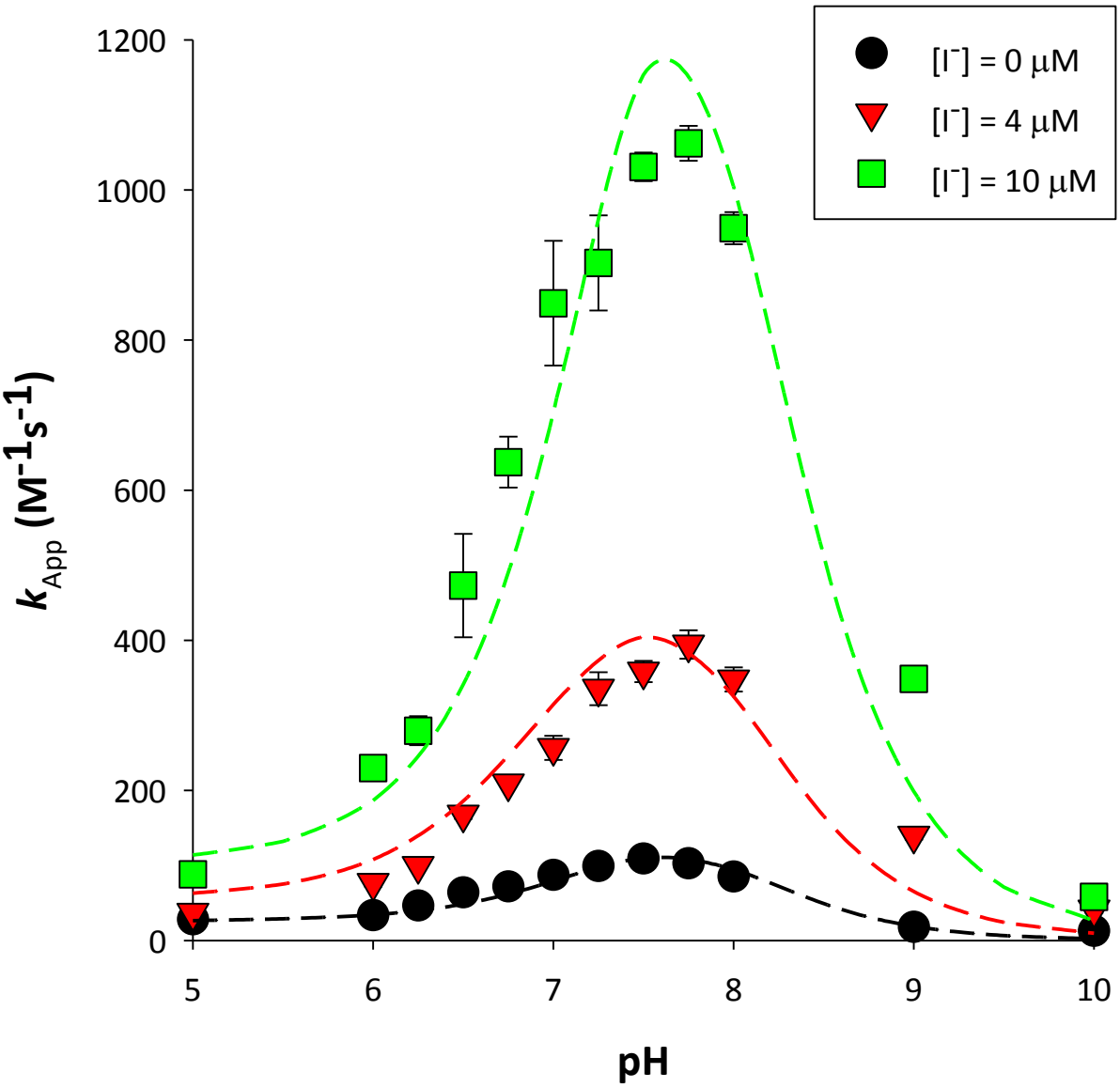

Figure 3.3: Experimental (points) and model-predicted (curves) apparent second-order reaction rate constants between pH of 5 to 10 with variable levels of iodide. Conditions: [Total Oxidant]$_i$ = 10.4-12.0 μM, [2,4-DCP]$_i$ = 100 μM, [$NaHCO_3$] = 2 mM. Error bars represent 95% confidence intervals.

$$\mathrm{HOI + HOCl + HOCl \xrightarrow{k_{3.16}} IO_3^- + 3H^+ + 2Cl^-} \qquad k_{3.16} = 8.3\times10^4\ \mathrm{M^{-2}s^{-1}} \tag{3.16}$$

Iodate is stable and non-reactive, making it a desirable sink for iodine during treatment processes because iodinated DBP formation potentials are reduced (56). However, for HOCl and I^- concentrations typical of drinking water treatment, the half-life of I^- is on the order of milliseconds (31), so under conditions where free chlorine is in excess, iodide is immediately and completely converted to HOI, which then equilibrates with the other free iodine species. The half-life of the HOI disproportionation reaction is on the order of ≈4 days (31) and the half-life of chlorine-mediated HOI oxidation is on the order of hours (56). Therefore, disproportionation and oxidation reactions are of little importance relative to the electrophilic substitution of phenols by free iodine since free iodine-phenol reactions have a half-life on the order of seconds. To ensure that iodate was an inconsequential iodide sink during our experiments, experimental solutions containing free chlorine and I^- were mixed for a period of only 20 seconds prior to initiating the reactions with phenols. This 20-second contact time is sufficient to ensure that iodide reached equilibrium with free chlorine and was present only as free iodine (i.e., H_2OI^+, I_2, I_3^-, HOI, OI^-, and HOI_2^-) or I^- but is not long enough for IO_3^- to form.

Modeling results. Because of the discrepancies between our results, the speciation analysis, and the mechanisms suggested in literature, a more comprehensive kinetic analysis was deemed necessary. To evaluate the oxidant consumption data, a model was developed using the Micromath Scientist software described previously. This computer model was designed to determine reaction rate constants using a sequential fitting approach where each parameter was systematically determined over a range of pH values. Inputs to the model included multiple pH values and variable initial free chlorine, iodide, and phenol concentrations.

Equations were included describing the relationships listed in Table 3.1 as well as the equilibrium relationship for 2,4-dichlorophenol speciation. Reactions describing each potential electrophilic substitution reaction are listed below.

$$Cl_2 + PhOH \xrightarrow{k_{3.17}} products + Cl^- \quad (3.17)$$

$$Cl_2 + PhO^- \xrightarrow{k_{3.18}} products + Cl^- \quad (3.18)$$

$$H_2OCl^+ + PhOH \xrightarrow{k_{3.19}} products \quad (3.19)$$

$$H_2OCl^+ + PhO^- \xrightarrow{k_{3.20}} products \quad (3.20)$$

$$HOCl + PhOH \xrightarrow{k_{3.21}} products \quad (3.21)$$

$$HOCl + PhO^- \xrightarrow{k_{3.22}} products \quad (3.22)$$

$$OCl^- + PhOH \xrightarrow{k_{3.23}} products \quad (3.23)$$

$$OCl^- + PhO^- \xrightarrow{k_{3.24}} products \quad (3.24)$$

$$I_2 + PhOH \xrightarrow{k_{3.25}} products + I^- \quad (3.25)$$

$$I_2 + PhO^- \xrightarrow{k_{3.26}} products + I^- \quad (3.26)$$

$$H_2OI^+ + PhOH \xrightarrow{k_{3.27}} products \quad (3.27)$$

$$H_2OI^+ + PhO^- \xrightarrow{k_{3.28}} products \quad (3.28)$$

$$HOI + PhOH \xrightarrow{k_{3.29}} products \quad (3.29)$$

$$HOI + PhO^- \xrightarrow{k_{3.30}} products \quad (3.30)$$

$$OI^- + PhOH \xrightarrow{k_{3.31}} products \quad (3.31)$$

$$OI^- + PhO^- \xrightarrow{k_{3.32}} products \quad (3.32)$$

$$HOI_2^- + PhOH \xrightarrow{k_{3.33}} \text{products} + I^- \quad (3.33)$$

$$HOI_2^- + PhO^- \xrightarrow{k_{3.34}} \text{products} + I^- \quad (3.34)$$

$$I_3^- + PhOH \xrightarrow{k_{3.35}} \text{products} + 2 \cdot I^- \quad (3.35)$$

$$I_3^- + PhO^- \xrightarrow{k_{3.36}} \text{products} + 2 \cdot I^- \quad (3.36)$$

Under excess 2,4-dichlorophenol conditions, the primary 'product' formed will be 2,4,6-trichlorophenol. The model was initially fit to experimental data obtained in the absence of iodide (Reactions 3.17-3.24). Results from previously published phenol chlorination studies have contradicting conclusions – some suggest that the mechanism controlling chlorination of 2,4-dichlorophenol is the reaction between HOCl and phenolate-2,4-DCP (reaction 3.22; refs. 1, 18), while another suggests reactions involving H_2OCl^+ (reactions 3.19-3.20) may be important (1), and a third concludes that Cl_2 (reactions 3.17-3.18) was responsible rather than H_2OCl^+ (29). To avoid bias and to test the capabilities of the model, differential equations describing total free chlorine loss were written to include both 2,4-DCP and phenolate- 2,4-DCP reactions with each of the four potential chlorine species:

$$\frac{d[\text{free chlorine}]}{dt} = -(k_{3.17}[Cl_2] + k_{3.19}[H_2OCl^+] + k_{3.21}[HOCl] + k_{3.23}[OCl^-])[PhOH]$$
$$-(k_{3.18}[Cl_2] + k_{3.20}[H_2OCl^+] + k_{3.22}[HOCl] + k_{3.24}[OCl^-])[PhO^-] \quad (3.37)$$

Rate constants for each of the 8 equations were initially determined by fitting six data sets obtained from experiments conducted at pH 5, 6, 7, 8, 9, and 10. The model rate constants were sequentially fit to oxidant consumption data collected at the pH values for which each respective reaction is most influential towards the total reactivity (a detailed description of the model fitting approach is included in Appendix B). Overall model fits were assessed while

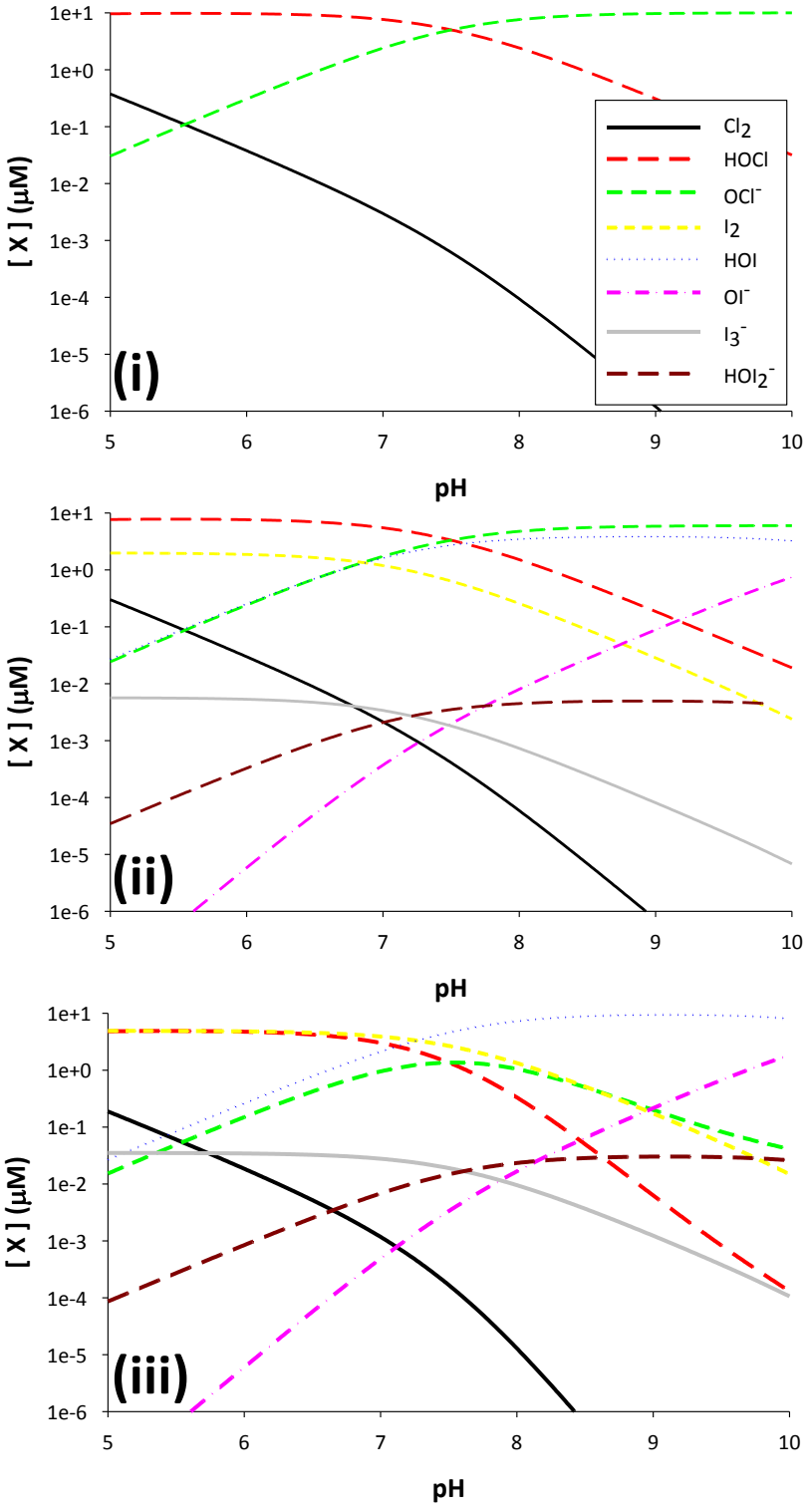

Figure 3.4: Oxidant speciation from pH 5 to 10 for 10 µM total oxidant when $[I^-]$ = 0 (i), 4 (ii), and 10 (iii) µM. H_2OI^+ concentrations never exceeded the 10^{-7} µM.

sequentially omitting reactions to determine the importance of each rate parameter. This approach enabled us to determine the importance of each individual reaction with respect to the overall numerical solution. These training sets identified the reactions most likely responsible for oxidant consumption and increased the precision of each reaction rate constant. Through this process, it was determined that free chlorine consumption in the presence of 2,4-dichlorophenol is described as follows:

$$-\frac{d[\text{free chlorine}]}{dt} = \frac{d[\text{Total DCP}]}{dt} = k_{3.21}[\text{HOCl}][\text{PhOH}] + k_{3.22}[\text{HOCl}][\text{PhO}^-] \quad (3.38)$$

where $k_{3.21}$ and $k_{3.22}$ were found to equal 26 (± 13) and 660 (± 130) $M^{-1}s^{-1}$, respectively. Upon relating this expression to equation 3.9, the apparent rate constant can be described as:

$$k_{\text{Cl,app}} = \left(k_{3.21} \cdot f_{\text{PhOH}} + k_{3.22} \cdot (1 - f_{\text{PhO}^-})\right) \cdot f_{\text{HOCl}} \quad (3.39)$$

with f_{PhOH} representing the fraction of 2,4-dichlorophenol in the neutral form and f_{HOCl} representing the fraction of free chlorine as HOCl.

To assess the model capabilities, it was used to predict solution reactivity for six additional solutions at pH values ranging from 5 to 10 (pH 6.25, 6.5, 6.75, 7.25, 7.5, and 7.75). The model results were compared to these "validation" data sets to assess the accuracy of the fitted rate constants. Overall, the model was able to predict oxidant consumption rates quite accurately for both the initial "training" data and the "validation" data (Figures 3.2-3.3).

A 1962 study suggests that the electrophilic substitution of a range of phenolic compounds, including 2,4-dichlorophenol, can be described simply by the reaction between HOCl and the PhO^- species (reaction 3.22; ref. 18). Using the results from the 1962 study, Gallard and von Gunten calculated second-order rate constants for several phenolic species, and determined a value for $k_{3.22}$ of 303 $M^{-1}s^{1-}$ for 2,4-dichlorophenol (1). In addition, Gallard and von Gunten

reassessed the reaction mechanism for several of the phenols, including unsubstituted phenol and 4-chlorophenol, discussed in the 1962 paper by performing additional experimentsand suggested that H_2OCl^+-PhOH and HOCl-PhOH reactions should also be considered (1). In each case, Gallard and von Gunten's new values for $k_{3.22}$ were different from what they calculated when using data from the 1962 study. Unfortunately, 2,4-dichlorophenol was not amongst the compounds that Gallard and von Gunten reassessed. Because 2,4-dichlorophenol was not reassessed during the study, a question is raised about the validity of the value for $k_{3.22}$ of 303 $M^{-1}s^{-1}$. As such, we expect some discrepancies between the value for $k_{3.22}$ determined in this study and that estimated by Gallard and von Gunten. Our value for $k_{3.22}$ is higher than the literature value but is of the same order of magnitude, thereby suggesting to some extent that our value is reasonable.

Contrary to what is currently reported in literature, this modeling exercise determined that neither H_2OCl^+ nor Cl_2 had a determinable effect on the observed reaction rate within our tested pH range. The speciation model illustrates that H_2OCl^+ was present at concentrations at least 5 orders of magnitude below that of HOCl at all tested pH values. Accordingly, were reactions involving H_2OCl^+ important they would require rate constants that approach the value for diffusion limited reactions (7.4×10^9 $M^{-1}s^{-1}$; ref. 63) to have a discernable influence on the overall reactivity, which is unlikely. The Cl_2 species makes up nearly 4% of total free chlorine at a pH of 5, however, inclusion of Cl_2 mediated electrophilic substitution reactions (i.e., non-zero $k_{3.17}$ and $k_{3.18}$) led to an overestimation of total oxidant loss and thus these terms were set to zero. However, Cl_2 is known to be highly reactive, so it is suspected that if the experimental solution pH were reduced below 5, non-zero values for $k_{3.17}$ and $k_{3.18}$ would be

measured. Significant amounts of OCl^- were present in the more basic solutions, but the model overestimated the kinetics of oxidant loss in these solutions if the rate constants for OCl^--mediated reactions with 2,4-DCP were set to anything other than zero. It is well established that rate constants for HOCl-PhO^- are much higher and would overshadow any possible OCl^- effects at pH values where the OCl^--PhOH reaction could be important.

The modeling procedure outlined above was replicated to determine rate constants for the free iodine reactions using experimental data collected with 10 μM of iodide present initially. As determined by the speciation model, free chlorine can still be present under these conditions so the iodine model includes the code for the chlorine model, though the free chlorine reaction rate constants were fixed to the previously determined values. Differential equations describing iodide and total free iodine concentration changes were developed as follows:

$$\frac{d[\mathrm{I}^-]}{dt} = -k_{3.8}[\mathrm{HOCl}][\mathrm{I}^-] + (k_{3.25}[\mathrm{I_2}] + k_{3.33}[\mathrm{HOI_2^-}] + 2k_{3.35}[\mathrm{I_3^-}])[\mathrm{PhOH}] + (k_{3.26}[\mathrm{I_2}] + k_{3.34}[\mathrm{HOI_2^-}] + 2k_{3.36}[\mathrm{I_3^-}])[\mathrm{PhO^-}] \quad (3.40)$$

$$\frac{d[\text{free iodine}]}{dt} = k_{3.8}[\mathrm{HOCl}][\mathrm{I}^-] - (k_{3.25}[\mathrm{I_2}] + k_{3.27}[\mathrm{H_2OI^+}] + k_{3.29}[\mathrm{HOI}] + k_{3.31}[\mathrm{OI^-}] + k_{3.33}[\mathrm{HOI_2^-}] + k_{3.35}[\mathrm{I_3^-}])[\mathrm{PhOH}] - (k_{3.26}[\mathrm{I_2}] + k_{3.28}[\mathrm{H_2OI^+}] + k_{3.30}[\mathrm{HOI}] + k_{3.32}[\mathrm{OI^-}] + k_{3.34}[\mathrm{HOI_2^-}] + k_{3.36}[\mathrm{I_3^-}])[\mathrm{PhO^-}] \quad (3.41)$$

Phenol substitution results in a single halide substitution on the ring structure. When species containing multiple iodine atoms react with phenol (i.e., I_2, HOI_2^-, and I_3^-), the released I^- can be oxidized by HOCl (equation 3.8). To account for this, each differential equation (including the

free chlorine equation from above) was modified to account for subsequent HOCl-iodide reactions to form HOI. As before, the sequential fitting procedure was repeated for rate constants of each possible reaction at pH values where the kinetics are maximized for that species while systematically omitting reactions until an optimal fit was achieved. The modeling exercise concluded that the change in the total iodine concentration can be described as follows:

$$\frac{d[\text{free iodine}]}{dt} = \frac{d[\text{Total DCP}]}{dt} = k_{3.8}[\text{HOCl}][\text{I}^-] - k_{3.25}[\text{I}_2][\text{PhOH}]$$

$$-(k_{3.26}[\text{I}_2] + k_{3.28}[\text{HOCl}])[\text{PhO}^-] \qquad (3.42)$$

where $k_{3.25}$, $k_{3.26}$, and $k_{3.28}$ were determined to be 240 (± 73), 1.0 (± 0.26) × 10^4, and 650 (± 150) $M^{-1}s^{-1}$, respectively. The apparent rate constant for free iodine reactions can be defined as:

$$k_{\text{I,app}} = \left(k_{3.25} \cdot f_{\text{PhOH}} + k_{3.26} \cdot (1 - f_{\text{PhO}^-})\right) \cdot f_{\text{I}_2} + k_{3.27} \cdot f_{\text{HOI}} \cdot (1 - f_{\text{PhO}^-}) \qquad (3.43)$$

The overall apparent rate constant accounting for both free chlorine and free iodide is:

$$k_{\text{Tot,app}} = k_{\text{Cl,app}} \cdot f_{\text{Cl/TOTOX}} + k_{\text{I,app}} \cdot f_{\text{I/TOTOX}} \qquad (3.44)$$

where $f_{\text{Cl/TOTOX}}$ and $f_{\text{I/TOTOX}}$ are defined as the fraction of total oxidant as free chlorine and free iodine, respectively. The validity of the fitted rate constants was again tested using the "validation" data sets. As a whole, the model was able to accurately predict oxidant loss over the entire pH range, and this was only the case when each of the reactions listed in Table 3.2 were included. The resulting program was able to predict model oxidant consumption rates to within 1-5% of experimentally measured concentrations for all data sets, further supporting the validity of the fitted rate constants (Table 3.2). The curves plotted on Figures 3.1-3.2 show the

final model predictions. Literature values are not available for iodine substitution to 2,4-dichlorophenol so no comparisons of reaction rate constants are possible.

The modeling results suggest that the reaction mechanism in free chlorine/iodide systems differs from that previously reported. Primarily, the differences involve changes in the oxidant species included in the rate determining reaction as a result of a thorough speciation analysis. The free chlorine mediated reactions include those described by equations 3.21-3.22, while iodide reactions include equations 3.25-3.26 and 3.28. To evaluate the applicability of the model under additional reaction conditions, we examined its capabilities using data from experiments with an iodide concentration of 4 μM. The model predictions fit the experimental data well (Figure 3.2) and the calculated k_{app} values reflect the trends in the experimental data (Figure 3.3). Once again, the calculated apparent reaction rates were able to predict the experimentally measured rates very closely, further supporting the model validity.

Additional experiments were performed at pH 7 with 10 μM of total initial oxidant and excess 2,4-dichlorophenol, where initial iodide concentrations of 1, 7, 15, and 25 μM were examined (Figure 3.5). This concentration variation was undertaken to test the constraints of the model and it was able to accurately predict oxidant loss for all data sets up to an iodide concentration of 10 μM. However, model predictions underestimated reaction rates for data sets obtained when iodide concentrations were greater than 10 μM (Figure 3.4). The speciation model was run for total iodide concentrations of 15 and 25 μM and found that the total oxidant was present completely as free iodine at pH 7. The slight increase in the kinetic model predictions between the 15 and 25 μM I^- runs was due to a slight shift it speciation towards I_2 as iodide

Table 3.2: Pertinent second-order reactions and their fitted rate constants for the oxidation of 2,4-dichlorophenol. Error reported as 95% confidence intervals.

	Reaction	k_{DCP} ($M^{-1}s^{-1}$)
3.21	$HOCl + PhOH \xrightarrow{k_{3.21}} products$	$2.6 (\pm 1.3) \times 10^{1}$
3.22	$HOCl + PhO^{-} \xrightarrow{k_{3.22}} products$	$6.6 (\pm 1.3) \times 10^{2}$
3.25	$I_2 + PhOH \xrightarrow{k_{3.25}} products + I^{-}$	$2.4 (\pm 0.7) \times 10^{2}$
3.26	$I_2 + PhO^{-} \xrightarrow{k_{3.26}} products + I^{-}$	$1.0 (\pm 0.3) \times 10^{4}$
3.28	$HOI + PhO^{-} \xrightarrow{k_{3.28}} products$	$6.5 (\pm 1.5) \times 10^{2}$

concentrations increased, but the speciation model did not provide any insight as to why it under-predicted the experimental results. It is hypothesized that while ICl is typically a short-lived intermediate during oxidation of iodide by HOCl, it may be present under conditions when iodide is in excess. To validate this theory, additional experiments would need to be performed. For the purposes of this study, since iodide would be in excess of free chlorine during drinking treatment only in extreme cases, further investigation was deemed unnecessary.

2,4-dichlorophenol consumption. Experiments were performed at pH 7.0 with 10 μM of initial 2,4-dichlorophenol, 20 μM of initial free chlorine, and initial iodide concentrations of 0 and 10 μM to assess the ability of the model to predict phenol loss over time. The model was run using the rate constants obtained from the previous modeling exercise and the initial oxidant and phenol concentrations for the new reaction conditions. The resulting predictions fit the observed experimental data quite well (Figure3.6-i). The accurate model predictions for 2,4-dichlorophenol loss further support the validity of the model's fitting capabilities.

Reactivity of other phenolic compounds. Experiments were performed in which total oxidant concentrations were measured over time in pH 7 solutions containing iodide concentrations of 0 and 10 μM for unsubstituted phenol, 4-chlorophenol, 4-iodophenol, and 2,4,6-trichlorophenol (Figure 3.6). The data was then used to calculate apparent reaction rates for each compound (1, 2) and these were compared to apparent rate constants calculated for pH 7 using rate constants from the literature (Table 3.3). The apparent rate constant for free chlorine and free iodine reactions for 2,4,6-trichlorophenol were determined to be 1.4 and 13.8

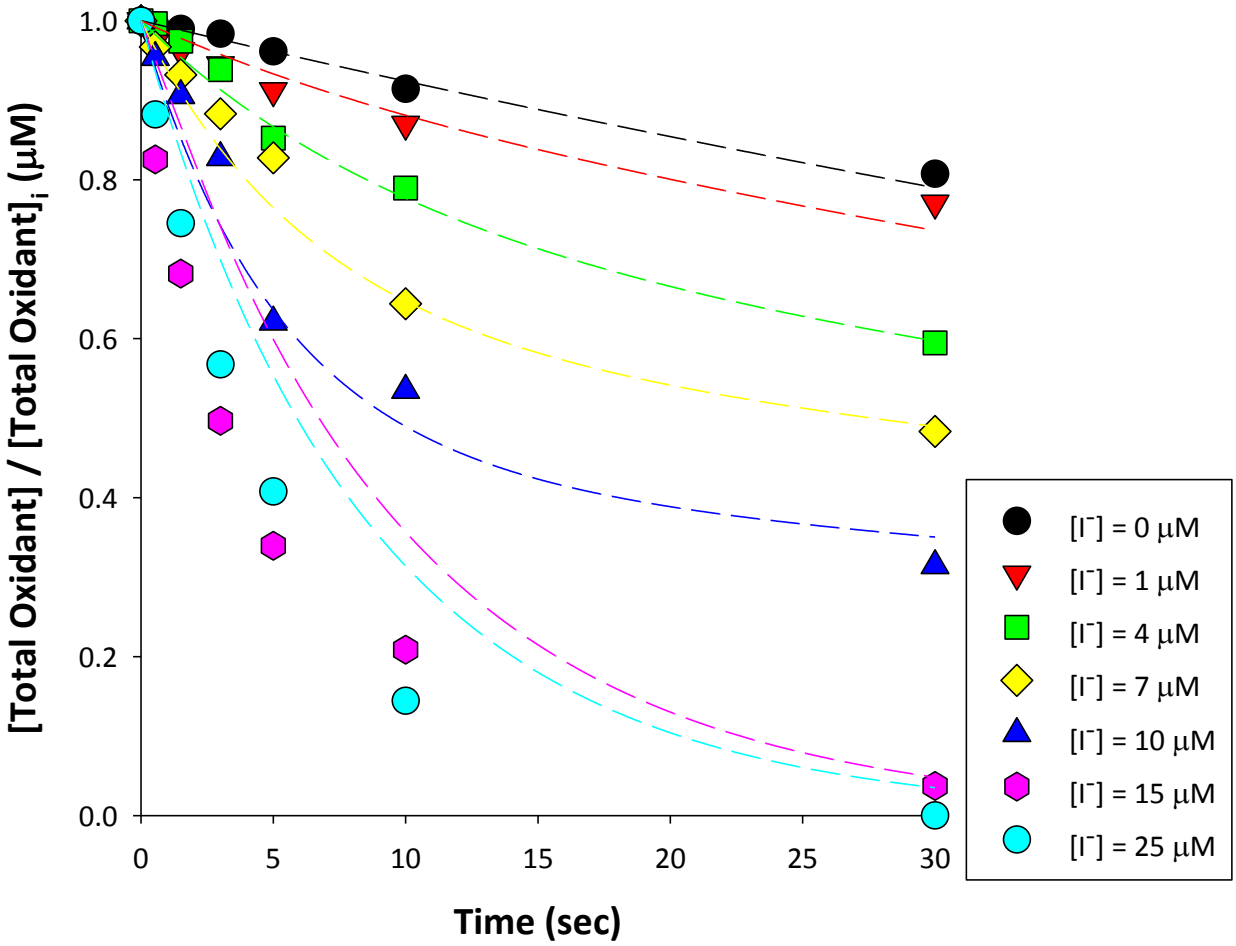

Figure 3.5: The effect of iodide concentration on oxidant consumption over time in the presence of 2,4-dichlorophenol. Conditions: pH = 7, $[2,4\text{-DCP}]_i$ = 100 μM, $[NaHCO_3]$ = 2 mM.

$M^{-1}s^{-1}$ (data shown in Figure 3.6) but were not included in this analysis because comparable apparent rate constants could not be found in the literature. The values for k_{app} from the literature for unsubstituted phenol, 4-chlorophenol, 4-iodophenol, and 2,4,6-trichlorophenol compare very well with those from this study. However, because of the noted inconsistencies in the reaction mechanism developed for 2,4-dichlorophenol reactivity detailed herein and that presented in the literature, we re-evaluated the data obtained in the previous studies. The k_{App} values obtained from the previous studies were used to produce theoretical oxidant consumption data for reaction times ranging from 0 to 10 seconds over a pH range corresponding to the range reported in each study. The theoretical oxidant data was calculated simply by plugging each value for k_{App} into the following equation:

$$[\text{total oxidant}]_t = [\text{total oxidant}]_i \cdot e^{-k_{App} \cdot [\text{total phenol}]_i \cdot t} \quad (3.45)$$

where $[\text{total oxidant}]_i$ = 10 μM and $[\text{total phenol}]_i$ = 100 μM.

Because the k_{App} values from the literature were shown to successfully predict the original apparent rate constant data from the corresponding study and also matched well with the limited experiments run in our study, they can be used to simulate oxidant demand data for variable starting concentrations of oxidant and phenol as a function of time. This should be the case even if the actual reaction mechanism differs from the mechanism determined in this study since the original experimental data was successfully modeled. The pH range used to reassess the data was between 5 and 10 for free chlorine electrophilic substitution reactions. For the iodination calculations, oxidant consumption was determined for pH 5 to between 7.5 and 8.5 to represent the range employed in the original study (2).

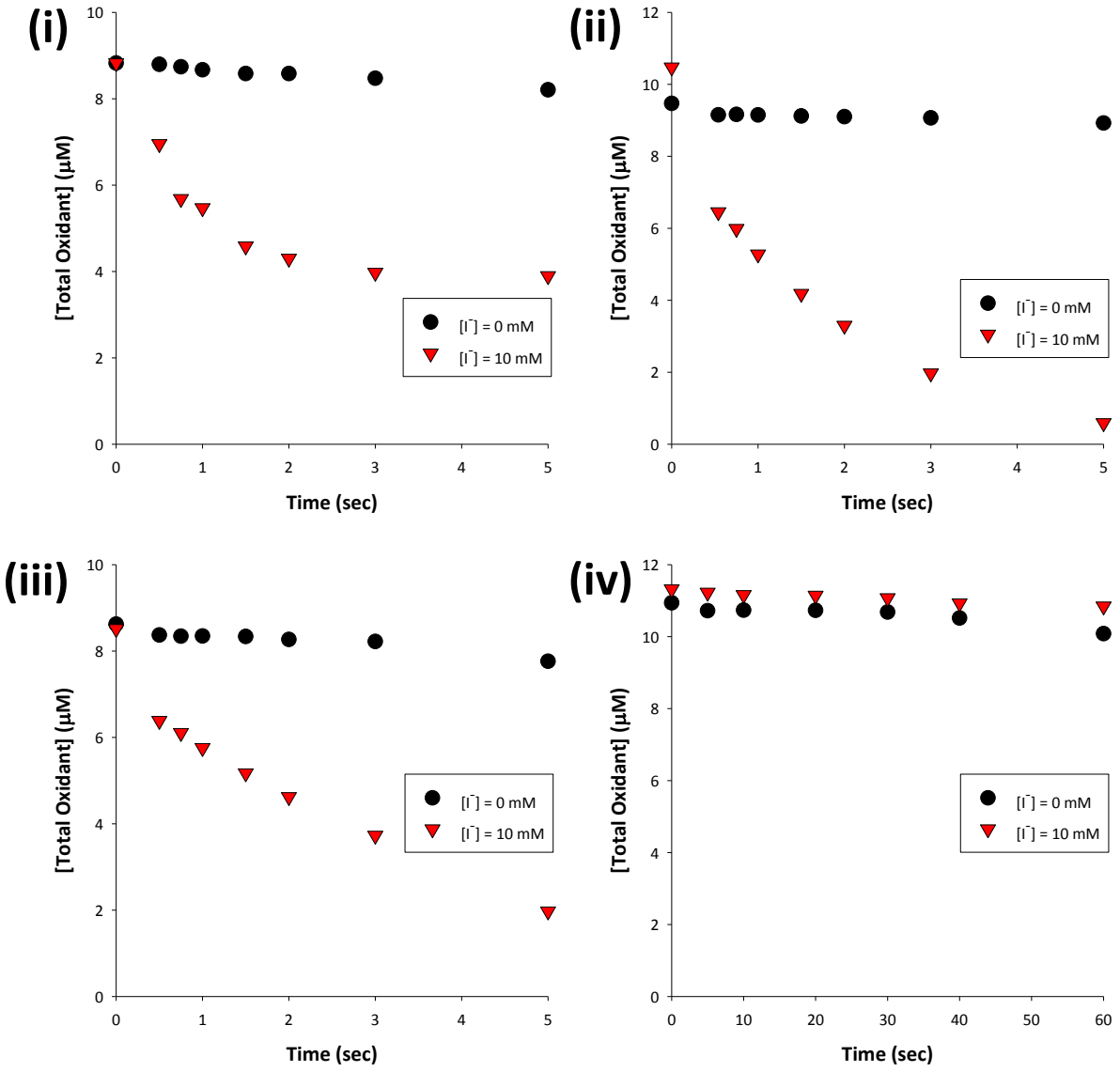

Figure 3.6: Plots of total oxidant versus time for (i) unsubstituted phenol, (ii) 4-chlorophenol, (iii) 4-iodophenol, and (iv) 2,4,6-trichlorophenol in the presence of 0 and 10 μM iodidne. Error is less than 0.2% for all data points. Conditions: pH = 7.0, $[phenol]_i$ = 10 μM (except for unsubstituted which contained 5 μM), $[total\ oxidant]_i$ = 8.5-11.3 μM, $[NaHCO_3]$ = 2 mM.

Table 3.3: Comparison between apparent rate constants of phenol, 4-chlorophenol, and 4-iodophenol calculated from experimental data in this study (experimental) and the apparent rate constants calculated from Gallard and von Gunten (2002) and Bichsel and von Gunten (2000).

compound	$k_{app,\ free\ chlorine}$ ($M^{-1}s^{-1}$)		$k_{app,\ free\ iodine}$ ($M^{-1}s^{-1}$)	
	(experimental)	(Gallard)	(experimental)	(Bichsel)
phenol	1.5 (± 0.6) × 10^1	1.8 (± 0.1) × 10^1	1.5 (± 0.2) × 10^3	2.1 (± 1.1) × 10^3
4-chlorophenol	9.0 (± 2.3)	6.3 (± 1.0)	1.9 (± 0.7) × 10^3	6.0 (± 1.9) × 10^2
4-iodophenol	3.7 (± 0.4) × 10^1	1.0 (± 0.3) × 10^1	9.5 (± 0.6) × 10^2	9.6 (± 5.1) × 10^3

Table 3.4: Rate constants fit for free chlorine and free iodine electrophilic substitution reactions for substituted phenols. Rate constants were fit using data from literature. Errors represent 95% confidence intervals.

Reaction	Rate constant ($M^{-1}s^{-1}$)		
	phenol	4-chlorophenol	4-iodophenol
HOCl + PhOH	7.1 (± 2.1) × 10^0	4.0 (± 1.2) × 10^0	3.4 (± 1.0) × 10^1
HOCl + PhO^-	3.6 (± 0.02) × 10^4	1.2 (± 0.05) × 10^4	2.2 (± 0.09) × 10^3
I_2 + PhOH	2.4 (± 0.10) × 10^2	1.4 (± 0.69) × 10^1	6.0 (± 1.1) × 10^1
I_2 + PhO^-	2.3 (± 0.14) × 10^6	2.8 (± 0.17) × 10^6	2.5 (± 0.15) × 10^5
HOI + PhO^-	1.8 (± 0.40) × 10^6	1.4 (± 0.31) × 10^5	1.4 (± 0.36) × 10^5

The theoretical data sets obtained using equation 3.45 were then analyzed using the model developed in this study. Other than adjusting the pK_a values for each phenolic species, our model could be used to analyze all of the theoretical data. For iodine-free data, the initial iodine parameter was set to zero in the final model and it automatically excluded any iodine-related calculations. Parameters were fit by the same sequential fitting approach as was described previously. The reaction mechanisms producing the optimized model fit were found to be the same as for the 2,4-dichlorophenol model fitting from this study. The newly determined individual rate constants are listed in Table 3.4 and were able to model the data very accurately.

Reaction rate constants were compared for each substituted phenol and as expected, the rate constants increased as the pK_a of the phenolic compound increases (i.e., as the Hammet value decreases). Figure 3.7 shows a linear free-energy relationship (LFER) plot of the rate constant for each phenol species versus the corresponding Hammet value. The σ^+ Hammet values, called Brown-Okamoto parameters ($\Sigma\sigma^+$), were used because they most appropriately describe electrophilic substitution while accounting for through-resonance between the chloro-ring substituents and the electron-deficient reaction center of the aromatic ring (64, 65). The rate constants in the plot include the 2,4,6-dichlorophenol rate values determined from this study as well as the phenol, 4-chlorophenol, and 4-iodophenol rate constants determined from our reanalysis of literature data. In general, if each phenolic species reacts with a given oxidant via the same mechanism, a plot of log (*k*) should form a roughly linear relationship. Figure 3.7 exhibits a roughly linear plot for each oxidant confirming that the rate determining step for each reaction is electrophilic substitution of a halogen onto the phenol ring. The reactivity of

the phenolic species can be ranked in the order of phenol>4-chlorophenol≈4-iodophenol>2,4-dichlorophenol. This is due to the presence of additional substituents on the ring structures of each compound. When halogens are present on the ring structures, their high electronegativity relative to H^+ leads to an increase in the stability of the molecule and lowers its susceptibility to electrophilic attack (47). 2,4-dichlorophenol is the most stable of the tested compounds since it contains 2 chlorine atoms on the ring structure. The degree by which each oxidant is affected by the increased number of substituents present on the ring is illustrated by the slope. The negative slope of each means that additional substitutions have a deactivating effect (i.e., the compound is increasingly stable so it is less prone to electrophilic attack). The increased steepness of the HOI curve relative to HOCl and I_2 means that its reactivity is more sensitive to the reactivity changes of the phenol. The LFER also shows that oxidant strength can be ranked as I_2>HOI>HOCl by the relative y-axis range of each oxidant set. The rate constants for the HOCl-PhOH and I_2-PhOH reactions were not included in the plot because they did not exhibit linear behavior. The reaction rate constants for the PhO^- reactions were several orders of magnitude larger than for the PhOH rates which made it difficult to fit the PhOH parameters because their effects were overshadowed. As a result, a great deal more uncertainty is associated with the rate constants describing PhOH reactions so they were omitted from the LFER plot.

2,4-dichlorophenol product formation kinetics at pH 7. For experiments in the absence of iodide, the buildup of 2,4,6-trichlorophenol was observed as reaction times are increased. Since free chlorine/2,4,6-trichlorophenol observed reaction rates (k_{App} = 1.4 $M^{-1}s^{-1}$) are an order of magnitude slower than those for 2,4-dichlorophenol (k_{App} = 87 $M^{-1}s^{-1}$), 2,4-DCP substitution

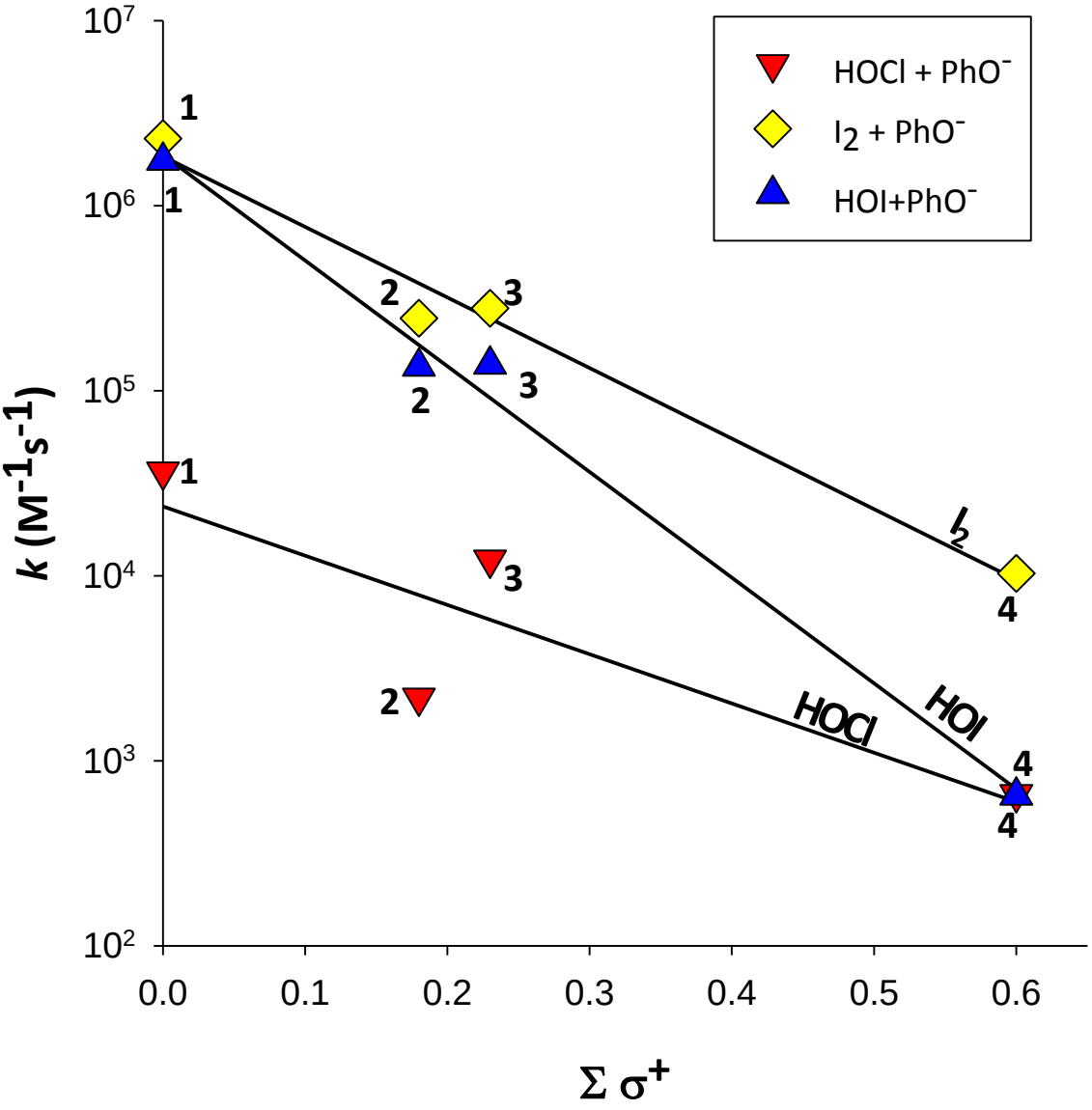

Figure 3.7: Plot of log *k* versus the Hammett value for substituted phenolic compounds. 1) phenol, 2) 4-iodophenol, 3) 4-chlorophenol, 4) 2,4-dichlorophenol. Conditions: $[\text{Total Oxidant}]_i$ = 10 μM, $[\text{phenol}]_i$ = 100 μM, $[NaHCO_3]$ = 2 mM. With the exception of 2,4-dichlorophenol the individual rate constants were fit using data from previous literature (1, 2).

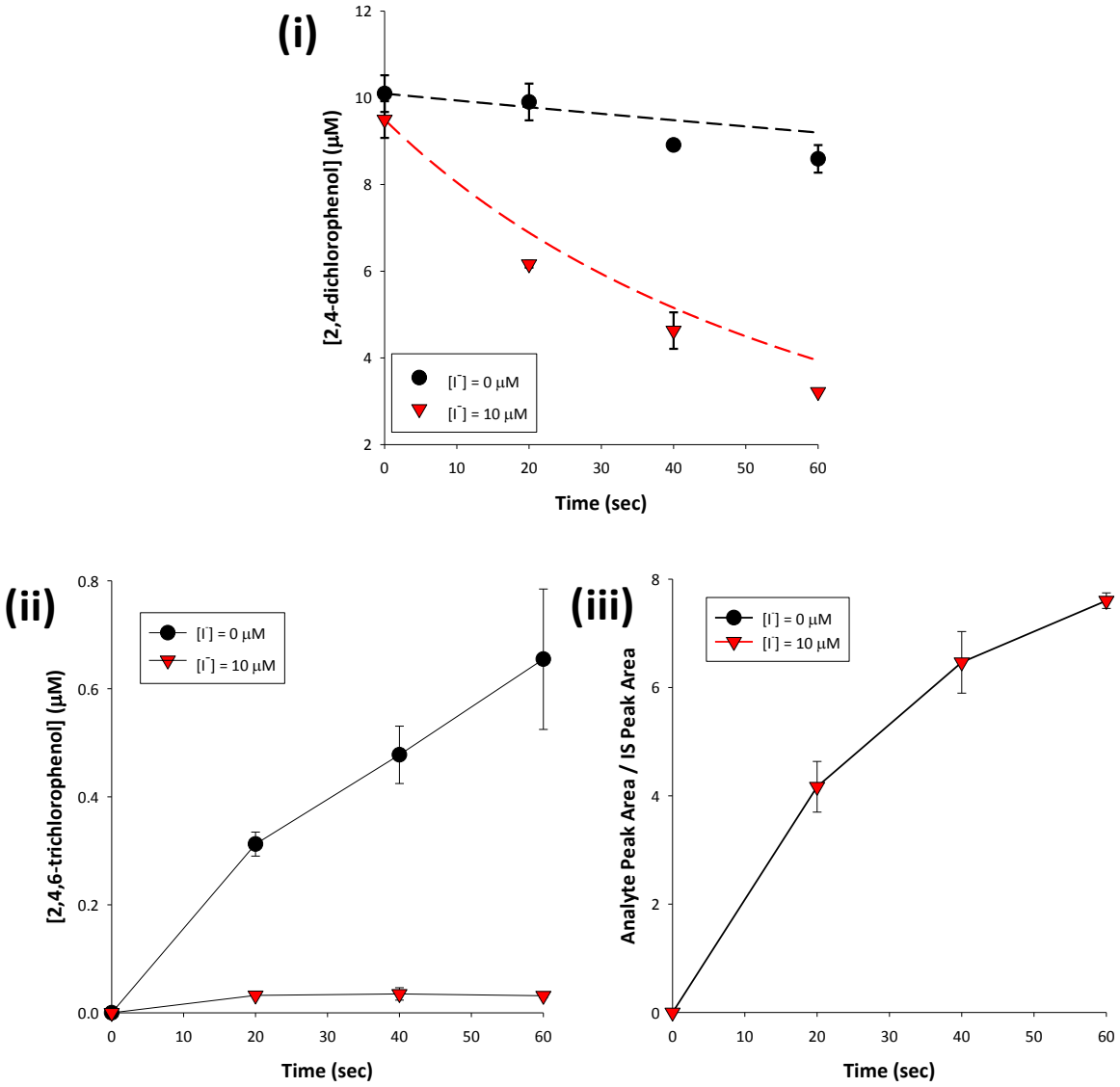

Figure 3.8: Electophilic substitution of 2,4-dichlorophenol (i) and formation of 2,4,6-trichlorophenol (ii) and 2,4-dichloro-6-iodophenol (iii) over time. Model predictions (dashed lines on plot i), experimental results (curves). Conditions: [free chlorine]i = 20 μM, [2,4-dichlorophenol]i = 9.5-10.1 μM, [NaHCO3] = 2 mM, pH = 7.0.

forms 2,4,6-TCP faster than 2,4,6-trichlorophenol is consumed, thus resulting in a significant buildup of 2,4,6-TCP (Figure 3.8). The failure to identify further substituted chlorophenols in any sample suggests that there was either inadequate free chlorine available for further substitution reactions to form detectable tetrachlorophenol or pentachlorophenol, or that additional chlorination results in ring cleavage of 2,4,6-trichlorophenol, as suggested in the literature, to produce chloroform and other THMs (16). The later theory is supported by the observed loss of 2,4-dichlorophenol in the amount of 1.5 μM over 60 seconds while only 0.65 μM of 2,4,6-trichlorophenol was formed over that same reaction time. One would expect to see a 2,4,6-TCP formation: 2,4-DCP loss ratio near a value of 1:1 if additional products were not forming. If 2,4,6-trichlorophenol were reacting, we would expect to measure less 2,4,6-TCP forming than the amount of 2,4-DCP that is lost. For experiments with 10 μM of I^-, less than 0.06 μM of 2,4,6-trichlorophenol was formed. With an initial free chlorine concentration of 20 μM and an experimental pH of 7.0, the fraction of the total oxidant present as free chlorine is considerably larger than that of free iodine (nearly 15 μM of free chlorine versus only ≈5 μM of I_2) so one might expect to observe a substantial buildup of 2,4,6-trichlorophenol. Instead, very little 2,4,6-trichlorophenol formation is detected and no buildup is observed. This result suggests that either free iodine inhibits free chlorine reactions or, more likely, that free iodine reacts more quickly with 2,4,6-trichlorophenol than chlorine reacts with 2,4-dichlorophenol. In reactions containing 10 μM of initial iodide, the 2,4-dichloro-6-iodophenol peak area increased with increasing reaction times. The relative increase in peak area magnitude, which corresponds to compound concentration, is proportional to those observed for 2,4,6-trichlorophenol in reactions where iodide was absent. The lack of dichloro-diiodophenol or

trichloro-iodophenol detection implies that further free chlorine or free iodine reactions result in production of other iodinated products, which combined with the lack of 2,4,6-trichlorophenol formation leads to the conclusion that the overall yield of byproducts is increased when iodide is present.

Product formation for substituted phenols. To further explore product formation with substituted phenols, experiments over extended time periods (t = 5 min) were performed where 10 μM of 4-chlorophenol, 4-iodophenol, and 4-bromophenol were contacted with excess free chlorine ($[HOCl]_i$ = 100 μM) at pH 7.0 (Figure 3.9). To increase our understanding of the overall fate of phenolic products during disinfection, experiments were performed with extended reaction times, excess free chlorine, and at a pH where observed reaction rates are elevated. Schematics describing product formation when 4-chlorophenol, 4-iodophenol, or 4-bromophenol reacts with free chlorine and free iodine are shown in Figure 3.10-3.12. In experiments in the absence of iodide, each phenolic compound underwent a single chlorine substitution, such as the chlorination of 4-CP to form 2,4-DCP or chlorination of 4-IP to form 2-chloro-4-iodophenol. Typically, the most favorable substitution reactions are those that occur at the reaction site with the least amount of required energy (66). For example, the most common chlorine substitution for an unsubstituted phenol occurs in the C-2 para-position because interactions between the electrophilic chlorine and the negatively charged C-1 hydroxyl group have an activating effect. Subsequent substitutions would most likely occur at the ortho C-6 position followed by the C-4 site so that interactions between the bulky halogen ions are minimized (17). Each added chlorine requires more energy to overcome repulsion forces from the others, so further chlorination typically does not occur. Appendix C includes

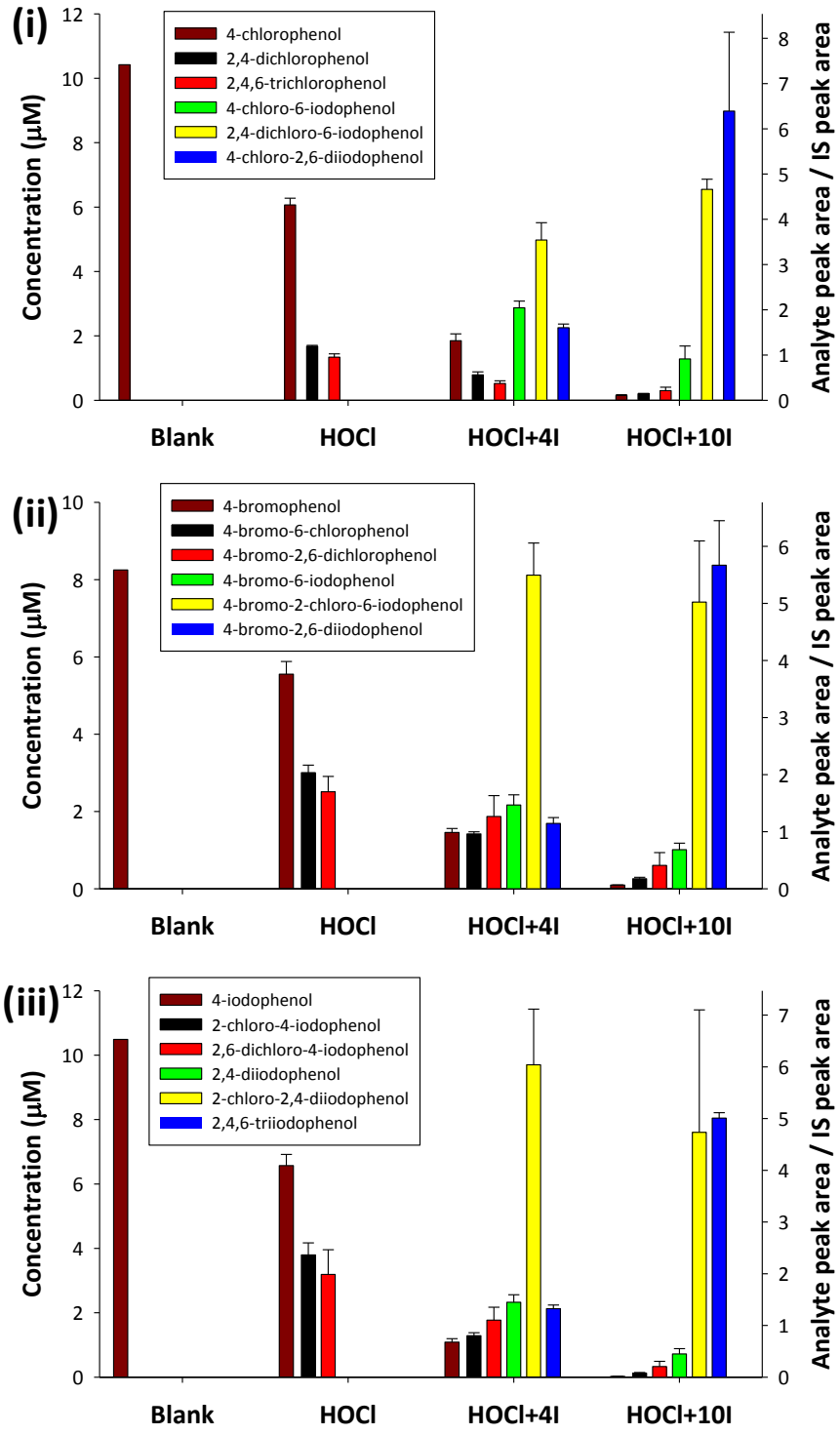

Figure 3.9: Product formation from 2,4-dichlorophenol reactions with free chlorine in the presence of 0 (i), 4 (ii), and 10 μM (iii) initial iodide. Conditions: pH 7.0, [2,4-DCP]i = 10 μM, [free chlorine]i = 20 μM, reaction time = 5 min.

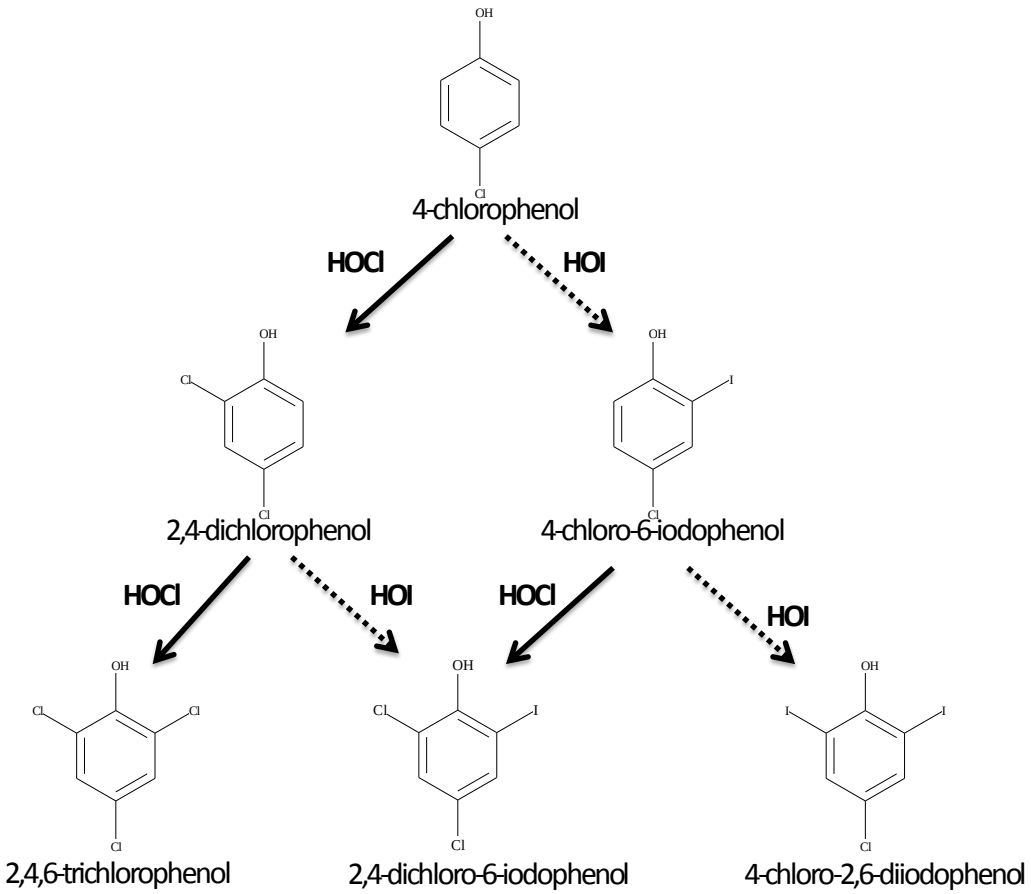

Figure 3.10: Proposed reaction pathway for the electrophilic substitution of 4-chlorophenol by free chlorine and free iodine.

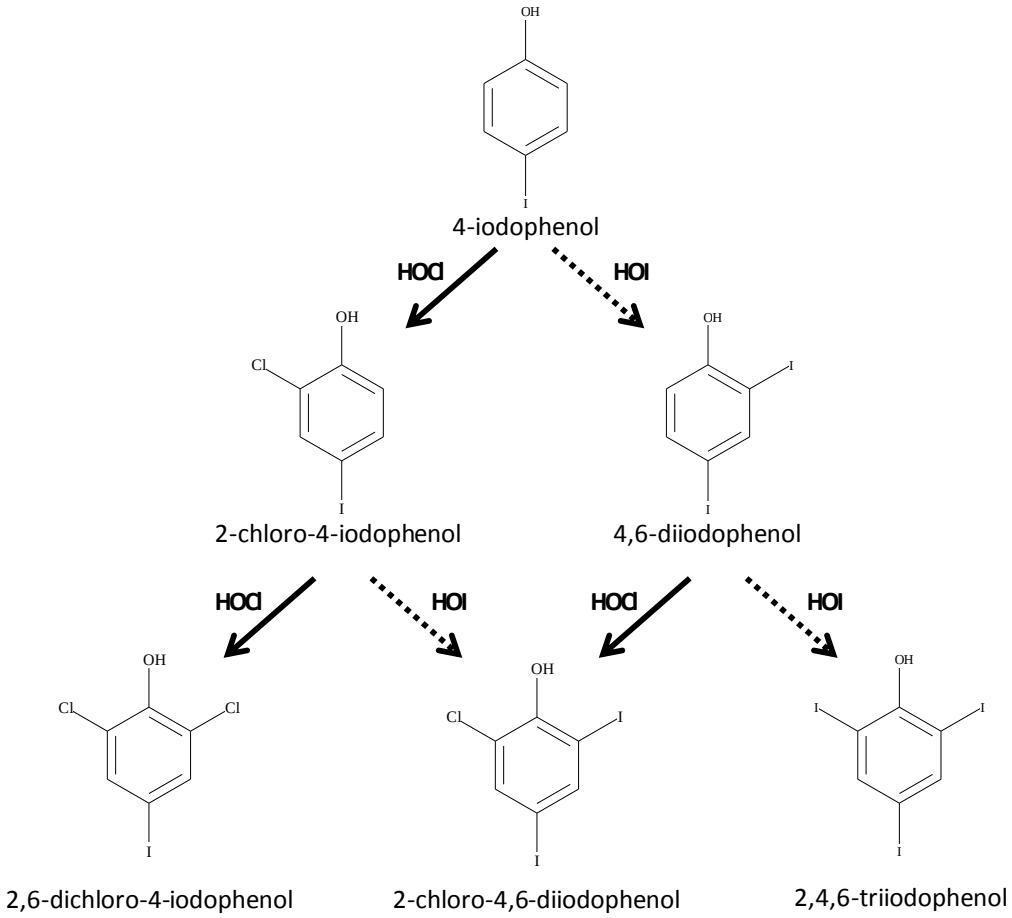

Figure 3.11: Proposed reaction pathway for the electrophilic substitution of 4-iodophenol by free chlorine and free iodine.

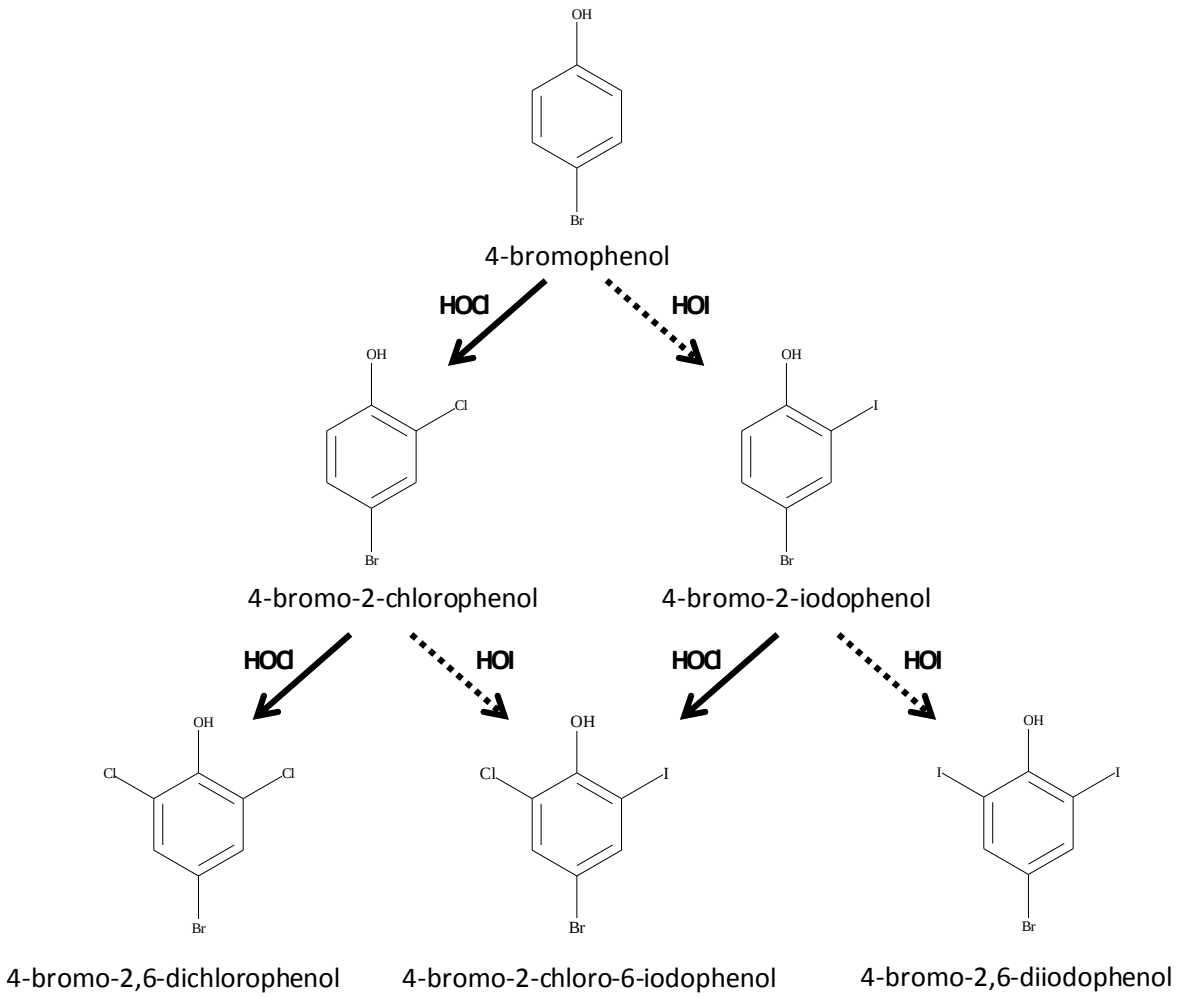

Figure 3.12: Proposed reaction pathway for the electrophilic substitution of 4-bromophenol by free chlorine and free iodine.

GC-MS spectra for 4-chlorophenol, 4-iodophenol, and 4-bromophenol in which as many as two additional chlorine substitutions have been observed. Even after 5 minutes in contact with excess free chlorine, 25-65% of the starting concentration of the parent compound could still be detected.

All product production data is shown in Figure 3.9. After 5 minutes of reaction time, the concentration of 4-chlorophenol was reduced from 9.8 to 5.1 μM while 2.6 and 1.2 μM of 2,4-DCP and 2,4,6-TCP were formed, respectively. The same reaction time resulted in a 3.8 μM loss of 4-iodophenol while substantial peaks were formed for 4-iodo-6-chlorophenol and 4-iodo-2,6-dichlorophenol. A 3.9 μM loss for 4-bromophenol also resulted in significant quantities of both monochlorinated and dichlorinated products.

In experiments containing iodide, the 5 minute reaction time was sufficient for almost complete consumption of each parent compound. Only 1.7, 1.0, and 1.5 μM of 4-CP, 4-IP, and 4-BP remained when 4 μM iodide was present. For 4-CP, both 2,4-DCP and 2,4,6-TCP formation was decreased by over 50% as compared to when iodide was absent (only 1.2 and 0.5 μM concentrations were measured, respectively). However, substantial peaks were detected for chloro-iodophenol, dichloro-iodophenol, and chloro-diiodophenol. The addition of iodide similarly reduced all chlorine substituted product peaks by over 60% for 4-BP and 4-IP while substantial peaks of monoiodo and diiodo substituted compounds were again detected. When the iodide concentration was increased to 10 μM, the 5 minute reaction time was sufficient for near complete consumption of all parent compounds. Chlorinated product formation was further reduced for all parent compounds by at least 75% as compared to the 4 μM iodide

reactions. The peak areas of all singly iodinated products were reduced by at least 50% while the diiodinated product peaks increased by 300 to 500% for each parent compound.

In general, as the abundance of iodinated products increased with a larger iodine concentration, the abundance of chlorinated products decreased. Since HOCl was in excess of iodide, however, the complete suppression of chlorinated products was never observed. The drastic decreases in the chlorinated product yields countered by equally large increases in iodinated products shows that free iodine reaction pathways are preferred over chlorination reactions and the presence of small iodide concentrations can cause a large shift in product formation potentials. The decrease in monoiodinated products when the iodide concentration was increased from 4 to 10 μM shows that a 5 minute contact time is sufficient for multiple iodine substitution reactions to occur so the formation of iodinated THMs would also likely happen very quickly. The findings that 2,4-dichloro-6-iodophenol continued to increase in concentration with each increase in iodide concentration during 4-chlorophenol reactions and that the monochlorinated and dichlorinated 4-chlorophenol products were not reduced as drastically as observed for 4-IP and 4-BP suggest that chlorine substitutions onto the ring structures have more of an inhibitory effect on iodine substitution than on additional chlorine substitution reactions. The increased consumption of parent compounds in the presence of iodide suggests that the total quantities of product being formed are also elevated. Overall, these results show that even small amounts of iodide present during chlorination can produce significant amounts of iodinated products.

3.4: Conclusions

- Free chlorine reactions with substituted phenolic compounds occur primarily through electrophilic substitution reactions as described by equations 3.21 and 3.22. Contrary to current literature, H_2OCl^+ was not included in the mechanism describing the chlorination of phenols.

$$\mathrm{HOCl} + \mathrm{PhOH} \xrightarrow{k_{3.21}} \mathrm{products} \quad (3.21)$$

$$\mathrm{HOCl} + \mathrm{PhO^-} \xrightarrow{k_{3.22}} \mathrm{products} \quad (3.22)$$

  It is suspected that Cl_2 reactions may play an important role at low pH but this was not verified during the course of this research. Prior to this study, overly simplistic modeling techniques utilized for the kinetic analysis of chlorination of phenolic compounds have resulted in incorrect rate constants for these reactions.

- Free iodine reactions with substituted phenolic compounds also occur primarily through electrophilic substitution as described by equations 3.25-3.26 and 3.28. The mechanism includes reactive I_2 as opposed to current literature which credits a H_2OI^+ species.

$$\mathrm{I_2} + \mathrm{PhOH} \xrightarrow{k_{3.25}} \mathrm{products} + \mathrm{I^-} \quad (3.25)$$

$$\mathrm{I_2} + \mathrm{PhO^-} \xrightarrow{k_{3.26}} \mathrm{products} + \mathrm{I^-} \quad (3.26)$$

$$\mathrm{HOI} + \mathrm{PhO^-} \xrightarrow{k_{3.28}} \mathrm{products} \quad (3.28)$$

  I_2 is found to be an extremely important reactant when describing free iodide reactions so rates determined without considering its presence cannot be used with confidence.

- Rate constants for each reaction were determined for 2,4-dichlorophenol, 4-chlorophenol, 4-iodophenol, and unsubstituted phenol as follows:

	$k_{3.21}$	$k_{3.22}$	$k_{3.25}$	$k_{3.26}$	$k_{3.28}$
2,4-dichlorophenol	26 (± 13)	6.6 (± 1.3) × 10^2	2.4 (± 0.73) × 10^2	1.0 (± 0.26) × 10^4	6.5 (± 1.5) × 10^2
4-chlorophenol	4.0 (± 1.2)	1.2 (± 0.05) × 10^4	1.4 (± 0.69) × 10^1	2.8 (± 0.17) × 10^6	1.4 (± 0.31) × 10^5
4-iodophenol	34 (± 10)	2.2 (± 0.09) × 10^3	6.0 (± 1.1) × 10^1	2.5 (± 0.15) × 10^5	1.4 (± 0.36) × 10^5
phenol	71 (± 21)	3.6 (± 0.02) × 10^4	2.4 (± 0.10) × 10^2	2.3 (± 0.14) × 10^6	1.8 (± 0.40) × 10^6

- Iodinated byproducts are formed quickly when iodide is present and form preferentially over chlorinated products at low iodide concentrations. The 20-fold increase in the rate of consumption of the parent compound suggests that overall byproduct yields are also increased.

3.5: References

1. Gallard, H.; Von Gunten, U., Chlorination of phenols: Kinetics and formation of chloroform. *Environ. Sci. Technol.* **2002,** *36*, (5), 884-890.

2. Bichsel, Y.; von Gunten, U., Formation of iodo-trihalomethanes during disinfection and oxidation of iodide containing waters. *Environ. Sci. Technol.* **2000,** *34*, (13), 2784-2791.

3. Vieno, N. M.; Harkki, H.; Tuhkanen, T.; Kronberg, L., Occurrence of pharmaceuticals in river water and their elimination a pilot-scale drinking water treatment plant. *Environ. Sci. Technol.* **2007,** *41*, (14), 5077-5084.

4. Stackelberg, P. E.; Gibs, J.; Furlong, E. T.; Meyer, M. T.; Zaugg, S. D.; Lippincott, R. L., Efficiency of conventional drinking-water-treatment processes in removal of pharmaceuticals and other organic compounds. *Science of the Total Environment* **2007,** *377*, (2-3), 255-272.

5. Boyd, G. R.; Palmeri, J. M.; Zhang, S. Y.; Grimm, D. A., Pharmaceuticals and personal care products (ppcps) and endocrine disrupting chemicals (edcs) in stormwater canals and bayou st. John in new orleans, louisiana, USA. *Science of the Total Environment* **2004,** *333*, (1-3), 137-148.

6. Snyder, S. A.; Westerhoff, P.; Yoon, Y.; Sedlak, D. L., Pharmaceuticals, personal care products, and endocrine disruptors in water: Implications for the water industry. *Environmental Engineering Science* **2003,** *20*, (5), 449-469.

7. Boyd, G. R.; Reemtsma, H.; Grimm, D. A.; Mitra, S., Pharmaceuticals and personal care products (ppcps) in surface and treated waters of louisiana, USA and ontario, canada. *the Science of the Total Environment* **2003,** *311*, 135-149.

8. Kolpin, D. W.; Furlong, E. T.; Meyer, M. T.; Thurman, E. M.; Zaugg, S. D.; Barber, L. B.; Buxton, H. T., Pharmaceuticals, hormones, and other organic wastewater contaminants in u.S. Streams, 1999-2000: A national reconnaissance. *Environ. Sci. Technol.* **2002,** *36*, 1202-1211.

9. Halling-Sorensen, B.; Nielsen, S. N.; Lanzky, P. F.; Ingerslev, F.; Lutzhoft, H. C. H.; Jorgensen, S. E., Occurrence, fate and effects of pharmaceutical substances in the environment - a review. *Chemosphere* **1998,** *36*, (2), 357-394.

10. Gallard, H.; Leclercq, A.; Croue, J. P., Chlorination of bisphenol a: Kinetics and by-products formation. *Chemosphere* **2004,** *56*, (5), 465-473.

11. Yamamoto, T.; Yasuhara, A., Chlorination of bisphenol a in aqueous media: Formation of chlorinated bisphenol a congeners and degradation to chlorinated phenolic compounds. *Chemosphere* **2002,** *46*, (8), 1215-1223.

12. Bedner, M.; Maccrehan, W. A., Transformation of acetaminophen by chlorination produces the toxicants 1,4-benzoquinone and n-acetyl-p-benzoquinone imine. *Environ. Sci. Technol.* **2006,** *40*, (2), 516-522.

13. Canosa, P.; Morales, S.; Rodriguez, I.; Rubi, E.; Cela, R.; Gomez, M., Aquatic degradation of triclosan and formation of toxic chlorophenols in presence of low concentration of free chlorine. *Anal. Bioanal. Chem.* **2005,** *383*, (7-8), 1119-1126.

14. Fiss, E. M.; Rule, K. L.; Vikesland, P. J., Formation of chloroform and other chlorinated byproducts by chlorination of triclosan-containing antibacterial products. *Environmental Science & Technology* **2007,** *41*, (7), 2387-2394.

15. Greyshock, A. E.; Vikesland, P. J., Triclosan reactivity in chloraminated waters. *Environmental Science and Technology* **2006,** *40*, 2615-2622.

16. Rule, K. L.; Ebbett, V. R.; Vikesland, P. J., Formation of chloroform and chlorinated organics by free-chlorine-mediated oxidation of triclosan. *Environmental Science and Technology* **2005,** *39*, 3176-3185.

17. Deborde, M.; von Gunten, U., Reactions of chlorine with inorganic and organic compounds during water treatment - kinetics and mechanisms: A critical review. *Water Res.* **2008,** *42*, (1-2), 13-51.

18. Lee, G. F.; Morris, J. C., Kinetics of chlorination of phenol-chlorophenolic tastes and odors. *Int. J. Air Water Pollut.* **1962,** *6*, 419-431.

19. Pinkston, K. E.; Sedlak, D. L., Transformation of aromatic ether-and amine-containing pharmaceuticals during chlorine disinfection. *Environ. Sci. Technol.* **2004,** *38*, (14), 4019-4025.

20. Onodera, S.; Nishikawa, T.; Suzuki, S., Chemical-changes of organic-compounds in chlorinated water .14. Characterization and determination of halogenated organics formed during chlorination of water from the tama river. *J. Chromatogr.* **1987,** *409*, 259-270.

21. Kanetoshi, A.; Ogawa, H.; Katsura, E.; Kaneshima, H., Chlorination of irgasan dp300 and formation of dioxins from its chlorinated derivatives. *J. Chromatogr.* **1987,** *389*, 139-153.

22. Soper, F. G.; Smith, G. F., The halogenation of phenols. *J. Am. Chem. Soc.* **1926,** *6*, 1582-1591.

23. Gallard, H.; von Gunten, U., Chlorination of natural organic matter: Kinetics of chlorination and of thm formation *Water Res.* **2002,** *36*, (1), 65-74.

24. Onodera, S.; Iino, N.; Matsuda, M.; Ishikura, S., Chemical-changes of organic-compounds in chlorinated water .6. Gas-chromatographic and mass-spectrometric studies of the reactions of phenylphenols with hypochlorite in dilute aqueous-solution. *J. Chromatogr.* **1983,** *265*, (2), 201-213.

25. Onodera, S.; Yamada, K.; Yamaji, Y.; Ishikura, S.; Suzuki, S., Chemical-changes of organic-compounds in chlorinated water .10. Formation of polychlorinated methylphenoxymethylphenols (predioxins) during chlorination of methylphenols in dilute aqueous-solution. *J. Chromatogr.* **1986,** *354*, 293-303.

26. Vikesland, P. J.; Rule, K. L.; Greyshock, A. E.; Ebbett, V. R.; Fiss, E. M., *Triclosan reactivity in chlorinated and monochloraminated waters*. AWWA Research Foundation: Denver, 2006.

27. Trussell, R. R.; Umphres, M. D., Formation of trihalomethanes. *Journal American Water Works Association* **1978,** *70*, (11), 604-612.

28. Rook, J. J., Formation of haloforms during chlorination of natural waters. *Water Treatment and Examination* **1974,** *23*, 234-243.

29. Cherney, D. P.; Duirk, S. E.; Tarr, J. C.; Collette, T. W., Monitoring the speciation of aqueous free chlorine from ph 1 to 12 with raman spectroscopy to determine the identity of the potent low-ph oxidant. *Applied Spectroscopy* **2006,** *60*, (7), 764-772.

30. Moran, J. E.; Oktay, S. D.; Santschi, P. H., Sources of iodine and iodine 129 in rivers. *Water Resources Research* **2002,** *38*, (8).

31. Bichsel, Y.; von Gunten, U., Oxidation of iodide and hypoiodous acid in the disinfection of natural waters. *Environmental Science & Technology* **1999,** *33*, (22), 4040-4045.

32. Plewa, M. J.; Wagner, E. D.; Richardson, S. D.; Thruston, A. D.; Woo, Y. T.; McKague, A. B., Chemical and biological characterization of newly discovered lodoacid drinking water disinfection byproducts. *Environmental Science & Technology* **2004,** *38*, (18), 4713-4722.

33. Hua, G. H.; Reckhow, D. A.; Kim, J., Effect of bromide and iodide ions on the formation and speciation of disinfection byproducts during chlorination. *Environ. Sci. Technol.* **2006,** *40*, (9), 3050-3056.

34. Nagy, J. C.; Kumar, K.; Margerum, D. W., Non-metal redox kinetics - oxidation of iodide by hypochlorous acid and by nitrogen trichloride measured by the pulsed-accelerated-flow method. *Inorganic Chemistry* **1988,** *27*, (16), 2773-2780.

35. Lengyel, I.; Li, J.; Kustin, K.; Epstein, I. R., Rate constants for reactions between iodine- and chlorine-containing species: A detailed mechanism of the chlorine dioxide/chlorite-iodide reaction. *J. Am. Chem. Soc.* **1996,** *118*, (15), 3708-3719.

36. Nagy, K.; Kortvelyesi, T.; Nagypal, I., Iodine hydrolysis equilibrium. *Journal of Solution Chemistry* **2003,** *32*, (5), 385-393.

37. Kazantseva, N. N.; Ernepesova, A.; Khodjamamedov, A.; Geldyev, O. A.; Krumgalz, B. S., Spectrophotometric analysis of iodide oxidation by chlorine in highly mineralized solutions. *Analytica Chimica Acta* **2002,** *456*, (1), 105-119.

38. Gottardi, W., Iodine and disinfection: Theoretical study on mode of action, efficiency, stability, and analytical aspects in the aqueous system. *Archiv Der Pharmazie* **1999,** *332*, (5), 151-157.

39. Gottardi, W.; Arnitz, R.; Nagl, M., N-chlorotaurine and ammonium chloride: An antiseptic preparation with strong bactericidal activity. *International Journal of Pharmaceutics* **2007,** *335*, (1-2), 32-40.

40. Schmitz, G., Inorganic reactions of iodine(+1) in acidic solutions. *International Journal of Chemical Kinetics* **2004,** *36*, (9), 480-493.

41. Lengyel, I.; Epstein, I. R.; Kustin, K., Kinetics of iodine hydrolysis. *Inorganic Chemistry* **1993,** *32*, (25), 5880-5882.

42. Wang, T. X.; Margerum, D. W., Kinetics of reversible chlorine hydrolysis - temperature-dependence and general acid base-assisted mechanisms. *Inorganic Chemistry* **1994,** *33*, (6), 1050-1055.

43. Morris, J. C., The acid ionization constant of hocl from 5 to 35°. *Journal of Physical Chemistry* **1966,** *70*, (12), 3798-3805.

44. Ge, F.; Zhu, L. Z.; Wang, J., Distribution of chlorination products of phenols under various phs in water disinfection. *Desalination* **2008,** *225*, (1-3), 156-166.

45. Veglia, A. V.; Rossi, R. H. d., Selectivity in the iodination of phenol in the presence of □-cyclodextrin. *Journal of Organic Chemistry* **1988,** *53*, 5281-5287.

46. Burttschell, R. H.; Rosen, A. A.; Middleton, F. M.; Ettinger, M. B., Chlorine derivatives of phenol causing taste and odor. *J. Am. Water Works Assoc.* **1959,** *51*, 205-214.

47. Schwarzenbach, R. P.; Gschwend, P. M.; Imboden, D. M., *Environmental organic chemistry*. 2nd ed.; John Wiley & Sons: Hoboken, NJ, 2003.

48. Mirlohi, S. Chemical identification and flavor profile analysis of iodinated phenols produced from disinfection of spacecraft drinking water. Virginia Polytechnic Institute and State University, Blacksburg, 1997.

49. Erling Grovenstein, J.; Aprahamian, N. S.; Bryan, C. J.; Gnanapragasam, N. S.; Kilby, D. C.; John M. McKelvey, J.; Sullivan, R. J., Aromatic halogenation. Iv. Kinetics and mechanism of iodination of phenol and 2,6-dibromophenol. *J. Am. Chem. Soc.* **1973,** *95*, (13), 4261-4270.

50. Cancho, B.; Ventura, F.; Galceran, M.; Diaz, A.; Ricart, S., Determination, synthesis and survey of iodinated trihalomethanes in water treatment processes. *Water Res.* **2000,** *34*, (13), 3380-3390.

51. Hua, G. H.; Reckhow, D. A., Comparison of disinfection byproduct formation from chlorine and alternative disinfectants. *Water Res.* **2007,** *41*, (8), 1667-1678.

52. Krasner, S. W.; Weinberg, H. S.; Richardson, S. D.; Pastor, S. J.; Chinn, R.; Sclimenti, M. J.; Onstad, G. D.; Thruston, A. D., Occurrence of a new generation of disinfection byproducts. *Environ. Sci. Technol.* **2006,** *40*, (23), 7175-7185.

53. Bichsel, Y. Behavior of iodine species in oxidative processes during drinking water treatment. Swiss Federal Institute of Technology Zurich, Zurich, 2000.

54. Sebok-Nagy, K.; Kortvelyesi, T., Kinetics and mechanism of the hydrolytic disproportionation of iodine. *International Journal of Chemical Kinetics* **2004,** *36*, (11), 596-602.

55. Truesdale, V. W.; Luther, G. W.; Greenwood, J. E., The kinetics of iodine disproportionation: A system of parallel second-order reactions sustained by a multi-species pre-equilibrium. *Physical Chemistry Chemical Physics* **2003,** *5*, (16), 3428-3435.

56. Bichsel, Y.; von Gunten, U., Hypoiodous acid: Kinetics of the buffer-catalyzed disproportionation. *Water Res.* **2000,** *34*, (12), 3197-3203.

57. Warner, J. A.; Casey, W. H.; Dahlgren, R. A., Interaction kinetics of i-2(aq) with substituted phenols and humic substances. *Environ. Sci. Technol.* **2000,** *34*, (15), 3180-3185.

58. Buffle, M. O.; Schumacher, J.; Salhi, E.; Jekel, M.; von Gunten, U., Measurement of the initial phase of ozone decomposition in water and wastewater by means of a continuous quench-flow system: Application to disinfection and pharmaceutical oxidation. *Water Res.* **2006,** *40*, (9), 1884-1894.

59. *Standard methods for the examination of water and wastewater*. 18th ed.; Washington, D.C., 1992.

60. Arnold, W. A.; Roberts, A. L., Pathways and kinetics of chlorinated ethylene and chlorinated acetylene reaction with fe(0) particles. *Environ. Sci. Technol.* **2000,** *34*, (9), 1794-1805.

61. Bell, R. P.; Gelles, E., 608. The halogen cations in aqueous solution. *Journal of the Chemical Society* **1951**, 2734-2740.

62. Burger, J. D.; Liebhafsky, H. A., Thermodynamic data for aqueous iodine solutions at various temperatures. *Analytical Chemistry* **1973,** *45*, (3), 600-602.

63. Espenson, J. H., *Chemical kinetics and reaction mechanisms*. McGraw Hill: New York, 2002.

64. Canonica, S.; Tratnyek, P. G., Quantitative structure-activity relationships for oxidation reactions of organic chemicals in water. *Environmental Toxicology and Chemistry* **2003,** *22*, (8), 1743-1754.

65. Li, C.; Hoffman, M. Z., One-electron redox potentials of phenols in aqueous solution. *Journal of Physical Chemistry B* **1999,** *103*, (32), 6653-6656.

66. Carroll, F. A., *Perspectives on structure and mechanism in organic chemistry*. Brooks/Cole Publishing Company: Pacific Grove, 1998.

Chapter 4: Halogenation Kinetics of Triclosan in Chlorinated Waters Containing Iodide

4.1: Introduction

Triclosan (5-chloro-2-(2,4-dichlorophenoxy)phenol) (Figure 2.2) is an antimicrobial agent found in many common household hygienic products, such as liquid soap, hand lotion, and toothpaste, at concentrations up to 0.3%. Although its actual effectiveness in the home is a topic of debate (1), triclosan is commonly added to many personal care products because it exhibits antibacterial as well as antifungal and antiviral properties (2). Because of incomplete wastewater treatment removal efficiencies and land application of triclosan laden bio-solids, triclosan can be found in nearly every aquatic environment, including wastewater treatment effluents, stream waters, lakes, and river sediments (3-6). Due to fears about the compound's acute toxicity, its potential to increase bacterial resistance, and other ill effects attributed to its use, many European countries have limited the use of triclosan-containing products (7). However, U.S. use of triclosan shows no signs of decline boasting an average nationwide usage of ~1500 kg/day (8). A comprehensive U.S.G.S. study detected triclosan in 57.6% of 139 streams tested (9).

Triclosan present in source waters used for drinking water supply can come into contact with disinfectants during drinking water treatment. In addition, many triclosan-containing products currently on the market are designed to be used during activities such as showering and dish washing. As such, these products may be in contact with a disinfectant for extended periods of

time at water temperatures that can range from 21-46 ^{o}C (10, 11). Most utilities in the U.S. use free chlorine for disinfection purposes and over 70% of all drinking water utilities use free chlorine to maintain a disinfectant residual (12). Studies have shown that triclosan and free chlorine readily react to form byproducts that include chlorinated phenoxy-phenols, chlorinated phenols, and trihalomethanes (13-17). These byproducts include 5,6-dichloro-2-(2,4-dichlorophenoxy)phenol, 4,5-dichloro-2-(2,4-dichlorophenoxy)phenol, 4,5,6-trichloro-2-(2,4-dichlorophenoxy)phenol, 2,4-dichlorophenol, 2,4,6-trichlorophenol, and chloroform. Some of these chlorinated intermediates and products are reported carcinogens, although insufficient studies have been performed to determine if that is the case for each compound.

An issue that has been overlooked in the majority of PPCP-disinfectant studies to date is the potential complicating effect caused by the presence of common salts, such as iodide, on these reactions. In natural waters, iodide is typically found at concentrations ranging from 0.5-100 μg/L (0.004 to 2 μM) (18) and is known to readily react with free chlorine to produce highly reactive hypoiodous acid (19-24). If iodide comes in contact with free chlorine, it can be oxidized to HOI by a complex series of fast reactions involving the intermediates $HOClI^-$ and ICl (23-26). Once equilibrium is reached, the possible free iodine species present include I_2, HOI, OI^-, I_3^-, H_2OI^-, and HOI_2^- (27-30), any of which can potentially react with triclsoan. Studies have shown that the intermediates (ICl and $HOClI^-$) are present at trace levels and react instantaneously to form HOI, so it can be assumed that they will have negligible effects on the overall reactivity of iodine towards triclosan (24).

In general, relatively little is known about the implications of PPCP iodination in natural waters. Iodination of phenolic compounds is of concern because some iodinated DBPs have

been shown to be 50-500× more toxic than their chlorinated analogues (21), and the presence of iodide during organic matter oxidation has been shown to produce iodinated THMs (20) and HAAs that are not produced by free chlorine alone (22). Free iodine has also been shown to react with natural organic matter nearly 15 times faster than HOCl (20). Accelerated reactions and increased product formation necessitate the need to better understand iodide interactions so that a true assessment of public health risk is possible.

Although prior studies have examined the effects of iodide on the electrophilic substitution of phenols, most have concentrated on product detection and distribution (22, 31-33) rather than reaction rates since accurate data for the extremely short reaction periods indicative of free iodine reactions with phenolic compounds can be difficult to accurately ascertain. Existing kinetics studies with iodide focused on disproportionation reactions forming iodate rather than on reactions with organic matter or phenols (19, 25, 34-37). The few kinetic studies that have looked at oxidation kinetics either utilized conditions that call the applicability of the results to drinking water into question (38) or used simplified models to fit rate constants (20). No studies to date have addressed the iodination of PPCPs. The objectives of this study were to perform a comprehensive analysis of the kinetic effects of iodide presence during drinking water chlorination in order to elucidate reaction mechanisms and product formation potentials for triclosan. This will be bolstered by the development of a computer model that is able to calculate reaction rate constants and predict the overall behavior of triclosan in this system.

4.2: Materials and Methods

Reagent grade water was purified by deionization and distillation. Glassware was cleaned by sequentially soaking it in a 10% nitric acid water bath and then in a concentrated chlorine bath.

Triclosan was purchased from Aldrich (>98% purity) and was used without further purification. Stock triclosan solutions were prepared by dissolving 100 mg of triclosan in 50 mL of reagent grade methanol. Stocks of free chlorine were prepared using a commercial solution of sodium hypochlorite (purified grade 4-6% NaOCl; Fisher Scientific). pH measurements were obtained with a Fisher Scientific model 60 pH meter coupled with a Thermo-Orion Ross PerpHect Combination Electrode.

Preparation of Experimental Solutions. Experimental solutions were prepared using reagent grade water containing 2 mM sodium bicarbonate buffer adjusted to the desired pH. Aliquots of stock solution were spiked into experimental solutions to obtain a desired concentration. After allowing 5 minutes for the solutions to equilibrate, each experimental solution was adjusted to the desired pH using sodium hydroxide and sulfuric acid. Sulfuric acid was used in order to minimize chloride addition since chloride ions shift the solution equilibrium from HOCl towards Cl_2/H_2OCl^+ at low pH values thereby causing enhanced reaction rates (17). All experiments were performed at 25 ^oC.

Total oxidant consumption. Oxidant consumption experiments were performed using a quench flow system (QFS) similar to a design by Buffle et al. (Appendix A; ref. (39). By keeping the flow-rate of the QFS constant, we achieved highly accurate and extremely fast reaction times (ranging from 0.25-5 seconds) by simply changing the volume of each flow loop. Total oxidant concentrations (defined as the sum of Cl_2, HOCl, OCl^-, I_2, H_2OI^+, HOI, and OI^- concentrations) were determined using a modified DPD colorimetric method with photometric detection at 515 nm developed for use with the QFS (40). To promote pseudo-first order conditions, oxidant demand experiments were performed with phenol concentrations in 10× excess relative to the

oxidant concentration. Following the reaction period, the final solution was mixed with DPD reagent and phosphate buffer to quench the reaction. The quenched solution then flowed through an additional flow loop to allow one minute for color development, at which time the solution was analyzed using a Cary5000 (Varian Inc.) UV-Vis-NIR spectrophotometer (λ = 515 nm) with a 1 cm pathlength flow-through cell. The absorbances of the solutions were measured for each reaction time until the absorbance signal stabilized for a minimum of 30 seconds (Appendix A, Figure A.2). The total oxidant concentration was then determined using the average absorbance over the 30 second collection period in conjunction with a total oxidant calibration curve. All experiments were performed in at least duplicate to ensure precision of the data (Appendix A, Figure A.3).

PPCP and Byproduct Analysis. Byproduct experiments were performed with a two- to ten-fold excess of oxidant using both the QFS system and batch reactors (13). Following an allotted reaction period, the experimental solutions were mixed with a slight excess of sodium sulfite to quench the reaction. Sodium sulfite was chosen as the quenching agent because it is generally unreactive towards PPCPs and their daughter products (17). QFS solutions were collected in 40 mL amber vials. Products were extracted from solution and analyzed using GC-MS for phenolic byproducts and using GC-ECD for THMs. Detailed experimental methods are described elsewhere (13, 17). Compounds and byproducts were identified by m/z ratios of fragment ions from their GC chromatograms. Calibration curves were produced for 2,4-dichlorophenol, 2,4,6-trichlorophenol, and triclosan to assess product concentrations. However, standards for the remaining byproducts were not available for purchase. As such, relative abundances will be focused upon in the discussion section.

Model Development. A computer model was developed using the chemical kinetics program MicroMath Scientist (Salt Lake City, UT) that can predict oxidant reactivity with triclosan (Appendix B). Variables such as species concentrations, pH, and temperature are assigned unique names. Differential equations and mass balances were developed that describe the chemical reactions for each reactant. The program utilizes differential equations that describe the dependence of reaction rates on temperature to calculate the specific rate constants for a given system. Using a sequential fitting approach, unknown rate parameters were systematically determined. These equations were then used to write a computer program where each equation is solved for a given set of variables over a number of iterations. The model initially sets each variable to the value that is input by the user. Scientist then inputs the assigned values to an EPISODE numerical integration package to solve the set of simultaneous differential equations for the variables of interest. The input values are updated by the software following each iteration as the equations are solved. By setting the model to perform a large number of iterations, it is able to make highly accurate predictions for complex chemical relationships over time.

4.3: Results and Discussion

Oxidant Consumption Kinetics. The kinetics of total oxidant loss due to the electrophilic substitution of triclosan were significantly enhanced when iodide was present relative to the kinetics in its absence (Figure 4.1). As discussed in Chapter 3, a pseudo-first-order approximation was utilized to describe the kinetics of reactions containing excess triclosan as a function of solution pH. For experiments performed with triclosan concentrations in excess of the total oxidant concentrations, apparent second-order rate constants ($k_{app} = k_{obs}$/[triclosan],

$M^{-1}s^{-1}$) were determined for each experimental data set for over a pH range from 5.5 to 10. The apparent second-order rate constants are pseudo-first-order rate constants that have been normalized with respect to the initial triclosan concentration to enable direct comparisons between experiments with different reaction conditions. The calculated k_{app} values show that both free chlorine and free iodine readily react with triclosan and that the kinetics are dependent upon both the solution pH and the iodide to free chlorine ratio (Figure 4.2). At circumneutral pH, the free iodine mediated reactions are ≈20× faster than those only involving free chlorine. In comparison, it was observed that free iodine mediated reactions are only 10× faster than free chlorine mediated reactions for 2,4-dichlorophenol (Chapter 3). The lower apparent reaction rates observed for 2,4-dichlorophenol result primarily from the presence of two chlorine substituents on the phenol ring. Each halide substitution onto a phenolic ring increases the stability of the overall phenolic compound. Chlorine atoms are highly electrophilic (i.e., electron loving) so when attached to an instable phenol ring, they attract the electrons from the ring effectively delocalizing the charge (41). As a result, 2,4-dichlorophenol, with its ortho and para positioned electron-accepting chlorines, is a much stronger acid; meaning the negatively charged phenolate form (PhO^-) is much more stable and resistant to subsequent electrophilic attack. Triclosan only has a single meta-substituted chlorine on the phenolic ring so it lacks the enhanced stability of 2,4-DCP. There is also an ortho-substituted O-$C_6H_3Cl_2$ group, but the stabilizing effect of this substituent is significantly lower than for a second chlorine substitution (42). The corresponding pK_a values illustrate these effects- the pK_a of 2,4-dichlorophenol is 7.85 compared to triclosan's pK_a of 8.14. The lower value for 2,4-DCP illustrates the fact that it is a stronger acid and therefore more stable in the PhO^- form than

triclosan. This means that free chlorine will more commonly be in the less reactive, negatively charged OCl^- form at circumneutral pH than would free iodine so reactions kinetics should be slower. In addition to the reactivity of the phenolic compound, the reactivity of the oxidant plays a major role in the overall reaction kinetics. The apparent reaction rate of triclosan is 20× greater with free iodine than it is with free chlorine, as opposed to ten-fold difference observed for 2,4-dichlorophenol. This is because free iodine is a more sensitive oxidant to substitution effects for the reaction with PhO^- anions than is free chlorine. Free iodine more affected by the presence of a halogen substituent on the ring of a phenolic compound because iodide is less electronegative than chlorine and is less able to compete with the substituents on a phenol ring for available electrons. Chlorine has a stronger electronegativity (or at least equal, in the case of a chlorine substitution) than the halogen substituents present on a phenol ring, so can compete for the sharing of electrons more easily.

Modeling results. To evaluate the collected oxidant consumption data, a model was developed using the Micromath Scientist software program. Reaction rate constants were fit to the data using a sequential fitting approach as described in Appendix B where individual rate constants were simultaneously fit to oxidant consumption data collected at multiple pH values. Parameters were initially fit for a subset of data over a pH range for which a given reaction has the largest influence on the overall solution reactivity. As shown by equations 4.22-4.24, differential equations describing each potential substitution reaction involving triclosan were developed to consider every possible reaction between the PhOH or PhO^- triclosan species and each of the potentially reactive free chlorine and free iodide species. These equations were developed analogous to equations 3.37, 3.40, and 3.41 in Chapter 3. For brevity, we only wrote

the final differential equations here as individual reactions are depicted by equations 3.17-3.36 in Chapter 3.

$$\frac{d[\text{free chlorine}]}{dt} = -(k_{4.1}[\mathrm{Cl_2}] + k_{4.3}[\mathrm{H_2OCl^+}] + k_{4.5}[\mathrm{HOCl}] + k_{4.7}[\mathrm{OCl^-}])[\mathrm{PhOH}]$$
$$-(k_{4.2}[\mathrm{Cl_2}] + k_{4.4}[\mathrm{H_2OCl^+}] + k_{4.6}[\mathrm{HOCl}] + k_{4.8}[\mathrm{OCl^-}])[\mathrm{PhO^-}] \quad (4.22)$$

$$\frac{d[\mathrm{I^-}]}{dt} = -k_{4.9}[\mathrm{HOCl}][\mathrm{I^-}] + (k_{4.10}[\mathrm{I_2}] + k_{4.18}[\mathrm{HOI_2^-}] + 2 \cdot k_{20}[\mathrm{I_3^-}])[\mathrm{PhOH}]$$
$$+(k_{4.11}[\mathrm{I_2}] + k_{4.19}[\mathrm{HOI_2^-}] + 2 \cdot k_{4.21}[\mathrm{I_3^-}])[\mathrm{PhO^-}] \quad (4.23)$$

$$\frac{d[\text{free iodine}]}{dt} = k_{4.9}[\mathrm{HOCl}][\mathrm{I^-}]$$
$$-(k_{4.10}[\mathrm{I_2}] + k_{4.12}[\mathrm{H_2OI^+}] + k_{4.14}[\mathrm{HOI}] + k_{4.16}[\mathrm{OI^-}] + k_{4.18}[\mathrm{HOI_2^-}] + k_{4.2}[\mathrm{I_3^-}])[\mathrm{PhOH}]$$
$$-(k_{4.11}[\mathrm{I_2}] + k_{4.13}[\mathrm{H_2OI^+}] + k_{4.15}[\mathrm{HOI}] + k_{4.17}[\mathrm{OI^-}] + k_{4.19}[\mathrm{HOI_2^-}] + k_{4.21}[\mathrm{I_3^-}])[\mathrm{PhO^-}]$$
(4.24)

This is the same general model as was utilized for the 2,4-DCP modeling exercise in Chapter 3. The primary change from the 2,4-dichlorophenol model was that the phenol pK_a was adjusted to the reflect the value for triclosan (pK_a = 8.14). Relative to 2,4-DCP, the higher pK_a of triclosan results in reduced concentrations of the more reactive PhO^- form at circumneutral pH.

At the onset of the fitting process, the $k_{4.6}$ rate constant was fixed at 5.4×10^3 $M^{-1}s^{-1}$ as determined in a recent study by Rule et al (17). The model was initially fit to experimental data obtained in the absence of iodide using only the free chlorine differential equation (Equation 4.22) and the equilibrium relationships described by equations 4.25-4.27. Each rate constant was sequentially fit to the data until an optimal data fit was obtained. Individual reactions were then sequentially omitted while continuing to assess the fits for the remaining parameters. By assessing whether the updated rate constants were able to estimate the experimental data

when a single reaction was omitted, the importance of each individual reaction could be determined and inconsequential reactions removed. This process simplified the programming and enabled faster optimization of the remaining reaction rates.

$$Cl_2 + H_2O \longleftrightarrow HOCl + Cl^- + H^+ \qquad K_{4.25} = 5.1\times10^{-4}\ M^2 \qquad (4.25)$$

$$HOCl \longleftrightarrow OCl^- + H^+ \qquad K_{4.3} = 2.9\times10^{-8}\ M \qquad (4.26)$$

$$PhOH \longleftrightarrow PhO^- + H^+ \qquad K_{4.27} = 7.24\times10^{-9}\ M \qquad (4.27)$$

This modeling exercise led to the conclusion that the electrophilic substitution of triclosan by free chlorine occurs by the same mechanism as that of 2,4-dichlorophenol. The rate controlling reactions over the experimental pH range are as follows:

$$HOCl + PhOH \xrightarrow{k_{4.5}} products \qquad (4.5)$$

$$HOCl + PhO^- \xrightarrow{k_{4.6}} products \qquad (4.6)$$

where PhOH and PhO^- are the neutral and phenolic forms of triclosan, respectively, and 'products' represents a monochlorinated triclosan species (i.e., 5,6-dichloro-2-(2,4-dichlorophenoxy)phenol or 4,5-dichloro-2-(2,4-dichlorophenoxy)phenol). For reactions with excess triclosan and limiting free chlorine, only a single chlorine substitution is expected and the rate equation is described by equation 4.28:

$$\frac{d[\text{free chlorine}]}{dt} = \frac{d[\text{triclosan}]}{dt} = -k_{4.5} \cdot [\text{HOCl}] \cdot [\text{PhOH}] - \text{k}_{4.6} \cdot [\text{HOCl}] \cdot [\text{PhO}^-] \qquad (4.28)$$

where [free chlorine] and [triclosan] represent the total concentrations of free chlorine (i.e., $[Cl_2]$ + [HOCl] + $[OCl^-]$) and triclosan (i.e. [triclosan] + [phenolate-triclosan]), respectively. The rate constant from Rule et al. (17) fit the data very well for circumneutral and more basic pH experiments. The model's predictive capabilities were enhanced at pH ≤ 7 by inclusion of reaction 4.5, with a $k_{4.5}$ value of 3.7 (± 0.3) × 10^2 $M^{-1}s^{-1}$. Because the value of $k_{4.5}$ was a little

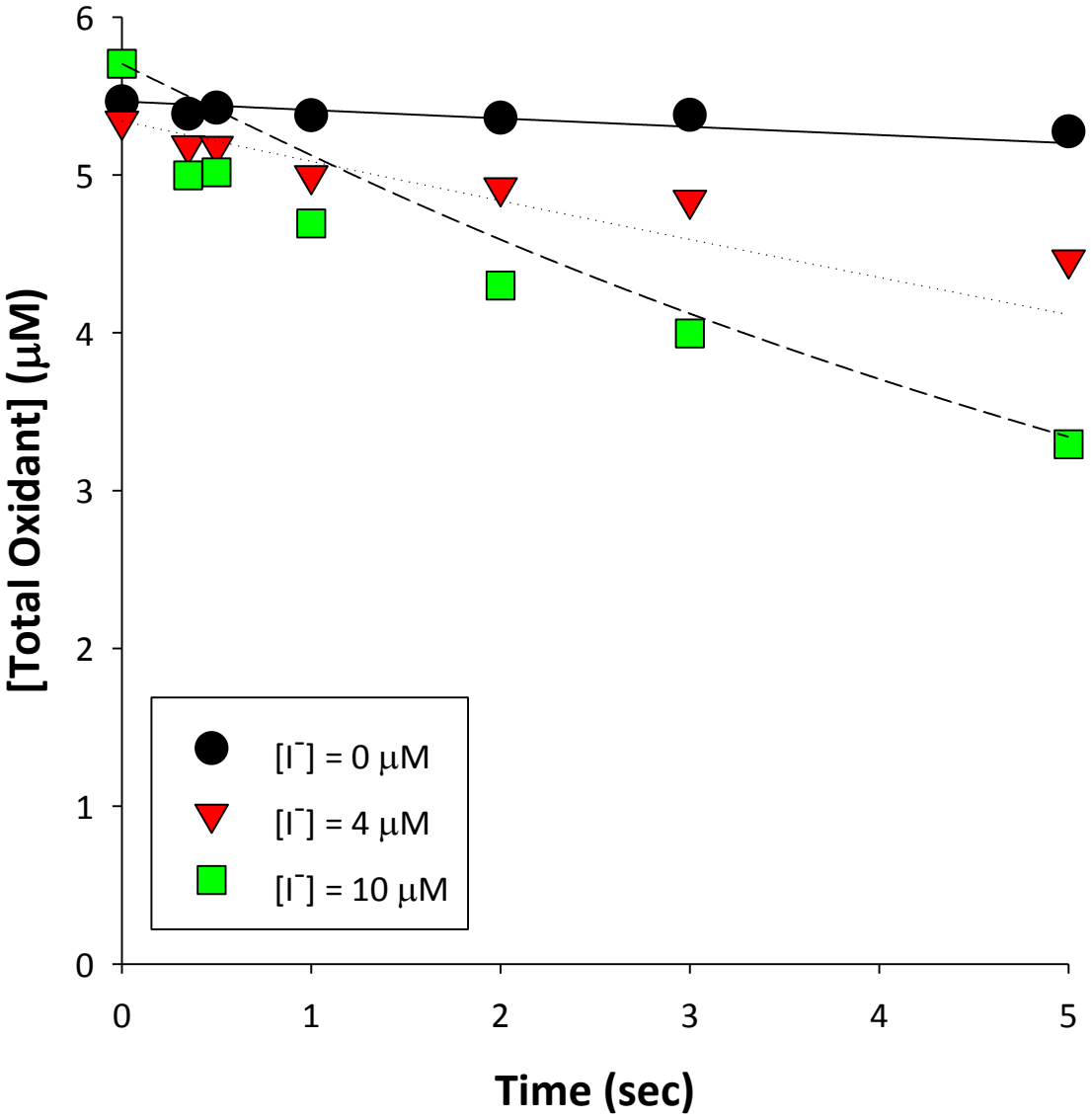

Figure 4.1: Total oxidant consumption over time due to reactions with triclosan with free chlorine in the presence of variable iodide. Curves represent model predictions. Conditions: pH = 6.5, $[\text{free chlorine}]_i$ = 5.3-5.7 μM, $[\text{triclosan}]_i$ = 25 μM, $[NaHCO_3]$ = 2 mM. Standard errors for individual data points are <0.1%.

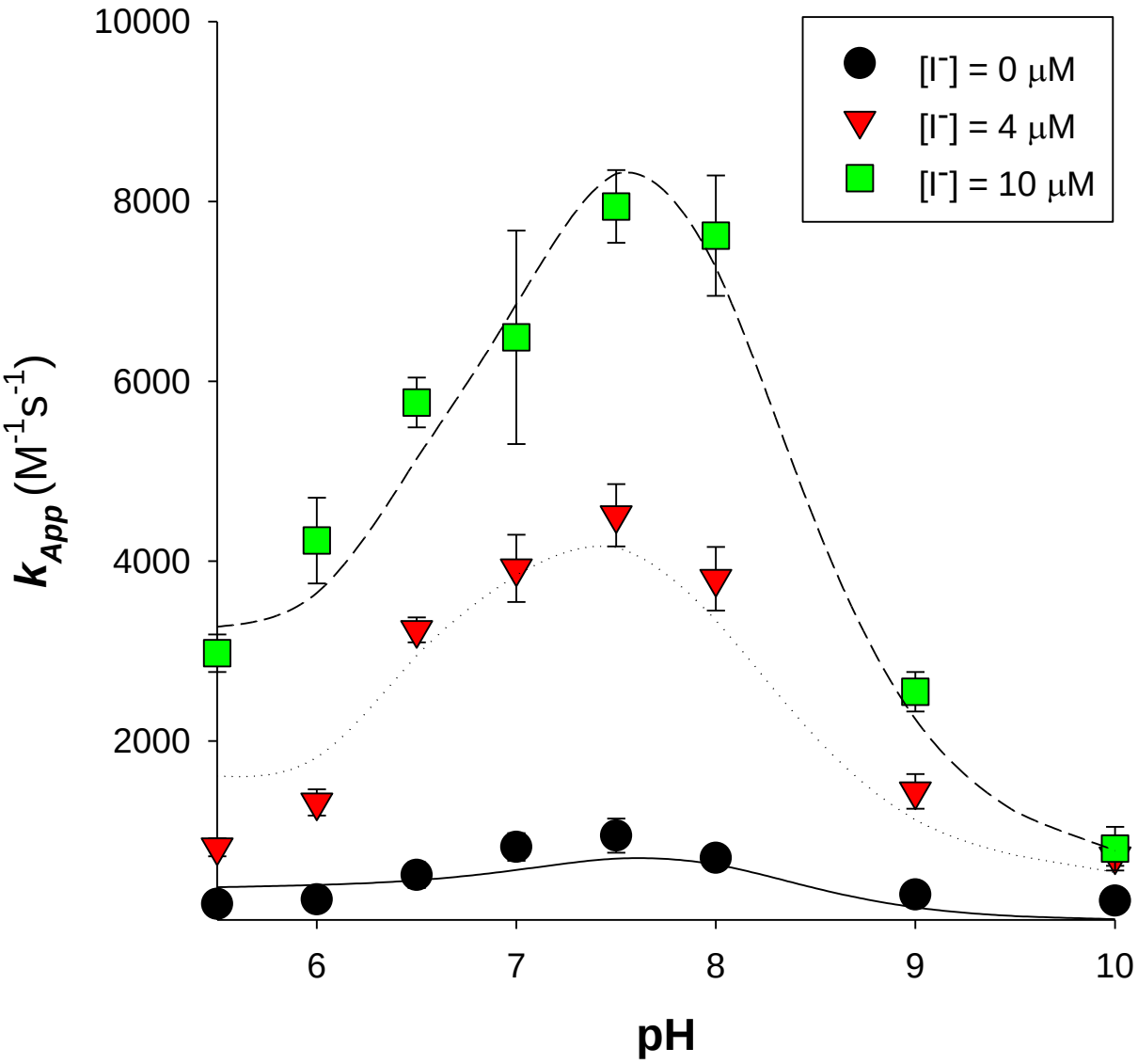

Figure 4.2: Psuedo-first-order observed rate constants plotted versus pH for variable iodide concentration. The model predictions are represented by the curves. Error bars represent 95% confidence intervals.

more than an order of magnitude lower than $k_{4.6}$, it makes sense that the concentration of PhOH-triclosan would need to be an order of magnitude higher than the PhO^- form before the influence of this reaction was observed. The point where reaction 4.5 becomes rate dominating would be near one pH unit below the pK_a (i.e. one log unit), which is the reason why the accuracy of model predictions were found to deteriorate below pH 7 as discussed previously. As was the case for 2,4-dichlorophenol, the experimental pH range did not extend far enough into the acidic range to assess the influence of Cl_2 reactivity. Since Cl_2 is a typically strong oxidant, we would anticipate that the Cl_2-PhOH reaction plays a role in triclosan substitution reactions.

The same modeling procedure as was used for the chlorine mediated reactions was used to obtain rate constants for the iodine mediated reactions using data obtained from experiments when 10 μM of iodide was initially present. For 10 μM initial free chlorine and 10 μM initial I^-, chlorine based oxidants can account for around 50% of the total oxidant concentration under acidic conditions (see Chapter 3). For this reason, each of the chlorine reactions described above was included in the modeling exercise with the rate constants fixed at the values previously determined. Differential equations accounting for free iodine reactivity and the consumption/production of I^- were developed as shown by equations 4.23-4.24. Equilibrium expressions of each iodine-containing species were included as illustrated by equations 4.29-4.33 as well as the oxidation of iodide to HOI by HOCl as described by equation 4.34.

$$I_2 + H_2O \longleftrightarrow HOI + I^- + H^+ \qquad K_{4.29} = 5.44\times10^{-13}\ M^2 \qquad (4.29)$$

$$HOI \longleftrightarrow OI^- + H^+ \qquad K_{4.30} = 2.3\times10^{-11}\ M \qquad (4.30)$$

$$I_2 + I^- \longleftrightarrow I_3^- \qquad K_{4.31} = 715\ M^{-1} \qquad (4.31)$$

$H_2OI^+ \longleftrightarrow HOI + H^+$ $K_{4.32} = 2$ M (4.32)

$HOI_2^- \longleftrightarrow HOI + I^-$ $K_{4.33} = 3.1\times10^{-3}$ M (4.33)

$HOCl + I^- \xrightarrow{k_{4.34}} HOI + Cl^-$ $k_{4.34} = 4.3 \times 10^8$ $M^{-1}s^{-1}$ (4.34)

This modeling exercise again led to the conclusion that electrophilic substitution of triclosan by free iodine could be described by the same general mechanism as 2,4-dichlorophenol. The rate controlling reactions are described by equations 4.10-4.11 and 4.15.

$I_2 + PhOH \xrightarrow{k_{4.10}} products + I^-$ (4.10)

$I_2 + PhO^- \xrightarrow{k_{4.11}} products + I^-$ (4.11)

$HOI + PhO^- \xrightarrow{k_{4.15}} products$ (4.15)

Since experiments were performed with excess triclosan, the primary reactions occurring would again be single electrophilic substitutions, so the 'products' formed by reactions 4.10, 4.11, and 4.15 would be monoiodinated triclosan (i.e., 5-chloro-6-iodo-2-(2,4-dichlorophenoxy)phenol or 5-chloro-4-iodo-2-(2,4-dichlorophenoxy)phenol). Kinetics of triclosan substitution by free iodine is described by equation 4.35:

$$\frac{d[\text{free iodine}]}{dt} = \frac{d[\text{Total DCP}]}{dt} = k_{4.34}[\text{HOCl}][\text{I}^-] - k_{4.10}[\text{I}_2][\text{PhOH}] - (k_{4.11}[\text{I}_2] + k_{4.15}[\text{HOCl}])[\text{PhO}^-] \quad (4.35)$$

where [free iodine] is the total concentration of free iodine (i.e., $[I_2]$ + $[HOI]$ + $[OI^-]$ + $[H_2OI^+]$ + $[HOI_2^-]$ + $[I_3^-]$). Rate constants for reactions 4.10-4.11 and 4.15, as determined through the sequential fitting approach, illustrate that $k_{4.10}$ and $k_{4.11}$ are the primary rate controlling reactions with rate constants of 4.0 (± 0.7) × 10^3 and 1.1 (± 0.1) × 10^5 $M^{-1}s^{-1}$, respectively. Reactions 4.10 and 4.11 have the greater effect upon the overall reaction rate at circumneutral

to slightly acidic pH. The influence of reaction 4.15 is observed in basic solutions ($k_{4.15}$ = 1.1 (± 0.6) × 10^3 $M^{-1}s^{-1}$). Reaction rates for all other species were fixed at zero because their inclusion in the model either negatively affected the overall accuracy of the predictions or had no discernible effect. For instance, while a reaction between HOI and neutral triclosan may occur, its magnitude is small enough to be dwarfed by the reactivity of I_2 with either triclosan species. This is exacerbated by the fact that HOI concentrations only begin to dominate above a pH of ≈7.3 and phenolate-triclosan becomes the dominant species at a pH of 8.14, so the overall influence of the HOI-triclosan reaction cannot be distinguished from other reactions.

The rate constants determined under conditions with a total initial iodide concentration of 10 μM were then used to predict oxidant demand for experiments with 4 μM of initial iodide. The model predictions, as shown by the plotted curves in Figure 4.1 and 4.2, are able to predict oxidant consumption over time very accurately for each tested iodide concentration. No literature values for the iodination of triclosan are available in the literature so these rate constants cannot be compared to published values.

Triclosan consumption and product formation kinetics. Kinetic experiments were performed in which the triclosan concentration was measured over time. These experiments were conducted to assess the ability of the model to predict triclosan consumption rates. The model was run with each rate constant being fixed at the values determined the in oxidant demand experiments. The reaction behavior as predicted by the model for a pH 7 solution (curves) is shown as compared to the experimentally measured triclosan concentrations (points) in Figure 4.3i. The predictions fit the experimental data quite well further supporting the validity of the model and illustrating its general predictive capabilities.

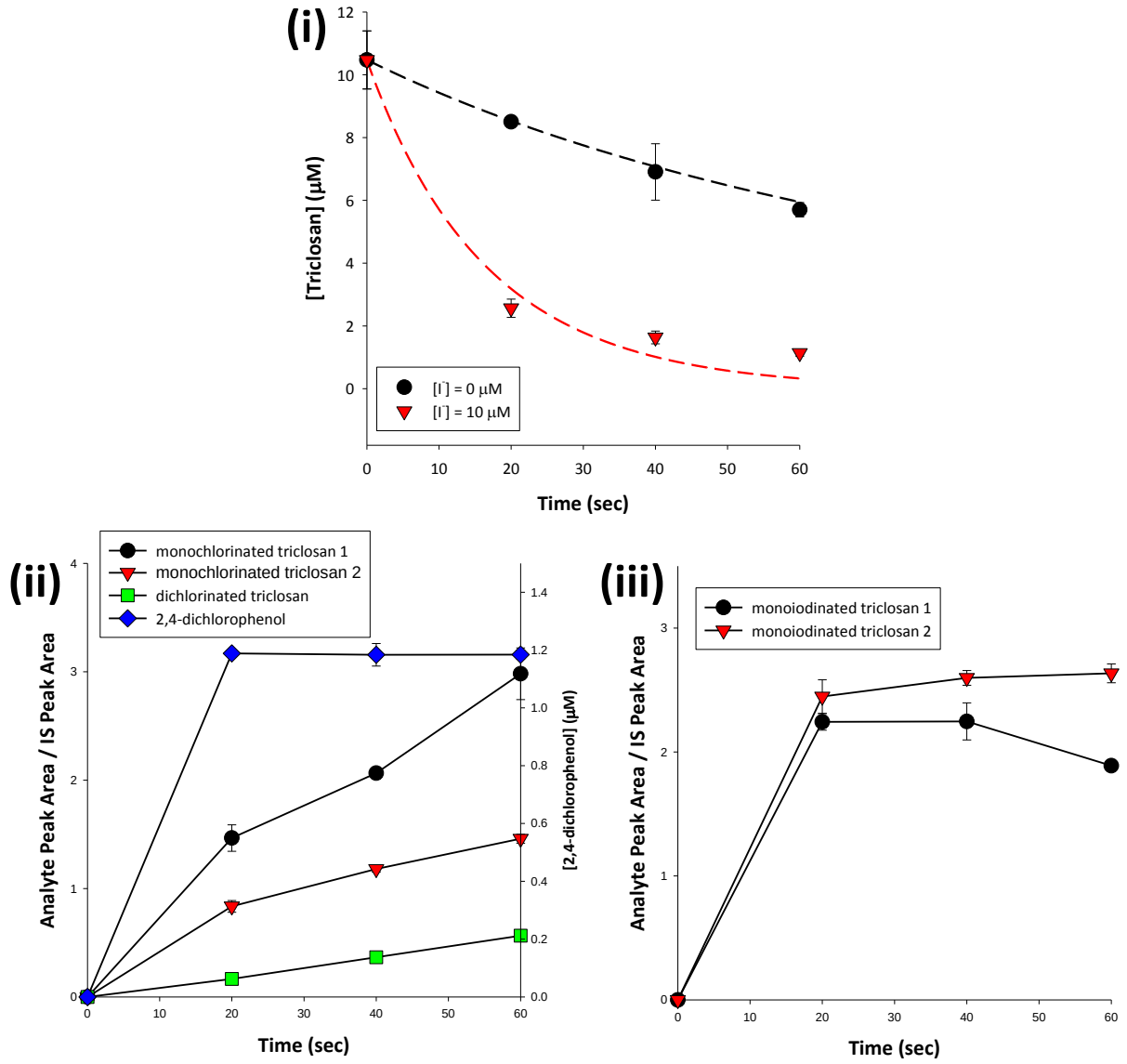

Figure 4-3: Electrophillic substitution of triclosan over time at pH 7 for experiments with [free chlorine]$_i$ = 20 μM, [triclosan]$_i$ = 10.4-10.5 μM, and [$NaHCO_3$] = 2 mM. Figures show triclosan loss (i) for initial iodide concentrations of 0 (ii) and 10 mM (iii). In the absence of I^-, four different daughter products were detected: 2,4-DCP, 5,6-dichloro-2-(2,4-dichlorophenoxy)phenol (monochlorinated triclosan 1), 4,5-dichloro-2-(2,4-dichlorophenoxy)phenol (monochlorinated triclosan 2), and 4,5,6-trichloro-2-(2,4-dichlorophenoxy)phenol (dichlorinated triclosan). With 10 μM iodide, only 5-chloro-6-iodo-2-(2,4-dichlorophenoxy)phenol (monoiodinated triclosan 1) and 5-chloro-4-iodo-2-(2,4-dichlorophenoxy)phenol (monoiodinated triclosan 2) were detected.

When iodide was absent, 4.8 μM of the starting 10.5 μM of triclosan was consumed over the 1 minute reaction period. As expected based on previous research (Rule et al.; Fiss et al.; refs. (13, 17)), the formation of two monochlorinated (5,6-dichloro-2-(2,4-dichlorophenoxy)phenol and 4,5-dichloro-2-(2,4-dichlorophenoxy)phenol) and one dichlorinated (4,5,6-trichloro-2-(2,4-dichlorophenoxy)phenol) triclosan daughter product were observed. Over the 1 minute reaction time period, the normalized peak areas of both the monochlorinated and dichlorinated triclosan daughter products continually increased in size. Since free chlorine was in excess of triclosan, it was not surprising that a second halogenation occurred. The increase in signal peak area directly corresponds to an increase in product concentration, so it is apparent that chlorine substitution reactions were occurring. When the normalized signal peak areas were plotted versus time (Figure 4.3ii), a steeper slope was observed for the formation of 5,6-dichloro-2-(2,4-dichlorophenoxy)phenol and 4,5-dichloro-2-(2,4-dichlorophenoxy)phenol than was observed for the 4,5,6-trichloro-2-(2,4-dichlorophenoxy)phenol slope. This result is consistent with the stepwise chlorination of triclosan to first form either 5,6-dichloro-2-(2,4-dichlorophenoxy)phenol or 4,5-dichloro-2-(2,4-dichlorophenoxy)phenol, followed by the chlorination of these daughter products to produce 4,5,6-trichloro-2-(2,4-dichlorophenoxy)phenol. The literature has illustrated that additional reactions with chlorine can cleave the ether bond between the two benzene rings in triclosan resulting in the formation of 2,4-dichlorophenol and 2,4,6-triclorophenol (17). In these experiments, 2,4-dichlorophenol was detected at a concentration of 1.2 μM after 20 seconds of reaction time and it remained fairly constant over the entire experimental time range. Formation of 2,4,6-trichlorophenol was not observed within the 60 second reaction period.

In the presence of 10 μM iodide, 9.4 μM of the initial 10.5 μM of triclosan was consumed over the reaction time period- nearly twice the amount consumed by free chlorine alone. Large product peaks were detected for two monoiodinated triclosan moieties (5-chloro-6-iodo-2-(2,4-dichlorophenoxy)phenol and 5-chloro-4-iodo-2-(2,4-dichlorophenoxy)phenol) after 20 seconds and the peak areas for these daughter products remained constant over the entire reaction time period (Figure 4.3iii). However, unlike the free chlorine mediated reactions, no diiodinated triclosan was detected. Furthermore, no chlorinated triclosan daughter products were detected nor were any products resulting from the cleavage of the ether bond. Since free iodine is largely present in the form of I_2 at pH 7, the starting triclosan concentration is in excess of free iodine so multiple iodine substitutions would be unexpected. Because the first iodine substitution occurs extremely quickly and seems to consume the majority of the available triclosan (> 80% of triclosan is consumed within the first 20 seconds), the lack of chlorine-substituted products may simply be due to the fact that not enough triclosan remains to react and that chlorine reactions with monoiodinated triclosan are slow. The reduced reactivity of free chlorine with iodine-substituted phenols is shown by Figure 3.8 in Chapter 3. Reactions were performed in which 20 μM of free chlorine was spiked into solutions containing 10.4 μM of 4-chlorophenol or 4-iodophenol at pH 7. Chlorine reactions with 4-CP in the absence of iodide resulted in a 10% greater loss of the parent compound than did 4-IP reactions with identical reaction conditions.

Product formation with 10× excess oxidant. To further explore triclosan daughter product formation, experiments over extended time periods (t = 5 min) were performed where 7.7-8.1 μM of triclosan was contacted with 100 μM of free chlorine in the presence of 0, 4, and 10 μM

iodide at pH 7 (Figure 4.4). An extended reaction time of 5 minutes was used to increase our understanding of the overall fate of triclosan during disinfection practices. For experiments in the absence of iodide, there remained ≈0.1 μM of triclosan at the completion of the experimental time period. As in the triclosan kinetic experiments, 5,6-dichloro-2-(2,4-dichlorophenoxy)phenol, 4,5-dichloro-2-(2,4-dichlorophenoxy)phenol and 4,5,6-trichloro-2-(2,4-dichlorophenoxy)phenol daughter products were detected in the absence of iodide due to the electrophilic substitution of chlorine onto the phenol ring. Additionally, oxidative cleavage of the carbon-oxygen bond between the phenol ring and the chlorobenzene ring in triclosan led to the formation of 2,4-dichlorophenol and ultimately 2,4,6-trichlorophenol. A reaction time of 5 minutes resulted in the formation of 0.76 and 0.49 μM of 2,4-DCP and 2,4,6-TCP, respectively.

At 4 μM initial iodide, only 0.06 μM of triclosan remained at the end of the 5 minute reaction time. As was the case for the free chlorine samples, the 5,6-dichloro-2-(2,4-dichlorophenoxy)phenol and 4,5-dichloro-2-(2,4-dichlorophenoxy)phenol peaks were again detected as well as the 4,5,6-trichloro-2-(2,4-dichlorophenoxy)phenol peak. The magnitudes of both the 5,6-dichloro-2-(2,4-dichlorophenoxy)phenol and 4,5-dichloro-2-(2,4-dichlorophenoxy)phenol peaks were virtually identical to those observed when only free chlorine was present and a slight decrease in the magnitude of the 4,5,6-trichloro-2-(2,4-dichlorophenoxy)phenol peak was observed. In addition to the chlorinated products, a peak matching the spectral breakdown of 4,5-dichloro-6-iodo-2-(2,4-dichlorophenoxy)phenol was identified (m/z = 630, 449). No discernable peaks were detected matching a singly or doubly iodinated triclosan, though the latter was not expected since triclosan was in excess of free iodine. Because free chlorine was also in excess of free iodine, the extended reaction times

allowed for chlorine substitutions to occur for 5-chloro-6-iodo-2-(2,4-dichlorophenoxy)phenol and 5-chloro-6-iodo-2-(2,4-dichlorophenoxy)phenol to an extent sufficient to prevent detection of either. Again, both 2,4-dichlorophenol and 2,4,6-trichlorophenol were identified, though concentrations were less than in the presence of only free chlorine ([2,4-DCP] = 0.52 μM and [2,4,6-TCP] = 0.30 μM). An additional peak was identified matching 2,4-dichloro-6-iodophenol (m/z = 468, 287).

For 10 μM initial iodine experiments, less than 0.03 mM triclosan remained after 5 minutes of reaction time. Both the 5,6-dichloro-2-(2,4-dichlorophenoxy)phenol and 4,5-dichloro-2-(2,4-dichlorophenoxy)phenol peaks were again detected as well as the 4,5,6-trichloro-2-(2,4-dichlorophenoxy)phenol peak. The monochlorinated peaks were of greater magnitude than for either of the previous experiments, while the dichlorinated triclosan peak area was reduced by over 80% as compared to the corresponding peaks for $[I^-]$ = 0 or 4 μM experiments. This trend is likely the result of the increased initial iodide concentration. The free chlorine oxidation of I^- consumed enough free chlorine so as to inhibit the occurrence of multiple chlorine substitutions within the allotted reaction time. Both 5-chloro-6-iodo-2-(2,4-dichlorophenoxy)phenol and 5-chloro-4-iodo-2-(2,4-dichlorophenoxy)phenol were detected, and a peak corresponding to 4,5-dichloro-6-iodo-2-(2,4-dichlorophenoxy)phenol was also identified. It is apparent that the single iodine-substitutions are occurring at two different sites since two peaks with identical spectra, both matched to that of monoiodinated triclosan daughter products (m/z = 594, 415), are eluting from the GC-MS column at different times. Two forms of the monochloro-monoiodo-triclosan (4,5-dichloro-6-iodo-2-(2,4-dichlorophenoxy)phenol and 5,6-dichloro-4-iodo-2-(2,4-dichlorophenoxy)phenol) are expected

to form, though only a single peak was identified. This suggests that the two sister compounds are of similar polarity and were not sufficiently separated during elution through the GC-MS column. No doubly-iodinated triclosan daughter products were detected. Since it was determined that 60 minutes is more than sufficient time to allow for the elution of diiodinated triclosan (monoiodinated triclosan elutes after 26 minutes), the lack of detection of multiple iodide substitutions on a single triclosan molecule was attributed to the fact that only 10 μM of iodine was initially present. That means the maximum amount of free iodine that could form would also be 10 μM. At pH 7, the total free iodine present is further limited by the presence of substantial amounts of I_2, so one might expect that only a single iodine substitution would occur. It follows that multiple iodine substitutions simply did not occur with enough frequency to allow for the detection of diiodinated products. Since free chlorine is present in concentrations nearing 10× that of iodine, substantial concentrations of free chlorine remain after the oxidation of I^- to HOI. This remaining free chlorine proceeds to react with the triclosan and monoiodotriclosan to produce chlorinated products, which explains the continued detection of substantial 5,6-dichloro-2-(2,4-dichlorophenoxy)phenol, 4,5-dichloro-2-(2,4-dichlorophenoxy)phenol, and 4,5,6-trichloro-2-(2,4-dichlorophenoxy)phenol daughter products. The products resulting from ring cleavage included 2,4-dichlorophenol and 2,4,6-trichlorophenol in concentrations of 0.26 and 0.01 μM, respectively, as well as an extremely small 2,4-dichloro-6-iodophenol peaks.

In general, increasing the iodine to free chlorine ratio resulted in reduced quantities of chlorine-substituted products and an increase in iodine-substituted products. The lack of detection of monoiodinated triclosan in the 4 μM iodine experiments is likely due to insufficient

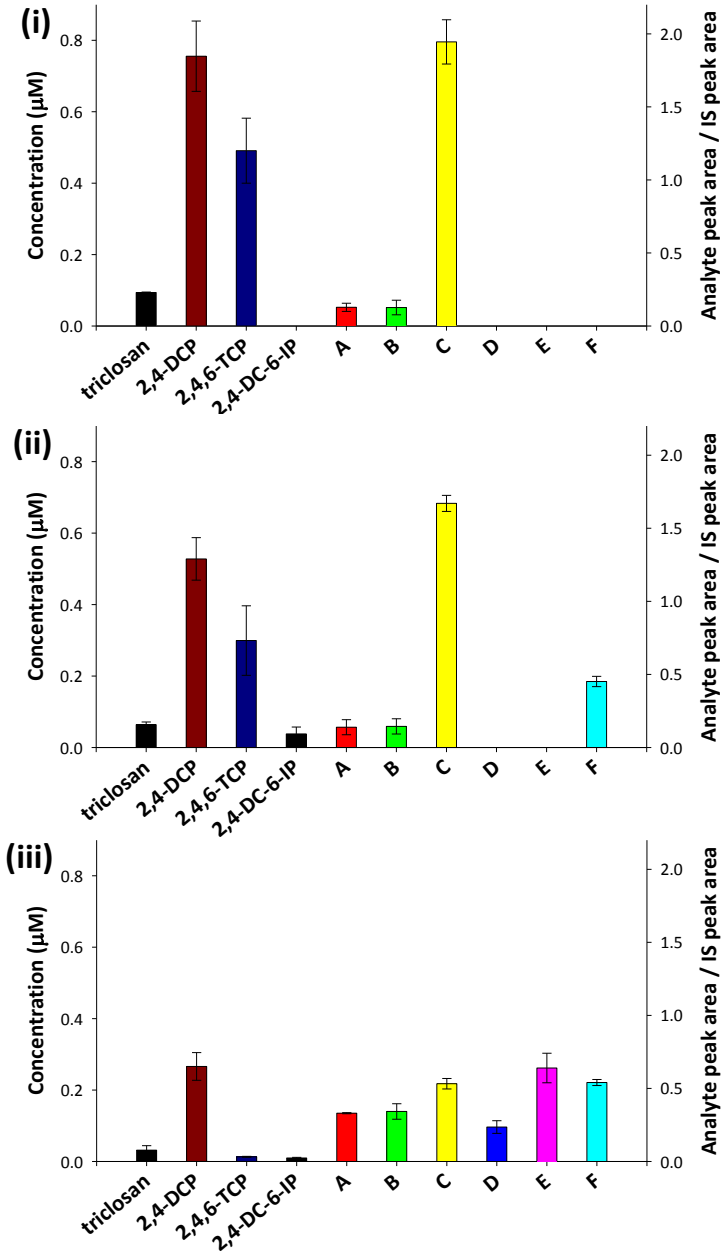

Figure 4.4: Product formation after a 5 minute reaction time for triclosan in the presence of free chlorine and 0 (i), 4 (ii), or 10 (iii) μM of initial iodide. Results reported as concentration for triclosan, 2,4-DCP, and 2,4,6-TCP and as normalized peak area for all other compounds. Conditions: $[\text{free chlorine}]_i$ = 100 μM, $[\text{triclosan}]_i$ = 7.74-8.11 μM, $[NaHCO_3]$ = 2 mM, pH = 7. Other products include 5,6-dichloro-2-(2,4-dichlorophenoxy)phenol (A), 4,5-dichloro-2-(2,4-dichlorophenoxy)phenol (B), 4,5,6-trichloro-2-(2,4-dichlorophenoxy)phenol (C), 5-chloro-6-iodo-2-(2,4-dichlorophenoxy)phenol (D), 5-chloro-4-iodo-2-(2,4-dichlorophenoxy)phenol (E), and 4,5-dichloro-6-iodo-2-(2,4-dichlorophenoxy)phenol (F).

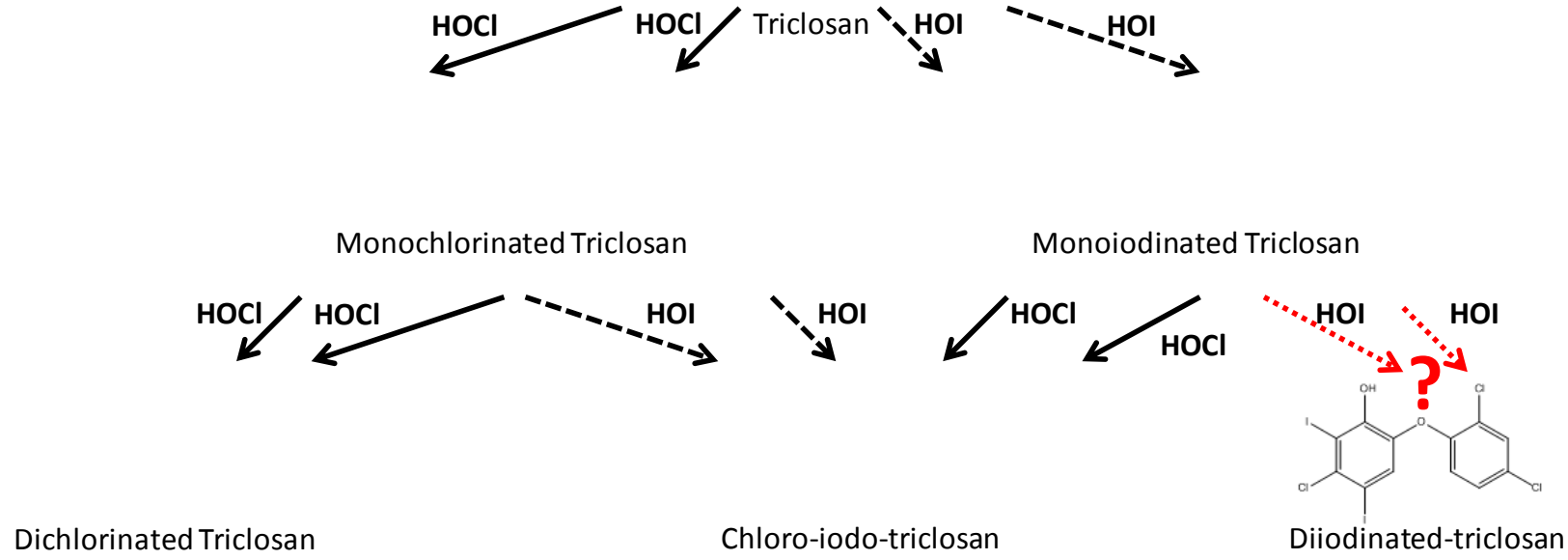

Figure 4.5: Proposed reaction pathway for the electrophilic substitution of triclosan by free chlorine and free iodine. Each product can undergo oxidataive cleavage of the ester bond between rings to form 2,4-dichlorophenol, 2,4,6-trichlorophenol, and 2,4-dichloro-6-iodophenol.

detection limits and does not mean that single iodine substitutions simply are not occurring. If excess iodine was present over that of triclosan, we would also expect to see the formation of diiodinated triclosan. Figure 4.5 illustrates the reaction mechanism for the electrophilic substitution of triclosan as suggested by our findings.

4.4: Conclusions

- Free chlorine reactions with triclosan initially occur through the electrophilic substitution reactions described by equations 4.5 and 4.6 with values for the rate constants as listed. The rate for reaction 4.6 was taken from a study by Rule et al. (17) while the value for $k_{4.5}$ was determined by our modeling exercise.

$$\mathbf{HOCl} + \mathrm{PhOH} \xrightarrow{k_{4.5}} \mathbf{products} \qquad k_{4.5} = 3.7\ (\pm 0.3) \times 10^2\ M^{-1}s^{-1} \qquad (4.5)$$

$$\mathrm{HOCl} + \mathrm{PhO^-} \xrightarrow{k_{4.6}} \mathrm{products} \qquad k_{4.6} = 5.4 \times 10^3\ M^{-1}s^{-1} \qquad (4.6)$$

  This new rate constant suggests that triclosan is more reactive in acidic conditions that previously thought.

- Free iodine reactions with triclosan also initially occur through electrophilic substitution as described by equations 4.10-4.11 and 4.15 with second-order reaction rates as follows:

$$\mathrm{I_2} + \mathrm{PhOH} \xrightarrow{k_{4.10}} \mathrm{products} + \mathrm{I^-} \qquad k_{4.10} = 4.0\ (\pm 0.7) \times 10^3\ M^{-1}s^{-1} \qquad (4.10)$$

$$\mathrm{I_2} + \mathrm{PhO^-} \xrightarrow{k_{4.11}} \mathrm{products} + \mathrm{I^-} \qquad k_{4.11} = 1.1\ (\pm 0.1) \times 10^5\ M^{-1}s^{-1} \qquad (4.11)$$

$$\mathrm{HOI} + \mathrm{PhO^-} \xrightarrow{k_{4.15}} \mathrm{products} \qquad k_{4.15} = 1.1\ (\pm 0.6) \times 10^3\ M^{-1}s^{-1} \qquad (4.15)$$

  This result is important because it suggests that iodine can result in much higher triclosan reactivity than observed with free chlorine.

- The presence of 10 μM of iodide results a 75-90% reduction in chlorinated products but increased the amount of triclosan consumed suggesting that even greater quantities of iodinated byproducts are formed. The toxicity of these byproducts needs to be further studied so that the risk to public health can be addressed.
- A theoretical simulation was run in which a pH 7.0 water which contained 100 ng/L triclosan, 2 mg/L free chlorine (typical of drinking water systems), and 1 μM of iodide. If no iodide was present, the half-life of triclosan in the system was predicted to be around 45 seconds due to chlorination processes. In comparison, the half-life when iodide was present was predicted to be only 40 seconds. The presence of iodide in concentrations typical of natural waters does affect the fate of organic contaminants, although the effect is expected to be moderate under the simulated conditions.

4.5: References

1. In *FDA Nonprescription Drugs Advisory Committee Meeting*, Washington D.C., 2005.

2. Jones, R. D.; Jampani, H. B.; Newman, J. L.; Lee, A. S., Triclosan: A review of effectiveness and safety in health care settings. *Am. J.Infect. Control* **2000,** *28*, 184-196.

3. Singer, H.; Muller, S.; Tixier, C.; Pillonel, L., Triclosan: Occurence and fate of a widely used biocide in the aquatic environment: Field measurements in wastewater treatment plants, surface waters, and lake sediments. *Environ. Sci. Technol.* **2002,** *36*, 4998-5004.

4. Kanda, R.; Griffin, P.; James, H. A.; Fothergill, J., Pharmaceutical and personal care products in sewage treatment works. *Journal of Environmental Monitoring* **2003,** *5*, 823-830.

5. Federle, T. W.; Kaiser, S. K.; Nuck, B. A., Fate and effects of triclosan in activated sludge. *Environmental Toxicology and Chemistry* **2001,** *21*, 1330-1337.

6. Lindstrom, A.; Buerge, I. J.; Poiger, T.; Bergqvist, P.-A.; Muller, M. D.; Buser, H.-R., Occurrence and environmental behavior of the bactericide triclosan and its methyl derivative in surface waters and in wastewater. *Environ. Sci. Technol.* **2002,** *36*, 2322-2329.

7. Glaser, A., The ubiquitous triclosan: A common antibacterial agent exposed. *Pesticides and You- Beyond Pesticides/ National Coalition Against the Misuse of Pesticides* 2004, pp 12-17.

8. McAvoy, D. C.; Schatowitz, B.; Jacob, M.; Hauk, A.; Eckhoff, W. S., Measurement of triclosan in wastewater treatment systems. *Environmental Toxicology and Chemistry* **2002,** *21*, 1323-1329.

9. Kolpin, D. W.; Furlong, E. T.; Meyer, M. T.; Thurman, E. M.; Zaugg, S. D.; Barber, L. B.; Buxton, H. T., Pharmaceuticals, hormones, and other organic wastewater contaminants in u.S. Streams, 1999-2000: A national reconnaissance. *Environ. Sci. Technol.* **2002,** *36*, 1202-1211.

10. Tancrede, M.; Yanagisawa, Y.; Wilson, R., Volatilization of volatile organic-compounds from showers .1. Analytical method and quantitative assessment. *Atmos. Environ. A-Gen.* **1992,** *26*, (6), 1103-1111.

11. Howard, C.; Corsi, R. L., Volatilization of chemicals from drinking water to indoor air: The role of residential washing machines. *J. Air Waste. Manage.* **1998,** *48*, (10), 907-914.

12. Committee, A. M. T. R., Committee report: Membrane processes. *J. Am. Water Works Assoc.* **1998,** *90*, (6), 91-105.

13. Fiss, E. M.; Rule, K. L.; Vikesland, P. J., Formation of chloroform and other chlorinated byproducts by chlorination of triclosan-containing antibacterial products. *Environ. Sci. Technol.* **2007,** *41*, (7), 2387-2394.

14. Onodera, S.; Ogawa, M.; Suzuki, S., Chemical-changes of organic-compounds in chlorinated water .13. Gas-chromatographic mass-spectrometric studies of the reactions of irgasan dp-300 [5-chloro-2-(2,4-dichlorophenoxy)phenol]with chlorine in dilute aqueous-solution. *J. Chromatogr.* **1987,** *392*, 267-275.

15. Kanetoshi, A.; Ogawa, H.; Katsura, E.; Kaneshima, H., Chlorination of irgasan dp300 and formation of dioxins from its chlorinated derivatives. *J. Chromatogr.* **1987,** *389*, 139-153.

16. Canosa, P.; Morales, S.; Rodriguez, I.; Rubi, E.; Cela, R.; Gomez, M., Aquatic degradation of triclosan and formation of toxic chlorophenols in presence of low concentration of free chlorine. *Anal. Bioanal. Chem.* **2005,** *383*, (7-8), 1119-1126.

17. Rule, K. L.; Ebbett, V. R.; Vikesland, P. J., Formation of chloroform and chlorinated organics by free-chlorine-mediated oxidation of triclosan. *Environmental Science and Technology* **2005,** *39*, 3176-3185.

18. Moran, J. E.; Oktay, S. D.; Santschi, P. H., Sources of iodine and iodine 129 in rivers. *Water Resources Research* **2002,** *38*, (8).

19. Bichsel, Y.; von Gunten, U., Oxidation of iodide and hypoiodous acid in the disinfection of natural waters. *Environmental Science & Technology* **1999,** *33*, (22), 4040-4045.

20. Bichsel, Y.; von Gunten, U., Formation of iodo-trihalomethanes during disinfection and oxidation of iodide containing waters. *Environmental Science & Technology* **2000,** *34*, (13), 2784-2791.

21. Plewa, M. J.; Wagner, E. D.; Richardson, S. D.; Thruston, A. D.; Woo, Y. T.; McKague, A. B., Chemical and biological characterization of newly discovered lodoacid drinking water disinfection byproducts. *Environ. Sci. Technol.* **2004,** *38*, (18), 4713-4722.

22. Hua, G. H.; Reckhow, D. A.; Kim, J., Effect of bromide and iodide ions on the formation and speciation of disinfection byproducts during chlorination. *Environmental Science & Technology* **2006,** *40*, (9), 3050-3056.

23. Nagy, J. C.; Kumar, K.; Margerum, D. W., Non-metal redox kinetics - oxidation of iodide by hypochlorous acid and by nitrogen trichloride measured by the pulsed-accelerated-flow method. *Inorganic Chemistry* **1988,** *27*, (16), 2773-2780.

24. Lengyel, I.; Li, J.; Kustin, K.; Epstein, I. R., Rate constants for reactions between iodine- and chlorine-containing species: A detailed mechanism of the chlorine dioxide/chlorite-iodide reaction. *J. Am. Chem. Soc.* **1996,** *118*, (15), 3708-3719.

25. Nagy, K.; Kortvelyesi, T.; Nagypal, I., Iodine hydrolysis equilibrium. *Journal of Solution Chemistry* **2003,** *32*, (5), 385-393.

26. Kazantseva, N. N.; Ernepesova, A.; Khodjamamedov, A.; Geldyev, O. A.; Krumgalz, B. S., Spectrophotometric analysis of iodide oxidation by chlorine in highly mineralized solutions. *Analytica Chimica Acta* **2002,** *456*, (1), 105-119.

27. Gottardi, W., Iodine and disinfection: Theoretical study on mode of action, efficiency, stability, and analytical aspects in the aqueous system. *Archiv Der Pharmazie* **1999,** *332*, (5), 151-157.

28. Gottardi, W.; Arnitz, R.; Nagl, M., N-chlorotaurine and ammonium chloride: An antiseptic preparation with strong bactericidal activity. *International Journal of Pharmaceutics* **2007,** *335*, (1-2), 32-40.

29. Schmitz, G., Inorganic reactions of iodine(+1) in acidic solutions. *International Journal of Chemical Kinetics* **2004,** *36*, (9), 480-493.

30. Lengyel, I.; Epstein, I. R.; Kustin, K., Kinetics of iodine hydrolysis. *Inorganic Chemistry* **1993,** *32*, (25), 5880-5882.

31. Cancho, B.; Ventura, F.; Galceran, M.; Diaz, A.; Ricart, S., Determination, synthesis and survey of iodinated trihalomethanes in water treatment processes. *Water Res.* **2000,** *34*, (13), 3380-3390.

32. Hua, G. H.; Reckhow, D. A., Comparison of disinfection byproduct formation from chlorine and alternative disinfectants. *Water Res.* **2007,** *41*, (8), 1667-1678.

33. Krasner, S. W.; Weinberg, H. S.; Richardson, S. D.; Pastor, S. J.; Chinn, R.; Sclimenti, M. J.; Onstad, G. D.; Thruston, A. D., Occurrence of a new generation of disinfection byproducts. *Environ. Sci. Technol.* **2006,** *40*, (23), 7175-7185.

34. Bichsel, Y. Behavior of iodine species in oxidative processes during drinking water treatment. Swiss Federal Institute of Technology Zurich, Zurich, 2000.

35. Sebok-Nagy, K.; Kortvelyesi, T., Kinetics and mechanism of the hydrolytic disproportionation of iodine. *International Journal of Chemical Kinetics* **2004,** *36*, (11), 596-602.

36. Truesdale, V. W.; Luther, G. W.; Greenwood, J. E., The kinetics of iodine disproportionation: A system of parallel second-order reactions sustained by a multi-species pre-equilibrium. *Physical Chemistry Chemical Physics* **2003,** *5*, (16), 3428-3435.

37. Bichsel, Y.; von Gunten, U., Hypoiodous acid: Kinetics of the buffer-catalyzed disproportionation. *Water Res.* **2000,** *34*, (12), 3197-3203.

38. Warner, J. A.; Casey, W. H.; Dahlgren, R. A., Interaction kinetics of i-2(aq) with substituted phenols and humic substances. *Environ. Sci. Technol.* **2000,** *34*, (15), 3180-3185.

39. Buffle, M. O.; Schumacher, J.; Salhi, E.; Jekel, M.; von Gunten, U., Measurement of the initial phase of ozone decomposition in water and wastewater by means of a continuous quench-flow system: Application to disinfection and pharmaceutical oxidation. *Water Res.* **2006,** *40*, (9), 1884-1894.

40. *Standard methods for the examination of water and wastewater*. 18th ed.; Washington, D.C., 1992.

41. Schwarzenbach, R. P.; Gschwend, P. M.; Imboden, D. M., *Environmental organic chemistry*. 2nd ed.; John Wiley & Sons: Hoboken, NJ, 2003.

42. Hansch, C.; A. Leo; Taft, R. W., A survey of hammett substituent constants and resonance and field parameters. *Chemical reviews* **1991,** *91*, (2), 165-195.

Chapter 5: Halogenation Kinetics of Bisphenol-A in Chlorinated Waters Containing Iodide

5.1: Introduction

Bisphenol-A (BPA, 2,2-bis-(4-hydroxy-phenyl)propane) (Figure 2.2) is a widely produced chemical used in the manufacture of a range of consumer products. It is used as a monomer in the synthesis of polycarbonates – a type of polymer utilized in the manufacture of plastic food containers and aluminum can liners – as well as a polymerization inhibitor in PVC pipes (1). The estimated U.S. production of bisphenol-A in 2004 was ≈2.3 billion pounds, 75% of which was used to manufacture polycarbonate resins for various consumer products (2). Such resins are commonly used in the production of food containers because they are highly transparent, have low weight, high heat resistance, and are virtually indestructible (2). As a result of its widespread use, a U.S.G.S. study detected BPA in over 41% of 139 streams tested (3).

Bisphenol-A is a well documented estrogen and endocrine disruptor that can be detrimental to human health (4). Long-term exposure can cause significant damage to the reproductive system and can enhance neurobehavioral problems like ADHD and autism (5). BPA exposure is most commonly due to the leaching of BPA from containers into food and other consumer products which are then ingested. For example, one study detected BPA in over 50% of samples taken from canned tomatoes (6). Much evidence suggests that BPA exposures typical of an average human living in a developed county are well within the range where adverse health effects are observed (5).

Bisphenol-A is regularly introduced into the environment by sewage treatment effluents, landfill leachates, and natural degradation of plastics leading to its detection in natural waters at concentrations up to 700 ng/L (7). During water treatment and due to the common use of PVC pipes in distribution systems, BPA commonly comes into contact with free chlorine. It is suggested that BPA migration from plastics into water used for cooking and storing water and food products can result in substantial contact with drinking water disinfectants. Several recent studies have shown that free chlorine can react with BPA to form a range of products including chlorinated BPA congeners, polychlorinated phenoxyphenols, and differentially substituted chlorophenols (8-10). The two hydroxyl groups on the molecule allow it to speciate between a neutral form ($PhOH_2$) and forms with negative one ($PhOH^-$) and negative two (PhO^{2-}) charges. The mechanism responsible for the production of BPA byproducts at circumneutral pH are believed to be the reactions between HOCl and the $PhOH^-$ and PhO^{2-} forms (10). Studies suggest that the binding affinity of chlorinated BPAs towards estrogen receptors is 24× greater than before chlorination. This finding indicates that chlorinated bisphenol-A is better able to mimic the effects of estrogen hormones than un-chlorinated BPA which in turn suggests that chlorination increases BPA estrogenic activity (8).

Studies have shown that, when in the presence of iodine during chlorination, other phenolic compounds can react to form a range of iodinated byproducts including iodinated phenols, trihalomethanes, and haloacetic acids (11-14). It has also been suggested that these iodinated byproducts are significantly more toxic than their chlorinated analogues (15). Since bisphenol-A can act as an endocrine disruptor, and chlorine substitution increases this effect, it is quite possible that iodine substitution will do so to an even greater degree. The iodination of BPA

could be a potentially important pathway for bisphenol-A fate in the environment. However, to date, no studies have been performed to assess the effects of iodide on bisphenol-A stability.

5.2: Materials and Methods

Reagent grade water was purified by deionization and distillation. Glassware was cleaned by sequentially soaking it in a 10% nitric acid bath and then in a concentrated chlorine bath. Bisphenol-A was purchased from Alfa Aesar (>98% purity) and was used without further purification. Stock BPA solutions were prepared by dissolving 2.5 g of BPA in 25 mL of reagent grade methanol. Dilute solutions were made by diluting this stock 100-fold in methanol. Stocks of free chlorine were prepared using a commercial solution of sodium hypochlorite (purified grade 4-6% NaOCl; Fisher Scientific). All pH measurements were obtained with a Fisher Scientific model 60 pH meter coupled with a Thermo-Orion Ross PerpHect Combination Electrode.

Preparation of Experimental Solutions. Experimental solutions were prepared using reagent grade water containing 2 mM sodium bicarbonate buffer adjusted to the desired pH. Aliquots of stock solution were spiked into experimental solutions to obtain a desired concentration. After allowing 5 minutes for the solutions to equilibrate, the pH of each was adjusted to the desired pH by addition of sodium hydroxide or sulfuric acid. Sulfuric acid was used in order to minimize chloride addition since chloride ions shift the solution equilibrium from HOCl towards Cl_2/H_2OCl^+ at low pH values thereby causing enhanced reaction rates (16). All experiments were performed at 25 ^oC.

Total oxidant consumption. Oxidant consumption experiments were performed using a quench flow system (QFS) similar to a design by Buffle et al. (Appendix A; ref. 17). By keeping the flow-

rate of the QFS constant, we achieved highly accurate and extremely fast reaction times (ranging from 0.25-5 seconds) by simply changing the volume of each flow loop. Total oxidant concentrations (defined as the sum of Cl_2, HOCl, OCl^-, I_2, H_2OI^+, HOI, and OI^- concentrations) were determined using a modified DPD colorimetric method with photometric detection at 515 nm developed for use with the QFS (18). To promote pseudo-first order conditions, oxidant demand experiments were performed with phenol concentrations in 10× excess relative to the oxidant concentration. Following the reaction period, the final solution was mixed with DPD reagent and phosphate buffer to quench the reaction. The quenched solution then flowed through an additional flow loop to allow one minute for color development, at which time the solution was analyzed using a Cary5000 (Varian Inc.) UV-Vis-NIR spectrophotometer (λ = 515 nm) with a 1 cm pathlength flowcell. The absorbance of a given solution was measured for each reaction time until the absorbance signal stabilized for a minimum of 30 seconds (Appendix A, Figure A.2). The total oxidant concentration was then determined using the average absorbance over the 30 second collection period in conjunction with a total oxidant calibration curve. All experiments were performed in at least duplicate to ensure the precision of the data (Appendix A, Figure A.3).

PPCP and Byproduct Analysis. Byproduct experiments were performed with a 10× excess of oxidant using both the QFS system and batch reactors (19). Following an allotted reaction period, the experimental solutions were mixed with a slight excess of sodium sulfite to quench the reaction. Sodium sulfite was chosen as the quenching agent because it is generally unreactive towards PPCPs and their daughter products (16). QFS solutions were collected in 40 mL amber vials. Products were extracted from solution and analyzed using GC-MS for phenolic

byproducts and using GC-ECD for THMs. Detailed experimental methods are described elsewhere (16, 19). Compounds and byproducts were identified by m/z ratios of fragment ions from their GC chromatograms. Calibration curves were produced for bisphenol-A and a range of substituted phenols to assess product concentrations. However, standards for the remaining byproductswere not available for purchase. As such, relative abundances will be focused upon in the discussion section.

Model Development. A computer model was developed using the chemical kinetics program MicroMath Scientist (Salt Lake City, UT) that can predict oxidant reactivity with bisphenol-A. Variables such as species concentrations, pH, and temperature are assigned unique names. Differential equations and mass balances were developed that describe the chemical reactions for each reactant. The program utilizes differential equations that describe the dependence of reaction rates on temperature to calculate the specific rate constants for a given system. Using a sequential fitting approach, unknown rate parameters were systematically determined. These equations were then used to write a computer program where each equation is solved for a given set of variables over a number of iterations. The model initially sets each variable to the value that is input by the user. Scientist then inputs the assigned values to an EPISODE numerical integration package to solve the set of simultaneous differential equations for the variables of interest. The input values are updated by the software following each iteration as the equations are solved. By setting the model to perform a large number of iterations, it is able to make highly accurate predictions for complex chemical relationships over time. A more detailed discussion of the modeling software and techniques are included in Appendix B.

5.3: Results and Discussion

Oxidant consumption kinetics. The kinetics of total oxidant loss in the presence of a fixed concentration of bisphenol-A were significantly enhanced when iodide was present (Figure 5.1). A pseudo-first-order approximation was utilized to describe the kinetics of the reactions when bisphenol-A was in excess. Apparent second-order rate constants (k_{app}, $M^{-1}s^{-1}$) were determined from experimental data obtained over a range of pH values and iodide concentrations using the method of initial rates. Apparent rate constants are pseudo-first order rate constants that have been normalized to the initial phenol concentration. This normalization allows comparison of reactivity for solutions with variable initial conditions. These experimentally determined k_{app} values were then plotted versus solution pH as shown in Figure 5.2. Figures 5.1 and 5.2 illustrate that bisphenol-A readily undergoes electrophilic substitution by both free chlorine and free iodine and that the reaction rates are dependent upon the solution pH and the amount of iodide relative to free chlorine. Observed reaction rates for the electrophilic substitution of bisphenol-A by free chlorine with 10 μM $[I^-]_i$ are more than 200× faster than observed rates for free chlorine alone for a pH range of 6.5-9.0. In the absence of iodide, the maximum reaction rate occurs around a pH of 8.5 and an increase or decrease in pH results in a substantial decline in the overall reactivity of the solution. As the initial iodide concentration is increased, apparent reaction rates below pH 7.5 exhibit an increased dependence upon the solution pH (i.e., the slope of the k_{app} plot is steeper at acidic pH when iodide concentrations are increased). This trend suggests that the relative concentrations of both the oxidant and bisphenol-A species involved in the rate-determining reactions increase as pH becomes more basic since the maximum apparent rate should occur at

the pH where both species are simultaneously present at optimal concentration. The steeper slope apparent when $[I^-]_i$ = 10 μM also implies that the rate determining reaction for iodine substitution of BPA is kinetically faster than the rate determining step for chlorine substitution. However, increased iodide concentrations seem to have the opposite effect within the pH range of 7.5 to 10. While the overall k_{app} is enhanced by the presence of iodide, an increase in iodide concentration from 4 to 10 μM seems to decrease the pH dependence of the overall reactivity within this pH range. When 10 μM of iodide is present, the apparent reaction rate plateaus between a pH of about 7.75 to above 10. The observance of a plateau in apparent reactivity over a range of pH is likely the result of the influence of multiple reactions that exhibit nearly equivalent effects on the overall reactivity over a given pH range. For example, the k_{app} values reach a maximum value around 7.75 and the overall reactivity remains relatively stable to pH 10. If a reaction has a maximum apparent rate occurring at pH 7.75, then as pH is increased above 7.75, the influence of the reaction on the overall apparent rate decreases. However, if a second reaction has a maximum apparent rate occurring at a higher pH, then increasing the pH above 7.75 increases the observed reactivity of the second reaction. If the two reaction rates are of similar magnitudes, then the decreasing influence of the first reaction on overall solution reactivity can be counteracted by the simultaneous increase in the influence of the second reaction, which would then result in a relatively stable overall solution reactivity over a significant pH range.

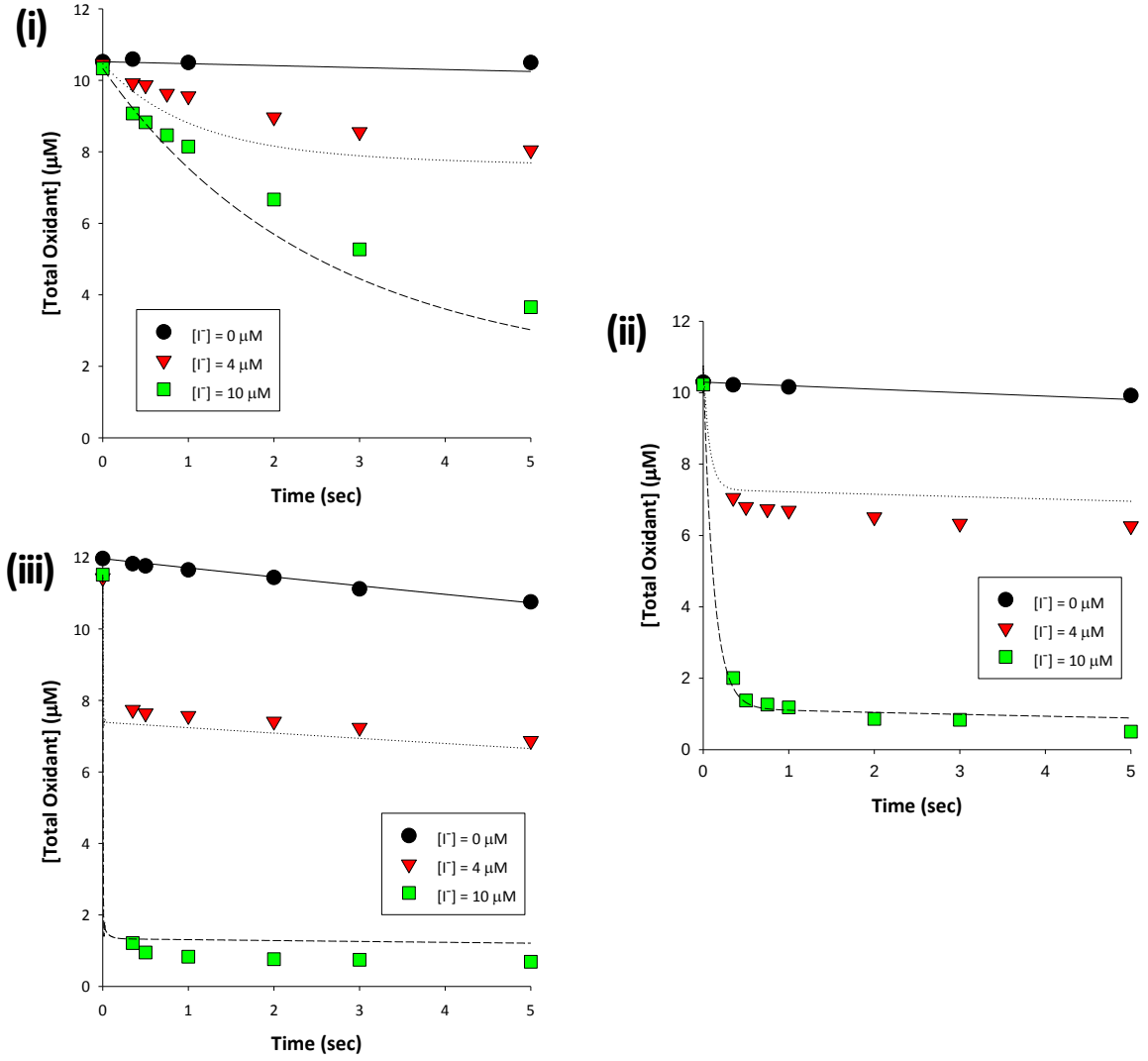

Figure 5-1: Total oxidant loss over time from reactions with bisphenol-A in the presence of iodide. Conditions: [free chlorine]$_i$ = 10 μM, [bisphenol-A]$_i$ = 100 μM, [$NaHCO_3$]$_i$ = 2 mM, pH = 5.5 (i), 7.0 (ii), and 9.0 (iii). The curves represent model simulations for a given condition. Standard errors for individual data points are <0.1%.

The literature suggests that the reactivity of free chlorine towards bisphenol-A can be described by the following reactions (Equations 5.1-5.4; Ref. 10):

$$\mathrm{PhOH_2} + \mathrm{H_2OCl^+} \xrightarrow{k_{5.1}} \text{products} \tag{5.1}$$

$$\mathrm{PhOH_2} + \mathrm{HOCl} \xrightarrow{k_{5.2}} \text{products} \tag{5.2}$$

$$\mathrm{PhOH^-} + \mathrm{HOCl} \xrightarrow{k_{5.3}} \text{products} \tag{5.3}$$

$$\mathrm{PhO^{2-}} + \mathrm{HOCl} \xrightarrow{k_{5.4}} \text{products} \tag{5.4}$$

where the dominant reactions at circumneutral pH are between HOCl and the $PhOH^-$ and PhO^{2-} forms of bisphenol-A. Gallard et al. determined rate constants for reactions 5.1-5.4 to be 3.78×10^7, 1.84, 3.10×10^4, and 6.62×10^4 $M^{-1}s^{-1}$, respectively (10). They then define the overall second-order apparent rate constant for bisphenol-A reactivity with free chlorine as follows:

$$k_{\mathrm{app}} = \frac{k_{5.1}[\mathrm{H^+}]+k_{5.2}[\mathrm{H^+}]^3+k_{5.3}\mathrm{K_{a_1}}[\mathrm{H^+}]^2+k_{5.2}\mathrm{K_{a_1}K_{a_2}}[\mathrm{H^+}]}{[\mathrm{H^+}]^3+(\mathrm{K_{a_1}}+\mathrm{K_{a_{Cl}}})[\mathrm{H^+}]^2+\left(\mathrm{K_{a_1}K_{a_{Cl}}}+\mathrm{K_{a_1}K_{a_2}}\right)[\mathrm{H^+}]+\mathrm{K_{a_1}K_{a_2}K_{a_{Cl}}}} \tag{5.5}$$

where $\mathrm{pK_{a_1}}$, $\mathrm{pK_{a_2}}$, and $\mathrm{pK_{a_{Cl}}}$ were set to 9.6, 10.2, and 7.54, respectively. Equation 5.5 was used to calculate k_{app} values using the reported second-order rate constants over a pH range from 5.5 to 10 and these model simulations were compared to the apparent rate constants determined from our experimental data (Figure 5.3). Gallard et al.'s apparent rate equation respectably predicting the data at basic pH, but it loses accuracy as the pH is dropped below 8.0. This discrepancy suggests that the previously determined rate constants, specifically $k_{5.1}$ and $k_{5.2}$, are too small. These rate constants were re-evaluated using the modeling program developed for this study. The observation that the maximum reactivity occurs at a pH of 8.5 supports the finding that the $PhOH^-$ and PhO^{2-} reactions are the rate determining reactions at

circumneutral pH. A pH of 8.5 is almost exactly half way between the pK_a of HOCl (pK_a = 7.54) and the pK_a of the neutral and $PhOH^-$ bisphenol-a species, meaning that HOCl and $PhOH^-$ and PhO^{2-} are at their maximum relative concentrations. If the electrophilic substitution of bisphenol-A by free chlorine is truly 'first order in the total concentration of chlorine and BPA (10)', then we would expect the maximal reactivity when both reactive species are at their relative maximum concentrations. The fact that the pH at which maximal reactivity was observed in our experiments matches up with the theoretical pH predicted for the maximum rate supports the finding that the $PhOH^-$ and PhO^{2-} bisphenol-A species are responsible for the observed reactivity. .

A recent study by Cherney et al., (2006) showed that Cl_2, rather than H_2OCl^+, is the primary reactive chlorine species in solution at low pH (20), thus suggesting that reaction 5.1 should be rewritten as:

$$\mathrm{PhOH_2} + \mathrm{Cl_2} \xrightarrow{k_{5.1\mathrm{r}}} \mathrm{products} + \mathrm{Cl^-} \qquad (5.1\mathrm{r})$$

Though inclusion of reaction 5.1 had negligible effects on the overall apparent rate calculations using equation 5.5 within our experimental pH range, reaction 5.1r could possibly have some influence on the measured k_{app} values at the low end of our pH range since the pK_a for Cl_2 is higher than that of H_2OCl^+ (3.6 for Cl_2 versus 1.5 for H_2OCl^+; ref. 20).

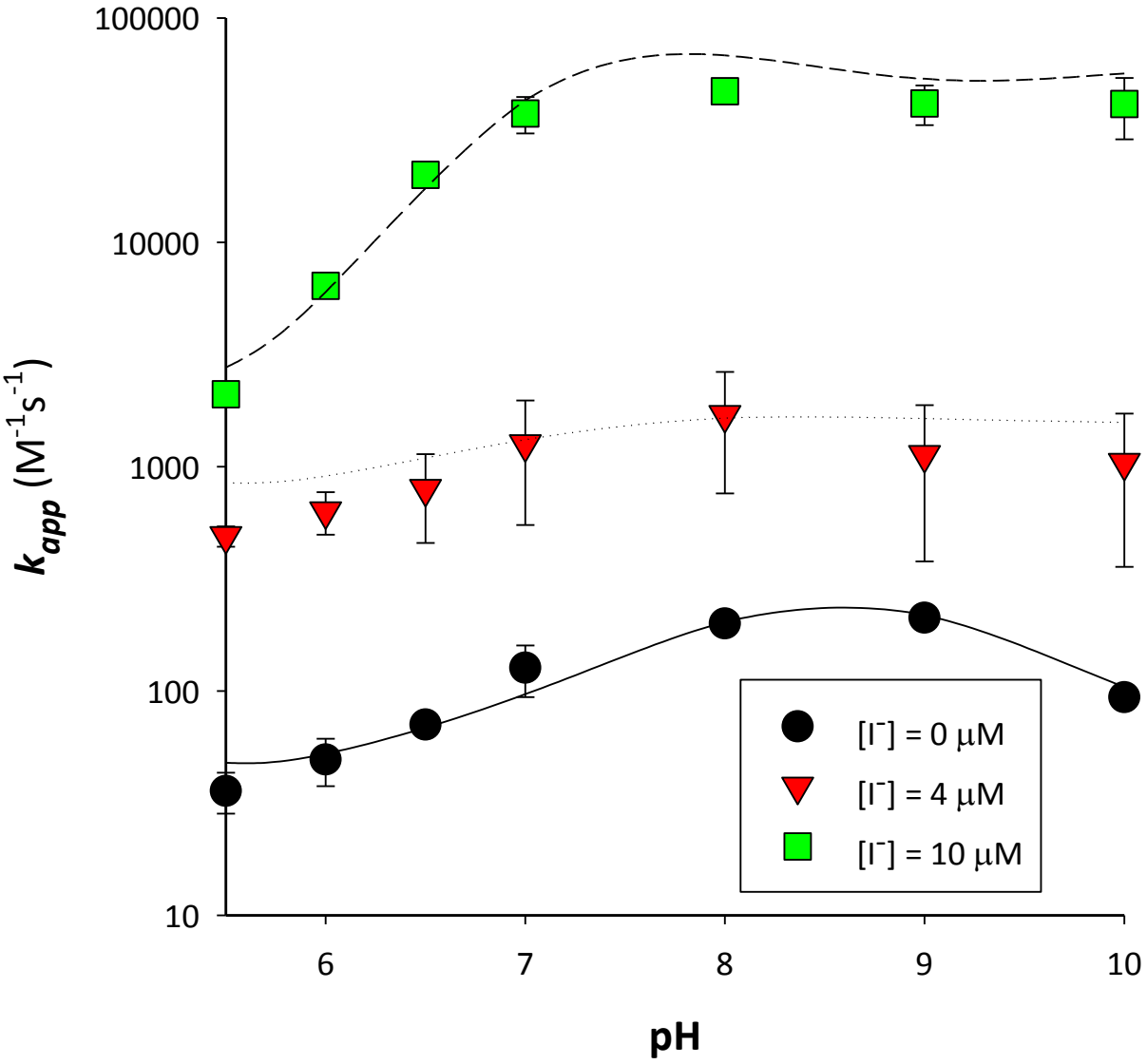

Figure 5-2: Experimental (points) and model predicted (curves) apparent psuedo-first-order reaction rates for bisphenol-A oxidation between pH 5.5 to 10. Conditions: [total oxidant]$_i$ = 9.9-12.0 μM, [bisphenol-A]$_i$ = 100 μM, [$NaHCO_3$] = 2 mM. Error bars represent 95% confidence intervals.

Modeling Results. A reactivity model was designed using Micromath Scientist to allow evaluation of the oxidant consumption data. A sequential fitting approach was used in which each parameter was systematically determined over the experimental pH range. Equations describing the equilibrium relationships for all possible reactive species were included (Equations 5.6-5.14) along with a rate expression describing HOCl oxidation of I^- to form HOI (Equation 5.15).

$$Cl_2 + H_2O \longleftrightarrow HOCl + Cl^- + H^+ \qquad K_{5.6} = 5.1\times10^{-4}\ M^2 \qquad (5.6)$$

$$HOCl \longleftrightarrow OCl^- + H^+ \qquad K_{5.7} = 2.9\times10^{-8}\ M \qquad (5.7)$$

$$I_2 + H_2O \longleftrightarrow HOI + I^- + H^+ \qquad K_{5.8} = 5.44\times10^{-13}\ M^2 \qquad (5.8)$$

$$HOI \longleftrightarrow OI^- + H^+ \qquad K_{5.9} = 2.3\times10^{-11}\ M \qquad (5.9)$$

$$I_2 + I^- \longleftrightarrow I_3^- \qquad K_{5.10} = 715\ M^{-1} \qquad (5.10)$$

$$H_2OI^- \longleftrightarrow HOI + H^+ \qquad K_{5.11} = 2\ M \qquad (5.11)$$

$$HOI_2^- \longleftrightarrow HOI + I^- \qquad K_{5.12} = 3.1\times10^{-3}\ M \qquad (5.12)$$

$$PhOH_2 \longleftrightarrow PhOH^- + H^+ \qquad K_{5.13} = 2.5\times10^{-10}\ M \qquad (5.13)$$

$$PhOH^- \longleftrightarrow PhO^{2-} + H^+ \qquad K_{5.14} = 2.5\times10^{-10}\ M \qquad (5.14)$$

$$HOCl + I^- \xrightarrow{k_{3.8}} HOI + Cl^- \qquad k_{5.15} = 4.3\times10^{8}\ M^{-1}s^{-1} \qquad (5.15)$$

Differential equations were then developed describing each potential bisphenol-A electrophilic substitution reaction. Equation 5.28 shows the differential equation describing free chlorine reactions with bisphenol-A.

$$\frac{d[\text{free chlorine}]}{dt} = -(k_{5.16}[Cl_2] + k_{5.19}[H_2OCl^+] + k_{5.22}[HOCl] + k_{5.25}[OCl^-])[PhOH_2]$$

$$-(k_{5.17}[Cl_2] + k_{5.20}[H_2OCl^+] + k_{5.23}[HOCl] + k_{5.26}[OCl^-])[PhOH^-]$$

$$-(k_{5.18}[Cl_2] + k_{5.21}[H_2OCl^+] + k_{5.24}[HOCl] + k_{5.27}[OCl^-])[PhO^{2-}] \qquad (5.28)$$

Similar equations were developed for free iodine, bisphenol-A, and iodide species (not shown). Each potential reaction was initially included in the model so that the relative importance of each could be assessed.

The model described by equations 5.6-5.28 was initially fit to data from experiments performed in the absence of iodide in order to determine rate constants for the chlorination reactions. Each rate constant in equation 5.28 was determined by fitting data sets obtained from experiments run at pH values ranging from 5.5 to 10.0. The model was fit repeatedly to the data while sequentially omitting one or more reaction. This approach allowed us to determine the importance of each individual reaction with respect to the overall numerical solution. These training sets allowed us to identify the reactions most likely responsible for oxidant consumption and to increase the precision of each reaction rate constant. Through this process, it was determined that free chlorine consumption due to reactions with bisphenol-A is best described by the following second-order reactions where the products are monochlorinated bisphenol-A daughter products:

$$\mathrm{HOCl} + \mathrm{PhOH_2} \longrightarrow \text{products} \qquad k_{5.22} = 47\ (\pm\ 25)\ \mathrm{M^{-1}s^{-1}} \qquad (5.22)$$

$$\mathrm{HOCl} + \mathrm{PhOH^-} \longrightarrow \text{products} \qquad k_{5.23} = 3.2\ (\pm\ 0.6) \times 10^4\ \mathrm{M^{-1}s^{-1}} \qquad (5.23)$$

$$\mathrm{HOCl} + \mathrm{PhO^{2-}} \longrightarrow \text{products} \qquad k_{5.24} = 5.5\ (\pm\ 0.7) \times 10^4\ \mathrm{M^{-1}s^{-1}} \qquad (5.24)$$

Reactions 5.22-5.24 correspond to reactions 5.2-5.4 but were renumbered here to simplify the discussion. In general, our results support the mechanistic findings from Gallard et al. (10) except that our rate parameter values differ from theirs. In our model, $k_{5.22}$ (47 (± 25) $\mathrm{M^{-1}s^{-1}}$) was found to be over an order of magnitude greater than the previously reported $k_{5.2}$ (1.84 $\mathrm{M^{-1}s^{-1}}$). This was not unexpected since the model shown in Figure 5.3 under-predicts the apparent

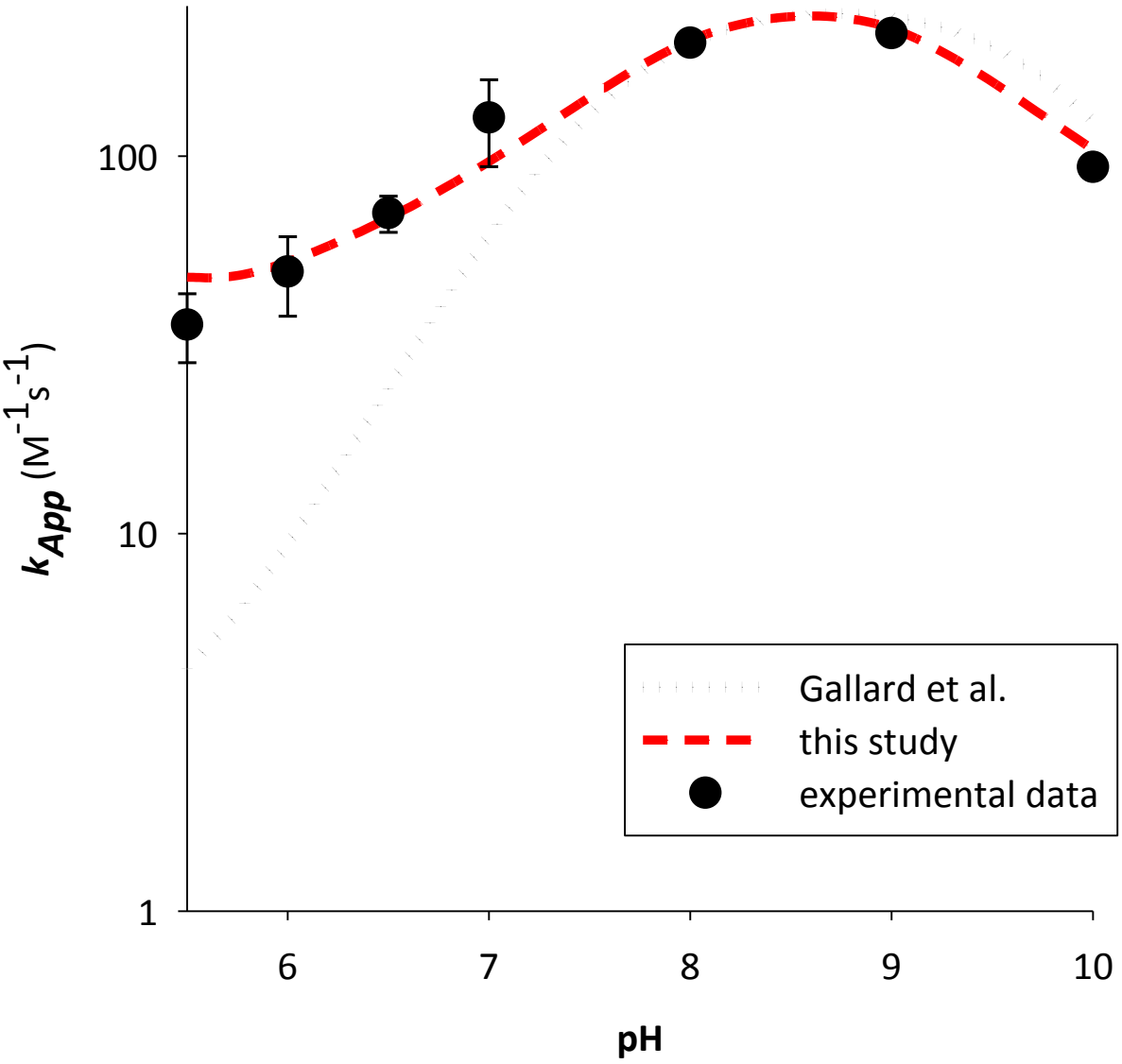

Figure 5-3: Comparison between observed second-order rate constants calculated using an equation (equation 5.5) derived by Gallard et al. (2004) as shown by the grey curve and values measured experimentally (points). The model predictions from this study were included for comparison (red curve). Error bars represent 95% confidence intervals for the experimental data.

reaction rates below a pH of 7, which is also the pH range where the HOCl-$PhOH_2$ reaction predominates. Our numerically determined values for $k_{5.23}$ (3.2 (± 0.6) × 10^4 $M^{-1}s^{-1}$) and $k_{5.24}$ (5.5 (± 0.7) × 10^4 $M^{-1}s^{-1}$) were quite similar to those previously reported ($k_{5.3}$ = 3.1 × 10^4 $M^{-1}s^{-1}$ and $k_{5.4}$ = 6.6 × 10^4 $M^{-1}s^{-1}$). The slight differences likely result from variability between labs. As illustrated by the curve representing our model predictions in Figure 5.3, the adjustments to the rate parameter values, though slight, significantly improved the accuracy in fitting the experimental data as compared to the predictions from the k_{app} equation (equation 5.5 from Gallard et al.). Our larger value for $k_{5.22}$ was the biggest improvement in that it caused the model predictions below pH 8 to fit the experimental data almost perfectly. We found that inclusion of reaction terms involving either H_2OCl^+ or Cl_2 to be unnecessary for fitting the data over the experimental pH range. Since the developed model includes equilibrium equations describing each reactive species, the concentration of each free chlorine species can be determined at any pH. This output showed that H_2OCl^+ never exceeds a concentration within 3 orders of magnitude of the Cl_2 concentration over the entire pH range of 1-14. Since Cl_2 is known to be highly reactive, it would be very unlikely that H_2OCl^+ would be sufficiently more reactive than Cl_2 so as to become important as a reactant. At low pH, we might expect Cl_2 to play an important role in the reaction kinetics. However, Cl_2 accounts for <0.1% of the total free chlorine within a pH range of 5.5-10, so it is likely that any reactions involving Cl_2 are simply overshadowed by reactions 5.22-5.24 at our tested pH values.

To determine the rate constants for the iodine-containing species, the reaction rate constants for free chlorine (equations 5.22-5.23) were fixed to the values determined in the iodide-free model. As before, fits were repeated for rate constants of each possible reaction while

systematically omitting reactions until an optimal fit was achieved. The mechanism responsible for iodination of bisphenol-A can be described by Equations 5.29-5.32 in which the products are monoiodinated BPA:

$$I_2 + PhOH_2 \longrightarrow products + I^- \qquad k_{5.29} = 4.0\ (\pm\ 1.8) \times 10^2\ M^{-1}s^{-1} \qquad (5.29)$$

$$I_2 + PhOH^- \longrightarrow products + I^- \qquad k_{5.30} = 3.1\ (\pm\ 0.4) \times 10^7\ M^{-1}s^{-1} \qquad (5.30)$$

$$HOI + PHOH_2 \longrightarrow products \qquad k_{5.31} = 2.4\ (\pm\ 0.2) \times 10^5\ M^{-1}s^{-1} \qquad (5.31)$$

$$HOI + PhOH^- \longrightarrow products \qquad k_{5.32} = 1.4\ (\pm\ 0.5) \times 10^7\ M^{-1}s^{-1} \qquad (5.32)$$

Interestingly, BPA^{2-} did not have a significant effect on the overall observed reactivity of free iodine. Possibly it may have played a more significant role if the experimental pH range was extended above 10 since, as shown in Figure 5-4, BPA^{2-} only becomes the dominant BPA species above a pH of 10.25. However, if the HOI-BPA^{2-} reaction rate was near the same order of magnitude as the HOI-BPA^- rate, one would expect to see some increase in overall reaction rate when increasing the pH from 7.5 to 10 due to the fact that the BPA^{2-} concentration increases from <0.01% to over 30% of total BPA within that pH range. The observation that the overall reaction rate plateaus as the pH is increased from 7.5 to 10 suggests that the HOI reaction with BPA^- is kinetically favorable (Figure 5-3). Rate constants for the iodination of BPA are nearly 3 orders of magnitude larger than those observed for HOCl.

The accuracy of the fitted rate constants was further assessed by examining their ability to fit data from experiments containing 4 μM of iodide. The model predictions are shown in Figures 5-1 and 5-2 by the plotted curves. In all cases, the model predictions obtained with the fitted rate constants were able to predict total oxidant degradation very closely. Overall, the model

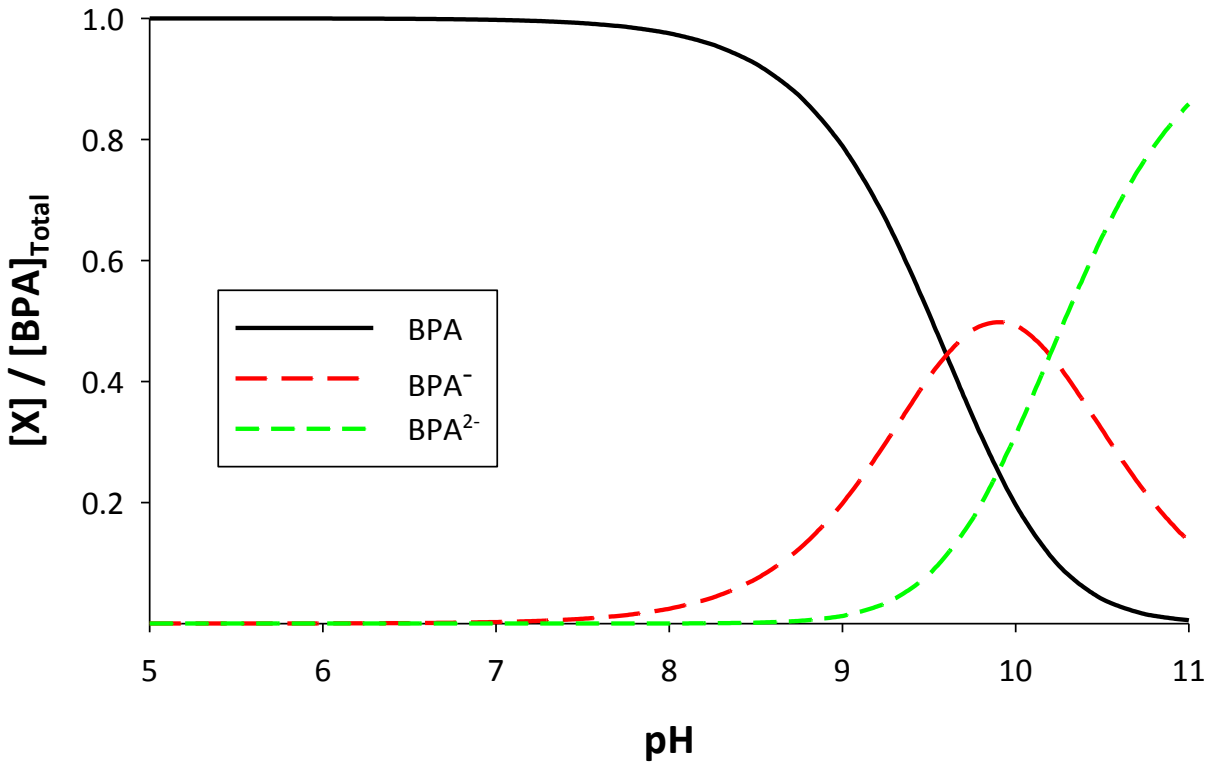

Figure 5.4: Plot of the fraction of bisphenol-A present as each species 'X' over a pH range from 5 to 11. pK_{a1} = 9.6, pK_{a2} = 10.2.

was highly successful at describing the reactivity of the solution despite the fact that free iodine mediated oxidation of BPA is extremely fast.

Product Formation. To further explore product formation for bisphenol-A, experiments over extended time periods (t = 5 min) were performed where 22.4-24.1 μM of bisphenol-A was contacted with 100 μM of free chlorine in the presence of 0, 4, and 10 μM iodide at pH 7 (Figure 5.5). An extended reaction time of 5 minutes was used to increase our understanding of the overall fate of bisphenol-A during disinfection practices. In experiments in the absence of iodide, one monochlorinated (2-(3-chloro-4-hydroxyphenyl)-2-(4-hydroxyphenyl)propane), two dichlorinated (2-(3-chloro-4-hydroxyphenyl)-2-(3-chloro-4-hydroxyphenyl)propane and 2-(3,5-dichloro-4-hydroxyphenyl)-2-(4-hydroxyphenyl)propane), one trichlorinated (2-(3,5-dichloro-4-hydroxyphenyl)-2-(3-chloro-4-hydroxyphenyl)propane), and one tetrachlorinated (2-(3,5-dichloro-4-hydroxyphenyl)-2-(3,5-dichloro-4-hydroxyphenyl)propane) daughter product was detected (Figure 5.5). 2-(3-chloro-4-hydroxyphenyl)-2-(3-chloro-4-hydroxyphenyl)propane and 2-(3,5-dichloro-4-hydroxyphenyl)-2-(4-hydroxyphenyl)propane are considered collectively in Figure 5.5 because it was not possible to separate the individual signals for the two peaks. Chlorination reactions occurred by step-wise electrophilic substitution forming 2-(3-chloro-4-hydroxyphenyl)-2-(4-hydroxyphenyl)propane first. Subsequent chlorine substitutions continued to occur to form the additional BPA daughter products. Further chlorination of these chlorinated BPA moieties resulted in cleavage of the tri-methyl group (propane) of BPA to form 2,4-dichlorophenol or 2,4,6-trichlorophenol from one phenol ring while the second ring retained the propane and could be singly or doubly chlorinated. Mass spectra of the

degradation products like 2,4-DCP and 2,4,6-TCP could be readily identified but were not quantifiable because they were below the detection limit and the peaks could not be defined.

When the iodide concentration was increased to 4 μM, a 2-(3-iodo-4-hydroxyphenyl)-2-(4-hydroxyphenyl)propane daughter product was identified. Except for 2-(3,5-dichloro-4-hydroxyphenyl)-2-(3,5-dichloro-4-hydroxyphenyl)propane, each chlorination product was still detected, although all chlorinated product peak magnitudes were decreased by over 25%. Multiple iodide substitutions were not detected nor were they expected. Because the iodide was present at much lower concentrations than the bisphenol-A, primarily a single electrophilic substitution should occur. In the presence of 4 μM iodide, no additional chlorine substitution was observed for iodinated bisphenol-A. When 10 μM of iodide was present, the chlorinated BPA products were reduced by over 50% and the 2-(3-iodo-4-hydroxyphenyl)-2-(4-hydroxyphenyl)propane daughter product peak increased by more than 500% relative to the 4 μM samples. Again, multiple iodine substitutions were not detected since BPA was in excess of iodide. However, an extremely small peak was identified as 2-(3-iodo-4-hydroxyphenyl)-2-(3-chloro-4-hydroxyphenyl)propane (or to a lesser extent possibly 2-(3-iodo-5-chloro-4-hydroxyphenyl)-2-(4-hydroxyphenyl)propane) in the 10 μM iodide experiments. It was not included in Figure 5.5 because it was of too small a magnitude to show up on the scale.

As the iodide concentration increased, the amount of bisphenol-A remaining in solution also decreased. When only free chlorine was present, nearly 9 μM of the initial 22.4 μM remained after 5 minutes. When 10 μM iodide was present, less than 5 μM of an initial 24.1 μM BPA remained at the completion of the experiment. This means that, not only does the addition of iodide form iodinated products rather than chlorinated ones, but it also increases the total

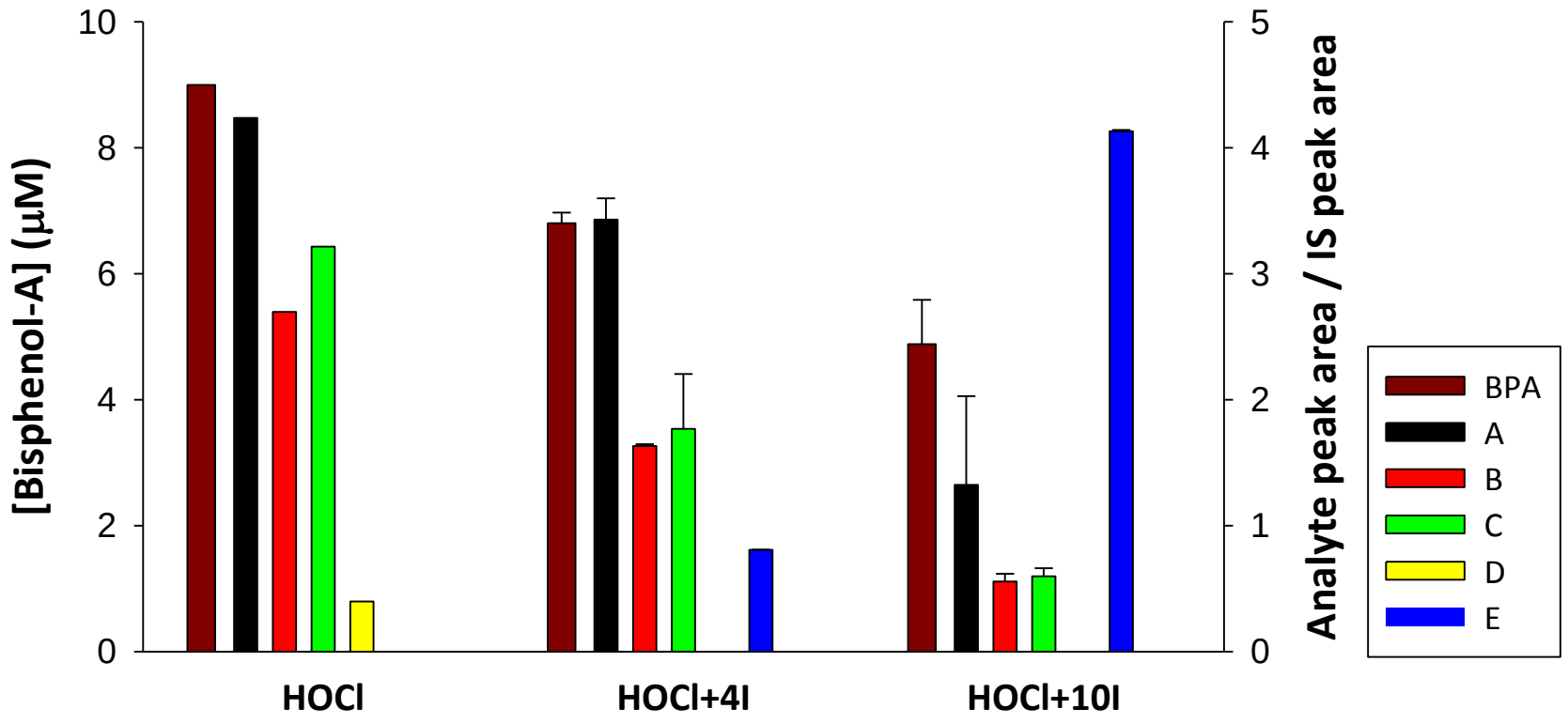

Figure 5.5: Product formation from the electrophilic substitution of bisphenol-A in the presence of free chlorine and iodide concentrations 0 (HOCl), 4 (HOCl+4I), and 10 mM (HOCl+10I). Conditions: pH = 7.0, $[BPA]_i$ = 22.4-24.1 mM, $[\text{free chlorine}]_i$ = 100 mM, reaction time = 5 minutes. Bisphenol-A is in concentration units while all other analytes are represented by normalized peak area. Monochloro-monoiodo-BPA was detected for 10 μM I^- but was too small in magnitude to show up on the scale. Products include 2-(3-chloro-4-hydroxyphenyl)-2-(4-hydroxyphenyl)propane (A), 2-(3-chloro-4-hydroxyphenyl)-2-(3-chloro-4-hydroxyphenyl)propane + 2-(3,5-dichloro-4-hydroxyphenyl)-2-(4-hydroxyphenyl)propane (B), 2-(3,5-dichloro-4-hydroxyphenyl)-2-(3-chloro-4-hydroxyphenyl)propane (C), 2-(3,5-dichloro-4-hydroxyphenyl)-2-(3,5-dichloro-4-hydroxyphenyl)propane (D), and 2-(3-iodo-4-hydroxyphenyl)-2-(4-hydroxyphenyl)propane (E).

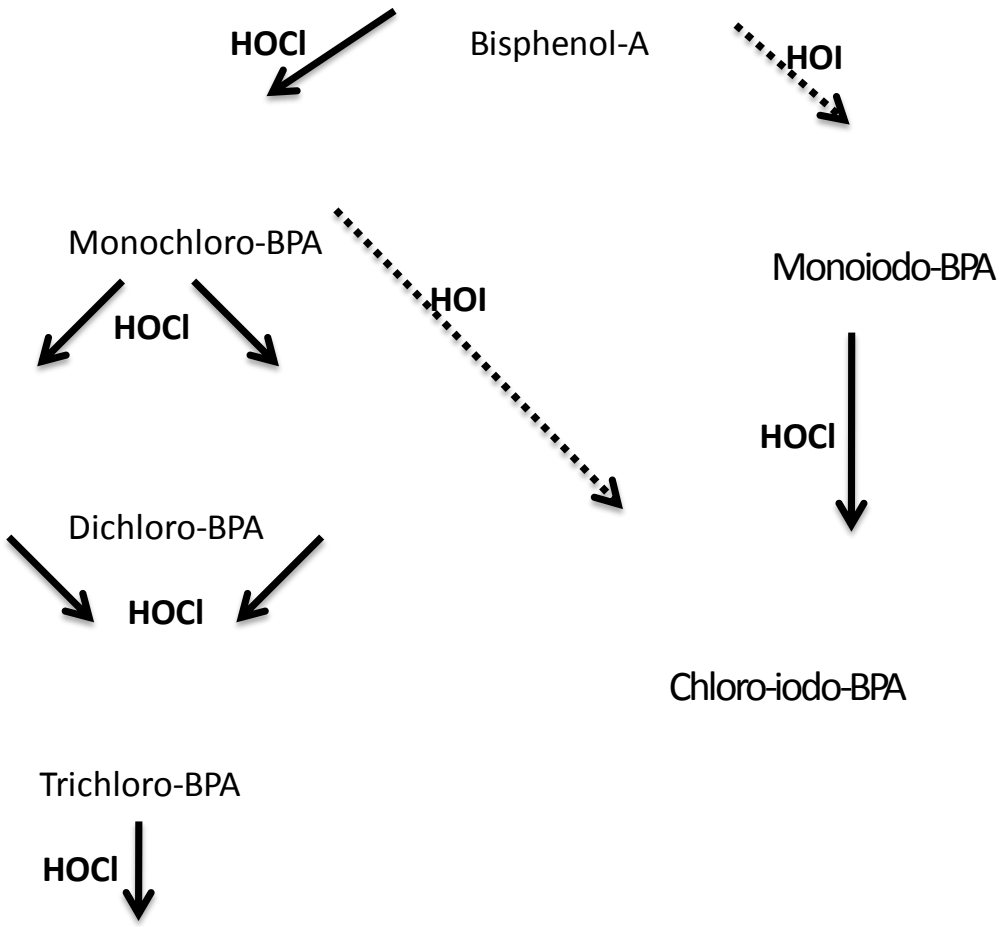

Figure 5.6: Reaction scheme showing reaction mechanisms and chemical structures for triclosan. All species were identified by mass spectral analysis. Other products not shown in this schematic include chlorinated phenols and other degradation products resulting from cleavage between the ring structures.

amount of bisphenol-A consumed so is increasing the volume of byproducts formed. Figure 5.7 illustrates the suspected mechanism of electrophilic substitution of bisphenol-A as suggested by our findings. Since iodinated products are known to be more toxic than chlorinated products, the presence of iodide during drinking water chlorination could result in significant health risks.

5.4: Conclusions

- Free chlorine reactions with bisphenol-A occur primarily through electrophilic substitution reactions described by equations 5.22-5.24 where the 'products' are monochlorinated BPA. The values determined for each parameter are as listed.

$$HOCl + PhOH_2 \longrightarrow \text{products} \qquad k_{5.22} = 47\ (\pm\ 25)\ M^{-1}s^{-1} \qquad (5.22)$$

$$HOCl + PhOH^- \longrightarrow \text{products} \qquad k_{5.23} = 3.2\ (\pm\ 0.6) \times 10^4\ M^{-1}s^{-1} \qquad (5.23)$$

$$HOCl + PhO^{2-} \longrightarrow \text{products} \qquad k_{5.24} = 5.5\ (\pm\ 0.7) \times 10^4\ M^{-1}s^{-1} \qquad (5.24)$$

- Free iodine reactions with bisphenol-A also occur primarily through electrophilic substitution as described by equations 5.29-5.32 to form monoiodinated BPA. For free iodine reactions, the effects on the overall reaction rate within a pH range from 5.5 to 10 of the PhO^{2-} form of BPA was found to be negligible.

$$I_2 + PhOH_2 \longrightarrow \text{products} + I^- \qquad k_{5.29} = 4.0\ (\pm\ 1.8) \times 10^2\ M^{-1}s^{-1} \qquad (5.29)$$

$$I_2 + PhOH^- \longrightarrow \text{products} + I^- \qquad k_{5.30} = 3.1\ (\pm\ 0.4) \times 10^7\ M^{-1}s^{-1} \qquad (5.30)$$

$$HOI + PHOH_2 \longrightarrow \text{products} \qquad k_{5.31} = 2.4\ (\pm\ 0.2) \times 10^5\ M^{-1}s^{-1} \qquad (5.31)$$

$$HOI + PhOH^- \longrightarrow \text{products} \qquad k_{5.32} = 1.4\ (\pm\ 0.5) \times 10^7\ M^{-1}s^{-1} \qquad (5.32)$$

These extremely fast reaction rates mean that any free iodine that comes into contact with bisphenol-A sill result in the production of iodinated products.

- The presence of iodide resulted in an increase in the amount of bisphenol-A consumed over an extended reaction time and preferentially formed iodinated byproducts over chlorinated ones. The estrogenic activity of these iodinated byproducts necessitates further study, but the fast reaction kinetics of free iodine reactions suggests that significant iodinated products can result with the presence of relatively small amount of iodide.
- A theoretical simulation was run in which a water at pH 7 which contained 100 ng/L bisphenol-A, 2 mg/L free chlorine (typical of drinking water systems), and 20 μg/L of iodide (the median in natural waters). If no iodide was present, the half-life of bisphenol-A in the system was predicted to be around 250 seconds due to chlorination processes. In comparison, the half-life of bisphenol-A when iodide was present was predicted to be only 13 seconds. The presence of iodide in concentrations typical of natural waters has an extremely large effect on the fate of organic contaminants.

5.5: References

1. Ash, M.; Ash, I., *Handbook of plastic and rubber additives*. Gower, Hampshire, UK, 1995.

2. *Ntp-cerhr expert panel report on the reproductive and developmental toxicity of bishpehnol a*; Center for the Evaluation of Risks to Human Reproduction: 2007.

3. Kolpin, D. W.; Furlong, E. T.; Meyer, M. T.; Thurman, E. M.; Zaugg, S. D.; Barber, L. B.; Buxton, H. T., Pharmaceuticals, hormones, and other organic wastewater contaminants in u.S. Streams, 1999-2000: A national reconnaissance. *Environ. Sci. Technol.* **2002,** *36*, 1202-1211.

4. Wetherill, Y. B.; Akingbemi, B. T.; Kanno, J.; McLachlan, J. A.; Nadal, A.; Sonnenscheing, C.; Watson, C. S.; Zoeller, R. T.; Belcher, S. M., In vitro molecular mechanisms of bisphenol a action. *Reproductive Toxicology* **2007,** *24*, (2), 178-198.

5. vom Saal, F. S.; Akingbemi, B. T.; Belcher, S. M.; Birnbaum, L. S.; Crain, D. A.; Eriksen, M.; Farabollini, F.; Guillette, L. J.; Hauser, R.; Heindel, J. J.; Ho, S. M.; Hunt, P. A.; Iguchi, T.; Jobling, S.; Kanno, J.; Keri, R. A.; Knudsen, K. E.; Laufer, H.; LeBlanc, G. A.; Marcus, M.; McLachlan, J. A.; Myers, J. P.; Nadal, A.; Newbold, R. R.; Olea, N.; Prins, G. S.; Richter, C. A.; Rubin, B. S.; Sonnenschein, C.; Soto, A. M.; Talsness, C. E.; Vandenbergh, J. G.; Vandenberg, L. N.; Walser-Kuntz, D. R.; Watson, C. S.; Welshons, W. V.; Wetherill, Y.; Zoeller, R. T., Chapel hill bisphenol a expert panel consensus statement: Integration of mechanisms, effects in animals and potential to impact human health at current levels of exposure. *Reproductive Toxicology* **2007,** *24*, (2), 131-138.

6. Grumetto, L.; Montesano, D.; Seccia, S.; Albrizio, S.; Barbato, F., Determination of bisphenol a and bisphenol b residues in canned peeled tomatoes by reversed-phase liquid chromatography. *Journal of Agricultural and Food Chemistry* **2008,** *56*, (22), 10633-10637.

7. Crain, D. A.; Eriksen, M.; Iguchi, T.; Jobling, S.; Laufer, H.; LeBlanc, G. A.; Guillette, L. J., An ecological assessment of bisphenol-a: Evidence from comparative biology. *Reproductive Toxicology* **2007,** *24*, (2), 225-239.

8. Hu, J. Y.; Aizawa, T.; Ookubo, S., Products of aqueous chlorination of bisphenol a and their estrogenic activity. *Environ. Sci. Technol.* **2002,** *36*, (9), 1980-1987.

9. Yamamoto, T.; Yasuhara, A., Chlorination of bisphenol a in aqueous media: Formation of chlorinated bisphenol a congeners and degradation to chlorinated phenolic compounds. *Chemosphere* **2002,** *46*, (8), 1215-1223.

10. Gallard, H.; Leclercq, A.; Croue, J. P., Chlorination of bisphenol a: Kinetics and by-products formation. *Chemosphere* **2004,** *56*, (5), 465-473.

11. Krasner, S. W.; Weinberg, H. S.; Richardson, S. D.; Pastor, S. J.; Chinn, R.; Sclimenti, M. J.; Onstad, G. D.; Thruston, A. D., Occurrence of a new generation of disinfection byproducts. *Environ. Sci. Technol.* **2006,** *40*, (23), 7175-7185.

12. Bichsel, Y.; von Gunten, U., Formation of iodo-trihalomethanes during disinfection and oxidation of iodide containing waters. *Environ. Sci. Technol.* **2000,** *34*, (13), 2784-2791.

13. Cancho, B.; Ventura, F.; Galceran, M.; Diaz, A.; Ricart, S., Determination, synthesis and survey of iodinated trihalomethanes in water treatment processes. *Water Res.* **2000,** *34*, (13), 3380-3390.

14. Hua, G. H.; Reckhow, D. A.; Kim, J., Effect of bromide and iodide ions on the formation and speciation of disinfection byproducts during chlorination. *Environ. Sci. Technol.* **2006,** *40*, (9), 3050-3056.

15. Plewa, M. J.; Wagner, E. D.; Richardson, S. D.; Thruston, A. D.; Woo, Y. T.; McKague, A. B., Chemical and biological characterization of newly discovered lodoacid drinking water disinfection byproducts. *Environ. Sci. Technol.* **2004,** *38*, (18), 4713-4722.

16. Rule, K. L.; Ebbett, V. R.; Vikesland, P. J., Formation of chloroform and chlorinated organics by free-chlorine-mediated oxidation of triclosan. *Environmental Science and Technology* **2005,** *39*, 3176-3185.

17. Buffle, M. O.; Schumacher, J.; Salhi, E.; Jekel, M.; von Gunten, U., Measurement of the initial phase of ozone decomposition in water and wastewater by means of a continuous quench-flow system: Application to disinfection and pharmaceutical oxidation. *Water Res.* **2006,** *40*, (9), 1884-1894.

18. *Standard methods for the examination of water and wastewater*. 18th ed.; Washington, D.C., 1992.

19. Fiss, E. M.; Rule, K. L.; Vikesland, P. J., Formation of chloroform and other chlorinated byproducts by chlorination of triclosan-containing antibacterial products. *Environ. Sci. Technol.* **2007,** *41*, (7), 2387-2394.

20. Cherney, D. P.; Duirk, S. E.; Tarr, J. C.; Collette, T. W., Monitoring the speciation of aqueous free chlorine from ph 1 to 12 with raman spectroscopy to determine the identity of the potent low-ph oxidant. *Applied Spectroscopy* **2006,** *60*, (7), 764-772.

Chapter 6: Conclusions and Importance of Research to Water Treatment

6.1: Summary of findings

As stated in Chapter 1, the objectives for the research described herein were two-fold: 1) to perform a comprehensive analysis of the effects of iodide on the electrophilic substitution oxidation of substituted phenols and PPCPs during drinking water chlorination and 2) to develop a reaction model able to calculate rate constants and predict the overall chemical behavior for each reactive oxidant and phenol species.

In agreement with the existing literature (1), the kinetics of the electrophilic substitution of phenolic compounds by free chlorine were significantly enhanced by the presence of iodide. When I^- is contacted with free chlorine, it is quickly oxidized by HOCl to form free iodine. Free iodine is highly reactive and can be present as I_2, HOI, OI^-, HOI_2^-, or H_2OI^+, depending on pH. For each compound tested, the observed reaction rates were dependent upon both the solution pH and the iodide to free chlorine ratio. In general, the reactivity of the phenolic compounds tested increased in the order 2,4-dichlorophenol<triclosan<4-chlorophenol~4-iodophenol<phenol<bisphenol-A with both free chlorine and free iodine. This trend in relative reactivities roughly correlates with the pK_a of each compound, as shown in Figure 6.1. In general, the pK_a of a compound is a descriptor of the compound stability, and as the pK_a increases the relative acid strength of a compound decreases. In the case of phenolic compounds, a stronger acid indicates that the ring structure has substituents with large

electron accepting capabilities. With the addition of electron acceptors, the negative charge associated with the PhO^- form of the compound is dispersed to the electron accepting substituents, which in turn decreases the reactivity of the compound. The relationship between phenol substituents and reactivity is often described using Hammett values, which when plotted versus the reaction rate typically form a straight line. Hammett values are generally better descriptors for phenol reactivity than pK_a values since they take into account resonance effects of substituents on a phenolic compound. However, because an accurate Hammett value for triclosan could not be found, the pK_a of each compound was used instead, but the plot still exhibits a roughly linear relationship. The steeper slope for the HOI rates suggests that its reactivity is more sensitive to additional substituents included on the phenol ring. Using this linear relationship formed by each oxidant, we can then predict rate constants for each oxidant with other phenolic compounds, including PPCPs, even if all we know about the phenolic compound is its pK_a.

The individual reactions, and their corresponding rate constants, involved in free chlorine mediated electrophilic substitution for each phenolic compoundare listed in Table 6.1. In agreement with current literature, it was determined that the chlorination reaction controlling the overall kinetics between pH 5 to 10 involves the reaction between HOCl and the PhO^- (and PhO^{2-} in the case of bisphenol-A) form of a given phenolic compound. The rate for the HOCl:bisphenol-A reaction was found to be an order of magnitude larger than the corresponding triclosan reaction and 2 orders of magnitude larger than for 2,4-dichlorophenol. In addition, the PhO^{2-} form of bisphenol-A was found to react even faster than the $PhOH^-$ form. The propane structure that joins the two bisphenol-A rings essentially make BPA act as two

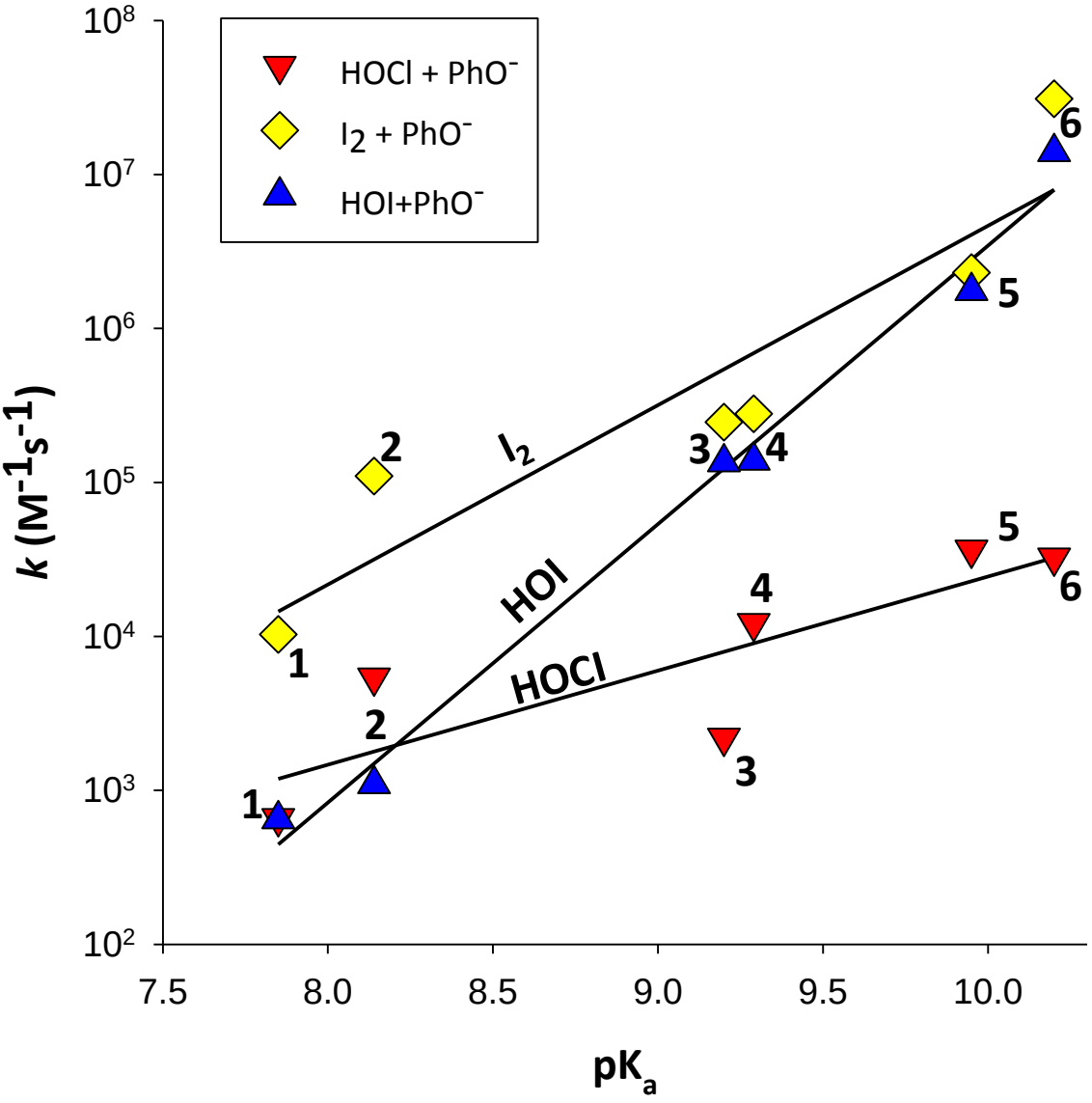

Figure 6.1: Plot of second-rate constants of 2,4-dichlorophenol (1), triclosan (2), 4-iodophenol (3), 4-chlorophenol (4), phenol (5), and triclosan (6) reactions with HOCl, HOI, and I_2.

separate moieties. When one side is negatively charged, the reactivity of BPA increases drastically. When both sides are negatively charged, the reactivity should essentially double since the reactivity of both rings should be the same. The values of the corresponding rate constants support this behavior. Reactions between HOCl and the neutral form of each species were also found to be of importance, although in each case the calculated rate constants were at least an order of magnitude lower than those determined for the phenolate form. To illustrate the importance of the different reactions listed in Table 6.1, Figure 6.2 plots the calculated rate for each free chlorine mediated electrophilic substitution reaction as a function of the solution pH. This analysis was conducted to illustrate the relative importance and magnitude of each reaction as pH changes. For each phenolic compound, reactions involving the PhO^- form dominate the kinetics above a pH of 6.5. Below 6.5, reactions between the PhOH form and HOCl become the dominant mechanism, but the overall solution reactivity is not as high as when the PhO^- reaction dominates.

The reaction mechanism and rates describing electrophilic substitution reactions by free iodine are listed in Table 6.1. An overall increase in observed reaction rates between iodide-containing species and the phenolic compounds again increased in the same fashion as observed for free chlorine reactions. Figure 6.3 illustrates the relative importance of each individual reaction versus solution pH for reactions occurring with 10 μM of iodide initially present. It was found that I_2 reactions with the PhO^- species were the dominant reaction mechanism at circumneutral pH. The rate constant for the I_2 reaction with the phenol form of each compound was significantly lower than observed with the phenolate form, but was higher than that determined for HOCl. This result is due to the fact that I_2 is a more potent oxidant

than HOCl so it exhibits a higher reactivity with the unionized phenols, but the phenolate form is substantially more reactive with either oxidant. For both 2,4-dichlorophenol and triclosan, the reactions between HOI and the unionized molecules have negligible effects on the overall reaction rate. This finding can be explained by looking at the speciation of each compound. 2,4-dichlorophenol and triclosan have pK_a values of 7.85 and 8.14, respectively, while HOI concentrations only exceed I_2 concentrations above a pH of ≈7.3. This difference in speciation means that one would expect the HOI:PhOH reaction to dominate within a relatively small pH range. Such a reaction likely occurs, but when compared to the extremely fast I_2: PhO^- reactions that occur over that same pH range, the effects on the overall reaction rates are comparably insignificant. For both compounds, HOI reactions with the phenolate-species were found to be significant when the solution pH approached 10. Bisphenol-A again exhibited the fasted observed reaction rates. Reactions between the $PhOH^-$ form of bisphenol-A and both I_2 and HOI were important within the experimental pH range. Unlike for 2,4-dichlorophenol and triclosan, the reaction between HOI and the neutral form was important for the description of the bisphenol-A reactivity. This is due to the fact that BPA has a pK_{a1} of 9.6, so both HOI and the neutral form of BPA are the dominant species over a much broader pH range than for2,4-dichlorophenol or triclosan. Surprisingly, reaction rates involving the BPA^{2-} species were found to be negligible within the experimental pH range. Because BPA has a pK_{a2} of 10.2, it is likely that BPA^{2-} simply is not present at sufficient concentrations to measure the reaction rate for the experimental pH range.

Overall, the main findings of this study demonstrate that the mechanism describing electrophilic substitution of phenols by free chlorine or free iodine differs from that reported in

Table 6.1: Summary of reaction mechanisms and rates for 2,4-dichlorophenol, triclosan, and bisphenol-A oxidation by free chlorine or hypoiodous acid.

Reaction	Rate ($M^{-1}s^{-1}$)		
	2,4-DCP	**triclosan**	**BPA**
$HOCl + \text{phenol} \xrightarrow{k_{6.1}} \text{products}$	26 (± 13)	370 (± 30)	47 (± 25)
$HOCl + \text{phenolate} - \text{phenol} \xrightarrow{k_{6.2}} \text{products}$	660 (± 130)	5.4×10^3	$3.2\ (\pm 0.6) \times 10^4$
$HOCl + \text{phenolate}^{-2} - \text{phenol} \xrightarrow{k_{6.3}} \text{products}$	N/A	N/A	$5.5\ (\pm 0.7) \times 10^4$
$I_2 + \text{phenol} \xrightarrow{k_{6.4}} \text{products}$	240 (± 73)	$4.0\ (\pm 0.7) \times 10^3$	400 (± 180)
$I_2 + \text{phenolate} - \text{phenol} \xrightarrow{k_{6.5}} \text{products}$	$1.0\ (\pm 0.26) \times 10^4$	$1.1\ (\pm 0.1) \times 10^5$	$3.1\ (\pm 0.4) \times 10^7$
$HOI + \text{phenol} \xrightarrow{k_{6.6}} \text{products}$	0	0	$2.4\ (\pm 0.2) \times 10^5$
$HOI + \text{phenolate} - \text{phenol} \xrightarrow{k_{6.7}} \text{products}$	650 (± 150)	$1.1\ (\pm 0.6) \times 10^6$	$1.4\ (\pm 0.5) \times 10^7$

the literature. These new findings are the result of in-depth modeling techniques that were able to assess the validity of the analyses used in past studies. With these conclusions, it will be necessary to revisit additional kinetic studies on phenol reactivity to better validate the published rate constant values.

Importance to Water Treatment. Overall, this study has made several important contributions to the environmental engineering field. We were able to better our understanding of a highly complex system of fast-occurring chemical reactions by using in-depth modeling techniques. The resulting model can be used as a predictive tool to assess the potential for free iodine formation in natural waters and the subsequent effects of free iodine on the overall fate of phenolic organic contaminants. As mentioned in the previous chapters, a theoretical simulation was run for both triclosan and bisphenol-A at conditions typical of natural waters. If 1 μM of iodide is present in water also containing 2 mg/L free chlorine and 100 ng/L of triclosan, the half-life of triclosan decreases from 45 seconds to 40 seconds when iodide is present. Though the change in kinetics does not seem significant, we have shown that iodinated products form in place of chlorinated products when iodide is present, so substantial quantities of iodinated daughter products are likely formed. However, when that same simulation was performed for 100 ng/L of bisphenol-A, only this time the iodine concentration was set to 0.2 μM which is the average concentration found in natural waters, a very different result occurred. The half-life of bisphenol-A when no iodide was present was 250 seconds, but when iodide was present, the half-life was only 13 seconds. Though the importance of iodide is dependent upon the organic compound involved, for some compounds, like bisphenol-A, it can have a profound effect.

In circumneutral pH environments, such as those found during drinking water treatment, it is apparent that aqueous disinfectants such as free chlorine and free iodine will react with the trace levels of PPCPs found in those environments to form potentially harmful byproducts. The reactivity of free iodine, produced by the oxidation of I^- by free chlorine, will enhance the rate at which parent PPCP compounds react and concomitantly will result in more rapid production of iodinated DBPs. Because iodinated DBPs are potentially more toxic than their chlorinated analogues such a finding has great significance to the drinking water community. The comprehensive reaction model developed through the course of this study has shown its general applicability to a range of different phenolic compounds and with further modifications has the potential to be applied to additional compounds. The present model is able to accurately predict both disinfectant and phenolic compound loss rates and future work should to be done to extend this model to predict DBP formation rates in chlorinated waters containing iodide. The existing model captures the complexity of these systems and does so using fundamental chemical reactions instead of empirical models. As such, this model is a significant step towards achieving a more complete understanding of these highly reactive systems.

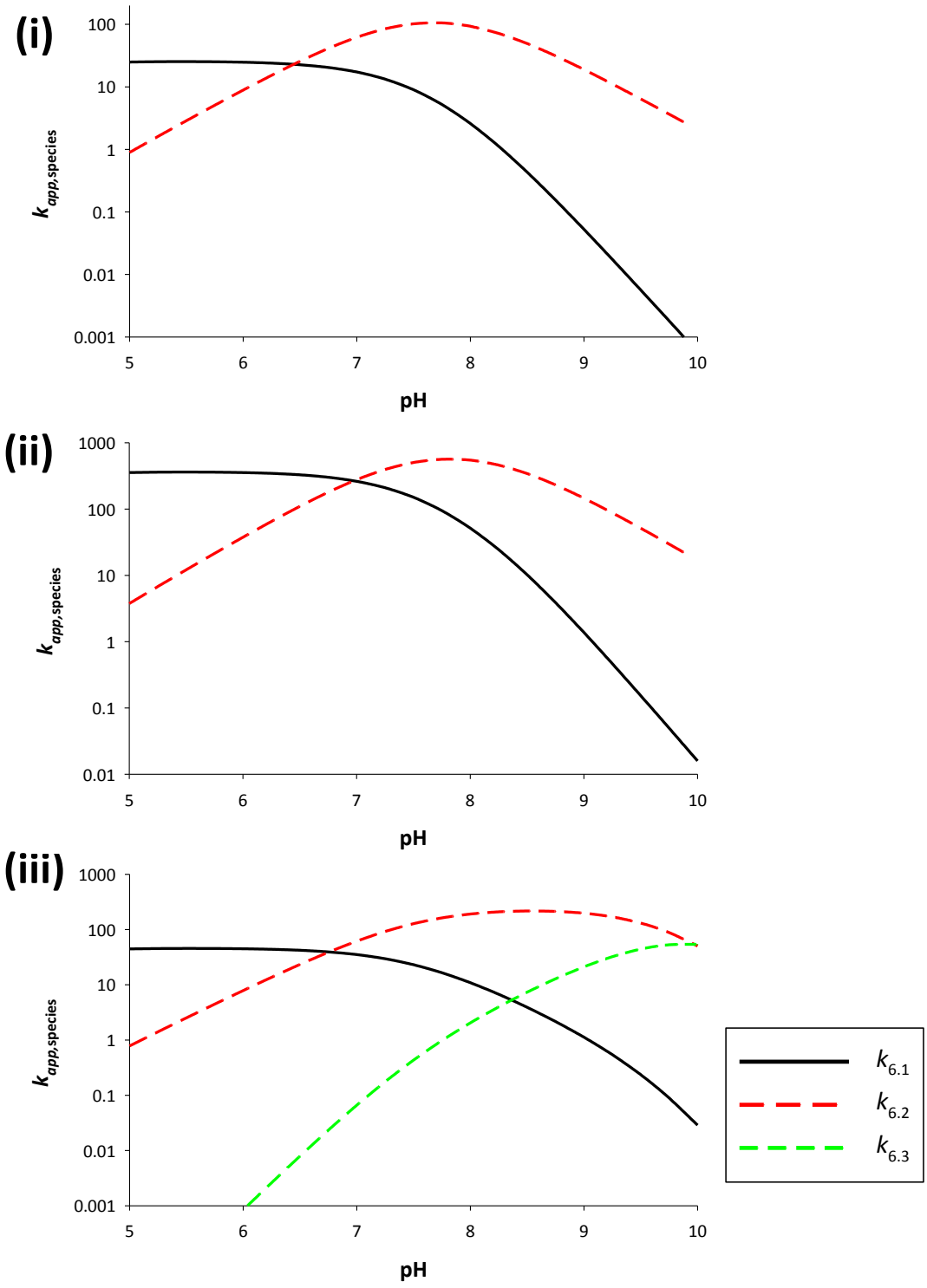

Figure 6.2: Plots of the apparent reactivity ($M^{-1}s^{-1}$) resulting from each individual reaction versus pH in the absence of iodide. Plots include reactions with 2,4-dichlorophenol (i), triclosan (ii), and bisphenol-A (iii).

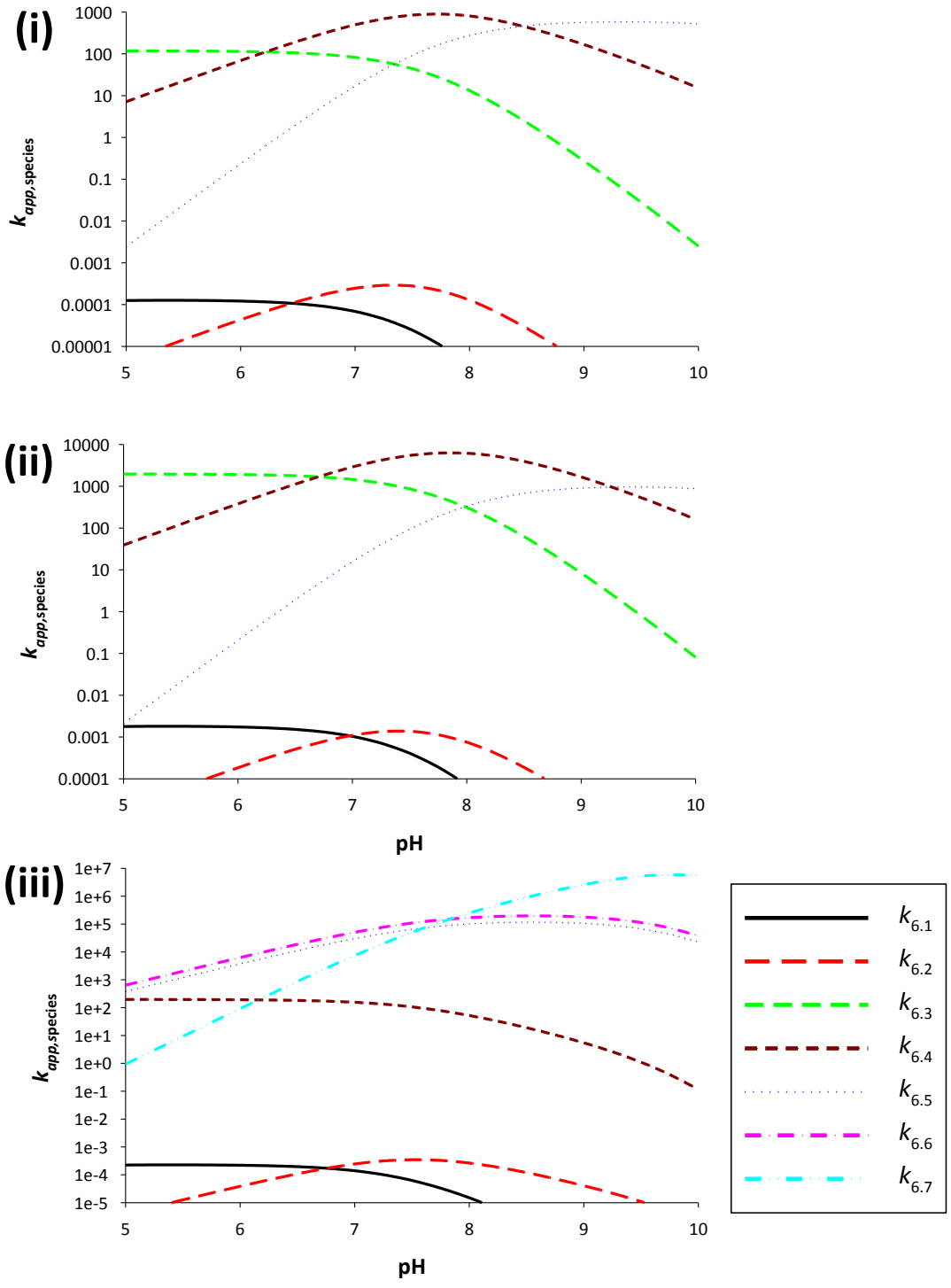

Figure 6.3: Plots of the apparent reactivity ($M^{-1}s^{-1}$) resulting from each individual reaction versus pH when 10 mM of iodide is present. Plots include reactions with 2,4-dichlorophenol (i), triclosan (ii), and bisphenol-A (iii).

6.2. References

1. Bichsel, Y.; von Gunten, U., Formation of iodo-trihalomethanes during disinfection and oxidation of iodide containing waters. *Environ. Sci. Technol.* 2000, *34*, (13), 2784-2791.

Appendix A: Quenched Flow System Description

Discussion A.1: Detailed description of Quenched Flow System.

Free chlorine and free iodine reactions with many PPCPs can be extremely fast, with a timescale on the order of seconds to minutes, and thus require a special experimental setup for accurate analysis. Continuously-stirred batch systems are ill suited for analysis of extremely fast reactions because of the speed required for reaction initiation and subsequent quenching, both of which require a syringe injection, prevents proper mixing for required solution volumes. This shortcoming is in addition to the inherent human error naturally involved when experiments are performed very quickly. As such, alternate reaction techniques were developed in order to accurately quantify reactions with half-lives of less than 1 minute. For this purpose, a quench flow system (QFS), inspired by a design described in Buffle et al (33), was constructed that enabled accurate analysis of reactions occurring on the order of several seconds (Figure A.1).

The system is composed of three syringe pumps, each mounted with 2 syringes, that contain the various different experimental stock solutions. Both syringes on Pump 1 are designated for the phenolic compound solution. Pump 2 contains one syringe designated for variably concentrated iodide solution and a second designated for chlorine solution. Pump 3 contains 2 syringes designated for DPD and phosphate buffer, respectively. Both pumps 1 and 2 are operated at a flow rate of 2.5 mL/min equaling a total flow rate of 10 mL/min for the combined 4 syringes. The iodide and free chlorine solutions are mixed via a mixing tee, thus beginning the oxidation of iodide to HOI. Iodide concentrations are varied between 0, 16, and 40 µM in order to obtain desired concentrations after a 1:4 dilution that forms the final mixed reaction

solution. The concentrated chlorine solution is also 4× concentrated. After mixing, the iodide and chlorine solutions travel through a flow loop of volume 6.7 mL to allow for 20 seconds of contact time. This was deemed sufficient for the oxidant solution to reach equilibration by use of the speciation model described in Chapter 3. The oxidant solution is then mixed with the phenol solution at a second mixing tee in order to initiate the reaction. The final mixed reaction solution then flows through one of thirteen flow loops of varying hydraulic residence time (t= 0.35, 0.5, 0.75, 1.0, 1.5, 2.0, 2.5, 3.0, 4.0, 5.0, 10.0, 20.0, and 30.0 seconds) to regulate contact time. A typical experiment involved eight sample loops (i.e., 8 time points) as determined by the rapidity of the reactions kinetics. By keeping the flow rates constant for Pumps 1 and 2, the hydraulic residence (reaction) times could be accurately controlled simply by varying the volumes of the different flow loops. The flow was directed between different flow loops usingfour separate Hamilton 8-way valves linked together on either side of the flow loops with Hamilton 3-way valves. Via this approach, contact times of 0.35-30 seconds could be readily achieved and accurately reproduced.

For oxidant consumption experiments, upon exiting the flow loop, the reaction solution was mixed through another mixing tee with DPD and phosphate buffer to quench the reaction. Pump 3 maintained a flow rate of 0.25 mL per minute so that the resulting solution would be at a 1:20 ratio of indicator to chlorine solution as directed by EPA Method 330.5. The quenched mixture was then analyzed in a flow-through cell via UV-Vis spectroscopy after being pumped through an additional length of tubing. The additional tubing length was sized to allow for 60 seconds of color development.

In the case of the phenol consumption and product formation experiments, the flow loop effluent tube was disconnected from the DPD/phosphate buffer mixing tee and connected to a modified 40 mL vial cap. The reaction solution was directly injected into a continuously-mixed 40 mL amber vial containing excess sodium sulfite to quench the reaction. Vials were then acidified, capped, and refrigerated until extractions were performed. Sample storage time never exceeded 12 hours prior to performing extractions.

To decrease the chance of contamination and to increase the speed of the reactions, a series of 1-way check valves were connected to an additional 3-way tee that was then connected into the syringe. One branch of the 3-way tee was connected to a tube leading to the corresponding experimental stock solution. A check valve was installed into the assembly such that solution flow was only able to enter the syringe. The tube assembly connected to the remaining branch of the 3-way tee contained a check valve that only allowed solution flow out of the syringe. The other end of this assembly was connected to the flow loop setup. The syringes then could be refilled between experiments by reversing the direction of each pump while ensuring that syringe outflow only was able to flow into the reaction-loop system. In order to prevent oxidant degradation or issues in color development due to sunlight, all flow loops were housed in a sealed box and all external tubing was painted black. Between experiments, all syringes and tubing were flushed with an H_2SO_4 solution of pH 2 followed by triplicate flushes with deionized water. When not in use, all liquids in the system were flushed out by pumping air through each flow loop to prevent dry rotting of the plastic connection nuts. Syringes and tubing were again flushed in triplicate with each respective reaction solution prior to starting an

experiment to prevent accidental dilution, to expunge air bubbles, and to allow the tubing to become saturated with the test compound to prevent sorption during experiments.

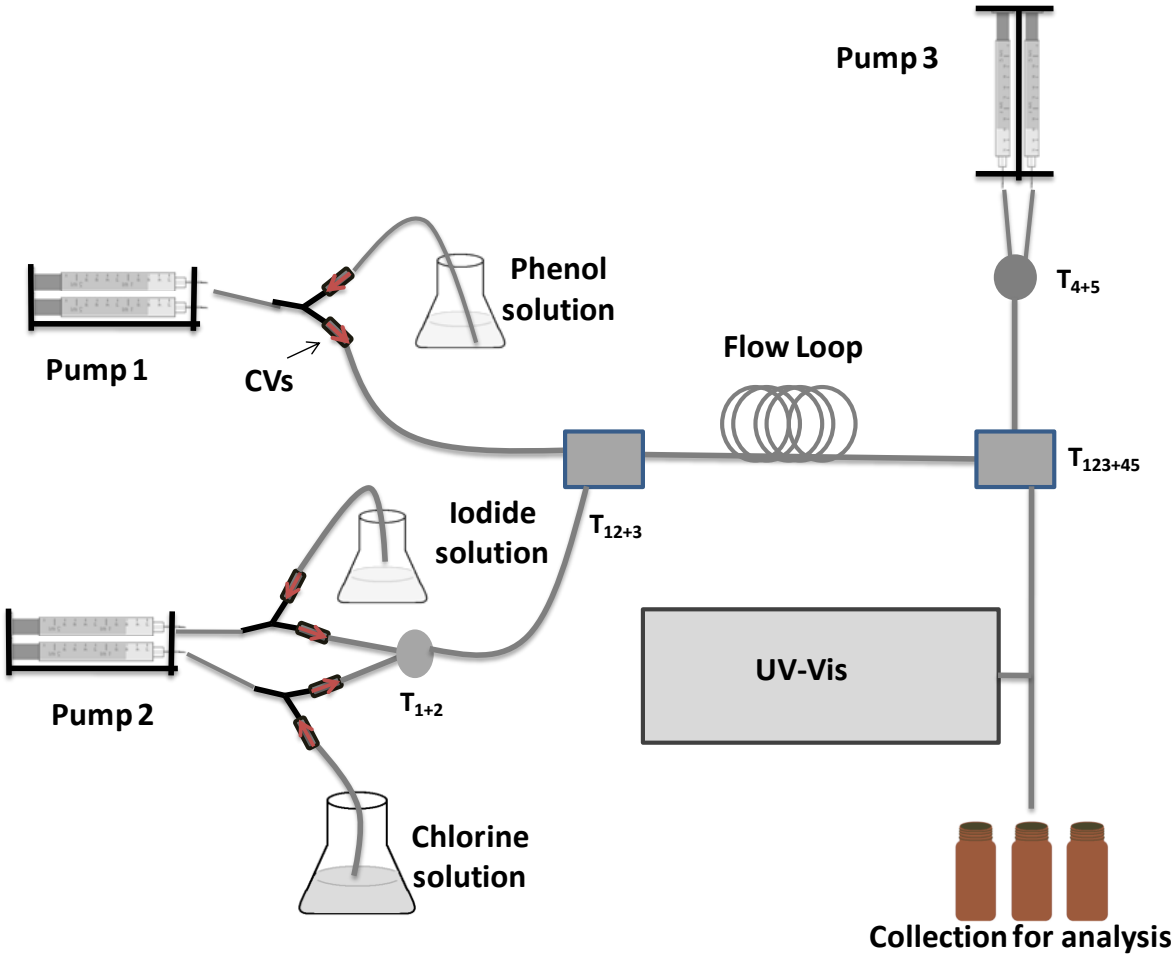

Figure A.1: Schematic of quench flow system (QFS) design.

Discussion A.2: Explanation of UV-Vis data file interpretation.

For oxidant consumption experiments, the 'kinetics' program on the UV-Vis was started. The detection wavelength was set to 515 nm and readings were zeroed using DI water as the blank sample. The signal was zeroed again after allowing 15 minutes for the lamps to warm up and for the signal to settle. The kinetics program was then set up to take continuous readings at a rate of 10 readings per second over a predetermined time period (typically 20 mins). All QFS syringes were filled with a corresponding volume of their respective reaction solutions (i.e., for a 20 min reading, each syringe would contain 50 mL of solution for a flow rate of 2.5 mL/min). The flow loop corresponding to a 0.35 sec reaction time was selected using the 8-way distribution valves. Pumps were set to infuse mode and started while simultaneously beginning the UV-Vis data collection. The absorbance readings initially fluctuate extensively as the flow system is flushed with fresh reaction solutions. After roughly 2-2.5 minutes, the reaction solution begins to reach steady-state and the absorbance signal levels out to a constant reading. After maintaining a constant absorbance reading for a minimum of a minute, the time showing on the UV-Vis count-down timer is recorded as the 'start time' for the sample reading. After an additional 30 seconds (designated as the sample 'stop time'), the reaction solution flow was diverted to the flow loop with a corresponding reaction time of 0.5 seconds. Flow can be diverted without disturbing pumping rates by simply selecting the correct reaction loop with the 8-way valves. The 'start time' for the 0.5 sample then began after a minimum of 30 seconds has passed after the absorbance readings once again show a steady signal. This process is repeated until measurements have been taken for all desired reaction times. The absorbance

data over the entire collection time for each respective time point is used to determine an average absorbance and standard deviation. The entire process was performed in duplicate for each experimental condition to ensure precision of results. Total oxidant concentrations for each time point were calculated using calibration curves.

Figure A.2 shows an example absorbance plot over time that is representative of the data collected for a typical oxidant consumption experiment. Absorbance readings were typically highly stable once equilibrium was obtained. Excess fluctuations were exclusively the result of a malfunction within the QFS system. When this occurred, the system was shut down to allow for all connections to be checked until the issue was corrected. Any data gathered at these instances was thrown out and the experiments were rerun. Figure A.3 shows an example plot of oxidant concentrations calculated for replicate experiments. This plot is representative of the high quality, highly reproducible results possible by use of the QFS.

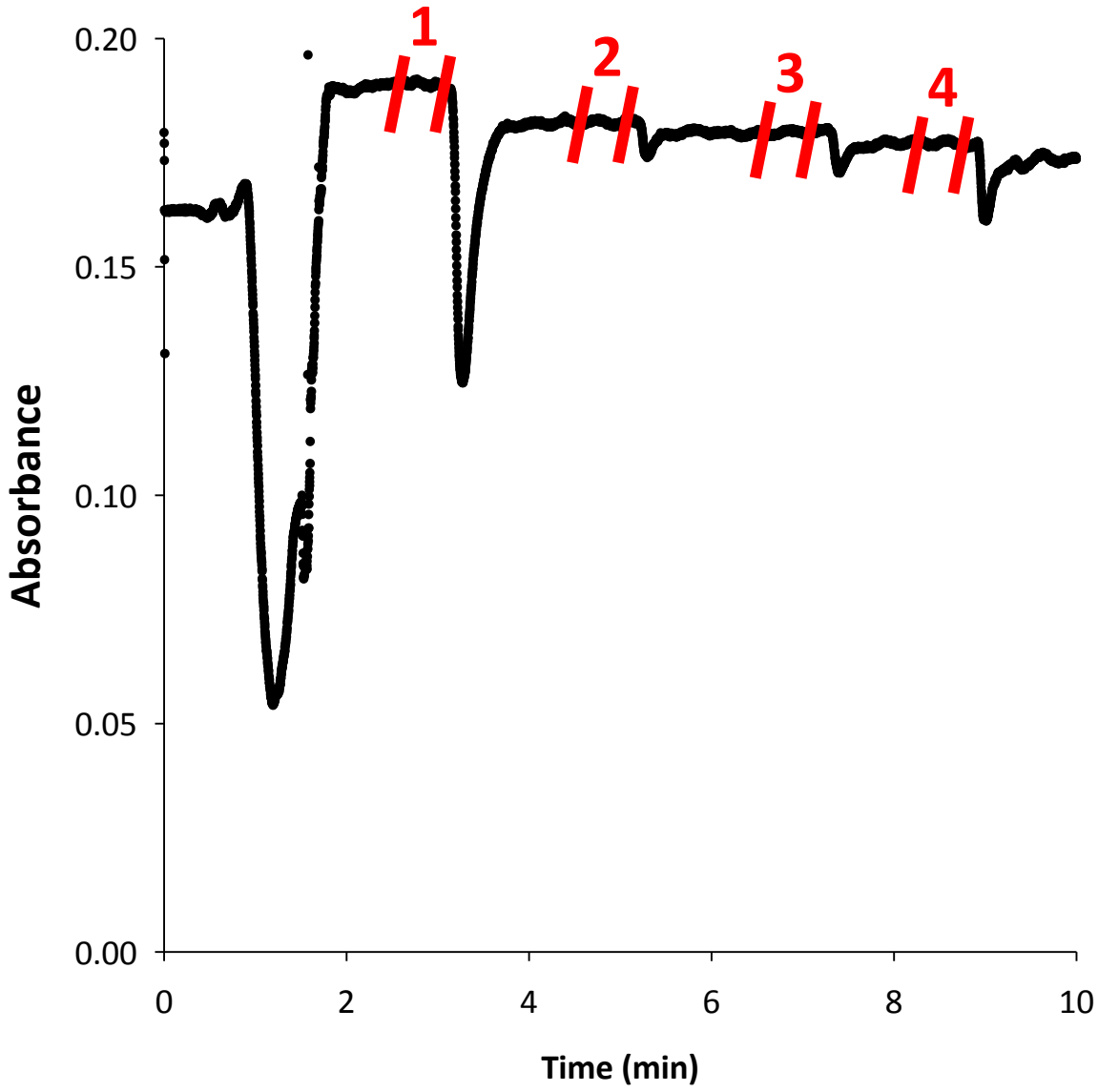

Figure A.2: Example of data file obtained from the UV-Vis during oxidant consumption experiments. Data was obtained by averaging 30 seconds of absorbance readings after allowing the signal to equilibrate for at least 30 seconds to obtain the average absorbance for each reaction time. The sections of data used for each time point are shown by sections above as follows: t = 0 (1), 0.35 (2), 0.5 (3), and 0.75 seconds (4). Conditions: $[2,4\text{-dichlorophenol}]_i$ = 100 μM, $[HOCl]_i$ = 10.42-10.48 μM, pH = 7.5, [NaHCO3] = 2 mM.

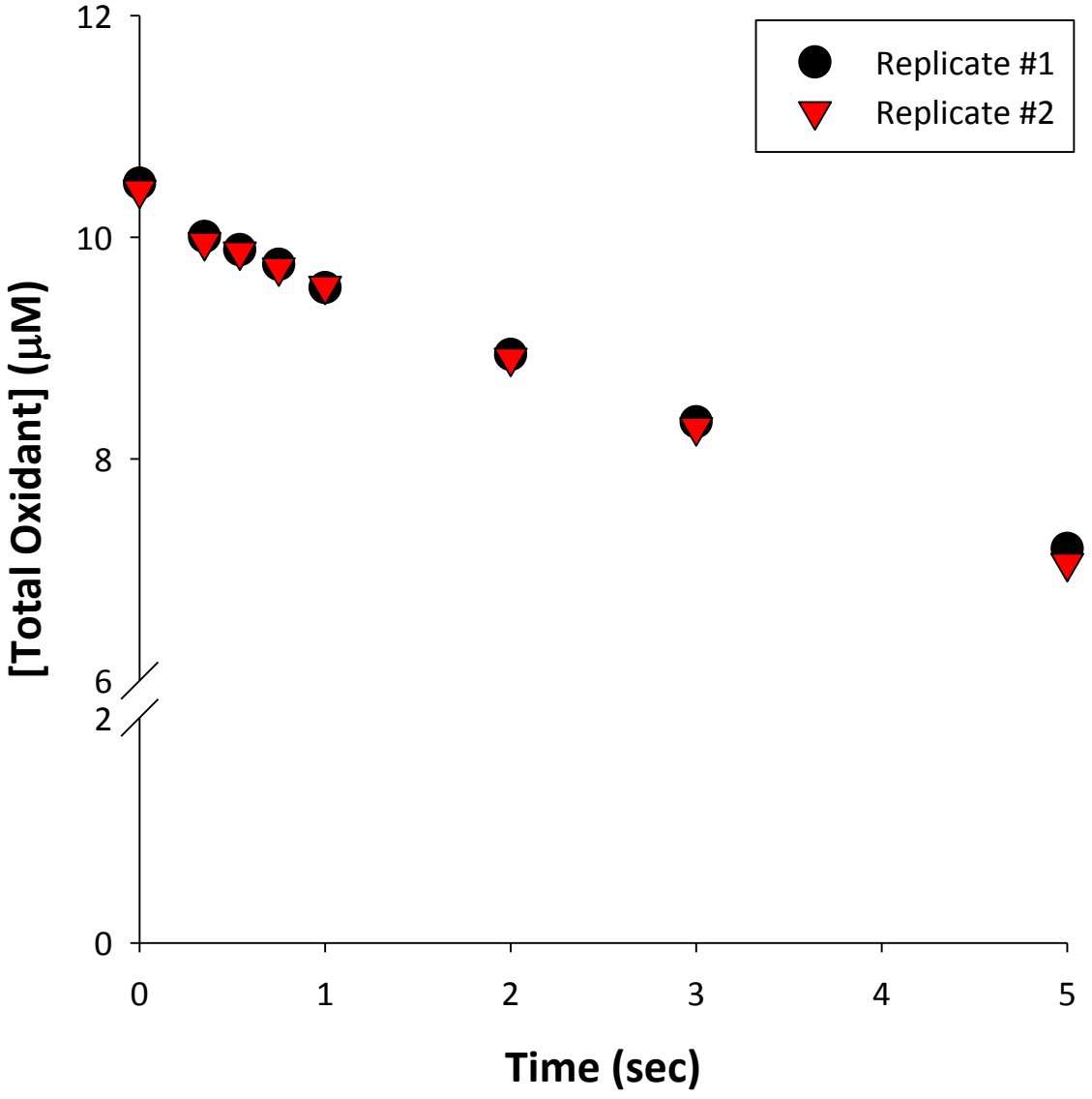

Figure A.3: Example plot of replicates for oxidant consumption measurements obtained from averaged absorbance. Each data point was obtained by averaging 30 seconds of absorbance readings for each reaction time. This plot is representative of the high quality, reproducible results possible using the QFS. The standard deviation for all points were <0.5 nM. Conditions: $[2,4\text{-dichlorophenol}]_i$ = 100 μM, $[HOCl]_i$ = 10.42-10.48 μM, pH = 7.5, $[NaHCO_3]$ = 2 mM.

Appendix B: Model Description

Discussion B.1: The following is an example of the code used to produce the models described within this study. This model simultaneously fits experimental oxidant concentrations over time at 6 different pH values for experiments performed with Bisphenol-A. Explanations of each portion of code are designated by bold font and were not in the original coding. All concentrations use units of µM.

//Iodide-HOCl model at user defined conditions
Independent variable=Time
These are fixed on spreadsheet to experimental reaction times
IndVars: T
Dependant variables=[total oxidant] at each pH
These are fixed on spreadsheet to experimental results
DepVars: TOTOX1, TOTOX2, TOTOX3, TOTOX4, TOTOX5, TOTOX6
Parameters: Iinit=[initial iodide], Pheninit=[total initial phenol]
These both remain constant. k values are rate constants for the following rxns.

$HOCl + BPA \rightarrow products$	**k1**
$OCl^- + BPA \rightarrow products$	**k2**
$HOCl + BPA^- \rightarrow products$	**k3**
$OCl^- + BPA^- \rightarrow products$	**k4**
$HOCl + BPA^{2-} \rightarrow products$	**k5**
$I_2 + BPA \rightarrow products + I^-$	**k6**
$I_2 + BPA^- \rightarrow products + I^-$	**k7**
$HOI + BPA \rightarrow products$	**k8**
$HOI + BPA^- \rightarrow products$	**k9**
$HOI + BPA^{2-} \rightarrow products$	**k10**
$OI^- + BPA \rightarrow products$	**k11**
$OI^- + BPA^- \rightarrow products$	**k12**
$OI^- + BPA^{2-} \rightarrow products$	**k13**

Params: Iinit, Pheninit, k1, k2, k3, k4, k5, k6, k7, k8, k9, k10, k11, k12, k13
Other pertinent equilibrium and rate constants

I2<--->HOI+I+H	**KI1**
HOI<--->OI+H	**KI2**
I2+I<--->I3	**KI3**
HOI+H<--->H2OI	**KI4**

HOI+I<--->HOI2 **KI5**
Cl2<--->HOCl+Cl+H **KCl1**
HOCl<--->OCl+H **KCl2**
HOCl+I---->HOI+Cl **kCl**

KI1=5.44e-13/Iinit
KI2=2.3e-11
KI3=715*Iinit
KI4=2
KI5=3.1e-3/Iinit
Kphenol1=10^(-9.6)
Kphenol2=10^(-10.2)
KCl1=2.56e-4
KCl2=3.16e-8
kCl=4.3e8

Initial values for variables

T=0
Pheninit1=Pheninit
Pheninit2=Pheninit
Pheninit3=Pheninit
Pheninit4=Pheninit
Pheninit5=Pheninit
Pheninit6=Pheninit
TOTOXi1=1e-5
TOTOXi2=1e-5
TOTOXi3=1e-5
TOTOXi4=1e-5
TOTOXi5=1e-5
TOTOXi6=1e-5
TOTOX1=TOTOXi1
TOTOX2=TOTOXi2
TOTOX3=TOTOXi3
TOTOX4=TOTOXi4
TOTOX5=TOTOXi5
TOTOX6=TOTOXi6
pH1=5
pH2=6
pH3=7
pH4=8
pH5=9
pH6=10
Cl1=TOTOXi1
Cl2=TOTOXi2
Cl3=TOTOXi3
Cl4=TOTOXi4

Cl5=TOTOXi5
Cl6=TOTOXi6
Initial I^- concentrations taken from speciation model output
I1=1.1734e-10
I2=1.196e-10
I3=1.4981e-10
I4=1.5161e-10
I5=1.4686e-10
I6=1.3539e-10
H1 = 10^(-PH1)
H2 = 10^(-PH2)
H3 = 10^(-PH3)
H4 = 10^(-PH4)
H5 = 10^(-PH5)
H6 = 10^(-PH6)
TOTphen1=Pheninit1
TOTphen2=Pheninit2
TOTphen3=Pheninit3
TOTphen4=Pheninit4
TOTphen5=Pheninit5
TOTphen6=Pheninit6
Phenol species concentrations
Phenol1=TOTPhen1/(1+Kphenol1/H1*(1+KPhenol2/H1))
Phenol2=TOTPhen2/(1+Kphenol1/H2*(1+KPhenol2/H2))
Phenol3=TOTPhen3/(1+Kphenol1/H3*(1+KPhenol2/H3))
Phenol4=TOTPhen4/(1+Kphenol1/H4*(1+KPhenol2/H4))
Phenol5=TOTPhen5/(1+Kphenol1/H5*(1+KPhenol2/H5))
Phenol6=TOTPhen6/(1+Kphenol1/H6*(1+KPhenol2/H6))
Phenolate1=KPhenol1*Phenol1/H1
Phenolate2=KPhenol1*Phenol2/H2
Phenolate3=KPhenol1*Phenol3/H3
Phenolate4=KPhenol1*Phenol4/H4
Phenolate5=KPhenol1*Phenol5/H5
Phenolate6=KPhenol1*Phenol6/H6
Phenolate2m1=KPhenol2*Phenolate1/H1
Phenolate2m2=KPhenol2*Phenolate2/H2
Phenolate2m3=KPhenol2*Phenolate3/H3
Phenolate2m4=KPhenol2*Phenolate4/H4
Phenolate2m5=KPhenol2*Phenolate5/H5
Phenolate2m6=KPhenol2*Phenolate6/H6
Oxidant species concentrations- Fspecies is fraction of the total
FHOI1=1/(1+KI2/H1 +H1/KI1*(1+KI3)+H1/KI4+1/KI5)
FHOI2=1/(1+KI2/H2 +H2/KI1*(1+KI3)+H2/KI4+1/KI5)
FHOI3=1/(1+KI2/H3 +H3/KI1*(1+KI3)+H3/KI4+1/KI5)

FHOI4=1/(1+KI2/H4 +H4/KI1*(1+KI3)+H4/KI4+1/KI5)
FHOI5=1/(1+KI2/H5 +H5/KI1*(1+KI3)+H5/KI4+1/KI5)
FHOI6=1/(1+KI2/H6 +H6/KI1*(1+KI3)+H6/KI4+1/KI5)
FOI1=KI2*FHOI1/H1
FOI2=KI2*FHOI2/H2
FOI3=KI2*FHOI3/H3
FOI4=KI2*FHOI4/H4
FOI5=KI2*FHOI5/H5
FOI6=KI2*FHOI6/H6
FI21=FHOI1*H1/KI1
FI22=FHOI2*H2/KI1
FI23=FHOI3*H3/KI1
FI24=FHOI4*H4/KI1
FI25=FHOI5*H5/KI1
FI26=FHOI6*H6/KI1
FCl21 = H1^2/(H1^2+KCl1*H1+KCl1*KCl2)
FCl22 = H2^2/(H2^2+KCl1*H2+KCl1*KCl2)
FCl23 = H3^2/(H3^2+KCl1*H3+KCl1*KCl2)
FCl24 = H4^2/(H4^2+KCl1*H4+KCl1*KCl2)
FCl25 = H5^2/(H5^2+KCl1*H5+KCl1*KCl2)
FCl26 = H6^2/(H6^2+KCl1*H6+KCl1*KCl2)
FHOCl1=FCl21*KCl1/H1
FHOCl2=FCl22*KCl1/H2
FHOCl3=FCl23*KCl1/H3
FHOCl4=FCl24*KCl1/H4
FHOCl5=FCl25*KCl1/H5
FHOCl6=FCl26*KCl1/H6
FOCl1=FHOCl1*KCl2/H1
FOCl2=FHOCl2*KCl2/H2
FOCl3=FHOCl3*KCl2/H3
FOCl4=FHOCl4*KCl2/H4
FOCl5=FHOCl5*KCl2/H5
FOCl6=FHOCl6*KCl2/H6
FI31=kI3*FI21
FI32=kI3*FI22
FI33=kI3*FI23
FI34=kI3*FI24
FI35=kI3*FI25
FI36=kI3*FI26
FHOI21=FHOI1/kI5
FHOI22=FHOI2/kI5
FHOI23=FHOI3/kI5
FHOI24=FHOI4/kI5
FHOI25=FHOI5/kI5

FHOI26=FHOI6/kI5
FH2OI1=FHOI1*H1/kI4
FH2OI2=FHOI2*H2/kI4
FH2OI3=FHOI3*H3/kI4
FH2OI4=FHOI4*H4/kI4
FH2OI5=FHOI5*H5/kI4
FH2OI6=FHOI6*H6/kI4
Using the following mass balances: TOTOI=I_2+HOI+OI^-+I_3^-+H_2OI^++HOI_2^-,
TOTI= I^-+2*I_2+HOI+OI^-+3*I_3^-+H_2OI^++2*HOI_2^-; then solved for TOTOI
TOTOI1=Iinit/(1+FI21+2*FI31+FHOI21)
TOTOI2=Iinit/(1+FI22+2*FI32+FHOI22)
TOTOI3=Iinit/(1+FI23+2*FI33+FHOI23)
TOTOI4=Iinit/(1+FI24+2*FI34+FHOI24)
TOTOI5=Iinit/(1+FI25+2*FI35+FHOI25)
TOTOI6=Iinit/(1+FI26+2*FI36+FHOI26)
HOI1=FHOI1*TOTOI1
HOI2=FHOI2*TOTOI2
HOI3=FHOI3*TOTOI3
HOI4=FHOI4*TOTOI4
HOI5=FHOI5*TOTOI5
HOI6=FHOI6*TOTOI6
I21=FI21*TOTOI1
I22=FI22*TOTOI2
I23=FI23*TOTOI3
I24=FI24*TOTOI4
I25=FI25*TOTOI5
I26=FI26*TOTOI6
OI1=FOI1*TOTOI1
OI2=FOI2*TOTOI2
OI3=FOI3*TOTOI3
OI4=FOI4*TOTOI4
OI5=FOI5*TOTOI5
OI6=FOI6*TOTOI6
TOTOCl1=TOTOX1-TOTOI1
TOTOCl2=TOTOX2-TOTOI2
TOTOCl3=TOTOX3-TOTOI3
TOTOCl4=TOTOX4-TOTOI4
TOTOCl5=TOTOX5-TOTOI5
TOTOCl6=TOTOX6-TOTOI6
Cl21=FCl21*TOTOCl1
Cl22=FCl22*TOTOCl2
Cl23=FCl23*TOTOCl3
Cl24=FCl24*TOTOCl4
Cl25=FCl25*TOTOCl5

Cl26=FCl26*TOTOCl6
HOCl1=FHOCl1*TOTOCl1
HOCl2=FHOCl2*TOTOCl2
HOCl3=FHOCl3*TOTOCl3
HOCl4=FHOCl4*TOTOCl4
HOCl5=FHOCl5*TOTOCl5
HOCl6=FHOCl6*TOTOCl6
OCl1=FOCl1*TOTOCl1
OCl2=FOCl2*TOTOCl2
OCl3=FOCl3*TOTOCl3
OCl4=FOCl4*TOTOCl4
OCl5=FOCl5*TOTOCl5
OCl6=FOCl6*TOTOCl6

These are the differential equations that are being solved over each iteration while fitting each value of k:

TOTOX'=TOTPhen'=

$$\frac{d[\mathbf{Total\ Oxidant}]}{dt} = -(k_1[\mathbf{HOCl}] + k_3[\mathbf{OCl}])[\mathbf{BPA}] - (k_2[\mathbf{HOCl}] + k_4[\mathbf{OCl}])[\mathbf{BPA^-}] - k_6[HOCl][BPA^{2-}] - (k_7[\mathbf{BPA}] + k_7[\mathbf{BPA^-}])[\mathbf{I_2}] - (k_8[\mathbf{BPA}] + k_9[\mathbf{BPA^-}] + k_{10}[\mathbf{BPA^{2-}}])[\mathbf{HOI}] - (k_{11}[\mathbf{BPA}] + k_{12}[\mathbf{BPA^-}] + k_{13}[\mathbf{BPA^{2-}}])[\mathbf{OI^-}]$$

I'=

$$\frac{d[\mathbf{Total\ I^-}]}{dt} = +(k_7[\mathbf{BPA}] + k_7[\mathbf{BPA^-}])[\mathbf{I_2}] - k_{\mathrm{ICL}}[\mathbf{HOCl}][\mathbf{I^-}]$$

TOTOI'=

$$\frac{d[\mathbf{Total\ HOI}]}{dt} = -(k_7[\mathbf{BPA}] + k_7[\mathbf{BPA^-}])[\mathbf{I_2}] - (k_8[\mathbf{BPA}] + k_9[\mathbf{BPA^-}] + k_{10}[\mathbf{BPA^{2-}}])[\mathbf{HOI}] - (k_{11}[\mathbf{BPA}] + k_{12}[\mathbf{BPA^-}] + k_{13}[\mathbf{BPA^{2-}}])[\mathbf{OI^-}] + k_{\mathrm{ICL}}[\mathbf{HOCl}][\mathbf{I^-}]$$

TOTOX1'=-k5*HOCl1*phenolate2m1+(-k1*HOCl1-k3*OCl1)*phenol1-
(k2*HOCl1+k4*OCl1)*phenolate1-(k6*phenol1+k7*phenolate1)*I21-

```
        (k8*phenol1+k9*phenolate1+k10*Phenolate2m1)*HOI1-
        (k11*phenol1+k12*phenolate1+k13*Phenolate2m1)*OI1
TOTOX2'=-k5*HOCl2*phenolate2m2+(-k1*HOCl2-k3*OCl2)*phenol2-
        (k2*HOCl2+k4*OCl2)*phenolate2-(k6*phenol2+k7*phenolate2)*I22-
        (k8*phenol2+k9*phenolate2+k10*Phenolate2m2)*HOI2-
        (k11*phenol2+k12*phenolate2+k13*Phenolate2m2)*OI2
TOTOX3'=-k5*HOCl3*phenolate2m3+(-k1*HOCl3-k3*OCl3)*phenol3-
        (k2*HOCl3+k4*OCl3)*phenolate3-(k6*phenol3+k7*phenolate3)*I23-
        (k8*phenol3+k9*phenolate3+k10*Phenolate2m3)*HOI3-
        (k11*phenol3+k12*phenolate3+k13*Phenolate2m3)*OI3
TOTOX4'=-k5*HOCl4*phenolate2m4+(-k1*HOCl4-k3*OCl4)*phenol4-
        (k2*HOCl4+k4*OCl4)*phenolate4-(k6*phenol4+k7*phenolate4)*I24-
        (k8*phenol4+k9*phenolate4+k10*Phenolate2m4)*HOI4-
        (k11*phenol4+k12*phenolate4+k13*Phenolate2m4)*OI4
TOTOX5'=-k5*HOCl5*phenolate2m5+(-k1*HOCl5-k3*OCl5)*phenol5-
        (k2*HOCl5+k4*OCl5)*phenolate5-(k6*phenol5+k7*phenolate5)*I25-
        (k8*phenol5+k9*phenolate5+k10*Phenolate2m5)*HOI5-
        (k11*phenol5+k12*phenolate5+k13*Phenolate2m5)*OI5
TOTOX6'=-k5*HOCl6*phenolate2m6+(-k1*HOCl6-k3*OCl6)*phenol6-
        (k2*HOCl6+k4*OCl6)*phenolate6-(k6*phenol6+k7*phenolate6)*I26-
        (k8*phenol6+k9*phenolate6+k10*Phenolate2m6)*HOI6-
        (k11*phenol6+k12*phenolate6+k13*Phenolate2m6)*OI6

TOTPhen1'=-k5*HOCl1*phenolate2m1+(-k1*HOCl1-k3*OCl1)*phenol1-
        (k2*HOCl1+k4*OCl1)*phenolate1-(k6*phenol1+k7*phenolate1)*I21-
        (k8*phenol1+k9*phenolate1+k10*Phenolate2m1)*HOI1-
        (k11*phenol1+k12*phenolate1+k13*Phenolate2m1)*OI1
TOTPhen2'=-k5*HOCl2*phenolate2m2+(-k1*HOCl2-k3*OCl2)*phenol2-
        (k2*HOCl2+k4*OCl2)*phenolate2-(k6*phenol2+k7*phenolate2)*I22-
        (k8*phenol2+k9*phenolate2+k10*Phenolate2m2)*HOI2-
        (k11*phenol2+k12*phenolate2+k13*Phenolate2m2)*OI2
TOTPhen3'=-k5*HOCl3*phenolate2m3+(-k1*HOCl3-k3*OCl3)*phenol3-
        (k2*HOCl3+k4*OCl3)*phenolate3-(k6*phenol3+k7*phenolate3)*I23-
        (k8*phenol3+k9*phenolate3+k10*Phenolate2m3)*HOI3-
        (k11*phenol3+k12*phenolate3+k13*Phenolate2m3)*OI3
TOTPhen4'=-k5*HOCl4*phenolate2m4+(-k1*HOCl4-k3*OCl4)*phenol4-
        (k2*HOCl4+k4*OCl4)*phenolate4-(k6*phenol4+k7*phenolate4)*I24-
        (k8*phenol4+k9*phenolate4+k10*Phenolate2m4)*HOI4-
        (k11*phenol4+k12*phenolate4+k13*Phenolate2m4)*OI4
TOTPhen5'=-k5*HOCl5*phenolate2m5+(-k1*HOCl5-k3*OCl5)*phenol5-
        (k2*HOCl5+k4*OCl5)*phenolate5-(k6*phenol5+k7*phenolate5)*I25-
        (k8*phenol5+k9*phenolate5+k10*Phenolate2m5)*HOI5-
        (k11*phenol5+k12*phenolate5+k13*Phenolate2m5)*OI5
```

```
TOTPhen6'=-k5*HOCl6*phenolate2m6+(-k1*HOCl6-k3*OCl6)*phenol6-
        (k2*HOCl6+k4*OCl6)*phenolate6-(k6*phenol6+k7*phenolate6)*I26-
        (k8*phenol6+k9*phenolate6+k10*Phenolate2m6)*HOI6-
        (k11*phenol6+k12*phenolate6+k13*Phenolate2m6)*OI6

I1'=(k6*phenol1+k7*phenolate1)*I21-kCl*I1*HOCl1
I2'=(k6*phenol2+k7*phenolate2)*I22-kCl*I2*HOCl2
I3'=(k6*phenol3+k7*phenolate3)*I23-kCl*I3*HOCl3
I4'=(k6*phenol4+k7*phenolate4)*I24-kCl*I4*HOCl4
I5'=(k6*phenol5+k7*phenolate5)*I25-kCl*I5*HOCl5
I6'=(k6*phenol6+k7*phenolate6)*I26-kCl*I6*HOCl6

TOTOI1'=-(k6*phenol1+k7*phenolate1)*I21-
        (k8*phenol1+k9*phenolate1+k10*Phenolate2m1)*HOI1-
        (k11*phenol1+k12*phenolate1+k13*Phenolate2m1)*OI1+kCl*I1*HOCl1
TOTOI2'=-(k6*phenol2+k7*phenolate2)*I22-
        (k8*phenol2+k9*phenolate2+k10*Phenolate2m2)*HOI2-
        (k11*phenol2+k12*phenolate2+k13*Phenolate2m2)*OI2+kCl*I2*HOCl2
TOTOI3'=-(k6*phenol3+k7*phenolate3)*I23-
        (k8*phenol3+k9*phenolate3+k10*Phenolate2m3)*HOI3-
        (k11*phenol3+k12*phenolate3+k13*Phenolate2m3)*OI3+kCl*I3*HOCl3
TOTOI4'=-(k6*phenol4+k7*phenolate4)*I24-
        (k8*phenol4+k9*phenolate4+k10*Phenolate2m4)*HOI4-
        (k11*phenol4+k12*phenolate4+k13*Phenolate2m4)*OI4+kCl*I4*HOCl4
TOTOI5'=-(k6*phenol5+k7*phenolate5)*I25-
        (k8*phenol5+k9*phenolate5+k10*Phenolate2m5)*HOI5-
        (k11*phenol5+k12*phenolate5+k13*Phenolate2m5)*OI5+kCl*I5*HOCl5
TOTOI6'=-(k6*phenol6+k7*phenolate6)*I26-
        (k8*phenol6+k9*phenolate6+k10*Phenolate2m6)*HOI6-
        (k11*phenol6+k12*phenolate6+k13*Phenolate2m6)*OI6+kCl*I6*HOCl6
```

Discussion B.2: Detailed description of the sequential fitting process used for fitting of all reaction rate constants. For purposes of simplicity, only the free chlorine- 2,4-dichlorophenol reaction rate parameter fitting approach is described below, though the same process was repeated for free iodide reactions.

The data file being fit contains the sample time points and the corresponding total oxidant concentration for experiments performed at pH 5, 6, 7, 8, 9, and 10. The parameters are fit using the differential equation as follows:

$$\frac{d[\text{Total HOCl}]}{dt} = -(k_{3.17}[\text{Cl}_2] + k_{3.19}[\text{H}_2\text{OCl}^+] + k_{3.21}[\text{HOCl}] + k_{3.23}[\text{OCl}^-])[\text{PhOH}]$$

$$-(k_{3.18}[\text{Cl}_2] + k_{3.20}[\text{H}_2\text{OCl}^+] + k_{3.22}[\text{HOCl}] + k_{3.24}[\text{OCl}^-])[\text{PhO}^-]$$

The model allows the user to select any number of total oxidant data sets at a given pH and minimizes the sum of squares error by varying parameter values over numerous iterations until a minimum is reached. The number of parameters being fit at a given time can also be selected by the user as well as the range limits for each value (i.e. $k \geq 0$, etc).

1. $k_{3.17}$, $k_{3.18}$, $k_{3.19}$, and $k_{3.20}$ are fit to pH 5 and pH 6 data sets. Rate constants are found to equal zero for $k_{3.18}$, $k_{3.19}$, and $k_{3.20}$. The $k_{3.17}$ rate constant is set to a value faster than the rate of diffusion limited reactions.

2. $k_{3.23}$ and $k_{3.24}$ are fit to pH 9 and 10 data sets. The rate constant is found to equal zero for $k_{3.23}$. $k_{3.24}$ also found to be extremely fast, though is highly unlikely since it involves 2 negatively charged species.

3. $k_{3.21}$ and $k_{3.22}$ are fit to pH 7 and 8 data sets and values are set at 87 and 451 $M^{-1}s^{-1}$, respectively.

4. $k_{3.17}$ and $k_{3.21}$ are fit to pH 5, 6, and 7 data sets. $k_{3.17}$ is fit to a value of 1.67×10^{-11} $M^{-1}s^{-1}$ so it is manually set to zero. $k_{3.21}$ remains unchanged.

5. $k_{3.21}$ fit is repeated for the same pH range. A slight change to 85 $M^{-1}s^{-1}$ is observed but the model's calculated total oxidant concentration at each time remains unchanged.

6. $k_{3.22}$ and $k_{3.24}$ are fit for pH 8, 9, and 10 data. $k_{3.24}$ is set to 2.05×10^{-13} $M^{-1}s^{-1}$ so it is also set manually to zero.

7. $k_{3.22}$ is again fit to the same data range with no change.

8. $k_{3.21}$ and $k_{3.22}$ are fit to the entire data set and values are adjusted to 25.5 and 664, respectively. A plot comparing the predicted and experimental oxidant concentrations over time shows that the model predicts the experimental concentrations very closely over the entire pH range.

9. $k_{3.21}$ is fixed at a value of 12.75 and $k_{3.22}$ is fit to data. The value of $k_{3.22}$ increases slightly but the error between model predictions and experimental data is significantly worse- especially at pH 5 and 6.

10. $k_{3.22}$ is set to 334 and $k_{3.21}$ is fit to data. The value of $k_{3.21}$ increases by an order of magnitude but predictions are much worse over the entire pH range.

11. A simultaneous fit of both $k_{3.21}$ and $k_{3.22}$ again results in values of 25.5 and 664, respectively.

12. To ensure that no other rate constant could substitute for either $k_{3.21}$ or $k_{3.22}$, $k_{3.21}$ was fixed to zero and $k_{3.22}$ was fixed at 664. One by one, each of the other parameters were again fit for the entire pH range. The rate constant fits did not change for any parameter except for Cl_2, but

again the assigned values was unrealistic and little improvement was observed for the overall predictions.

13. Step 12 was repeated, only this time $k_{3.21}$ was fixed at 25.5 and $k_{3.22}$ was fixed to zero. The model was unable to get the sum of squares error to within acceptable range by varying any rate constant.

14. Steps 12 and 13 were repeated while fitting each parameter only to the data sets at pH values where they are most likely important. Nearly identical results were observed.

14. All rate constants were again set to zero. All parameters were selected to adjust for an optimal overall fit for the entire data set. Once again, $k_{3.21}$ and $k_{3.22}$ were the only parameters to change, and once again, the resulting values were 25.5 and 664 $M^{-1}s^{-1}$.

The model fitting repeatedly found the only mechanisms necessary to include to be reactions between the PhOH or PhO^- 2,4-DCP species and HOCl. The model repeatedly tried to fit the Cl_2-HOCl reaction rate at a pH of 5, but resulting values were greater than diffusion limited reaction rates, and effects on model outputs were negligible. This leads to the conclusion that $k_{3.21}$ and $k_{3.22}$ are the only mechanisms that occur at circumneutral pH that affect the overall observed reactivity. The repeated attempts to fit the Cl_2 rate suggest that it likely would become important in more acidic conditions.

Appendix C: GC-MS Spectra for Phenols and Byproducts

Prior to analysis by GC-MS, the phenolic compounds in each sample were extracted through a solid phase extraction procedure. Each extracted sample then went through a derivitization step in which each was injected with a solution of pentafluorobenzyl bromide (PFBBr) and heated to 80 ^{o}C for 45 minutes. This basically caused the PFBBr to attach to the hydroxyl group on each phenol and results in an increased detection sensitivity for the GC-MS.

When run through the GC-MS, compounds are separated as they flow through a column and then they are bombarded by electrons which allows the charged particles to be analyzed and the composition to be determined. When bombarded by this electron beam, the compounds break apart in a specific pattern and the mass to charge ratio can be calculated for each particle. The results are given as spectra that show the quantities of particles and corresponding mass to charge (m/z) ratio. The m/z ratios spectra, as shown by the following figures, can be used to identify compounds since we can structurally determine the way each compound breaks apart when in the mass spectrophotometer. As a result of the derivitization step and because the molecular weight of PFBBr is 181 g/mol, the primary component detected for each phenol is represented by an m/z ratio of 181. In the case of phenol, the molecular weight is 94.1 g/mol. When the PFBBr attaches to phenol, the hydrogen on the hydroxyl group is lost, so the corresponding m/z ratio detected would be at 274 (94.1 g/mol for phenol - 1 g/mol for H^{+} + 181 g/mol for PFBBr). This is typically the second largest peak in the spectra as

compared to the PFBBr peak. The next largest peak results from phenols that either are not derivatized (i.e., do not attach to PFBBr) or in which the PFBBr is broken off by the electron beam. In either case, the hydrogen is detached so the m/z ratio would be 93. In the case of chlorine, it is typically found as one of two stable isotopes with molecular weights of 35 or 37 grams per mole. As such, if a single chlorine is substituted on a phenol, corresponding m/z ratios detected would be at 308 and 127 for ^{35}Cl and at 129 and 310 for ^{37}Cl. Additional peaks show up that correspond to the hydroxyl group fracturing off and a range of other occurrences. For bisphenol-A, it's two hydroxyl groups allow for the bonding of two PFBBr molecules, so a third set of peaks corresponding to double PFBBr substitutions are also found. This process was used to identify the compound associated with each figure below.

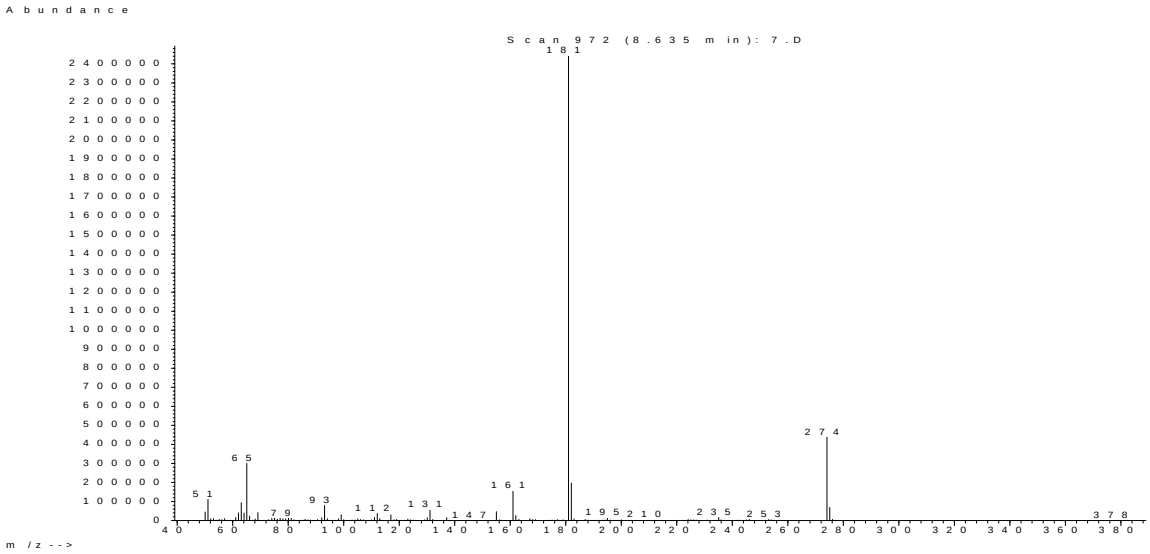

Figure C.1: GC-MS spectra for phenol. MW = 94.1 g/mol, m/z = 274, 93.

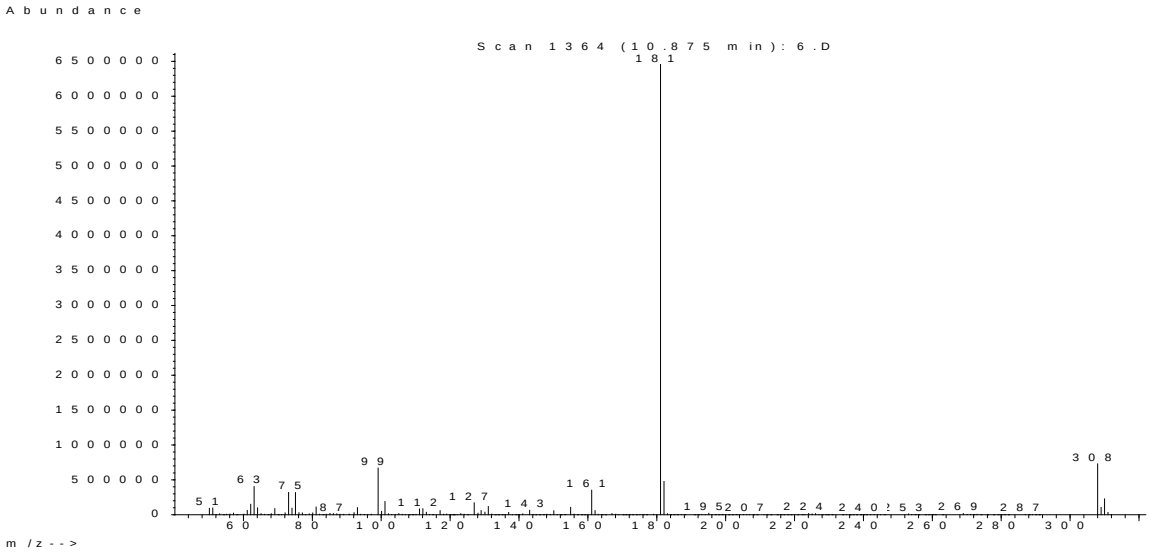

Figure C.2: GC-MS spectra for 4-chlorophenol. MW = 128.6 g/mol, m/z = 308, 127.

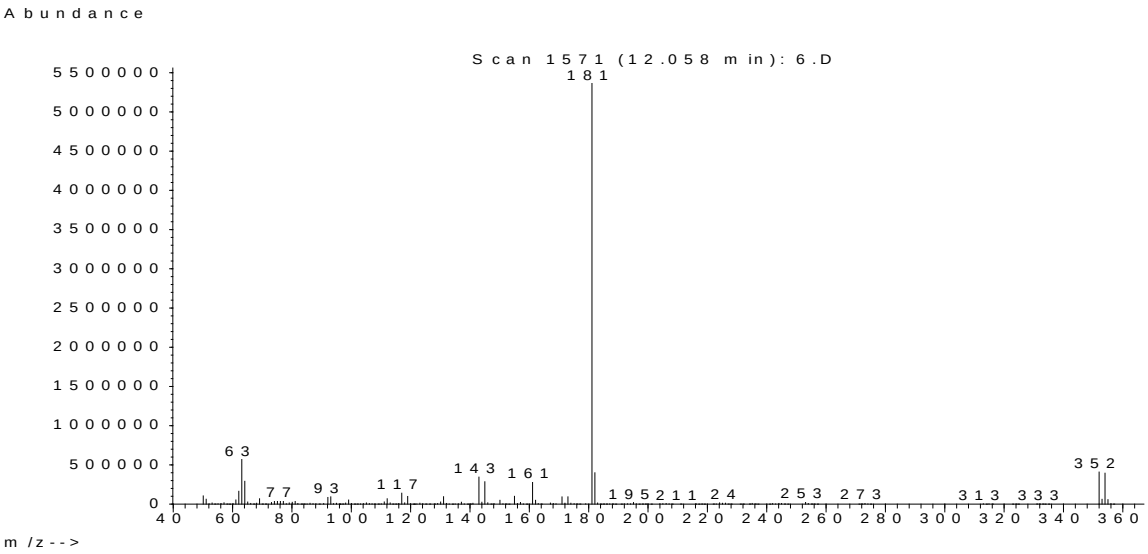

Figure C.3: GC-MS spectra for 4-bromophenol. MW = 173 g/mol, m/z = 352, 171.

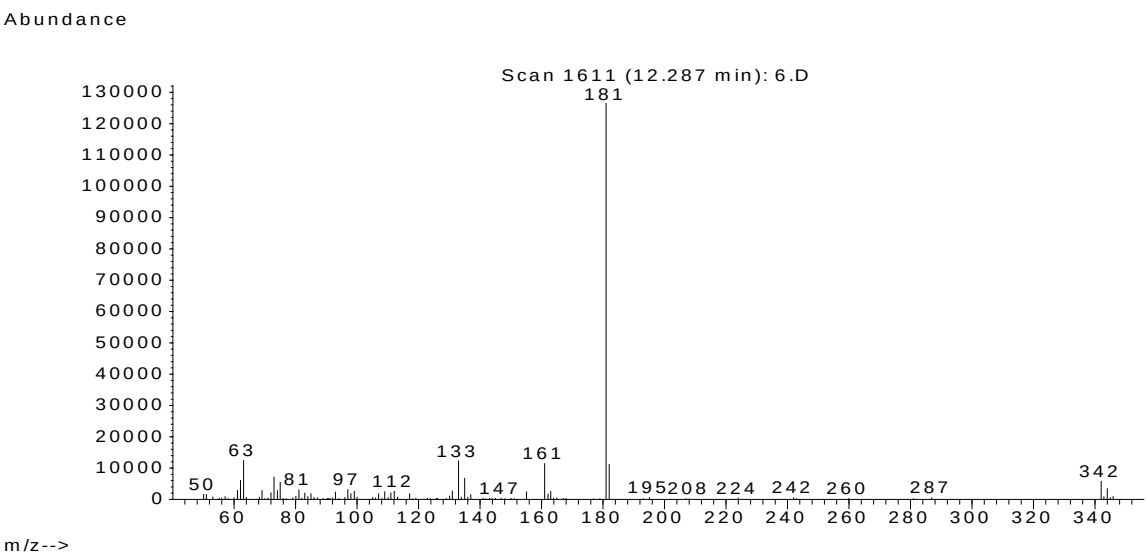

Figure C.4: GC-MS spectra for 2,4-dichlorophenol. MW = 163 g/mol, m/z = 342, 161.

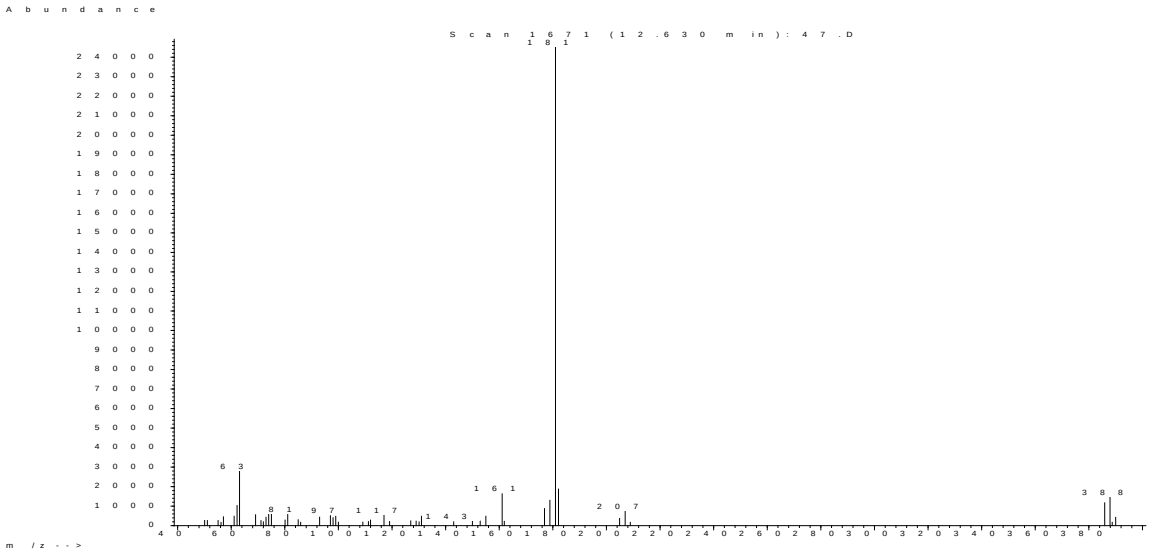

Figure C.5: GC-MS spectra for 4-bromo-6-chlorophenol. MW = 207 g/mol, m/z = 386, 207.

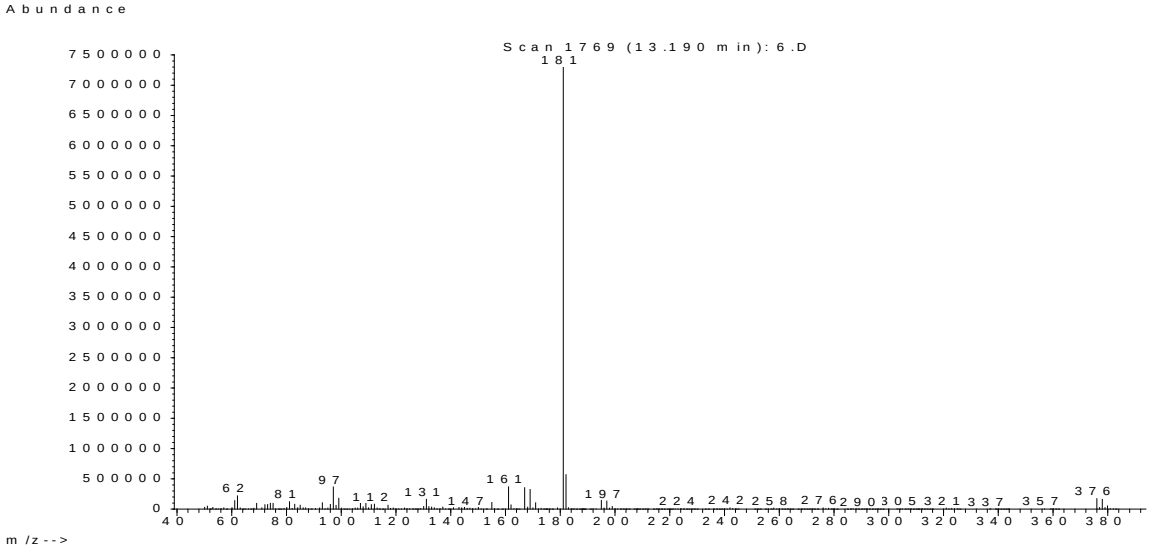

Figure C.6: GC-MS spectra for 2,4,6-trichlorophenol. MW = 197.4 g/mol, m/z = 376, 197.

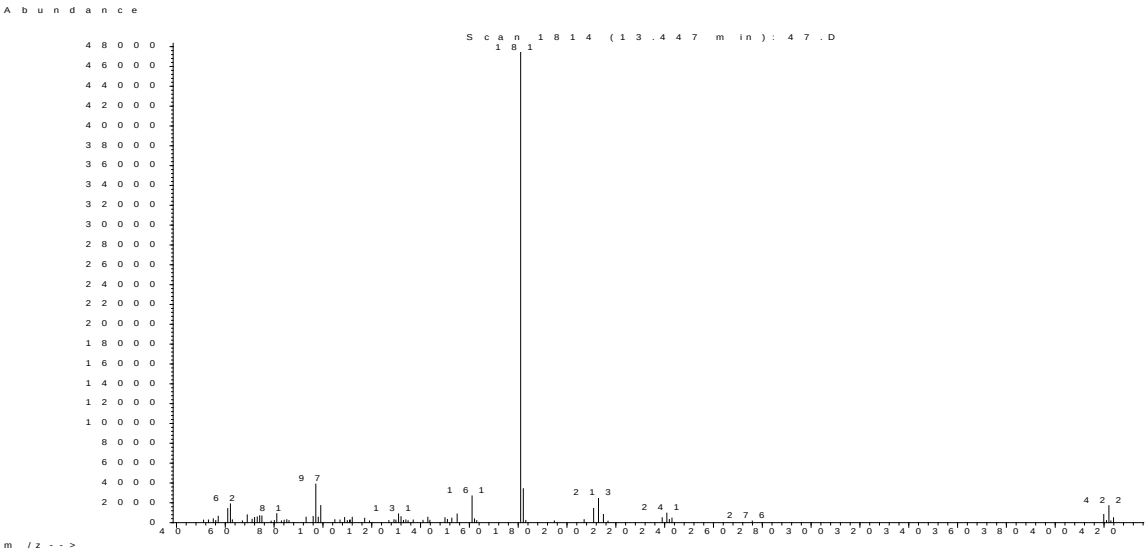

Figure C.7: GC-MS spectra for 4-bromo-2,6-dichlorophenol. MW = 242 g/mol, m/z = 422, 241.

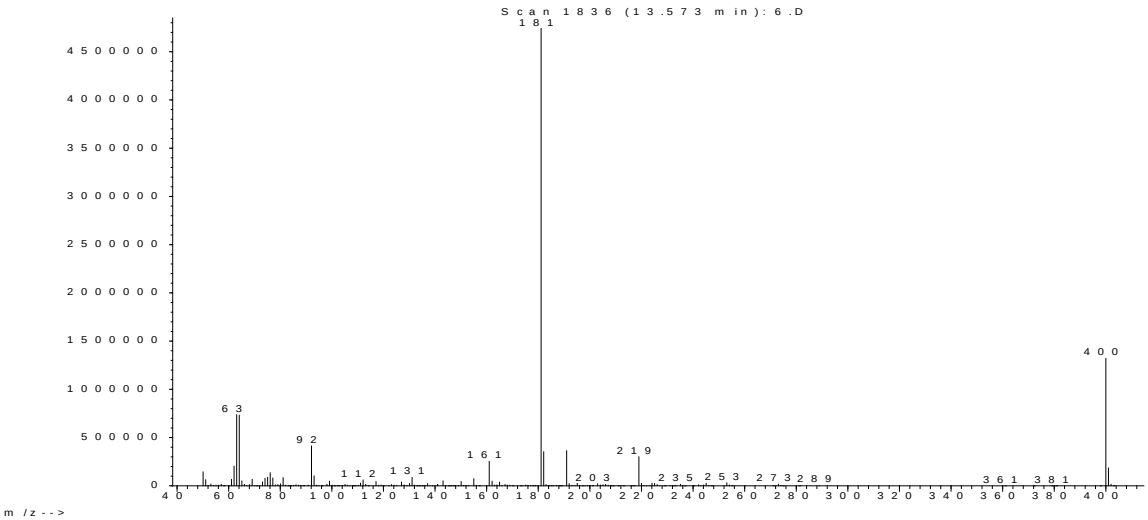

Figure C.8: GC-MS spectra for 4-iodophenol. MW = 220 g/mol, m/z = 400, 219.

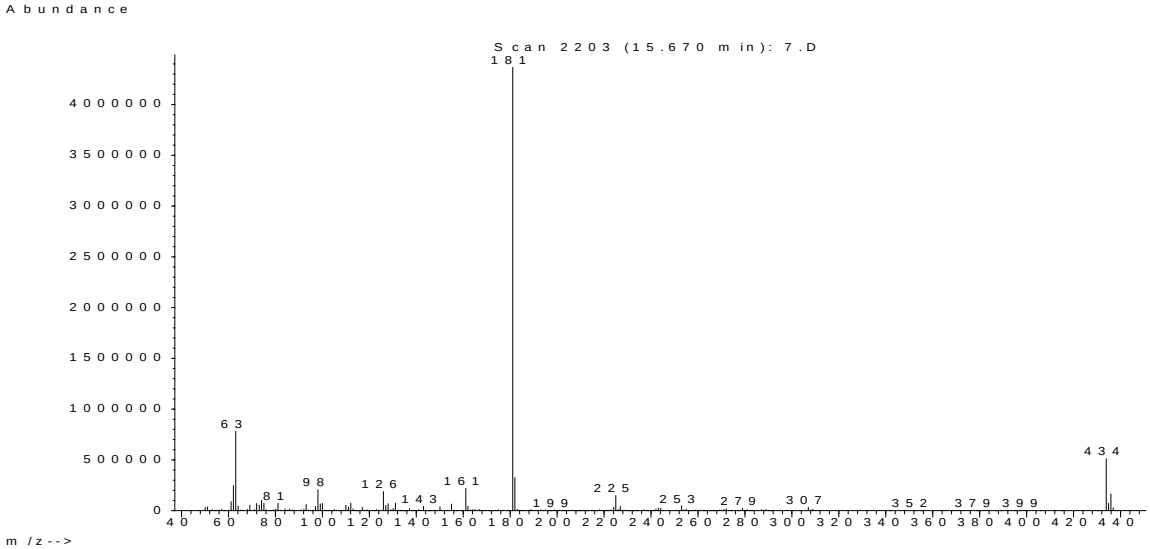

Figure C.9: GC-MS spectra for 4-chloro-3-iodophenol. MW = 254.5 g/mol, m/z = 434, 253.

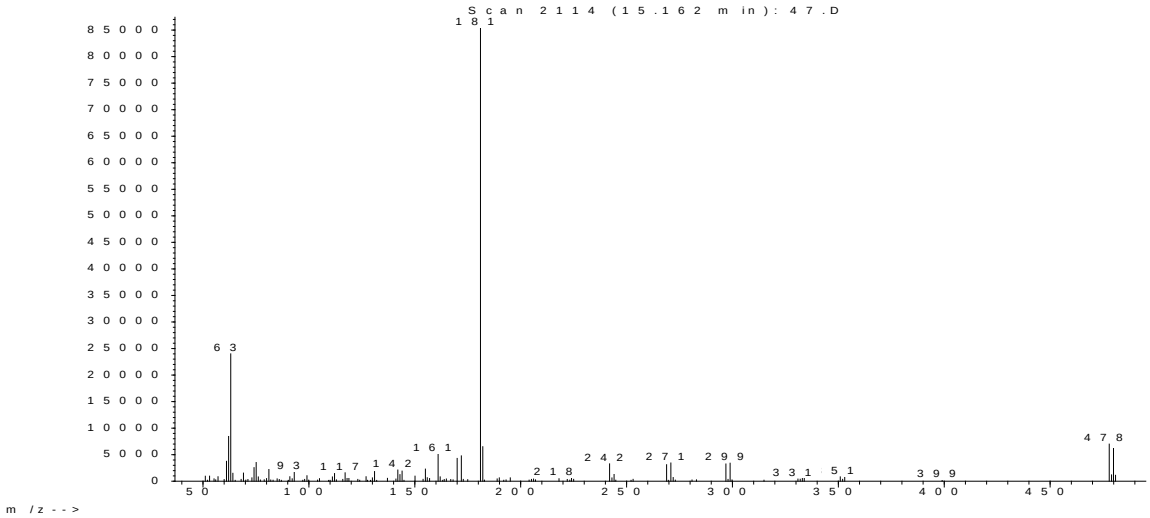

Figure C.10: GC-MS spectra for 4-bromo-6-iodophenol. MW = 300 g/mol, m/z = 478, 299.

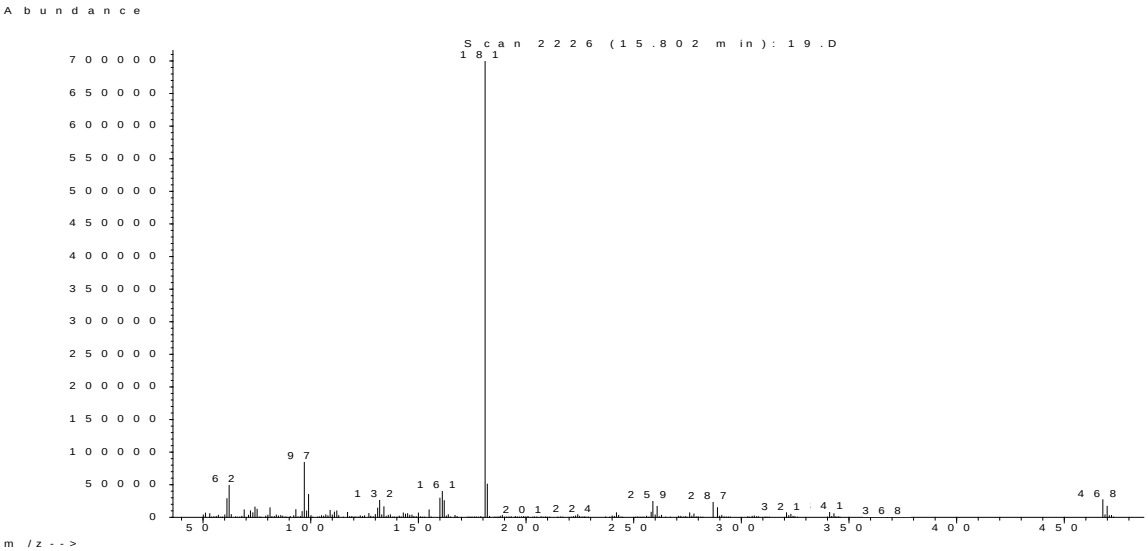

Figure C.11: GC-MS spectra for 2,4-dichloro-6-iodophenol. MW = 254.5 g/mol, m/z = 468, 287.

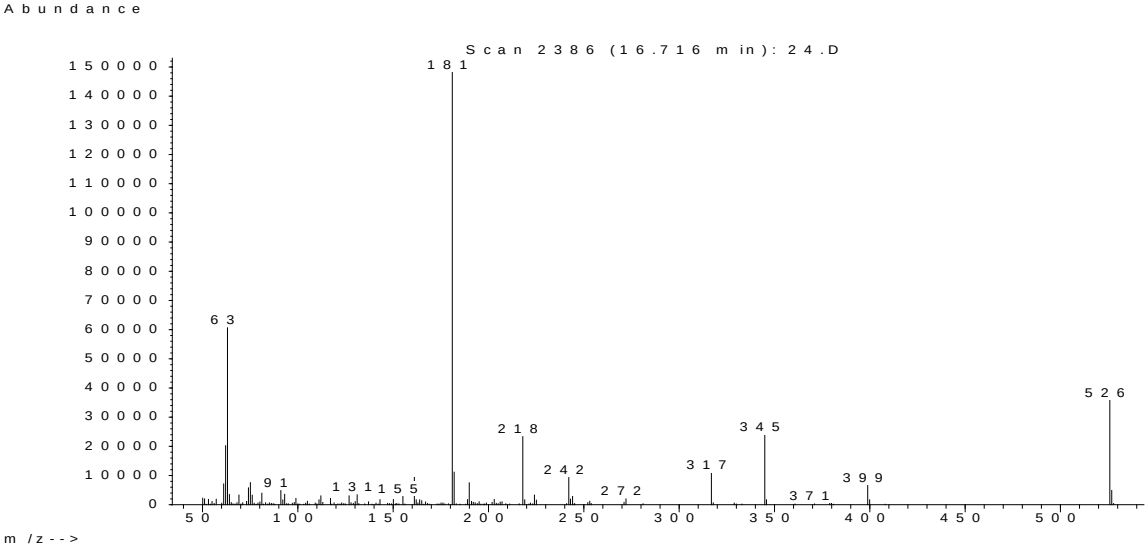

Figure C.12: GC-MS spectra for 2,4-diiodophenol. MW = 346 g/mol, m/z = 526, 345.

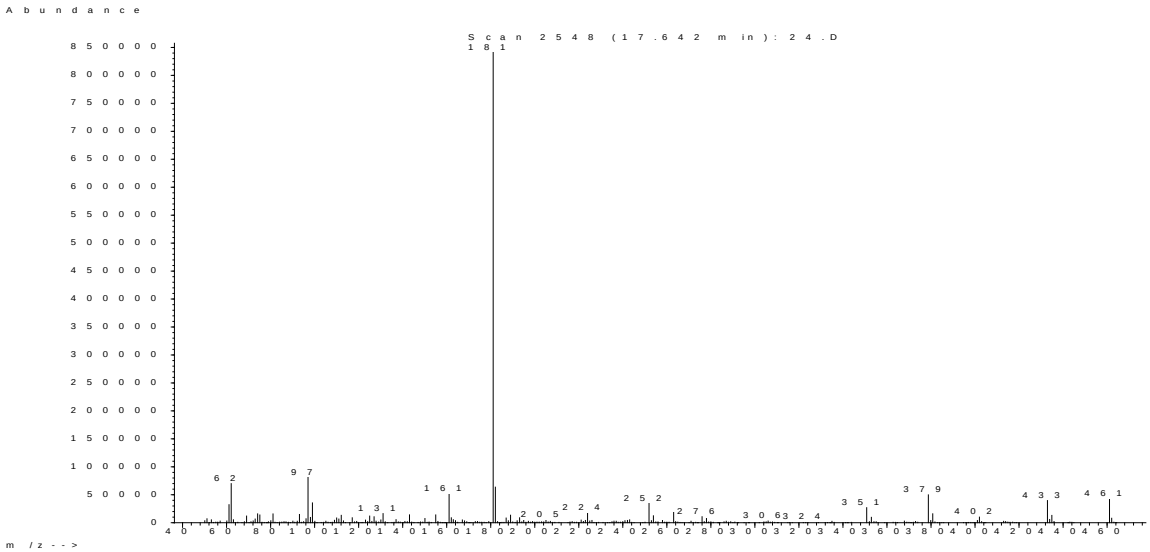

Figure C.13: GC-MS spectra for 2-chloro-4,6-diiodophenol. MW = 381 g/mol, m/z = 560, 379. (Scan range = 50 - 550)

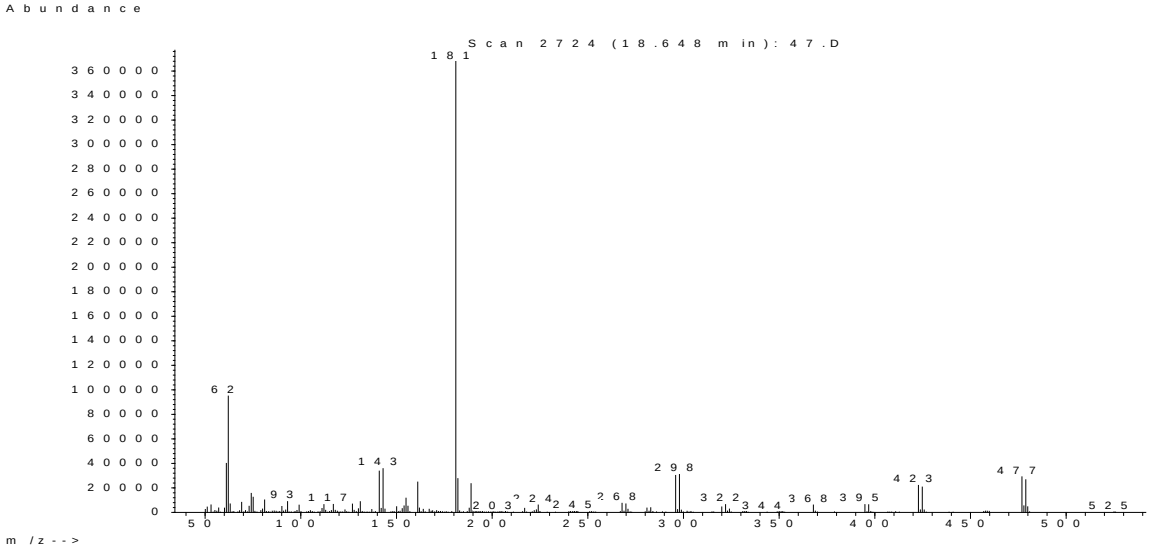

Figure C.14: GC-MS spectra for 4-bromo-2,6-diiodophenol. MW = 422 g/mol, m/z = 604, 421. (Scan range = 50 - 550)

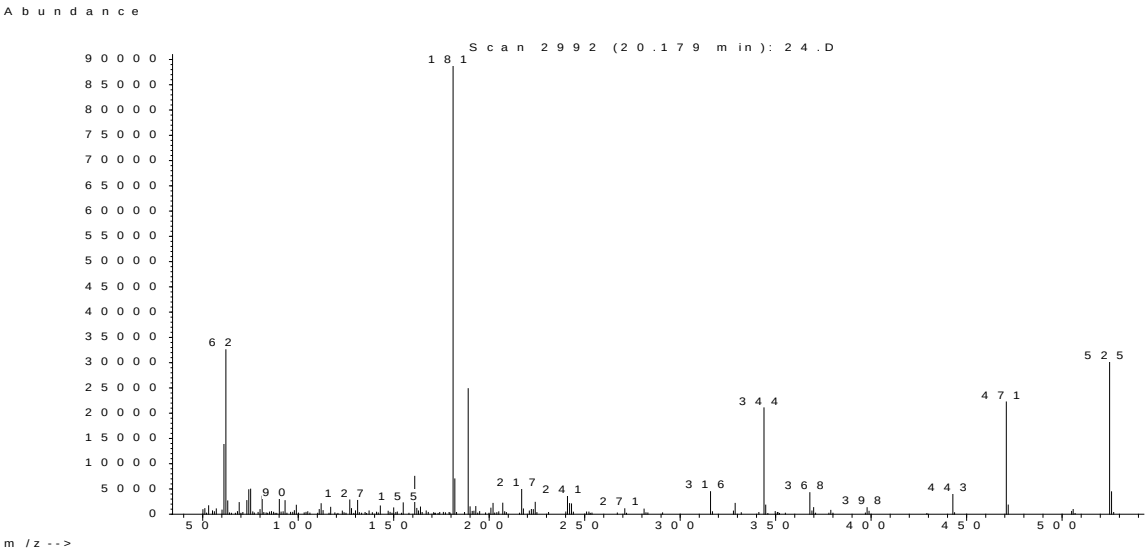

Figure C.15: GC-MS spectra for 2,4,6-triiodophenol. MW = 471.8 g/mol, m/z = 651, 471. (Scan range = 50 - 550)

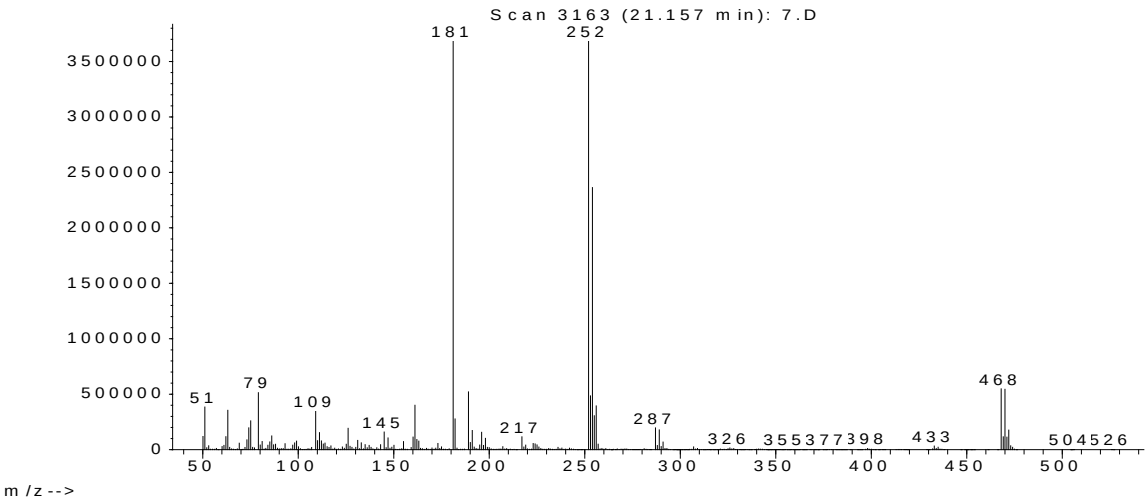

Figure C.16: GC-MS spectra for triclosan. MW = 289.5 g/mol, m/z = 468, 287.

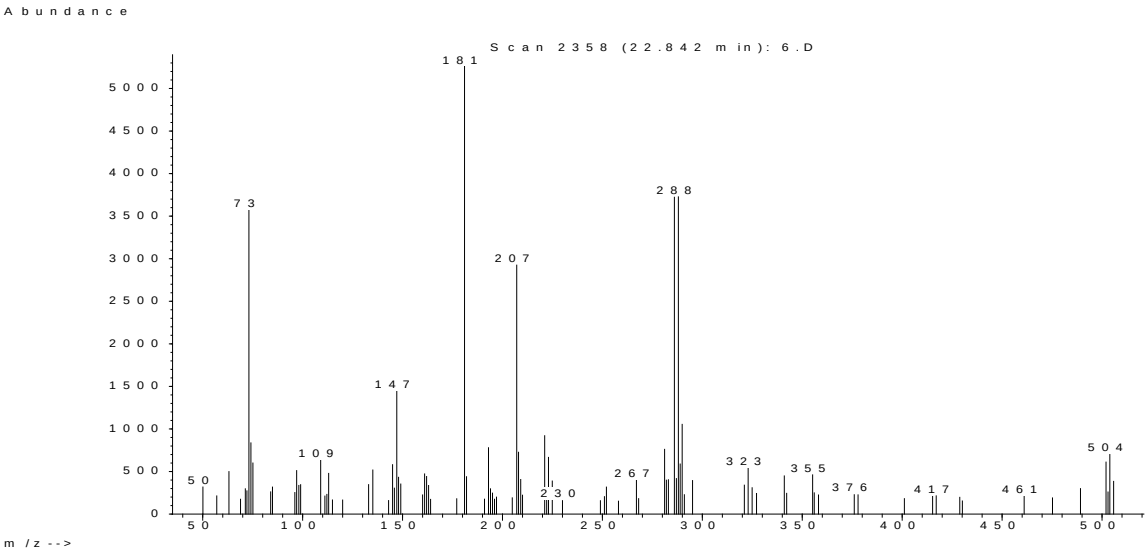

Figure C.17: GC-MS spectra for monochloro-triclosan. MW = 322.5 g/mol, m/z = 504, 323.

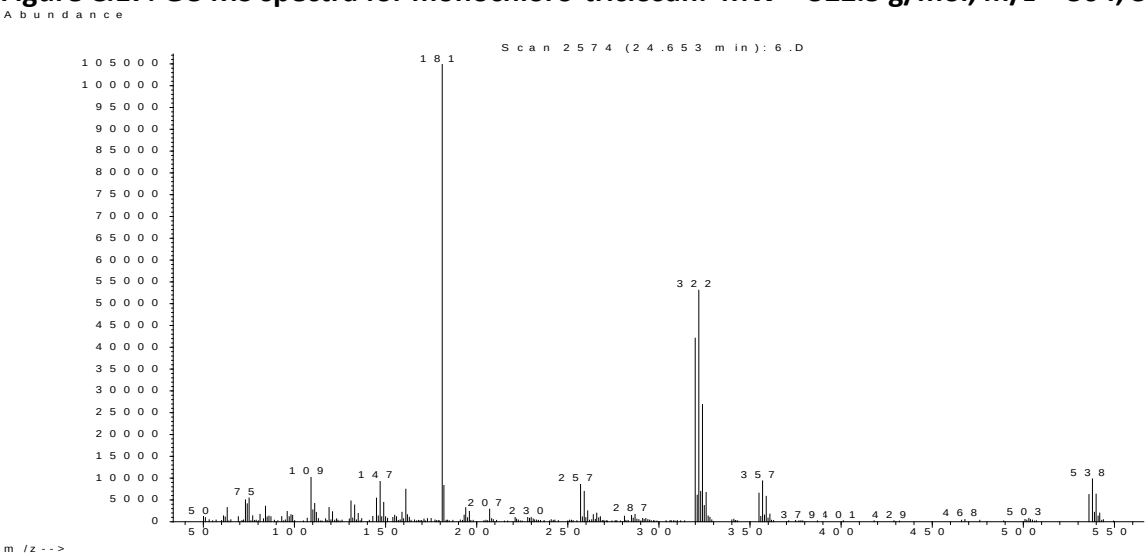

Figure C.18: GC-MS spectra for dichloro-triclosan. MW = 358.5 g/mol, m/z = 538, 357.

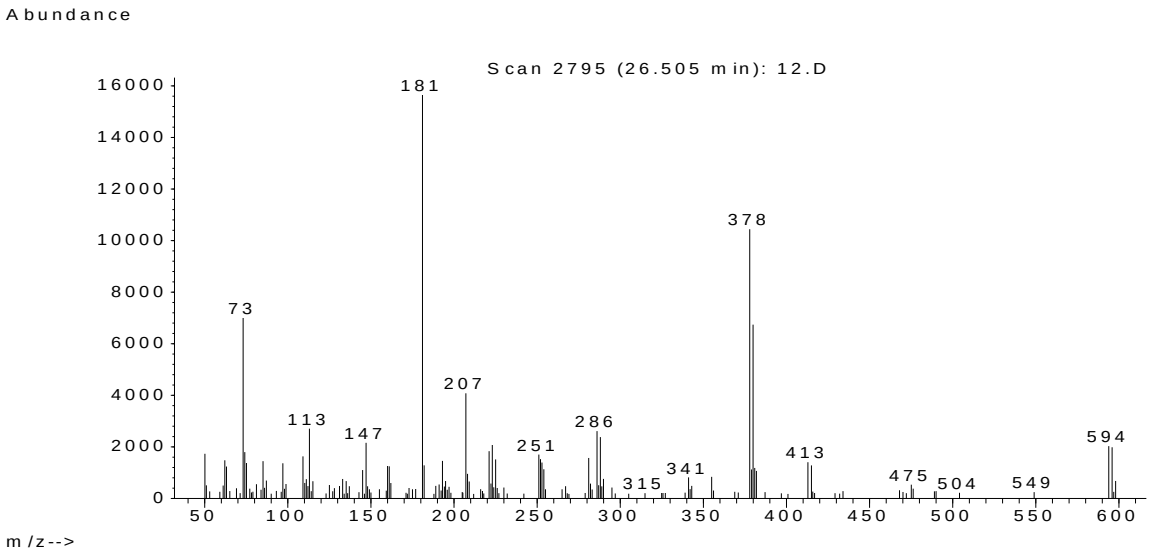

Figure C.19: GC-MS spectra for monoiodo-triclosan. MW = 414.5 g/mol, m/z = 594, 413.

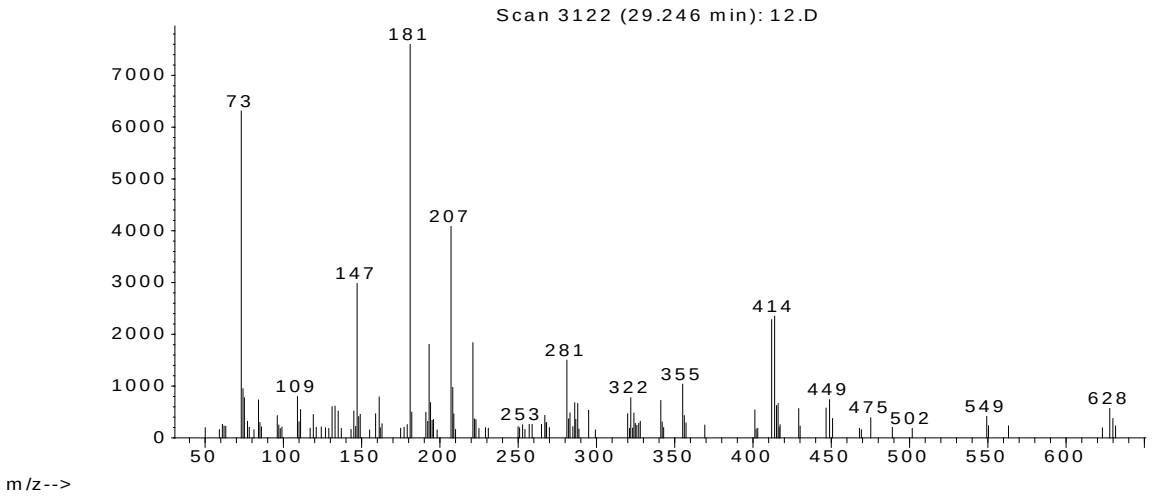

Figure C.20: GC-MS spectra for monochloro-monoiodo-triclosan. MW = 449.5 g/mol, m/z = 628, 449.

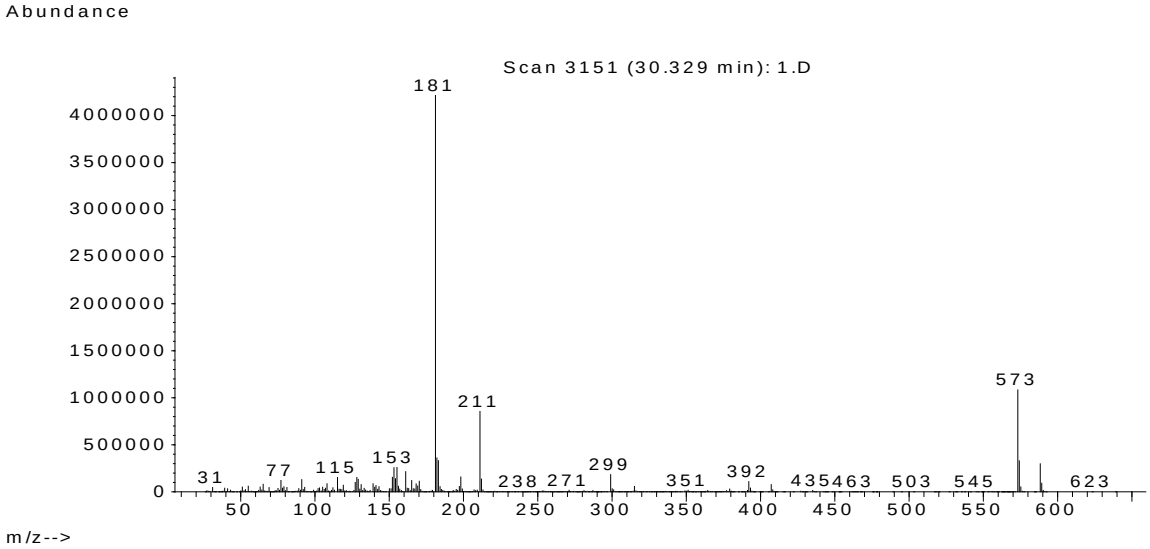

Figure C.21: GC-MS spectra for bisphenol-A. MW = 228.3 g/mol, m/z = 588, 407, 226.

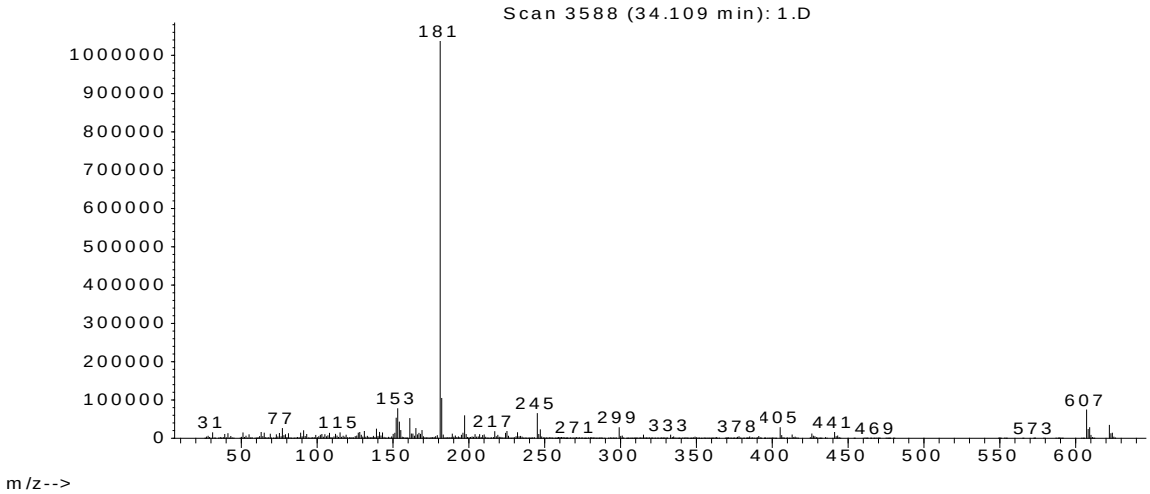

Figure C.22: GC-MS spectra for monochloro-BPA. MW = 262 g/mol, m/z = 622, 441, 260.

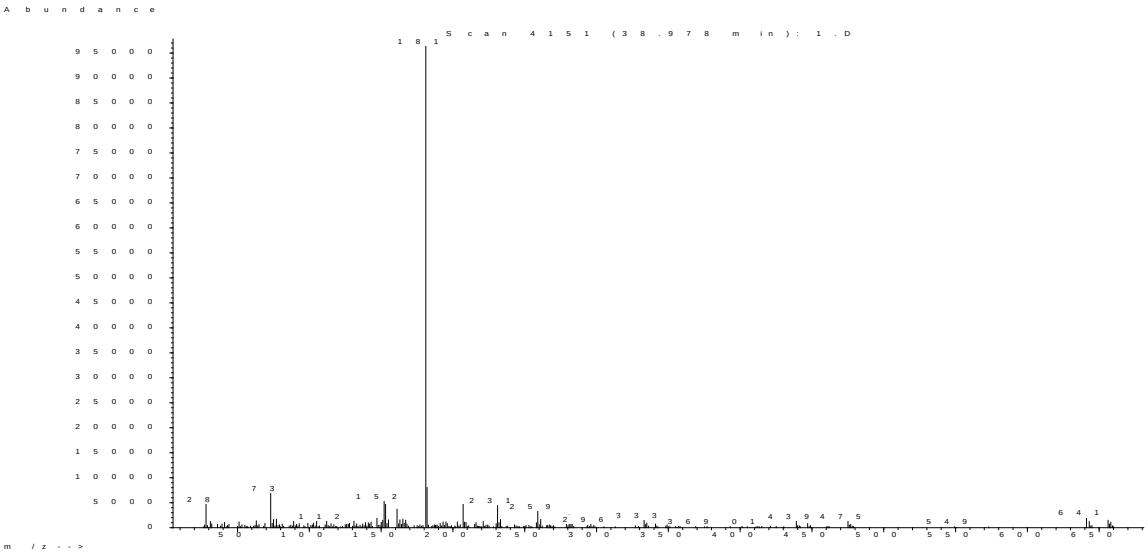

Figure C.23: GC-MS spectra for dichloro-BPA. MW = 296 g/mol, m/z = 656, 475, 294.

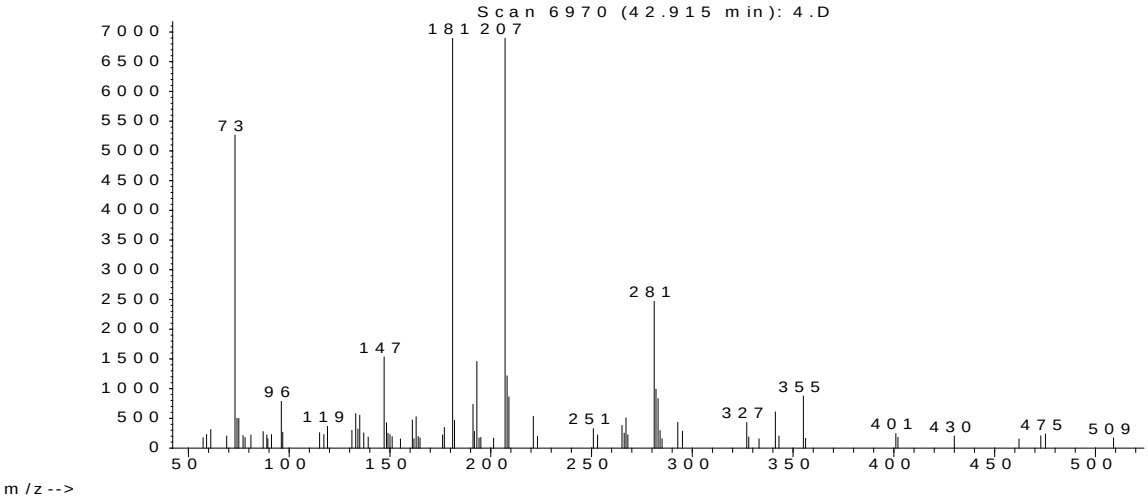

Figure C.24: GC-MS spectra for trichloro-BPA. MW = 330 g/mol, m/z = 690, 509, 328. (Scan range = 50 - 550)

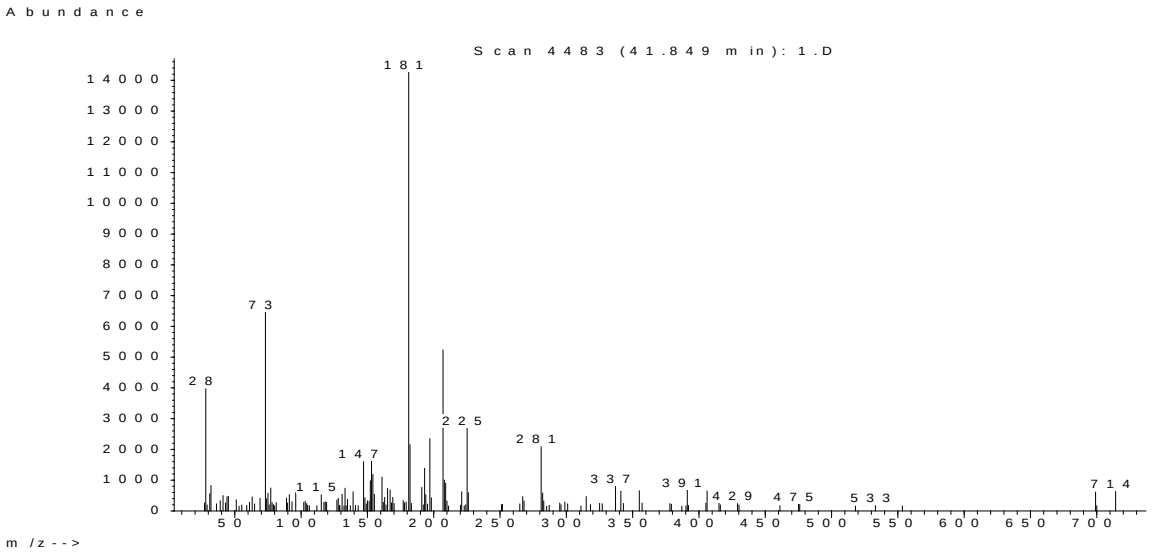

Figure C.25: GC-MS spectra for monoiodo-BPA. MW = 352 g/mol, m/z = 714, 533, 352.

Appendix D: Raw Experimental Data Tables

Note: The indicated standard deviations (STDEV) in the following tables are the deviation between two replicates.

Table D.1: Oxidant consumption over time. Conditions: pH = 5.0, [2,4-dichlorophenol] = 100 µM, [$NaHCO_3$] = 2 mM.

	Total Oxidant Concentration (µM)			STDEV (µM)		
Reaction Time (sec)	[I-] = 0 µM	[I-] = 4 µM	[I-] = 10 µM	[I-] = 0 µM	[I-] = 4 µM	[I-] = 10 µM
0	11.80026	11.96842	11.96842	0.00000	0.00000	0.00000
0.54	11.78866	11.94335	11.85144	0.05478	0.02078	0.04158
2	11.72853	11.88051	11.70665	0.01587	0.05722	0.07388
5	11.60736	11.77291	11.43014	0.00107	0.03133	0.69079
10	11.46629	11.52737	11.49917	0.21404	0.01916	0.05922

Table D.2: Oxidant consumption over time. Conditions: pH = 6.0, [2,4-dichlorophenol] = 100 µM, [$NaHCO_3$] = 2 mM.

	Total Oxidant Concentration (µM)			STDEV (µM)		
Reaction Time (sec)	[I-] = 0 µM	[I-] = 4 µM	[I-] = 10 µM	[I-] = 0 µM	[I-] = 4 µM	[I-] = 10 µM
0	10.60832	10.70850	10.80868	0.00000	0.00000	0.00000
0.54	10.60505	10.56879	10.77648	0.05276	0.10199	0.08018
0.75	10.57621	10.53677	10.75930	0.01185	0.10705	0.04740
1	10.58013	10.50892	10.71336	0.03633	0.12330	0.04846
1.5	10.56231	10.47541	10.62812	0.04312	0.10351	0.04390
2	10.51383	10.43146	10.55443	0.02725	0.10300	0.03921
3	10.49267	10.38276	10.42649	0.03492	0.09392	0.08196
4	10.46038	10.33965	10.33584	0.04094	0.11483	0.08395
5	10.45161	10.30130	9.95914	0.03477	0.06173	0.08926
10	10.35629	10.01549	9.05758	0.01449	0.02015	0.10926

Table D.4: Oxidant consumption over time. Conditions: pH = 6.25, [2,4-dichlorophenol] = 100 µM, [$NaHCO_3$] = 2 mM.

	Total Oxidant Concentration (µM)			STDEV (µM)		
Reaction Time (sec)	[I-] = 0 µM	[I-] = 4 µM	[I-] = 10 µM	[I-] = 0 µM	[I-] = 4 µM	[I-] = 10 µM
0	11.35936	11.35684	11.27419	0.00000	0.00000	0.00000
0.54	11.25944	11.31942	11.16572	0.01216	0.02396	0.00851
1.5	11.25483	11.22192	11.00177	0.00476	0.04305	0.04816
3	11.17509	11.03558	10.65372	0.00869	0.01715	0.02326
5	11.19539	10.75573	9.74120	0.04850	0.04078	0.09462
10	11.31264	10.20791	8.41521	0.07177	0.04632	0.07621

Table D.5: Oxidant consumption over time. Conditions: pH = 6.5, [2,4-dichlorophenol] = 100 µM, [$NaHCO_3$] = 2 mM.

	Total Oxidant Concentration (µM)			STDEV (µM)		
Reaction Time (sec)	[I-] = 0 µM	[I-] = 4 µM	[I-] = 10 µM	[I-] = 0 µM	[I-] = 4 µM	[I-] = 10 µM
0	11.75334	11.75018	11.83624	0.00000	0.00000	0.00000
0.54	11.69368	11.59949	11.08600	0.01216	0.02396	0.00851
1.5	11.66178	11.47829	9.93379	0.00476	0.04305	0.04816
3	11.55759	11.16229	9.81224	0.00869	0.01715	0.02326
5	11.39180	10.86069	9.25734	0.04850	0.04078	0.09462
10	11.21149	10.22416	8.08795	0.07177	0.03176	0.14190

Table D.6: Oxidant consumption over time. Conditions: pH = 6.75, [2,4-dichlorophenol] = 100 µM, [$NaHCO_3$] = 2 mM.

	Total Oxidant Concentration (µM)			STDEV (µM)		
Reaction Time (sec)	[I-] = 0 µM	[I-] = 4 µM	[I-] = 10 µM	[I-] = 0 µM	[I-] = 4 µM	[I-] = 10 µM
0	11.85837	11.76657	11.73157	0.00000	0.00000	0.00000
0.54	11.80492	11.61443	11.27886	0.01623	0.04933	0.01302
1.5	11.72497	11.35005	10.76368	0.00171	0.02299	0.02212
3	11.60259	11.04184	10.01557	0.03494	0.02566	0.03453
5	11.43620	10.49055	8.35960	0.00398	0.04497	0.08217
10	11.00575	9.31200	5.89336	0.07876	0.05698	0.20040

Table D.7: Oxidant consumption over time. Conditions: pH = 7, [2,4-dichlorophenol] = 100 µM, [$NaHCO_3$] = 2 mM.

	Total Oxidant Concentration (µM)							
Reaction Time (sec)	**[I-] = 0 µM**	**[I-] = 1 µM**	**[I-] = 4 µM**	**[I-] = 7 µM**	**[I-] = 10 µM**	**[I-] = 15 µM**	**[I-] = 25 µM**	**[I-] = 50 µM**
0	10.52229	11.34747	10.62323	11.45391	10.72418	11.28907	11.21932	11.51924
0.54	10.45498	11.50789	10.58270	11.07789	10.23017	9.25712	9.50810	10.25907
0.75	10.46147		10.54726		10.10456			
1	10.44808		10.48161		9.97273			
1.5	10.41078	11.37115	10.34945	10.67430	9.71453	7.67173	8.00722	9.25830
2	10.40272		10.21636		9.40126			
3	10.34902	11.16532	9.96987	10.11328	8.87737	5.59011	6.06274	7.90319
4	10.26271		9.70513		8.36215			
5	10.11494	10.77796	9.05337	9.02812	6.65776	2.95907	3.45066	5.56644
10	9.61799	10.28105	7.84644	7.37615	3.29898	0.65081	0.92359	2.43796
	STDEV (µM)							
Reaction Time (sec)	**[I-] = 0 µM**	**[I-] = 1 µM**	**[I-] = 4 µM**	**[I-] = 7 µM**	**[I-] = 10 µM**	**[I-] = 15 µM**	**[I-] = 25 µM**	**[I-] = 50 µM**
0	0.00000	0.00000	0.14276	0.00000	0.00000	0.00000	0.00000	0.00000
0.54	0.03126	0.14639	0.14986	0.02934	0.01896	0.08606	0.01123	0.13076
0.75	0.00823		0.13749		0.01567			
1	0.01980		0.16211		0.05520			
1.5	0.03600	0.06684	0.14251	0.00169	0.11777	0.03812	0.04577	0.14926
2	0.02597		0.11688		0.03967			
3	0.01317	0.11328	0.08692	0.01856	0.03118	0.02490	0.08618	0.14419
4	0.02328	0.11405	0.10886	0.04335	0.02491	0.03445	0.06107	0.15246
5	0.00734	0.01699	0.17637	0.05900	0.03874	0.05652	0.04294	0.10901
10	0.30828	0.06155	0.02478	0.17470	0.28254	0.00000	0.00000	0.03170

Table D.8: Oxidant consumption over time. Conditions: pH = 7.25, [2,4-dichlorophenol] = 100 µM, [$NaHCO_3$] = 2 mM.

	Total Oxidant Concentration (µM)			STDEV (µM)		
Reaction Time (sec)	[I-] = 0 µM	[I-] = 4 µM	[I-] = 10 µM	[I-] = 0 µM	[I-] = 4 µM	[I-] = 10 µM
0	11.90101	11.57361	11.01914	0.00000	0.00000	0.00000
0.54	11.61855	11.21050	10.02925	0.01028	0.06654	0.00175
1.5	11.50640	10.81269	9.20695	0.03128	0.05238	0.07406
3	11.40350	10.37810	8.12607	0.02136	0.09030	0.11820
5	10.99860	9.70018	6.88502	0.04369	0.06029	0.16655
10	10.77344	8.76569	5.08900	0.18563	0.20225	0.18115

Table D.9: Oxidant consumption over time. Conditions: pH = 7.5, [2,4-dichlorophenol] = 100 µM, [$NaHCO_3$] = 2 mM.

	Total Oxidant Concentration (µM)			STDEV (µM)		
Reaction Time (sec)	[I-] = 0 µM	[I-] = 4 µM	[I-] = 10 µM	[I-] = 0 µM	[I-] = 4 µM	[I-] = 10 µM
0	10.37823	10.43046	10.44870	0.06051	0.02794	0.04460
0.35	10.31026	10.16636	9.97975	0.03321	0.05404	0.03459
0.54	10.31344	10.14256	9.87779	0.01452	0.04867	0.01070
0.75	10.27096	10.04830	9.74013	0.01599	0.00335	0.01940
1	10.21479	9.97193	9.55303	0.04437	0.06129	0.01194
2	10.20486	9.73930	8.92580	0.04648	0.08400	0.01969
3	10.19411	9.46773	8.30917	0.01837	0.03998	0.03345
5	10.08232	8.95848	7.20403	0.07468	0.01594	0.11324

Table D.10: Oxidant consumption over time. Conditions: pH = 7.75, [2,4-dichlorophenol] = 100 µM, [$NaHCO_3$] = 2 mM.

	Total Oxidant Concentration (µM)			STDEV (µM)		
Reaction Time (sec)	[I-] = 0 µM	[I-] = 4 µM	[I-] = 10 µM	[I-] = 0 µM	[I-] = 4 µM	[I-] = 10 µM
0	10.75177	10.82795	10.79257	0.00356	0.02803	0.06119
0.35	10.65814	10.48720	10.24304	0.03535	0.03743	0.04272
0.54	10.65222	10.42065	10.13764	0.04414	0.02430	0.02482
0.75	10.61155	10.33324	9.98835	0.00516	0.00000	0.04338
1	10.62049	10.23546	9.81325	0.03378	0.06524	0.03877
2	10.57052	9.92528	9.11986	0.03234	0.00962	0.05131
3	10.47451	9.59210	8.45611	0.07632	0.02569	0.02750
5	10.37883	8.98273	7.21821	0.03906	0.05464	0.03715

Table D.11: Oxidant consumption over time. Conditions: pH = 8.0, [2,4-dichlorophenol] = 100 µM, [$NaHCO_3$] = 2 mM.

	Total Oxidant Concentration (µM)			STDEV (µM)		
Reaction Time (sec)	[I-] = 0 µM	[I-] = 4 µM	[I-] = 10 µM	[I-] = 0 µM	[I-] = 4 µM	[I-] = 10 µM
0	10.70650	10.98644	10.71168	0.39589	0.00000	0.00000
0.54	10.60184	10.72864	10.28127	0.50763	0.00556	0.07632
0.75	10.54902	10.60863	10.03471	0.51885	0.01518	0.03216
1	10.51857	10.48609	9.79858	0.51762	0.00204	0.04244
1.5	10.45945	10.27769	9.39415	0.53501	0.04676	0.04846
3	10.34406	9.80849	8.29763	0.55276	0.01798	0.10482
5	10.23070	9.28423	6.55963	0.44373	0.05589	0.12406
10	9.89151	8.30939	4.21609	0.50769	0.09609	0.04712

Table D.12: Oxidant consumption over time. Conditions: pH = 9.0, [2,4-dichlorophenol] = 100 µM, [$NaHCO_3$] = 2 mM.

	Total Oxidant Concentration (µM)			STDEV (µM)		
Reaction Time (sec)	[I-] = 0 µM	[I-] = 4 µM	[I-] = 10 µM	[I-] = 0 µM	[I-] = 4 µM	[I-] = 10 µM
0	10.49964	10.49964	10.53565	0.00000	0.00000	0.00000
0.54	10.40011	10.36063	10.22267	0.01097	0.06458	0.00318
0.75	10.36552	10.28658	10.10145	0.01612	0.06111	0.02494
1	10.34195	10.23834	10.01639	0.02619	0.05913	0.01775
1.5	10.30455	10.13203	9.84824	0.00946	0.05878	0.02610
3	10.28783	9.95902	9.49245	0.01521	0.02217	0.07163
5	10.24517	9.58263	8.74175	0.03841	0.09721	0.10926
10	10.04600	8.90450	7.42462	0.01076	0.12334	0.12027

Table D.13: Oxidant consumption over time. Conditions: pH = 10.0, [2,4-dichlorophenol] = 100 µM, [$NaHCO_3$] = 2 mM.

	Total Oxidant Concentration (µM)			STDEV (µM)		
Reaction Time (sec)	[I-] = 0 µM	[I-] = 4 µM	[I-] = 10 µM	[I-] = 0 µM	[I-] = 4 µM	[I-] = 10 µM
0	11.22360	11.23196	11.28153	0.00000	0.00000	0.00000
0.54	11.31502	11.19938	11.17418	0.00246	0.01269	0.05479
1	11.19262	11.07425	11.09691	0.03423	0.00381	0.10374
2	11.18617	11.05625	11.08701	0.01287	0.03670	0.07953
5	11.00525	10.89265	10.93492	0.01965	0.04183	0.03654
10	10.84001	10.66896	10.88392	0.01349	0.02035	0.17837

Table D.14: Oxidant consumption over time. Conditions: pH = 5.5, [bisphenol-A] = 100 µM, [$NaHCO_3$] = 2 mM.

	Total Oxidant Concentration (µM)			STDEV (µM)		
Reaction Time (sec)	**[I-] = 0 µM**	**[I-] = 4 µM**	**[I-] = 10 µM**	**[I-] = 0 µM**	**[I-] = 4 µM**	**[I-] = 10 µM**
0	10.52042	10.46152	10.33308	0.05901	0.00707	0.02731
0.35	10.58995	9.91992	9.07370	0.01316	0.05199	0.04712
0.5		9.86595	8.82579		0.02242	0.07481
0.75		9.62694	8.46376		0.00887	0.06693
1	10.49732	9.55451	8.14786	0.00375		0.03969
2		8.96734	6.66663		0.04175	0.11446
3		8.55511	5.27083			0.08628
5	10.49717	8.04602	3.65514	0.16392	0.03629	0.14332

Table D.15: Oxidant consumption over time. Conditions: pH = 6.0, [bisphenol-A] = 100 µM, [$NaHCO_3$] = 2 mM.

	Total Oxidant Concentration (µM)			STDEV (µM)		
Reaction Time (sec)	**[I-] = 0 µM**	**[I-] = 4 µM**	**[I-] = 10 µM**	**[I-] = 0 µM**	**[I-] = 4 µM**	**[I-] = 10 µM**
0	10.82594	10.69656	10.93565	0.00366	0.01499	0.02848
0.35	10.69163	9.72450	7.93171	0.09187	0.02011	0.26862
0.5	10.67176	9.45032	6.93144	0.04720	0.07229	0.14610
0.75	10.65634	9.22943	6.36702	0.10560	0.12588	0.22439
1	10.72809	9.00624	5.25009	0.10011	0.10854	0.23345
2	10.64329	8.42281	3.01243	0.10110	0.15174	0.10471
3	10.69804	8.00810	1.94932	0.11662	0.12401	0.18590
5	10.62354	7.58757	0.99556	0.13247	0.07821	0.22355

Table D.16: Oxidant consumption over time. Conditions: pH = 6.5, [bisphenol-A] = 100 µM, [$NaHCO_3$] = 2 mM.

	Total Oxidant Concentration (µM)			STDEV (µM)		
Reaction Time (sec)	[I-] = 0 µM	[I-] = 4 µM	[I-] = 10 µM	[I-] = 0 µM	[I-] = 4 µM	[I-] = 10 µM
0	9.91129	10.28366	10.27216	0.25596	0.01924	0.11460
0.35	9.95948	7.85446	4.12014	0.17963	0.01350	0.02530
0.5		7.53294	3.20139		0.00749	0.10909
0.75		7.25241	2.45146		0.02346	0.11710
1	9.91114	7.15764	2.19051		0.02298	0.17384
2		6.54366	0.72314		0.07203	0.04002
3		6.42648	0.44822		0.07616	0.01676
5	9.76152	6.39391	0.37780	0.24790	0.03263	0.00217

Table D.17: Oxidant consumption over time. Conditions: pH = 7.0, [bisphenol-A] = 100 µM, [$NaHCO_3$] = 2 mM.

	Total Oxidant Concentration (µM)			STDEV (µM)		
Reaction Time (sec)	[I-] = 0 µM	[I-] = 4 µM	[I-] = 10 µM	[I-] = 0 µM	[I-] = 4 µM	[I-] = 10 µM
0	10.82198	10.76758	10.75111	0.05362	0.02330	0.00000
0.35	10.74120	7.46230	2.22737	0.01784	0.14293	0.08331
0.5		7.19933	1.57741		0.19892	0.08967
0.75		7.13432	1.45785		0.17454	0.09083
1	10.68013	7.09121	1.37481	0.00564	0.19341	0.09165
2		6.90022	1.04177		0.16107	0.09490
3		6.71410	1.01351		0.18781	0.09518
5	10.43309	6.64145	0.67106	0.12711	0.17605	0.09852

Table D.18: Oxidant consumption over time. Conditions: pH = 8.0, [bisphenol-A] = 100 µM, [$NaHCO_3$] = 2 mM.

	Total Oxidant Concentration (µM)			STDEV (µM)		
Reaction Time (sec)	[I-] = 0 µM	[I-] = 4 µM	[I-] = 10 µM	[I-] = 0 µM	[I-] = 4 µM	[I-] = 10 µM
0	10.78928	10.72479	11.61118	0.02131	0.01580	0.01028
0.35	10.70675	6.74923	1.53097	0.01076	0.02168	0.03261
0.5	10.63583	6.59510	1.23544	0.01985	0.01510	0.01035
1	10.52095	6.51131	1.01018	0.01305	0.01548	0.01790
2	10.38217	6.38963	0.72406	0.01046	0.01172	0.01299
3	10.16056	6.22274	0.56273	0.05113	0.03067	0.01022
5	9.73280	5.95357	0.38763	0.04556	0.02638	0.00721

Table D.19: Oxidant consumption over time. Conditions: pH = 9.0, [bisphenol-A] = 100 µM, [$NaHCO_3$] = 2 mM.

	Total Oxidant Concentration (µM)			STDEV (µM)		
Reaction Time (sec)	[I-] = 0 µM	[I-] = 4 µM	[I-] = 10 µM	[I-] = 0 µM	[I-] = 4 µM	[I-] = 10 µM
0	11.96772	11.42510	11.51771	0.00000	0.00000	0.00000
0.35	11.82317	7.73867	1.21257	0.24856	0.11213	0.23726
0.5	11.76088	7.64031	0.94974	0.19314	0.11920	0.34382
1	11.65084	7.56788	0.83149	0.16378	0.06130	0.31931
2	11.44026	7.40983	0.76135	0.10276	0.01787	0.34674
3	11.11902	7.23726	0.74562	0.18000	0.04044	0.30994
5	10.75527	6.86923	0.68900	0.01741	0.01199	0.31470

Table D.20: Oxidant consumption over time. Conditions: pH = 10.0, [bisphenol-A] = 100 µM, [$NaHCO_3$] = 2 mM.

	Total Oxidant Concentration (µM)			STDEV (µM)		
Reaction Time (sec)	[I-] = 0 µM	[I-] = 4 µM	[I-] = 10 µM	[I-] = 0 µM	[I-] = 4 µM	[I-] = 10 µM
0	10.90607	10.97882	11.15783	0.04714	0.01991	0.03339
0.35	10.93737	6.49923	1.40903	0.01150	0.11460	0.00544
0.5		6.38114	1.17081		0.11911	0.00400
1	10.80666	6.18300	1.07999		0.11020	0.02948
2		6.02025	1.04095		0.12013	0.01843
3	10.62019	5.91841	1.00789	0.08078	0.06176	0.01786
5	10.40361	5.79316	0.85999	0.02815	0.18294	0.01532

Table D.21: Oxidant consumption over time. Conditions: pH = 5.5, [triclosan] = 25 µM, [$NaHCO_3$] = 2 mM.

	Total Oxidant Concentration (µM)			STDEV (µM)		
Reaction Time (sec)	[I-] = 0 µM	[I-] = 4 µM	[I-] = 10 µM	[I-] = 0 µM	[I-] = 4 µM	[I-] = 10 µM
0	5.72098	5.79426	5.84614	0.01215	0.00968	0.00986
0.35	5.64732	5.68957	5.48491	0.02469	0.02603	0.03244
0.5	5.68467	5.71038	5.46693	0.02489	0.02007	0.01440
1	5.60683	5.61733	5.18369	0.01474	0.02404	0.02905
2	5.65381	5.54282	4.87523	0.01394	0.01492	0.02000
3	5.64845	5.59240	4.54414	0.04579	0.04046	0.03708
5	5.57401	5.36159	4.03427	0.05739	0.05646	0.02777

Table D.22: Oxidant consumption over time. Conditions: pH = 6.0, [triclosan] = 25 µM, [$NaHCO_3$] = 2 mM.

	Total Oxidant Concentration (µM)			STDEV (µM)		
Reaction Time (sec)	[I-] = 0 µM	[I-] = 4 µM	[I-] = 10 µM	[I-] = 0 µM	[I-] = 4 µM	[I-] = 10 µM
0	5.46557	5.34230	5.70371	0.01039	0.01042	0.02726
0.35	5.38698	5.18600	4.99753	0.01411	0.01576	0.02415
0.5	5.42578	5.18251	5.01659	0.01196	0.01236	0.01183
1	5.37753	4.99578	4.69306	0.03303	0.02647	0.02614
2	5.36233	4.91921	4.29925	0.01000	0.00875	0.01519
3	5.38067	4.84033	3.99601	0.03204	0.02738	0.02626
5	5.27594	4.46273	3.29347	0.03148	0.02637	0.04788

Table D.23: Oxidant consumption over time. Conditions: pH = 6.5, [triclosan] = 25 µM, [$NaHCO_3$] = 2 mM.

	Total Oxidant Concentration (µM)			STDEV (µM)		
Reaction Time (sec)	[I-] = 0 µM	[I-] = 4 µM	[I-] = 10 µM	[I-] = 0 µM	[I-] = 4 µM	[I-] = 10 µM
0	4.99571	5.00722	4.50214	0.01580	0.03433	0.01461
0.35	4.78935	4.54150	3.84081	0.01308	0.02240	0.01914
0.5	4.82530	4.47801	3.70997	0.01154	0.01499	0.01137
1	4.67928	4.10529	3.21809	0.02091	0.02288	0.01403
2	4.67212	3.69858	2.60267	0.01085	0.02302	0.01813
3	4.62924	3.20357	2.10079	0.01642	0.04513	0.03000
5	4.47076	2.67871	1.45485	0.04955	0.02193	0.00803

Table D.24: Oxidant consumption over time. Conditions: pH = 7.5, [triclosan] = 25 µM, [$NaHCO_3$] = 2 mM.

	Total Oxidant Concentration (µM)			STDEV (µM)		
Reaction Time (sec)	[I-] = 0 µM	[I-] = 4 µM	[I-] = 10 µM	[I-] = 0 µM	[I-] = 4 µM	[I-] = 10 µM
0	4.56487	4.85199	4.91641	0.01434	0.01112	0.00877
0.35	4.37536	4.36427	4.25455	0.01453	0.01037	0.01061
0.5	4.37949	4.29247	4.17849	0.01035	0.01093	0.01075
1	4.33274	3.98159	3.78363	0.01832	0.01260	0.01054
2	4.24273	3.47023	3.01958	0.01701	0.00972	0.01008
3	4.23867	3.02032	2.41198	0.01377	0.01385	0.00890
5	3.88708	2.25343	1.54074	0.02204	0.02097	0.01086

Table D.25: Oxidant consumption over time. Conditions: pH = 8.0, [triclosan] = 25 µM, [$NaHCO_3$] = 2 mM.

	Total Oxidant Concentration (µM)			STDEV (µM)		
Reaction Time (sec)	[I-] = 0 µM	[I-] = 4 µM	[I-] = 10 µM	[I-] = 0 µM	[I-] = 4 µM	[I-] = 10 µM
0	5.52864	5.24121	5.30201	0.02131	0.02800	0.02446
0.35	5.42307	4.71245	4.56314	0.01076	0.02299	0.01976
0.5	5.44147	4.65128	4.45283	0.01985	0.01725	0.04164
1	5.36514	4.34441	3.99275	0.01305	0.02143	0.01023
2	5.29609	3.89849	3.40646	0.01046	0.01892	0.01476
3	5.23581	3.47718	2.80200	0.05113	0.04390	0.05043
5	5.09672	2.76702	2.12533	0.04556	0.03683	0.02440

Table D.26: Oxidant consumption over time. Conditions: pH = 9.0, [triclosan] = 25 µM, [$NaHCO_3$] = 2 mM.

	Total Oxidant Concentration (µM)			STDEV (µM)		
Reaction Time (sec)	[I-] = 0 µM	[I-] = 4 µM	[I-] = 10 µM	[I-] = 0 µM	[I-] = 4 µM	[I-] = 10 µM
0	5.68279	5.63791	5.74640	0.01609	0.02002	0.01299
0.35	5.64959	5.43626	5.45348	0.00794	0.01322	0.01401
0.5	5.63147	5.37514	5.38422	0.01051	0.01515	0.01419
1	5.62394	5.24042	5.23747	0.02009	0.01432	0.01703
2	5.58992	4.95482	4.89869	0.01256	0.01682	0.01569
3	5.58244	4.60229	4.54257	0.02726	0.02396	0.03215
5	5.53348	4.34477	4.19166	0.04036	0.03182	0.04973

Table D.27: Oxidant consumption over time. Conditions: pH = 10.0, [triclosan] = 25 µM, [$NaHCO_3$] = 2 mM.

	Total Oxidant Concentration (µM)			STDEV (µM)		
Reaction Time (sec)	[I-] = 0 µM	[I-] = 4 µM	[I-] = 10 µM	[I-] = 0 µM	[I-] = 4 µM	[I-] = 10 µM
0	5.36989	5.43037	5.42114	0.01226	0.00984	0.04091
0.35	5.26340	5.26230	5.18031	0.01832	0.01715	0.02544
0.5	5.24888	5.25195	5.19040	0.01526	0.01793	0.01726
1	5.25238	5.20642	5.13157	0.01597	0.01868	0.01053
2	5.22191	5.14494	5.07524	0.01742	0.01348	0.01530
3	5.19054	5.04667	4.87575	0.01705	0.01254	0.01353
5	5.14280	4.91550	4.84387	0.02173	0.01625	0.01855

Table D.28: Oxidant consumption over time. Conditions: pH = 4.5, [phenol] = 100 µM, [$NaHCO_3$] = 2 mM.

	Total Oxidant Concentration (µM)			STDEV (µM)		
Reaction Time (sec)	[I-] = 0 µM	[I-] = 4 µM	[I-] = 10 µM	[I-] = 0 µM	[I-] = 4 µM	[I-] = 10 µM
0	11.87012	11.87012	11.87012	0.18569	0.18569	0.18569
5	12.07880	11.87344	11.14010	0.14472	0.29974	0.44822
7.5	11.96229	11.70731	10.91961	0.15430	0.31021	0.32371
10	11.97442	11.58637	10.62930	0.11915	0.25613	0.35297
15	11.34035	10.78770	9.91237	0.05521	0.33845	0.66113
20	11.87556	11.25688	9.67556	0.19011	0.26330	0.72195
30	11.63067	10.90430	9.04056	0.04695	0.30732	0.79382
45	11.45301	10.47932	8.40173	0.09184	0.12621	0.69510
60	11.44766	10.22987	7.79792	0.05789	0.07722	0.86434

Table D.29: Oxidant consumption over time. Conditions: pH = 6, [phenol] = 100 µM, [$NaHCO_3$] = 2 mM.

	Total Oxidant Concentration (µM)			STDEV (µM)		
Reaction Time (sec)	[I-] = 0 µM	[I-] = 4 µM	[I-] = 10 µM	[I-] = 0 µM	[I-] = 4 µM	[I-] = 10 µM
0	8.82474	8.82474	8.82474	0.18569	0.18569	0.18569
0.25	8.79083	7.76742	7.22685	0.12292	0.22592	0.13399
0.5	8.79557	7.46966	6.95292	0.22229	0.20665	0.06770
0.75	8.73897	6.67214	5.68080	0.67187	0.27377	0.16787
1	8.66977	6.53517	5.46812	0.29479	0.40165	0.02541
1.5	8.58199	6.37884	4.58267	0.27123	0.22717	0.06691
2	8.58199	6.18274	4.29916	0.48248	0.46526	0.18663
2.5	8.47257	5.94009	3.97240	0.63863	0.05702	0.13377
5	8.20429	5.58523	3.89487	0.84029	0.91194	0.12556

Table D.30: Oxidant consumption over time. Conditions: pH = 7, [phenol] = 100 µM, [$NaHCO_3$] = 2 mM.

	Total Oxidant Concentration (µM)			STDEV (µM)		
Reaction Time (sec)	[I-] = 0 µM	[I-] = 4 µM	[I-] = 10 µM	[I-] = 0 µM	[I-] = 4 µM	[I-] = 10 µM
0	10.45288	10.38859	10.38859	0.05362	0.02330	0.00000
0.25	10.34487	8.56502	7.00130	0.01784	0.14293	0.08331
0.5	10.40731	8.46137	6.58195	0.06176	0.19892	0.08967
0.75	10.42835	8.36498	6.60699	0.18294	0.17454	0.09083
1	10.39040	8.15309	6.28943	0.00564	0.19341	0.09165
1.5	10.36965	8.07620	6.12531	0.01786	0.16107	0.09490
2	10.36965	7.93559	5.97538	0.01532	0.18781	0.09518
2.5	10.16714	7.86285	5.93167	0.12711	0.17605	0.09852
5	10.11379	7.78918	5.86044	0.12711	0.17605	0.09852

Table D.31: Oxidant consumption over time. Conditions: pH = 8, [phenol] = 100 µM, [$NaHCO_3$] = 2 mM.

	Total Oxidant Concentration (µM)			STDEV (µM)		
Reaction Time (sec)	[I-] = 0 µM	[I-] = 4 µM	[I-] = 10 µM	[I-] = 0 µM	[I-] = 4 µM	[I-] = 10 µM
0	10.6078	10.5991	10.5040	0.0000	0.0000	0.0000
0.25	10.6033	8.3624	6.6510	0.2486	0.1121	0.2373
0.5	10.6025	8.3088	6.5604	0.1931	0.1192	0.3438
0.75	10.6023	8.1355	6.3909	0.1638	0.0613	0.3193
1	10.5939	8.0513	6.3114	0.1028	0.0179	0.3467
1.5	10.5659	8.0312	6.2857	0.1800	0.0404	0.3099
2	10.5659	7.9644	6.2067	0.0174	0.0120	0.3147
2.5	10.4350	7.9091	6.1648	0.1146	0.0054	0.1102
5	10.3934	7.8470	6.0691	0.1191	0.0040	0.1201

Table D.32: Oxidant consumption over time. Conditions: pH = 7, [4-chlorophenol] = 100 µM, [$NaHCO_3$] = 2 mM.

	Total Oxidant Concentration (µM)			STDEV (µM)		
Reaction Time (sec)	[I-] = 0 µM	[I-] = 4 µM	[I-] = 10 µM	[I-] = 0 µM	[I-] = 4 µM	[I-] = 10 µM
0	9.46896	9.33410	10.47219	0.12995	0.06879	0.06801
0.5	9.15067	8.72483	6.44907	0.08215	0.08946	0.11490
0.75	9.16115	8.66270	5.98577	0.07739	0.07898	0.06916
1	9.14827	8.55941	5.27576	0.09143	0.10254	0.04562
1.5	9.11897	8.38215	4.18239	0.09340	0.10326	0.04514
2	9.10030	8.19452	3.29638	0.04395	0.08361	0.03267
3	9.06612	7.91638	1.97188	0.05619	0.08221	0.04352
5	8.92546	7.28051	0.58962	0.10596	0.04346	0.03636

Table D.33: Oxidant consumption over time. Conditions: pH = 7, [4-bromophenol] = 100 µM, [$NaHCO_3$] = 2 mM.

	Total Oxidant Concentration (µM)			STDEV (µM)		
Reaction Time (sec)	[I-] = 0 µM	[I-] = 4 µM	[I-] = 10 µM	[I-] = 0 µM	[I-] = 4 µM	[I-] = 10 µM
0	10.14919	9.46891	9.31016	0.04804	0.00829	0.02186
0.5	9.97556	8.80174	6.01101	0.04879	0.03039	0.66874
0.75	9.98828	8.67645	5.48133	0.04001	0.07470	0.63792
1	9.96941	8.55211	4.79150	0.04360	0.04393	0.59978
1.5	9.95280	8.31567	3.86027	0.04476	0.06715	0.69756
2	9.90297	8.07966	2.96170	0.04992	0.08577	0.69011
3	9.88784	7.78835	1.71806	0.05382	0.09499	0.59438
5	9.82380	7.05228	0.40997	0.00733	0.08477	0.44514

Table D.33: Oxidant consumption over time. Conditions: pH = 7, [4-iodophenol] = 100 µM, [$NaHCO_3$] = 2 mM.

	Total Oxidant Concentration (µM)			STDEV (µM)		
Reaction Time (sec)	[I-] = 0 µM	[I-] = 4 µM	[I-] = 10 µM	[I-] = 0 µM	[I-] = 4 µM	[I-] = 10 µM
0	8.62134	8.64740	8.51356	0.01790	0.01366	0.07509
0.5	8.36990	7.83308	6.38560	0.01160	0.01691	0.18068
0.75	8.34239	7.72826	6.10464	0.01330	0.03440	0.18205
1	8.34747	7.57333	5.75634	0.01963	0.04331	0.15899
1.5	8.33542	7.33305	5.17083	0.02635	0.02697	0.16975
2	8.26637	7.15649	4.62090	0.02770	0.02985	0.21596
3	8.21809	6.78655	3.72658	0.03987	0.01498	0.29321
5	7.76336	5.88164	1.97263	0.03016	0.02494	0.15897